40

SEP 18 1963

CONFIDENTIAL

MASTER

PWAC-632
LCRE AND SNAP 50-DR-1 PROGRAMS
ENGINEERING PROGRESS REPORT
April 1, 1963 - June 30, 1963

AEC RESEARCH AND DEVELOPMENT REPORT

PRATT & WHITNEY AIRCRAFT
DEPENDABLE ENGINES

RESTRICTED DATA

This document contains restricted data as defined in the Atomic Energy Act of 1954. Its transmittal or the disclosure of its contents in any manner to an unauthorized person is prohibited.

PRATT & WHITNEY AIRCRAFT
DIVISION OF UNITED AIRCRAFT CORPORATION
CANEL
MIDDLETOWN • CONNECTICUT

CONFIDENTIAL

DISCLAIMER

[redacted]

M-3679 (30th Ed.) CATEGORY C-93a
ADVANCED CONCEPTS FOR FUTURE APPLICATION-REACTOR EXPERIMENTS

PWAC-632
LCRE AND SNAP 50-DR-1 PROGRAMS ENGINEERING PROGRESS REPORT
April 1, 1963 - June 30, 1963

AEC RESEARCH AND DEVELOPMENT REPORT

CONTRACT AT(30-1)-2789

Issued August 26, 1963

[redacted]

PRATT & WHITNEY AIRCRAFT
DIVISION OF UNITED AIRCRAFT CORPORATION
CANEL
MIDDLETOWN • CONNECTICUT

[redacted]

DISTRIBUTION

Category C-93a Advanced Concepts for Future Application-Reactor Experiments

	Copy No.
Aerojet-General Corporation (NASA)	1
Aerojet-General Nucleonics	2
Aeronautical Systems Division	3 - 8
Aerospace Corporation	9
Air Force Weapons Laboratory	10 - 11
Airesearch Manufacturing Company, Phoenix	12
Albuquerque Operations Office	13
Allison Division-GMC	14
Argonne National Laboratory	15
Army Combat Developments Command	16
ARO, Inc.	17
Atomic Energy Commission, Washington	18 - 23
Atomics International	24
Battelle Memorial Institute	25
Brookhaven National Laboratory	26
Bureau of Naval Weapons	27 - 28
Bureau of Ships	29 - 30
California Patent Group	31
Canoga Park Area Office	32 - 33
Chicago Patent Group	34
Cincinnati Area Office	35
Director of Defense Research and Engineering (OAP)	36
duPont Company, Aiken	37
Foreign Technology Division (AFSC)	38
General Atomic Division	39
General Dynamics/Astronautics (NASA)	40
General Dynamics/Forth Worth	41
General Electric Company, Cincinnati	42 - 45
General Electric Company, Richland	46 - 48
Jet Propulsion Laboratory	49 - 50
Johns Hopkins University (APL)	51
Knolls Atomic Power Laboratory	52 - 53
Ling Temco Vought, Inc.	54
Lockheed-Georgia Company	55
Lockheed Missiles and Space Company (NASA)	56
Los Alamos Scientific Laboratory	57
Mound Laboratory	58
Marquardt Corporation	59
Martin-Marietta Corporation	60 - 61
Martin-Marietta Corporation, Denver	62
NASA Langley Research Center	63
NASA Lewis Research Center	64 - 68
NASA Manned Spacecraft Center	69
NASA Marshall Space Flight Center	70
NASA Scientific and Technical Information Facility	71 - 73
National Aeronautics and Space Administration, Washington	74 - 75
Naval Air Development Center	76

	Copy No.
Naval Air Engineering Center	77
Naval Ordnance Laboratory	78
Naval Postgraduate School	79
Naval Radiological Defense Laboratory	80
New York Operations Office	81
New York Operations Office, CANEL Project Office	82
North American Avaiation, Inc., Downey	83
Oak Ridge Operations Office	84
Office of Naval Research	85 - 86
Office of the Assistant General Council for Patents (AEC)	87
Office of the Chief of Naval Operations	88
Office of the Chief of Transportation	89
Phillips Petroleum Company (NRTS)	90 - 91
Pratt & Whitney Aircraft Division (NASA)	92
RAND Corporation	93
Rocketdyne (NASA)	94 - 95
Sandia Corporation	96
San Francisco Operations Office	97
School of Aerospace Medicine	98
Space Technology Laboratories, Inc.	99
Tennessee Valley Authority	100
Union Carbide Nuclear Company (ORNL)	101 - 110
United Nuclear Corporation (NDA)	111
USAF Headquarters	112
University of California, Livermore	113 - 114
Walter Reed Army Medical Center	115
Westinghouse Bettis Atomic Power Laboratory	116 - 118
Westinghouse Electric Corporation, Lima	119
Westinghouse Electric Corporation (NASA)	120
Division of Technical Information Extension	121 - 160

SPECIAL EXTERNAL DISTRIBUTION

Mr. W. H. Pennington	161 - 163
Col. E. M. Douthett, HQS, AEC	164 - 167
Mr. J. Simmons, HQS, AEC	168 - 169
Reports and Statistics Branch, HQS, AEC	170
Mr. H. Potter, NY, Patent Office	171
Mr. J. E. McLaughlin, NY	172
Mr. S. Meyers, MCR Project Office	173
Dr. M. Balicki, NY	174
Mr. H. M. Leppich, ID	175

PRATT & WHITNEY AIRCRAFT

CANEL	176 - 200

TABLE OF CONTENTS

TABLE OF FIGURES

I. SUMMARY

Prepared under the Direction of the
New York Operations Office
United States Atomic Energy Commission

CONFIDENTIAL
RESTRICTED DATA
CLASSIFICATION

AUTHORIZED CLASSIFIER

August 19, 1963
DATE

I. SUMMARY

This report covers work accomplished during the second quarter of 1963 on the Lithium-Cooled Reactor Experiment (LCRE), and the SNAP-50/SPUR powerplant development program. It is submitted to the U. S. Atomic Energy Commission in partial fulfillment of Contract AT(30-1)-2789.

A. LCRE

A study of fuel pin design resulted in a 7.5 inch increase in void length to accommodate the higher internal gas release which exceeded original design assumptions. This redesign increased the operating time limit from 7200 to 20,000 hours. Results of Cb-1 Zr alloy strength testing indicated the pin cladding strength to be below original design levels. Evaluation was continued on carburizing, nitriding, and solution heat treatment methods for improving pin cladding strength. Carbon coating increased the strength of cladding samples by 50 percent while solution treatment of tubing resulted in a 15 percent strength increase.

The ten-inch lithium-filled pressure vessel completed a 10,000-hour test at 1900F to 2000F. Examination of the vessel is in progress. One four-inch pressure vessel has completed 4746 hours (1600F) and the other has completed 3503 hours (2000F) of scheduled 10,000-hour tests. The full-scale pressure vessel has completed 408 hours of a scheduled 10,000-hour (2000F) test.

The Non-Nuclear Systems Test completed 206.5 operation hours (5 Mw and 2000F) without incident. All phases of startup were accomplished in a much shorter time that in the previous startup. A calibration program and design point operation are being conducted.

Examination of 866 of the 906 test-soak fuel pin specimens was completed. Metallographic and chemical analyses are underway to evaluate those fuel specimens which leaked lithium.

Examination of fuel specimens from one inpile capsule test was completed and examination of two other test specimens was begun.

The Reliability Data Center became fully operational.

A specification was completed and issued to prospective bidders covering design, procurement, fabrication, and installation of the Auxiliary Systems. Following review of proposals, the Auxiliary System contract will be awarded in September, 1963.

Title I support facility design was completed. Title II design is scheduled for completion in August.

B. SNAP-50/SPUR

Powerplant pump power requirements were revised following a review of the first flight powerplant. Studies indicate that revisions in the heat rejection system and radiator are desirable.

A mathematical model of the 300 Kwe SNAP-50/SPUR powerplant system has been checked out on the analog computer.

Fuel-to-cladding compatibility tests indicated the cladding effectiveness of tantalum and the excellent compatibility of stoichiometric uranium carbide versus tungsten-lined Cb-1 Zr alloy in out-of-pile testing. Inpile capsule testing has confirmed tantalum as an effective barrier between uranium carbide and Cb-1 Zr alloy.

Primary pump studies indicated the possibility of significant efficiency gains from revisions of shaft speed and inlet pressures.

Two-phase operation of a boiling potassium loop was terminated after 200 hours and testing began on an improved version of the loop

C. ADVANCED APPLICATION STUDIES

A preliminary study was completed (PWAC-406) for adapting the SNAP-50/SPUR powerplant to provide electrical power for a manned lunar base. Two types of powerplants were considered. A study was started to investigate the use of the LCRE reactor in a portable electrical power-generating system.

II. LITHIUM-COOLED REACTOR EXPERIMENT

A. LCRE ANALYSIS AND DESIGN

1. Reactor

A complete review was conducted of the LCRE structural design and thermal performance based on materials properties and component performance information available from recent tests. In addition, more detailed analyses were performed where required to support the LCRE design. These analyses are to be incorporated in the LCRE Design Report, which is currently being prepared. Fig 1 is a isometric drawing of the current concept of the physical relationship of the Primary, Reflector, and Secondary systems.

A study of the LCRE fuel pin design was conducted to evaluate the effects of increased helium production and additional experimental data on gas release and reduced fuel pin cladding strength.

The results of the study (Summary of LCRE Fuel Element Design Including Supporting Experimental Data) showed that the fuel pins are subjected to a higher internal gas pressure from released helium and fission gases than was believed in initial design assumptions. This increase is due, primarily, to higher cross-sections for production of helium in BeO. In addition, as results of long time tests of Cb-1 Zr alloy tubing became available, the fuel pin cladding strength was found to be below original design levels. The fuel pin design is being revised to provide the required gas containment by increasing the over-all length of the fuel pin by 3.0 inches, increasing the fuel pin void volume by shortening each end reflector 2.5 inches, and compensating for the reactivity change by increasing the fueled core length 0.5 inch. This provides a net increase of void length of 7.5 inches. In addition, the hot end void spacer has been redesigned to increase the buckling strength of the pin, thereby making it possible to seal the fuel pins by high vacuum electron beam welding, which further reduces the contained gas. The changes are based on restoration of strength to the Cb-1 Zr alloy cladding by carbon addition and solution heat treatment, according to the results of tests of treated material which show improved strength during accelerated strength testing. Carbon addition resulted in a 50 percent increase in 10,000-hour rupture strength at 2200F and solution heat treatment increased rupture strength by 15 percent for 10,000 hours at 2200F. The effect of these changes on operating time limit is shown in the following tabulation:

Gas Release Assumption	Design Case	Operating Time Limit, hr*
20% He and 2% Fission	Original LCRE Design	7,200
20% He and 2% Fission	7 inches of void length added	12,100
20% He and 2% Fission	7 inches of void length added plus vacuum fill	20,000

*These operating time limits are based on cladding strength criteria not exceeding one-half of the stress rate-to-rupture for operation to the specified time.

Further review was made of information on cross-sections for neutron reactions in beryllium, leading to helium production in the fuel pins. Fig 2 shows the values

LCRE INSTALLATION

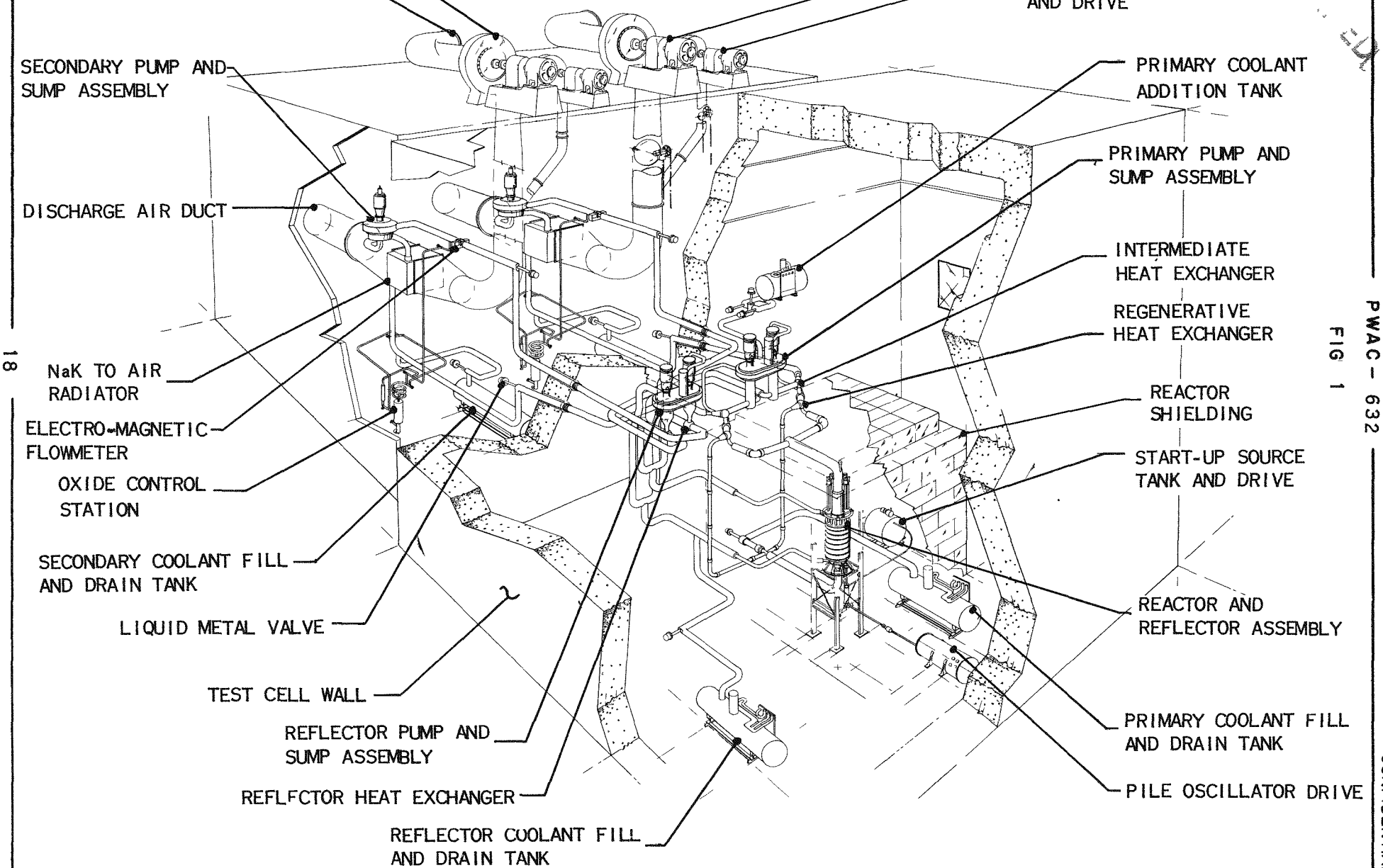

PWAC - 632
FIG 1

FIG 2

Be (n,2n) CROSS SECTION VERSUS ENERGY

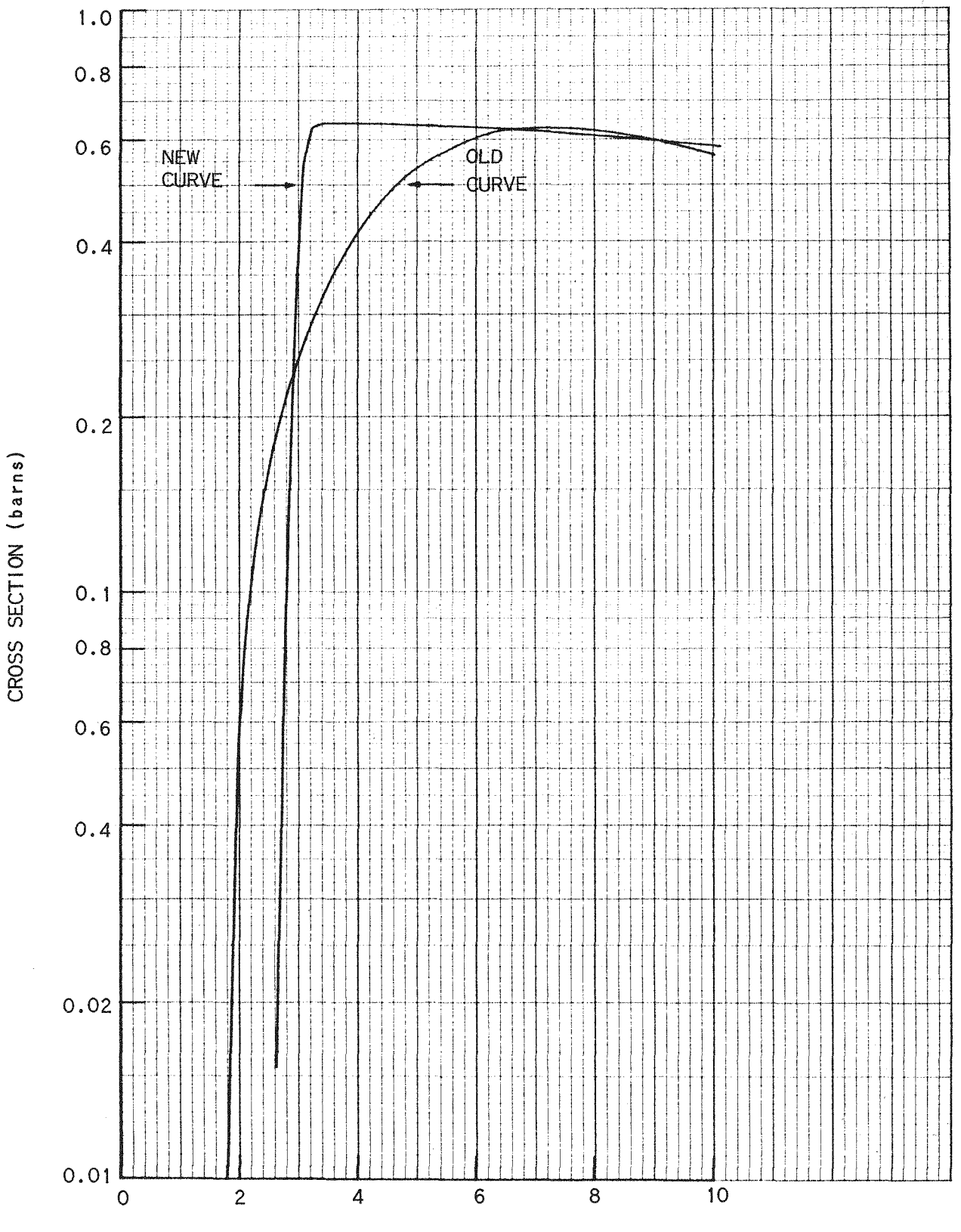

previously used and suggested new cross-section curves for the predominant n, 2n reaction. Multigroup average cross-sections were derived from the new curve, and helium generation rates in the LCRE were re-calculated. The following data shows the results for this reaction and others which produce significant amounts of helium. The results are given for the central pin, since the helium generation is maximum at that location.

Helium Production Rate at 10 Mw

Reaction	Core (Central Pin) He Atoms/cc Fuel, sec	End Reflector (Central Pin) He Atoms/cc BeO, sec
Be^9 (n, 2n)	2.48×10^{12}	0.79×10^{12}
Be^9 (n, α)	0.33×10^{12}	0.13×10^{12}
O^{16} (n, α)	0.05×10^{12}	Negligible
Ternary Fission	0.10×10^{12}	---
Total	2.96×10^{12}	0.92×10^{12}

These calculated results are about 40 percent greater than those obtained using the old cross-section curve. However, an uncertainty of plus or minus 50 percent exists until the final results of inpile measurements of helium generation in beryllium specimens are available.

A further analysis of the fuel pin hot channel factors to evaluate increasing the edge pin flow blockage path has been completed. The method of analysis has been revised to include two of the factors associated with fuel element internal power and flow conditions (orificing power distribution and fuel element flow mixing) as dependent factors associated with the nominal thermal gradients and not as hot channel factors. The analysis resulted in the hot channel factors shown in Fig 3. A tabulation of the fuel pin cladding hot spot temperatures for the drums turned outward 60 degrees (minimum anticipated start-up control drum position) and turned 160 degrees (maximum anticipated end-of-life control drum position) is presented below for pins located in the hot test core regions. Since the hot spot temperatures are considerably affected by control drum position, the temperatures can be reduced if actual drum movement required over reactor lifetime is less than the 100 degrees considered above.

Fuel Pin Cladding Hot Spot Temperatures

Location	Drum Position 60 Degrees, F	Drum Position 160 Degrees, F
Center Can		
Clad, center pin	2194	2124
Inner Full Can, R=1.88 inches		
Clad, inner passage	2247	2169
outer passage	2170	2095
Outer Full Can, R=6.74 inches		
Clad, inner passage	2125	2208
outer passage	2058	2235
Outer Partial Can, R=6.85 inches		
Clad, inner passage	2115	2227
outer passage	2050	2255

HOT CHANNEL CALCULATION TABLE FOR DETERMINING

FUEL PIN CLAD TEMPERATURES

PIN LOCATION IN CORE: INNER FULL FUEL ELEMENT
CORE RADIUS - 1.878 INCH, INNER PASSAGE
CONTROL DRUM POSITION - 60 DEGREES OUT, MINIMUM STARTUP

Hot Channel Items	Coolant Temperature Rise = 535F			Film Temperature Difference = 9F			Clad Temperature Difference = 10F			$\Sigma\sigma$	$[\Sigma\sigma]^2$
	F	σ'	$\sigma=\Delta T\sigma'$	F	σ'	$\sigma=T\sigma'$	F	σ'	$\sigma=\Delta T\sigma'$		
Power Density	1.15	0.075	40.0	1.15	0.075	0.7	1.15	0.075	0.8	41.5	1720
Flow											
Channel Design Tolerance	1.004	0.002	1.1	1.004	0.002	0.02	--	--	--	1.1	1
Distribution in Plenums	1.00	--	--	--	--	--	--	--	--	--	--
Orificing Design, Tolerance	1.01	0.005	2.7	1.004	0.002	0.02	--	--	--	2.7	7
Heat Flux											
Fuel Density and Composition	1.012	0.006	3.2	1.03	0.015	0.2	1.03	0.015	0.2	3.6	13
Matrix to Clad Eccentricity	--	--	--	--	--	--	1.30	0.150	1.5	1.5	2
Fuel Pin Internal Tolerance	1.004	0.002	1.1	1.004	0.002	0.02	1.068	0.034	0.4	1.5	2
Other											
Heat Transfer Coefficient	--	--	--	1.30	0.150	1.4	--	--	--	1.4	2
Clad Conductivity	--	--	--	--	--	--	1.05	0.025	0.3	0.3	--
Accuracy in Power Measurement	1.075	0.0375	20.0	1.075	0.0375	0.3	1.075	0.0375	0.4	20.7	429
											2176

F = Hot channel factor assumed to be 2 standard mean deviations
σ' = Fraction, single mean deviation
σ = Standard mean deviation

$T_{max\ clad} = T_{reactor\ in} + \Delta T_{cool,\ nominal} + \Delta T_{film} + \Delta T_{clad} + 2\sigma$
$= 1600 + 535 + 9 + 10 + 93 = 2247F$
$T_{max\ clad} = 2247F^*$ (97% probability of not being exceeded)

*Temperature reduced to 2200F after a maximum of 4000 hours of operation

$\Sigma[\Sigma\sigma]^2 = 2176$

$\sigma = [2176]^{.5} = 46.5F$

$2\sigma = 93F$

These temperatures occur at the upper surface of the fueled core. They are based on the use of two standard deviations from the mean and, thus, have a 97 percent probability of not being exceeded during operation. A 25F increase in cladding temperature is estimated due to total pin cladding creep at the end of life, assuming hot channel conditions occur over the complete reactor lifetime. The pin cladding hot spot temperature in the inner full can is above the 2200F design level for less than 4000 hours in the early stages of operation when the cladding stresses are less than 600 psi, but is below this level at the end of life when creep and rupture are accelerated due to the higher internal pressure. The fuel pins in the outer cans, both partial and full, reach their maximum temperature at the end of life, approximately 30F above the design value, but the gas generation and, subsequently, the internal pressure in these pins is approximately 67 percent of that in the inner pin. The higher temperature, lower pressure combination associated with the edge pin, based on available structural data, is a less severe condition than that experienced by pins located in the center region of the core. Thus, the fuel pin gas containment cladding design temperature of 2200F is properly acceptable.

Transport theory heating calculations in the boron carbide poison segment of the control drums indicate higher heating than previously estimated. Work is in progress to determine the effect of this higher heating on the temperature distribution in the control drum B_4C segment when it is positioned at 75 degrees, the reactor startup condition which has highest heating. Using the maximum helium gap between the B_4C and the poison container which can result from build-up of fabrication tolerances, the maximum temperature in the B_4C is approximately 1200F. Tolerances will be changed and fabrication procedures revised to keep this gap to a minimum and, thereby, limit the temperature to 1000F.

Two-dimensional physics calculations were made using a fine R, Θ mesh in order to check the effectiveness of reducing the uranium loading in the corner pins of each hexagonal fuel element. This would prevent overheating where the lithium flow is reduced by the corner. For most corner pins, the reduction in power density is directly proportional to the reduction in U^{235} loading. On the core periphery, however, a very strong possibility exists that low energy flux returning from the reflector will be absorbed in the first row of pins, even with reduced U^{235} loading. In this peripheral region, calculations indicate that a 30 percent reduction in U^{235} will result in a 25 percent reduction in the power density when the control drum position is turned outward. For drums turned inward, essentially no low energy flux enters the core, and the reduction in power density is proportional to the reduction in U^{235}.

The reactivity effects of thermal bowing of fuel elements have been calculated using experimental values of distributed reactivity coefficients for fuel, structure and coolant from critical experiments, and previously calculated radial displacements due to bowing at various reactor power levels. The results are shown in Figs 4 and 5 for control drums at 60 and 160 degrees. The changes in slopes of these curves are due to changes in the mode of bowing as various interferences occur between adjacent fuel elements and between the outer fuel elements and the filler pieces in the assumed physical model. Since the reactor power distribution changes with the position of the drum, the reactivity effect of bowing is correspondingly altered as shown. These extended results show that over much of the operating range the bowing coefficient is negative. Relationship of the new results to reactor stability analyses is being examined.

A study of a backup design arrangement of the reactor control drives is in progress to locate the electrical components in a reduced radiation environment outside the shield. The study includes an arrangement which extends the drives vertically through the shield and an arrangement with 90 degree angle drives to extend the drives through the side of the shield. These changes are being studied to evaluate design and development problems.

FIG 4

REACTIVITY CHANGE DUE TO FUEL ELEMENT BOWING VERSUS REACTOR POWER LEVEL

DRUM POSITION 60°

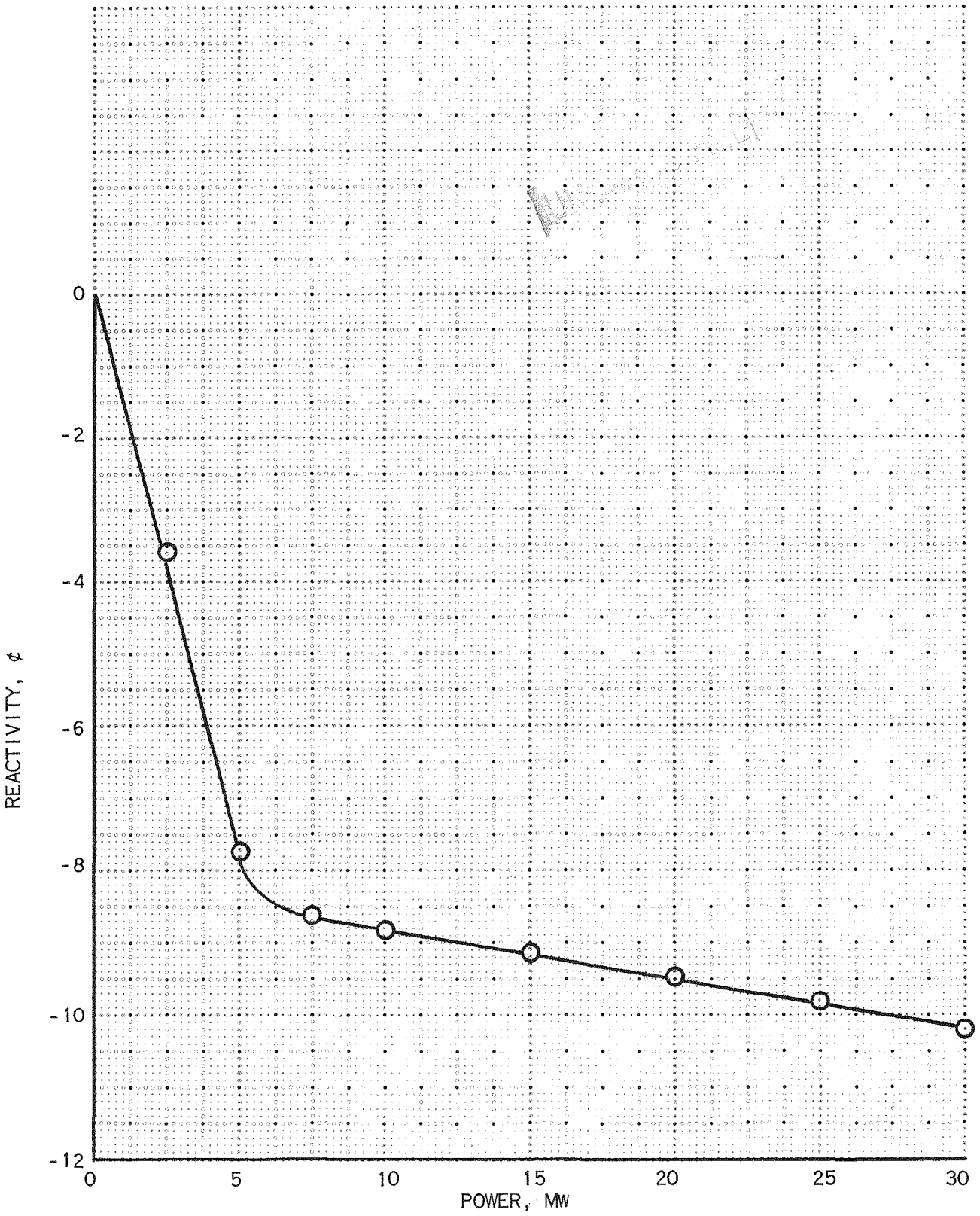

FIG 5

REACTIVITY CHANGE DUE TO FUEL ELEMENT BOWING VERSUS REACTOR POWER LEVEL

DRUM POSITION 160°

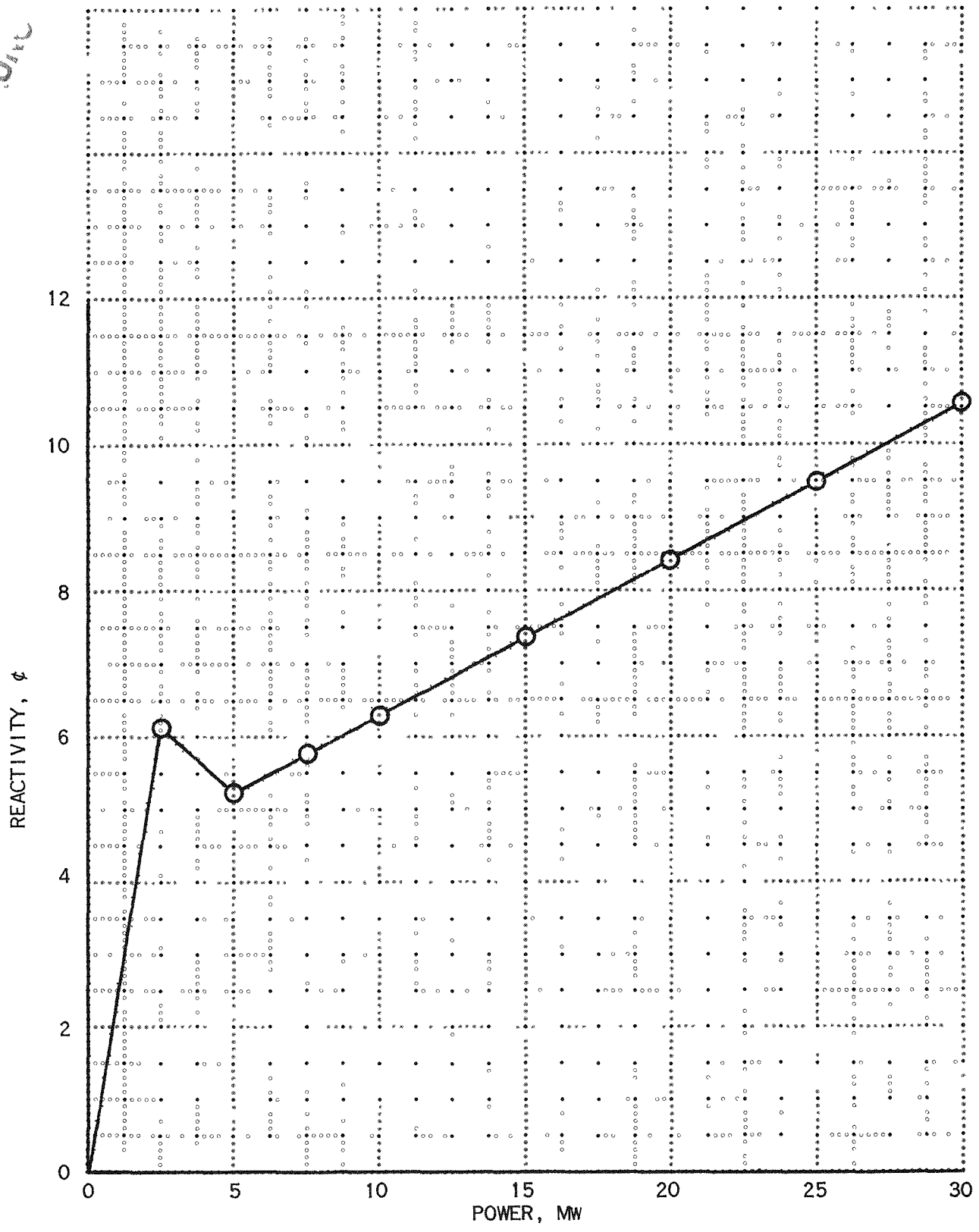

2. Shield

Gamma dose rates in the LCRE test cell were computed for a full power operation (activity in coolant pipes, heat exchangers and sump tanks) at a number of locations where organic lubricants, insulation or sealing materials will be used. The bremsstrahlung from Li^8 activity in the primary loop and from the equilibrium gamma activity in the NaK reflector coolant loop was considered. In addition, dose rates from accidental fission product activity in the primary loop were calculated postulating a continuous release to the coolant stream of 0.1 percent of all volatile fission products (i.e., boiling points below 2600F). The equilibrium activity in the entire primary loop under this condition is 6.8×10^{14} Mev/sec.

As part of estimating test cell radiation levels during operation, calculations were made to determine the neutron streaming fluxes at lithium pipe penetrations of the shield. The results for thermal, intermediate and fast fluxes were approximately $2x10^9$, $7x10^9$ and $2x10^8$ neutrons/cm^2 sec, respectively. The need for patch shielding is being evaluated.

Two-dimensional radiation heating calculations for the reactor shield were finished. Mappings were made of heating rate distributions due to boron (n,α) neutron elastic slowing down and gamma heating in the borated stainless steel, graphite, boral and concrete regions of the shield. Heating rates were also obtained in the control drum drive motors and shafts.

The shield coolant passage orifice sizes are being reviewed to evaluate the pressure drop in all the passages and to determine the orifice requirements for adequate cooling of shield components with this heating.

Radiation levels in shield gas cooling channels were estimated in order to determine the suitability of asbestos or other fibrous material for sealing shield penetrations. Midplane radiation doses are up to 10^{11} rads of gamma and 10^{20} nvt fast neutrons at the inner graphite annulus, and 10^{10} rads of gamma and 10^{18} nvt fast neutrons at the inner concrete annulus.

Work was performed on the LCRE over-all shield design to provide coolant gas seals at the location of penetrations, and to provide means for orificing coolant flow passages for flow control. The majority of this work is completed in design layout form, and is to be verified on the LCRE mock-up to ensure that methods of fabrication and assembly are satisfactory.

3. Primary and Reflector Systems

A design layout of devices for detection of lithium in the primary system jacket has been completed. The proposed detectors utilize a liquid metal level probe installed to collect leakage and produce a signal proportional to the quantity collected.

A design layout of electrical heaters for regenerative heat exchanger piping and for revised regenerator heaters was completed. The revised heaters on the regenerative heat exchanger extend heater coverage to include the end spheres of the heat exchanger. This layout completes definition of the primary heating system.

The control mode of the LCRE was rechecked on the analog computer, using latest estimates of temperature coefficient of reactivity. The responses were satisfactory. Analog computer analysis of the control stability effect of moving the reactor outlet thermocouples further downstream was conducted, showing that the control response remained stable.

The possibility of relocation of these thermocouples in order to reduce the neutron flux environment of the thermocouples is being held, pending the results of tests to determine the possible magnitude of a thermocouple calibration shift due to transmutations.

A redesign of the primary sump inlet weld has been completed. The weld redesign reduces the stresses and warpage at this joint when the weld is made. A review of the stresses in the primary pumping unit support structure under one-g side earthquake loads revealed excessive stresses at the base of the column supporting the sump. A redesign is in progress to provide the required strength.

A change was made in the insulation material of the liquid metal pump insulation cans from a material with structural strength to a material without strength. This change necessitated an increase in the can thickness to prevent buckling.

Reflector NaK flow rate was reduced from 210 gpm to 175 gpm to reduce NaK pressure inside the reflector case from 58 psia to 42 psia (Fig 6). This was done to reduce the buckling load on the inner reflector case. Studies of reflector heat exchanger stress, reflector case stress, revised B_4C heating values, reflector coolant flow distribution and associated coolant stream temperature rise were investigated in support of the flow rate revision.

A minimum reflector inner coolant channel thickness of 0.10 inch was established because of coolant temperature rise in that channel. The tolerance build-up may require that some inner beryllium pieces be fitted at assembly to maintain acceptable flow passages.

4. Secondary System

Heat transfer analysis of the secondary piping test cell wall pass-through showed that concrete temperatures would reach 450F if no cooling were supplied. Since this exceeds the allowable temperature of 150F, a means of providing cooling is being designed (Fig 7).

A design layout of shielding for the secondary piping test cell wall pass-through was completed and approved (Fig 8). Evaluation was made of the effectiveness of this shielding. The predicted dose rate is 20 mrad per hour at the outer surface of the four-foot thick shield, at a point directly opposite the ducts which view most of the NaK sump.

The detail design of the hot trap installation in the secondary coolant system is in progress. The design is based on pipe locations selected from a flexibility analysis of the piping system. The selected locations do not significantly change the pipe system deflections or end reactions.

A study is being made to determine the effect of isolation valve closing time on hydrodynamic impulse in the system. The valve closing time will be controlled by orificing to prevent excessive pressure rises.

5. Auxiliary Systems

A design review of test facility systems drawings was completed. The modifications required to make these systems conform to the requirements of the experiment were compiled and given to the architect-engineer for consideration.

The construction detail drawings and wiring diagrams of the control consoles are about 80 percent completed. Wiring diagrams of the 34 "P" Area (PWAC-631, Fig 2) instrument racks are approximately 80 percent complete. The flux monitoring system electrical schematics were completed and released.

LCRE REACTOR HEAT REMOVAL SYSTEM

SCHEMATIC DIAGRAM OPERATING CONDITIONS

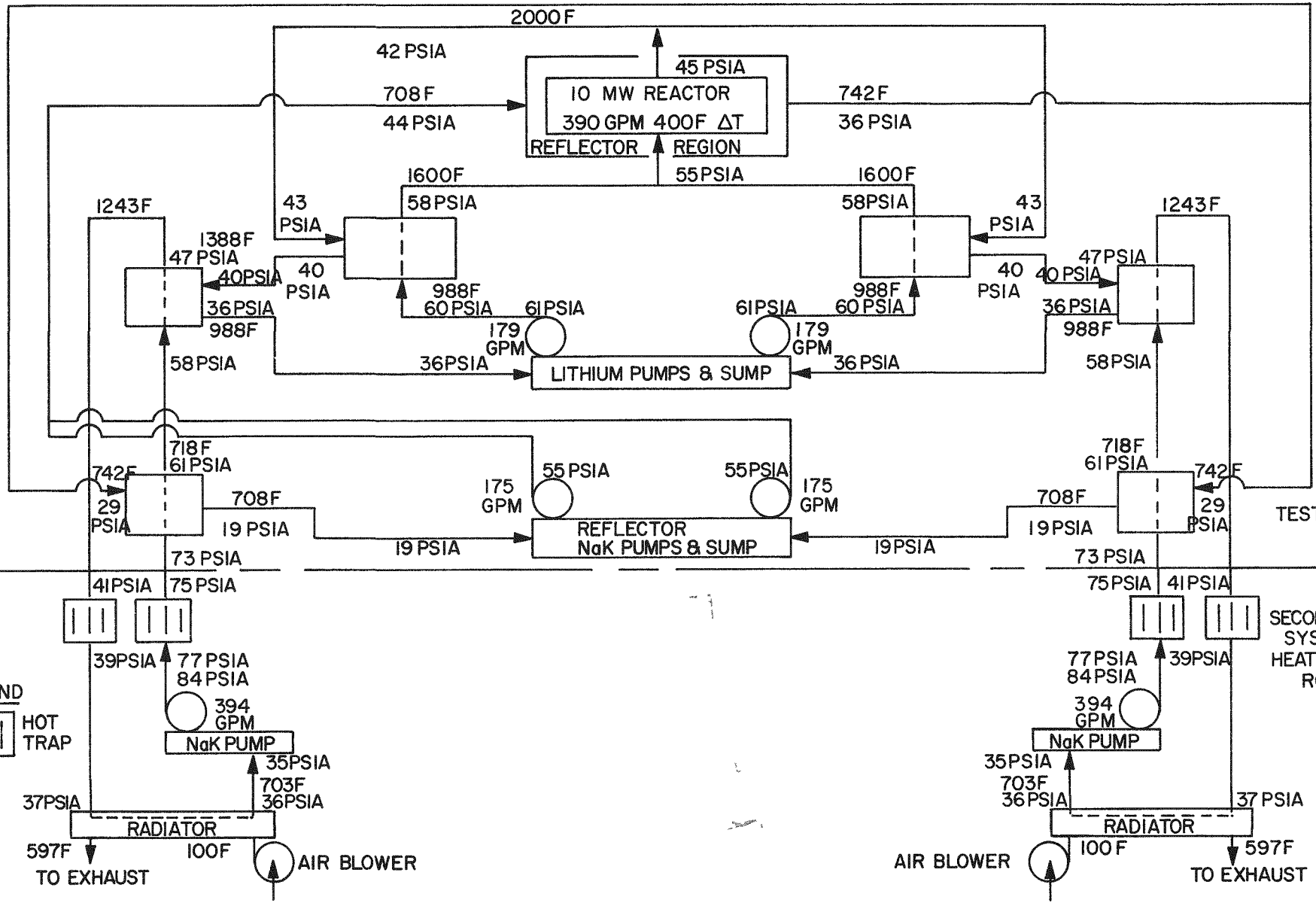

FIG 6

PWAC - 632

TEST CELL PENETRATION DESIGN

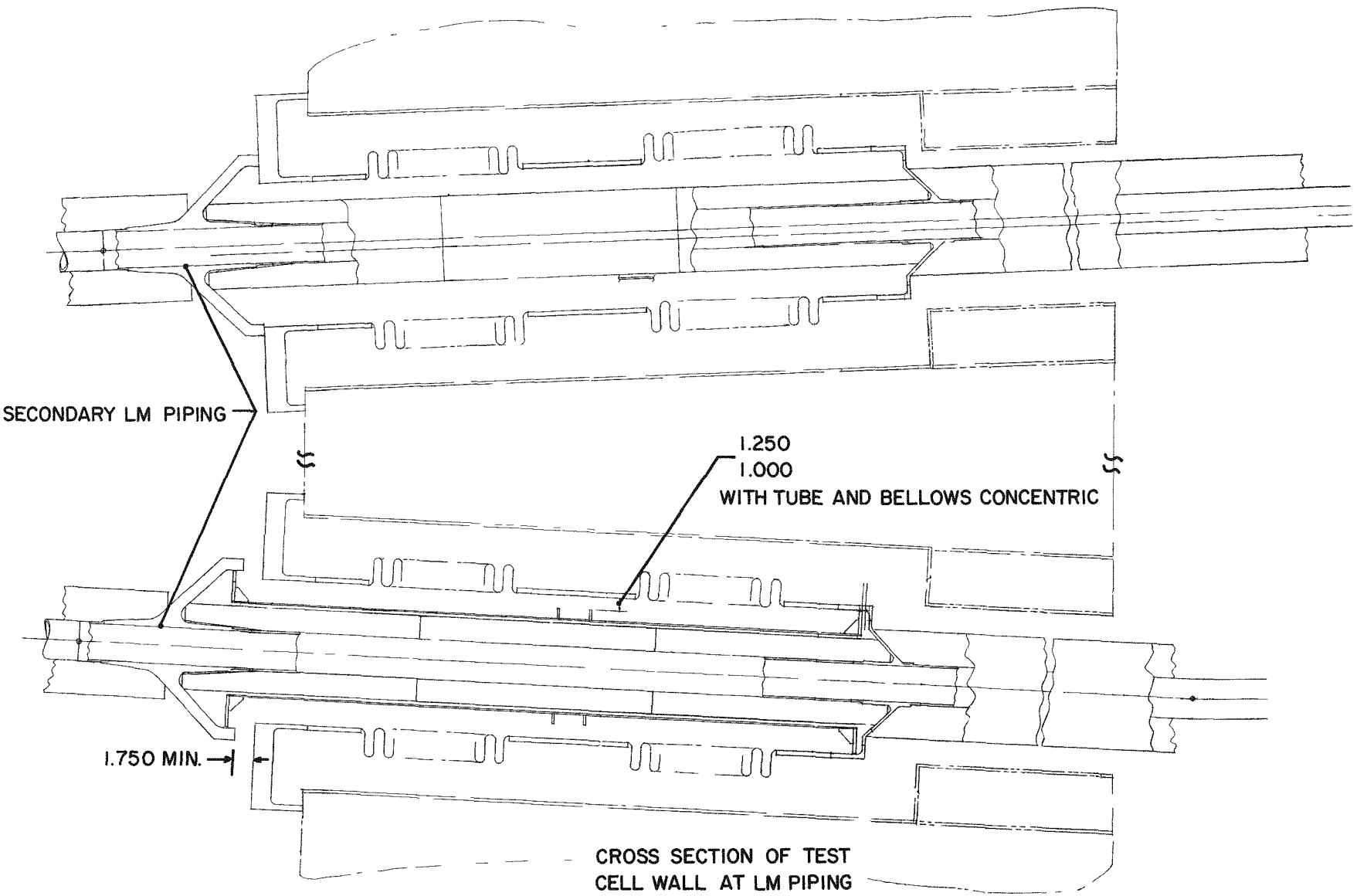

TEST CELL PENETRATION SHIELDING

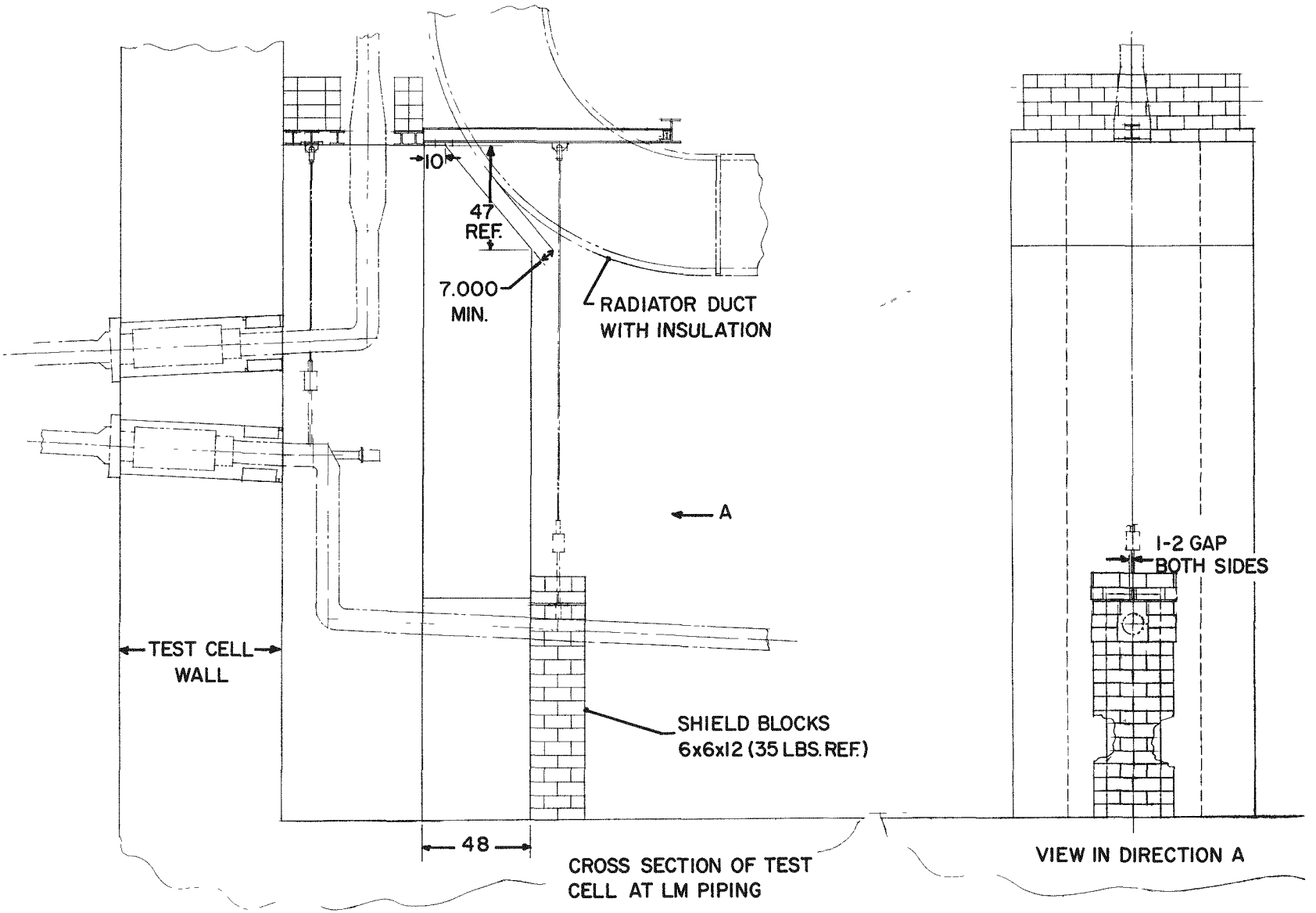

The over-all status of system design at the end of this quarter is shown in Fig 9. Approximately 75 percent of the design work to be done at CANEL has been completed.

A Subcontract for design of the cryogenic traps (non-nuclear process) was placed and this work will start on July 1. The remaining design work concerned with the nuclear cryogenic traps and the installation drawings for all systems will be started by the Auxiliary System Contractor (ASC) when this contract is awarded in the third or fourth quarter of this year. During the past quarter, the functional design of all systems (Instrumentation Flow Diagrams exceeded 95 percent completion (Fig 10).

The need for a pump green run test station in Idaho was recognized. This test station will provide electric power, cover gas, lubrication, and controls to check the liquid metal pumps for possible damage incurred in transit from CANEL and prior to final installation in the test cell and/or heat sink rooms.

Development tests show that the six vapor traps in the test cell will require approximately 200 scfh of cooling gas flow with a 3.8 to 5.1 psi pressure drop through the traps. The following methods of providing this cooling gas were examined:

a. A recirculating nitrogen system, open to the test cell, employing compressors to achieve the necessary head rise.

b. A nitrogen system, open to the test cell and vented to the stack, employing a liquid nitrogen source.

c. A recirculating nitrogen system, closed to the test cell, and employing compressors.

d. An air system, closed to the test cell, using instrument air from the Facility Instrument Air System.

The latter (d) method was found to be superior, based on relative cost and reliability considerations. Hazards problems associated with the possible introduction of air into the test cell will be satisfied by monitoring the system continuously for leakage. This air system will be incorporated into the systems design to serve all vapor traps (System 11, 14-17, 22-25, Fig 10).

After reviewing the cost of the Primary, Secondary, and Reflector Pump Lubrication Oil Systems, the total number of lubrication oil units which supply cooling and lubricating oil to the liquid metal pumps was reduced from 15 to 11 (including spares). The reliability of these systems will be maintained by valving between units to assure a continuous lubrication oil supply in the event of a failure of a lubrication unit. These changes will be incorporated into the lubrication oil systems (Nos. 34 through 36) during the next quarter.

A plan for shutting off all gas lines to and from the test cell is being developed to prevent general spread of radioactive particles in the event of a nuclear incident which might result in the release of fission products within the cell. The proposed system involves the use of approximately 20 gas valves located in the test cell helium, argon, air, and nitrogen supply and exhaust lines. The valves are normally open and will feature a special fail-safe actuator under administrative control from the control room. If actuation of these valves is required and an electric signal is not available, the valves are capable of being hand-operated from a safe distance.

Schematic drawings for all systems were completed in sufficient detail to permit bidding by those contractors interested in performing the installation of Auxiliary and Control Systems in Idaho.

FIG 9A

STATUS OF LCRE LAYOUT AND DETAIL DESIGN

A. Status Summary of Design Work in Progress	Percent Completion
1. Reactor and Shield	
a. Alternate Control Drive Arrangement	20
b. Control Drive Wiring	75
c. Control Drive Cooling	30
d. Control Drive Thrust Bearing Dedesign	95
e. Pile Oscillator Support	90
f. Pile Oscillator Cooling	90
g. Pile Oscillator Electrical System	75
h. Center Source Cans	30
i. Control Drum Positive Stop	30
j. Shield Seals	40
k. Shield Orificing	20
l. Inner Shield Support Change	75
m. Lower Shield Change	40
n. Cooling Duct System	50
o. Power Plant Electrical	75
p. Reactor Assembly Revisions	20
2. Primary and Reflector Systems	
a. Pumping Unit Gamma Monitoring System	30
b. Pump Thermocouple Change	30
c. Vapor Trap Thermocouple Change	30
d. I & J Probe Changes	75
e. Primary Pipe Support Changes	30
f. Heater Changes	50
g. Primary Leak Probe Installation	30
h. Primary Jacket Changes	30
i. Valve Changes	90
j. Reflector System Electrical Installation	75
k. Thermocouple Attachment Change	40

STATUS OF LCRE LAYOUT AND DETAIL DESIGN

B. Work to be Started

1. Reactor and Shield
   a. Control Drive Thermocouple Installation
   b. Control Drive Gas Line Installation
   c. Reactor ΔT Thermocouple Relocation Study

2. Primary and Reflector Systems
   a. Leak Detector Study
   b. Pump Gas Line Rerouting
   c. Pump Vibration Pick-ups
   d. Pump Drive Coupling Change
   e. Primary Outlet Pipe Cooling Jacket Variable Seal
   f. Reflector Sump Shielding
   g. Hoke Valve Installation (gas evaluation, liquid-metal fill and drain lines)
   h. Insulation Installation

3. Secondary System
   a. Pipe Support Hangers

STATUS OF LCRE INSTRUMENTATION FLOW DIAGRAMS

		Instrument Flow Diagram (Reference)	Percent Design Work Completed at CANEL
Reactor Instrumentation and Control Systems			
1.	Reactor Control System	CLR-10410-9	100
2.	Reactor Safety System	CLR-10411-9	95
3.	Reactor Flux Monitoring System	CLR-10412-9	99
4.	Chamber Drive System	CLR-10443-9	100
5.	Chamber Check Source Drive	CLR-10441-9	100
6.	Startup Source Drive	CLR-10444-9	100
7.	Gamma Monitoring System	CLR-10430-9	100
8.	Battery Power Supply	CLR-10450-9	70
9.	Pile Oscillator	CLR-10440-9	90
10.	Control Room Prime Viewing Console and Panel Wiring Diagrams	ALL	80
Liquid Metal Systems Instrumentation			
11.	Primary Circuit	CLR-10416-9	97
12.	Secondary Circuit	CLR-10417-9	97
13.	Reflector Circuit	CLR-10418-9	97
14.	Primary Fill and Drain	CLR-10413-9	92
15.	Secondary Fill and Drain	CLR-10414-9	92
16.	Reflector Fill and Drain	CLR-10415-9	92
17.	Primary Coolant Addition	CLR-10419-9	93
18.	Secondary Oxide Control System	CLR-10437-9	95
Electric Heating Systems			
19.	Primary Electric Heating	CLR-10420-9	75
20.	Secondary Electric Heating	CLR-10446-9	75
21.	Gas Line Heating	CLR-10489-9	50

STATUS OF LCRE INSTRUMENTATION FLOW DIAGRAMS

		Instrument Flow Diagram (Reference)	Percent Design Work Completed at CANEL
Gas Systems			
22.	Primary Seal and Sweep Gas	CLR-10431-9	93
23.	Secondary Seal and Sweep Gas	CLR-10432-9	93
24.	Reflector Seal and Sweep Gas	CLR-10433-9	93
25.	Jacket Gas	CLR-10421-9	95
26.	Gear Box Gas	CLR-10490-9	95
27.	Helium Supply and Purification	CLR-10426-9	95
28.	Shield Cooling - CANEL Instrumentation	CLR-10427-9	75
29.	Cryogenic Trap (Nuclear Instrumentation)	CLR-10428-9	100
30.	Cryogenic Trap (Non-Nuclear Process)	Design Spec.	100
Mechanical and Electrical Systems and Equipment			
31.	Primary Pump Drives	CLR-10422-9	70
32.	Secondary Pump Drives	CLR-10423-9	70
33.	Reflector Pump Drives	CLR-10424-9	70
34.	Primary Lube Oil System	CLR-10434-9	30
35.	Secondary Lube Oil System	CLR-10435-9	30
36.	Reflector Lube Oil System	CLR-10436-9	30
37.	Heat Sink System	CLR-10425-9	80
38.	Liquid Metal Handling	CLR-10439-9	80
39.	Fuel Loading Experiment	CLR-10488-9	85
40.	Pump Green Run Test Station		5
41.	Pretest Gas Analysis System	CLR-10429-9	95
42.	Core Installation Monitor	CLR-10449-9	100

Design studies for the 28-hp primary and reflector pump motors were received from three vendors and are being evaluated. The major design problems which these vendors were asked to resolve were:

a. Type of magnet wire insulation (design total gamma dose, 10^9 rads).

b. Bearing and bearing lubrication design (15,000 hour life, using NRRG 159 grease).

c. Allowable vibration level, 0.0001 inch amplitude, peak-to-peak based on liquid metal pump seal requirements.

All designs feature magnet wire insulated with double-layer glass fiber impregnated with silicon varnish and regreasable bearings (regreasing must be done remotely during operation of the LCRE). Development tests are required to finalize the grease supply design details in each motor. After technical review during July, a design will be selected for the primary and reflector pump motors.

Designs were completed of leak-tight test cell pass-throughs for gas, lube oil, and electric power service into the test cell. It is planned to procure a small quantity for evaluation to check primarily the effect of field welding heat on electrical and gas seals.

6. Hazards

Critical experiments were performed by Oak Ridge National Laboratory to obtain information needed to establish nuclear safety criteria for the storage and handling of LCRE fuel pins and fuel elements. Measurements were made of the numbers of fuel pins required for criticality when moderated and fully reflected by water for a range of spacings which included the most reactive spacing. The reactivity effects of perturbations of temperature, material composition and fuel pin configuration were also studied.

Basic criticality measurements were made at 20C with water-flooded fuel pins containing 55 v/o UO_2 in the fueled portion but identical in all other respects to LCRE fuel pins, except that the gas expansion volumes were not included. Uniform hexagonal arrays with side-to-side spacings from 0 to 1.25 inches were investigated, and the results are summarized below.

Critical Numbers of 55 v/o UO_2 LCRE Fuel Pins
In Water-Flooded Hexagonal Arrays

Side-to-Side Spacing, in.	Critical Number of Fuel Pins
0	312
0.25	164
0.50	89
0.75	78
1.0	93
1.25	182

The critical numbers of fuel pins for the zero-inch and 1.25-inch spacings were obtained by extrapolation of subcritical data obtained with at least 150 pins, while criticality for the other spacings was actually achieved with the tabulated numbers of fuel pins. By inter-

polation of this data, it was determined that the minimum number of water-flooded 55 v/o UO_2 fuel pins required for criticality is 77.5 at a temperature of 20C. It was further concluded that 91 fuel pins clamped in a single, close-packed, hexagonal array such as an LCRE fuel element, may be safely stored in a container which is not necessarily watertight.

The results of other experiments done at the 0.75-inch side-to-side fuel pins spacing to measure reactivity effects may be briefly summarized as follows:

a. Raising the temperature of the water and fuel pin array from 20C to 50C reduced the minimum number of pins for criticality to 76.

b. The replacement of 6.9-inch long BeO end-reflector segments in the fuel pins by water was found to have no measurable effect.

c. Axial displacement of a fraction of the fuel pins, causing introduction of BeO end-reflectors into the fueled region of the array, resulted in a loss of reactivity.

d. The replacement of several 55 v/o fuel pins by 50 v/o UO_2 fuel pins, (or, in effect, a substitution of BeO for UO_2) resulted in a reactivity loss of approximately 0.4 cents per volume percent per fuel pin.

e. The replacement of water moderator by Zyglo dye-penetrant fluid resulted in a loss of reactivity.

A number of calculations were performed to assist in evaluating the criticality hazards of posttest handling. Reactivity effects of incidental reflection by NaK and stainless steel were evaluated. With no reflector, the reactor with beginning-of-life fuel inventory and lithium filled was calculated to be 18 dollars subcritical.

The proposed outline of PWAC-395, Core Assembly and Installation Hazards Summary Report for the LCRE, was completed. Copies have been distributed for review and comment.

The following schedules have been established for submission of the two LCRE Hazard Summary Reports to the AEC:

Report No.	Title	Submission Date
PWAC-395	Core Assembly and Installation Hazards Summary Report for the LCRE	January, 1964
PWAC-396	Final Hazards Summary Report for the LCRE	November, 1964

B. LCRE REACTOR SPECIFICATIONS

General Reactor Data	
Reactor power, Mw	10
Design lifetime, hr	10,000
Critical mass, kg-U^{235}	86.1
Core coolant	Lithium (99.99% Li^7)
Reactor coolant inlet temperature, F	1600
Reactor coolant outlet temperature, F	2000
Type of fuel	UO_2-BeO ceramic
Nominal volume percent UO_2 in matrix	47
Reactor structural material, fuel element cladding and core filler pieces	Cb-1 Zr alloy
Side reflector material	Beryllium
End reflector material	Beryllium oxide
Reflector structural material	Type 316 stainless steel
Reflector coolant	NaK (78 w% K)
Method of reactor control	Rotating poison drums
Poison material	B_4C (natural B)
Weight of reactor package, lb	3300
Reactor Configuration	
Equivalent active core diameter, in.	13.5
Active fueled core length, in.	13.5
End reflector thickness, in.	6.9
Side reflector thickness (nominal), in.	6.9
Core filler OD (nominal), in.	14.476
Pressure vessel ID (nominal), in.	14.716
Pressure vessel OD (nominal), in.	15.136
Reactor jacket ID (nominal), in.	15.381
Reactor jacket OD (nominal), in.	15.557
Reflector outer shell diameter, in.	30.12
Core filler material	Cb-1 Zr alloy
Number of core filler pieces	6
Core Operating Conditions	
Average power density, kw/cc	0.469
Average heat flux, Btu/hr-ft^2	2.30×10^5
Average ΔT film, F	8
Average ΔT clad, F	10
Center pin maximum fuel matrix temperature, drums 60^o, F	2745
Center pin total temperature rise, bulk coolant to fuel centerline, at maximum temperature plane, F	610
Maximum fuel matrix temperature-corner pin, edge can, F	2250 (0.75 power)
Coolant inlet pressure, psia	55
Coolant outlet pressure, psia	45
Coolant flow direction	Upward
Power from core, Mw	10
Coolant flow rate in fueled core, lb/sec	22.8
Mixed mean core outlet temperature, F	2006
Core bypass coolant flow rate, lb/sec	1.14
Mixed mean temperature of bypass coolant outlet, F	1920
Average coolant velocity in core, fps	8.25
Average Reynolds number in core	3710
Average film coefficient in core, Btu/hr ft^2 F	32,000

Maximum to average power ratio for thermal design

	Center Pin	Edge Peaking
Axial	1.11	1.78 (R=0 to 6.65 in.) 0.95 (R=6.65 to 6.75 in.)
Radial	1.42 at 60^o	2.8 at 160^o

Fuel Element Specifications	
Type of fuel	UO_2-BeO ceramic
Type of fuel element	Cylindrical pins in hexagonal array
Fuel pin OD, in.	0.305
Fuel pin cladding thickness, in.	0.015
Helium thermal bond thickness, in.	0.001
Fuel matrix diameter, in.	0.273
Active fuel matrix length, in.	13.5
Length of top and bottom end reflectors, in.	6.9
Fuel pin fission gas void length, in.	8.0
Number of fuel pins in hexagonal can, full	91
Number of fuel pins in hexagonal can, partial	78
Equivalent number of hexagonal cans in core	18.14
Distance across flats, nominal fuel pin bundle, full can, in.	2.946
Fuel can wall thickness, in.	0.030
Distance across flats of hexagonal can (maximum), in.	3.021
Diameter of can perimeter flow blockage rods, in.	0.070
Fuel pin cladding material	Cb-1 Zr alloy
Fuel can material	Cb-1 Zr alloy

Material Volume Fractions	Core	Side Reflector	End Reflector
UO_2	0.3167		
BeO	0.3571		0.6738
Li	0.1011		0.1011
Cb	0.2153		0.2153
He	0.0098	0.0012	0.0098
B_4C		0.1293	
Be		0.7435	
NaK (78 w% K)		0.0753	
Type 316 stainless steel		0.0507	

Side Reflector Configuration	
Control drum	
Number of control drums	10
Control drum arrangement	Close packed
Control drum diameter, in.	6.478
Diameter of control drum circle, in.	22.632
Poison material	B_4C (natural B)
Poison arrangement	Canned assembly of solid segments
Poison segment angle, degrees	120
Poison length above core midplane, in.	12.2
Poison length below core midplane, in.	13.7
Poison segment gas containment volume, $in.^3$	83.7
Beryllium length, in.	27.5
Bearing materials	
Journal (inner) and bearing (outer)	90 w/o WC-8 Mo-2 Cb
Reflector material	Beryllium
Stationary Reflector and Vessel	
Number of stationary reflector pieces	
Inner	10
Outer	10
Length of stationary reflector pieces, in.	27.5
Inner reflector vessel ID, in.	15.381
Inner reflector vessel OD, in.	15.557
Inner stationary reflector piece ID, in.	15.755
Outer stationary reflector piece OD, in.	29.750
Reflector jacket ID, in.	29.870
Reflector jacket OD, in.	30.120

Control drum well ID, in.	6.746
Control drum well OD, in.	6.836
Clearance between control drum well and fixed reflector pieces, minimum, in.	0.002
Reflector material	Beryllium
Reflector structural material	Type 316 stainless steel
Reflector coolant	NaK (78 w% K)
Side Reflector Operating Conditions	
Coolant flow direction	Upward
Coolant inlet temperature, F	710
Coolant temperature rise, mixed mean, F	25
Coolant flow rate, total lb/sec	45.2
Coolant inlet pressure, psia	58
Coolant pressure drop, inlet feeder to exit collector	3.0
Stationary Region	
Heating per reflector piece	
Inner, kw	2.9
Outer, kw	1.12
Heat leakage from reactor, kw	80
Coolant temperature, rise	
Inner passage, F	50
Outer passage, F	4
Maximum temperature rise in beryllium, F	6
Maximum temperature in beryllium, F	760
Coolant flow rate external to drum well, lb/sec	23.2
Average coolant velocity, ft/sec	2.8
Pressure drop through stationary piece length, psi	0.3
Control Drum	
Heating per drum	
Beryllium region, kw	8.5
Poison region, kw	4.2
Coolant temperature rise drum annulus, F	30
Maximum temperature rise in beryllium, F	73
Maximum beryllium temperature, F	800
Maximum temperature rise in B_4C, F	52
Maximum B_4C temperature, F	1000
Coolant flow rate in drum annulus, lb/sec	2.2
Average coolant velocity, ft/sec	2.44
Pressure drop through drum length, psi	0.3
Helium pressure in poison cans	
Initial fill, psia	0.1
After 10,000 Mw Hr (10% release), psia	74
Nuclear Specifications	
Fission burnup, percent mass (100,000 MwH)	5.05
Total burnup, percent	6.57
B^{10} burnup, percent	1.1
Total control drum worth, Δk	0.09
Operational reactivity losses, Δk	
Fuel burnup	0.0300
Fuel growth (estimated)	0.0053
Xe^{135} equilibrium	0.0005
Xe^{135} buildup, after shutdown	0.0000
Sm^{149}	0.0044
Permanent poison buildup	0.0089
Li^6 buildup	0.0031
Total	0.0522
Temperature - reactivity losses, Δk	
70F to 1000F, wet reflector	0.0067
1000F to 1800F, (1) wet core and reflector	0.0033

(1) Reflector attains maximum temperature of 750F approximately

NaK worth in reflector, 70F, Δk	0.0030
Lithium worth in core, 1000F, Δk	0.0075
Unusable portion of shim control worth, Δk	0.0100
Maximum excess reactivity required, 1000F, Δk	0.06
Minimum shutdown margin, 1000F, Δk	0.03

Helium generation, atoms (100,000 MwH)

B_4C in all control drums	5×10^{24}
BeO in all fuel pins	8×10^{24}
Be in side reflector	7×10^{24}

Spectrum of neutrons causing fission

Percent thermal	
Drums in	0.1
Drums out	2.0
Median energy, kev	
Drums in	170
Drums out	100

Flux leakage into shield, percent of total neutrons

Side leakage	10
End leakage	2
Total	12

Maximum total flux, core center, n/cm^2-sec: 10^{15}

Power distribution ratios

Axial (averaged radially)	Calculated	Experimental
Center to average	1.18	1.08
Minimum to average	0.71	0.90
Maximum to average	1.18	1.68

Radial (average axially)	Drums In	Drums Out		
	Diffusion Theory	Diffusion Theory	Transport Theory	Experimental
Center to average	1.45	1.20	1.23	1.12
Minimum to average	0.55	0.85	0.84	0.875
Edge to average	0.55	1.65	1.95	3.0

Prompt neutron generation time, seconds

Drums in	1.5×10^{-7}
Drums out	1.8×10^{-6}

Effective delayed neutron fraction, $\epsilon\beta$: 0.007

Temperature coefficients, Δk per degree F x 10^6

Coolant expansion	
Core lithium	-0.8
Reflector NaK	-0.8
Axial expansion	
Fuel	-2.6
Reflector	-1.0
Core radial expansion	
Top	-0.3
Center	-0.9
Bottom	-0.3
Reflector radial expansion	
Top	-1.1
Bottom	-1.1
Bulk	-3.3
Doppler (U^{235}), 2000F	+0.85

Bowing coefficient; 10 Mw power, drums 160 degrees, cents/Mw: +0.2

C. LCRE RESEARCH AND DEVELOPMENT

1. Fuel

Following disassembly, an examination by phenolphthalein test, and in some cases metallography of 866 of the 906 lithium soak test pin specimens with various combinations of weld variables was completed. The following data was obtained after a cumulative, 15-cycle, 100-hour lithium soaking at 1600F, 100 hours at 2000F, and 100 hours at 900F to 2000F on approximately 300 welds of each type:

End Cap Material	No. Weld Leaks by X-Ray		Additional Possible Weld Leaks By Destructive Examination	
	Cb-1 Zr	Cb-5 Zr	Cb-1 Zr	Cb-5 Zr
As-welded	10	2	4	1
As-welded, 2200F anneal	0	0	1	3
As-welded, 2350F anneal	0	0	0	0

The four following specimens which leaked lithium are being given complete metallographic and chemical analyses to investigate the cause and extent of leakage.

Specimen No.	Specimen History	Radiographic Examination	Destructive Examination
1 & 2	Cb-1 Zr end cap, no post-weld anneal	Positive leak	Leak
3	Cb-5 Zr end cap, no post-weld anneal	Positive leak	Leak
4	Cb-5 Zr end cap, 2200F post-weld anneal	No leak	Leak

Metallography showed positive reduction of UO_2 to metallic uranium in the first three specimens, but the UO_2 in the fourth appeared normal in all respects. Quantitative chemical analysis by water leaching of the pellets, followed by alkalinity and flame photometer analysis, identified lithium in all four specimens but the quantity of lithium in Nos. 1, 2 and 3 was approximately 100 times more than that of No. 4. Forty Cb-1 Zr alloy pins from this test (including as-welded, 2200F and 2350F annealed) are being re-soaked in lithium at 2000F.

In the evaluation of anti-galling treatments to aid fuel element assembly, three hex cans have been nitrided and three have been carburized, using the aquadag brush application technique. Considerable difficulty was encountered in removing the excess carbon from the carburized inner surface and some removal of carbide case resulted in a subsequent pickling operation.

Depleted fuel pins of 0.3055 inch diameter were loaded in a carburized can and extreme galling was encountered which caused can buckling. Metallography of this can showed an irregular case, and a gas carburization technique was developed to effect improvement of the case. A fuel element was loaded with depleted fuel pins for water flow tests to determine fuel element pressure drop. Attempts to assemble this fuel element using a gas-carburized hex can were unsuccessful; the element was assembled using a gas-

nitrided can. Additional effort on can carburization is being directed towards improvement of carbide case properties by varying time-temperature cycles during gas carburization.

Tube burst testing of carburized and solution heat-treated Cb-1 Zr alloy fuel tubing is continuing. Studies to date indicate a 2900F heat treatment will not coarsen grain structure and will yield 1500 psi, 10,000-hour, 2200F rupture strength. Accelerated 2400F tests have been run for up to 700 hours. The use of nitrogen as a strengthening agent has been stopped. This work is reported in greater detail in Section II-C-10.

An examination was conducted on 50 v/o UO_2-BeO fuel specimens removed from inpile capsule PW26-42, after 1494 hours at 2100F. Microexamination of the pellets showed that there was some minor migration of UO_2 into microcracks within the pellets. No other anomalies were present. The results of U^{235} fission burnup studies based upon Cs^{137} follow.

Specimen No.	Percent Burnup	Fissions/cc	Power Density, kw/cc
459C (Middle)	1.34	1.48×10^{20}	0.79
460C (Bottom)	1.44	1.59×10^{20}	0.85

An examination was begun on the three 50 v/o UO_2-BeO fuel specimens tested in inpile capsule PW26-15 for 6173 hours at 2000F. Diameter measurements of the specimens showed no increase.

An examination was started on the three 50 v/o UO_2-BeO fuel specimens tested in inpile capsule PW26-18 for 6573 hours at 2000F. Measurements showed no diameter increases. Specimen cover gas pressures were essentially the same as gas pressure at fill. Microexamination of the cladding showed a recrystallized structure and no evidence of incompatibility. The pellets appeared to have a dense, nearly homogeneous structure with no grain boundaries evident to a depth of 40 to 50 mils from the outside of the pellets. Beyond this 50-mil zone to the center of the pellets, the typical BeO-UO_2 network was visible. The average helium release was 25 percent. U^{235} fission burnup studies and fission gas release studies are in progress.

Measurements were started of retained and released helium in beryllium and BeO specimens, irradiated in the BMI reactor to determine the (n, 2n) fast flux cross section in beryllium. Preliminary results indicated a cross section of 463 ± 60 millibarns.

The following status of the inpile test program on 50 v/o UO_2-BeO fuel is summarized in Fig 11.

STATUS AND SUMMARY OF LCRE CAPSULE IRRADIATION PROGRAM

Capsule Number	Duration of Irradiation, hr	*** Average Operating Temp of Specimen Surface, F	Test Facility Thermal Flux, nv	*** Cesium^{137} U^{235} Burnup, %	Fission Density Fissions/cc	Power Density Kw/cc	% Xe Release	% He Release	Cladding OD Change, mils	Cladding Reaction	Irradiation Dates
A. Pin-type specimens (Cb-1 Zr alloy cladding), 0.312 OD x 0.035 wall cladding, 50 v/o BeO, 0.238 inch D x 0.5 inch long pellet height, 1 kw/cc in Li at 2000F design											
PW26-10	10,000*	1990**	1.7×10^{13}	9.7*	--	--	--	--	--	--	5/62-1/64*
PW26-11	1,120	1990	1.6×10^{13}	0.8	8.6×10^{19}	0.68	0.44	20.0 (2)	None	None	1/62-4/62
PW26-12	3,599	1989**	1.6×10^{13}	2.4	2.6×10^{20}	0.66	0.08	15.0 (2)	None	None	4/62-10/62
PW26-13	3,513	1998**	1.5×10^{13}	2.5	2.7×10^{20}	0.70	0.85 (2)	18.0 (2)	None	None	2/62-8/62
PW26-14	324	911 (1)	1.3×10^{13}	0.2	2.0×10^{19}	0.56	0.04	6.3 (2)	None	None	2/62-3/62
PW26-15	6,173	1987**	1.5×10^{13}	6.0*	--	--	--	--	--	--	5/62-5/63
PW26-16	10,000*	2004**	1.6×10^{13}	9.7*	--	--	--	--	--	--	4/62-1/64*
PW26-17	735	1985**	1.7×10^{13}	0.7	7.3×10^{19}	0.9	0.71	17.0 (2)	None	None	3/62-4/62
PW26-18	6,573	1994**	1.6×10^{13}	6.0*	--	--	--	--	--	--	4/62-5/63
B. Pin-type specimens (Cb-1 Zr alloy cladding), 0.305 OD x 0.015 wall cladding, 50 v/o UO_2-50 v/o BeO, 0.272 inch D x 0.72 inch long pellet height, 1 Kw/cc in Li at 2200F design											
PW26-40	1,000*	2201	2.7×10^{13}	1.0*	--	--	--	--	--	--	4/63-8/63
PW26-41	1,803	2161	2.5×10^{13}	1.3	1.4×10^{20}	0.7	2.1	16.0 (2)	2.4	Grain Growth	10/62-12/62
PW26-42	1,494	2101	2.8×10^{13}	1.3	--	--	--	17.0	--	--	12/62-3/63
PW26-45	10,000*	2193	2.7×10^{13}	9.4*	--	--	--	--	--	--	1/63-6/64*
C. Pin-type specimens (Cb-1 Zr alloy cladding), 0.305 OD x 0.015 wall cladding, 60 v/o UO_2-40 v/o BeO, 0.262 inch D x 0.75 inch long pellet height, 1 Kw/cc in Li of 2000F design											
PW26-50	1,228	1904	1.5×10^{13}	0.7	8.9×10^{19}	0.65	0.92	18.0***	None	None	6/62-8/62
PW26-52	1,228	1979**	1.4×10^{13}	0.6	7.7×10^{19}	0.56	0.82	17.0***	None	None	6/62-8/62
D. Pin-type specimens (Cb-1 Zr alloy cladding), 0.305 OD x 0.015 wall cladding, 50 v/o UO_2-50 v/o BeO, 0.272 inch D x 0.72 inch long pellet height, 1 Kw/cc in Li at 2200F design											
PW26-60	6,000*	2174	2.8×10^{13}	5.8*	--	--	--	--	--	--	2/63-2/64*
PW26-61	10,000*	2183	2.5×10^{13}	9.4*	--	--	--	--	--	--	1/63-7/64*
PW26-62	10,000*	2199	2.5×10^{13}	9.4*	--	--	--	--	--	--	1/63-7/64*
E. Pin-type specimens (Cb-1 Zr alloy cladding - E.B. welded), 0.305 OD x 0.015 wall cladding, 50 v/o UO_2-50 v/o BeO, 0.272 inch D x 0.72 inch long pellet height, 1 Kw/cc in Li at 2200F design											
PW26-80	1,000*	2200*	2.7×10^{13}	1.0*	--	--	--	--	--	--	6/63-8/63*
PW26-81	3,000*	2200*	2.8×10^{13}	3.0*	--	--	--	--	--	--	6/63-12/63*
F. Pin-type specimens - ETR Core Experiments (Cb-1 Zr alloy cladding), 0.350 OD x 0.15 wall cladding, 1 specimen containing BeO and 2 specimens per capsule 50 v/o depleted UO_2-50 v/o BeO, in Li at 2200F design											
PW28-10	1,000*	2200*	6.7×10^{13}*	--	--	--	--	--	--	--	7/63*-10/63*
PW28-11	3,000*	2200*	6.7×10^{13}*	--	--	--	--	--	--	--	9/63*-4/64*

* *Design or estimated values*
** Approximate temperature - thermocouples are questionable
*** Center test specimen
(1) Heater failed at start up because of an operator error
(2) Top test specimen

Capsule	Center Specimen Cladding Temp, F	Approximate Hours thru June 30
PW26-10	2000	7009
PW26-16	2000	7409
PW26-45	2210	2660
PW26-60	2180	2035
PW26-61	2180	2421
PW26-62	2200	2421
PW26-40	2200	500
PW26-80	2200	100
PW26-81	2200	100

2. Critical Experiments and Physics

Measurements to investigate the variation of LCRE material reactivity coefficients with critical assembly core composition were carried out on the CCA-6 assembly with a 13.5-inch diameter and a 12-inch long core. With control drums at the zero degree orientation (poison sections facing the core) 13 kg of beryllium oxide (or approximately one-half of the normal core content) were removed from the core and replaced by 30 kg of columbium to shift the neutron spectrum to higher energies. The critical mass of U^{235} increased by 11.8 kg which was about one kg less than predicted by the normal spectrum core material reactivity coefficients. Material reactivity coefficients in the core and reflector regions were changed by only small amounts against the estimate of experimental errors. The same changes in the BeO and columbium content of the core were then made to the normal core loading with the control drums at 180 degrees. In this case, the critical mass of U^{235} increased by 9.7 kg, or approximately 3 kg less than that predicted from the normal spectrum core material reactivity coefficients. Material reactivity coefficient measurements indicated no apparent changes for aluminum and aluminum oxide. The core-averaged coefficients for U^{235} changed from 81 to 86 cents per kilogram; for beryllium oxide they changed from 62 to 58 cents per kilogram and for columbium from -5.1 to -2.2 cents per kilogram.

3. Reactor Control and Safety Systems

The Control System portion of the LCRE Control and Safety Systems mock-up was operated for 1068 hours during the quarter. This was an endurance run of all control system circuits under conditions simulating either manual or automatic modes of control. Each control drum was exercised 32 times on a periodic basis over its full range of motion in both directions. This cycle of operation is considerably greater than that which will be experienced in a startup and shutdown cycle of the LCRE. During the endurance run the only failures experienced involved five light bulbs located in the drum selector push-button switch assemblies. This has been corrected.

The mock-up was shut down following the above period of testing to permit the incorporation of a series of LCRE Safety System design changes and the installation of additional electrical interconnections required to make the mock-up a full scale operator trainer. When complete, the trainer will consist of a full eight-bay LCRE control console and 25 instrument racks, housing LCRE instruments, circuit chassis and simulated reactor components and mechanisms.

A number of breadboard and prototype safety system circuit assemblies were endurance-tested with satisfactory results. The following is a tabulation of the status of this testing as of the end of the reporting period:

Unit	Test Hours	Cycles of Operation
Scram Static Contactor Breadboard No. 1	2700	1100
Scram Static Contactor Breadboard No. 2	500	50
Scram Static Contactor Prototype Assembly	1870	200
Contactor Controller Breadboard	2210	750
Contactor Controller Prototype Assembly	1150	150
Low Voltage d-c Power Supply Breadboard	5000	--
Alarm Light Breadboard	3300	--
OR Logic Circuit Breadboard	900	--

In addition to the above, testing of a developmental nature was accomplished on an alarm light prototype assembly and a TWO-AND logic circuit breadboard. The prototype of the alarm light unit exhibited some self-tripping of individual channels because of an overheating in the SCR circuits. Preliminary testing of design modifications now indicates satisfactory performance.

The breadboard model of the TWO-AND unit has completed approximately 3500 hours of development testing. This has included many hours of endurance running with different circuit components of different values, in an effort to optimize performance. Considerable difficulty was experienced in eliminating spurious tripping of this and other logic circuits by electrical noise on the power circuits in the laboratory. The objective was to stabilize the basic trip-circuit to within one percent of the value of the gate signal which would trip the silicon-controlled rectifier in the circuit. It was found that the circuit, as presently designed, is stable for all input gate signals up to within two percent of the tripping values. However, when the input signal was adjusted to 99 percent of the tripping value, the unit tripped spuriously. The cause for this was found to be powerline clock synchronizing pulses and starting transients caused by major electrical equipment on the power line. The use of filtering capacitors and isolation transformers has diminished the effects of these disturbances to the point where circuit performance is acceptable. The behavior of these logic circuits emphasizes the importance of providing electric power sources for LCRE instrumentation which are essentially noise-free.

4. Reactor Components

The ten-inch, Cb-1 Zr alloy pressure vessel filled with lithium completed a scheduled 10,000 hour test. After 4370 hours of operation at 2000F with an effective hoop stress of 2000 psi in the vessel cylinder, the upper heating zone of the test rig burned out and the test temperature dropped to approximately 1900F. The effective hoop stress in the

vessel cylinder was increased to 2300 psi to compensate for the loss in temperature. This stress and temperature were held for the remainder of the test. Examination of the test pressure vessel is in process.

The two, four-inch, columbium foil-wrapped, Cb-1 Zr alloy pressure vessels are still in test. One of these vessels, pressurized to produce a hoop stress of 6000 psi at 1600F, has completed 4746 hours of a scheduled 10,000 hour test. The second vessel, pressurized to produce a hoop stress of 1200 psi at 2000F, has completed 3503 hours of a scheduled 10,000 hour test.

The Cb-1 Zr alloy full scale test vessel, filled with lithium and pressurized to produce a hoop stress of 1600 psi at 2000F, has completed 408 hours of a scheduled 10,000 hour test. No apparent damage to the pressure vessel was observed following the failure of the containment vessel tube during its initial heating to test temperature (PWAC-631). The failure was caused by differential thermal expansion in parts of the containment vessel. A section of Inconel tube was removed just above the break and a piece of the outer layer of tantalum foil was removed and examined. The foil contained 15,000 ppm O_2. The layer of foil directly beneath this area was ductile and was not discolored. The break was repaired so that the parts could expand freely.

5. Control Drives

Three, 600F, dry, non-lubricated, double-row ball harmonic bearing tests were completed this period, as listed below:

Part Number	Material: Rings	Material: Balls	Material: Cage	Cycles	Speed (RPM)
1022912	440-C Mod	M-2	17-4 PH	5×10^6	10
1029732	440-C Mod	M-2	Inconel X	5×10^6	10
1029732	440-C Mod	M-2	Inconel X	failed at 2×10^6	10

The failure to achieve test objectives in the third test above was due to high drag, resulting from silver pile-up in the race grooves. Posttest inspection of balls and rings from the first two tests showed no significant deterioration to the bearing parts.

To experimentally determine the fatigue limit in AMS 5616 flex tubes, five tubes were reused in bearing and flex gear test stands. These tubes have been subjected to 7 to 14 million reverse stress cycles to date, and continue to remain mass spectrometer leak-tight.

High temperature synchro transmitters continue to indicate that the innate fragility of their construction is leading to failures. To overcome this, the magnet wire size has been increased from AWG 33 to AWG 28. Further, alternate shaft angle transducers are being investigated and a sample lot of high temperature potentiometers is on order.

Two, 2000-hour, dry-spur gear tests in 600F helium continue with 1770 and 1630 operational hours, respectively. The gear materials are M-2 tool steel and PWA-724.

A printed circuit scram actuating motor having identical internal geometry to the LCRE type was scram-cycled 10,000 times in 500F helium. Brush and commutator wear were well within acceptable limits.

Three high-temperature shim actuating motors operating in 500F argon have completed 940, 670, and 340 hours to date and the tests continue. Materials of construction are Ceramic-Eze magnet wire, Sauereisen and Duramic potting compounds.

Two tungsten carbide and one columbium carbide type control drum radial bearing pairs were cycled in 900F NaK for 2000 hours. Torque values were within acceptable limits throughout the tests and no significant surface deterioration was observed.

An M-50 tool steel drum thrust bearing with a Rollube 3 cage was subjected to 2000 hours of reverse cycling at 600F in NaK. The axial load was 100 pounds. The load-carrying region showed insignificant wear and the torque required to drive the system was less than six pound-inches.

Two flex-gear tests under 600F in NaK were completed this period. The gear meshes were subjected to a reversing torque load of 250 pound-inches. The gear pair test, using an M-2 tool steel harmonic bearing, completed 1.3 million torque cycles with no appreciable tooth form wear. The second gear test, using a modified 440-C harmonic bearing, failed from loss of eccentricity in the wave shape.

The in-pile test of a shim actuating motor stack (Fig 12), containing Ceramic-Eze windings in Sauereisen potting cement was completed. The total dose for the 793-hour test was 2.0×10^{19} n/cm^2, fast flux. Electrical resistances across the encapsulated coil and the coil-to-case resistance did not change significantly.

6. Primary and Reflector System Components

Three Cb-1 Zr alloy, primary system, pipe static tests have completed 8098, 7960, and 6520 hours of the scheduled 10,000 hour test program. These pipe test specimens contain lithium and are operating at 2000F, pressurized to 56.5 psi.

Two of the three primary system pipe mechanical strain cycling rigs were put on test during this period. These rigs are designed to subject samples of primary pipe to mechanical cycling loads while pressurized to 71 psi at 2000F. The first of these test rigs has completed 1664 hours with 400 cycles at 0.002 inch-per-inch strain, 400 cycles at 0.004 inch-per-inch strain, and 28 cycles at 0.006 inch-per-inch strain. The second rig has completed 400 cycles at 0.002 inch-per-inch strain and 320 cycles at 0.004 inch-per-inch. The third test rig is in the final stages of fabrication.

Experiments were conducted on the LCRE jacket heat transfer test rig to obtain data for an evacuated assembly, a vertically-mounted assembly and heater spacing with 18 inches of unheated jacket length. A cursory evaluation of the experimental data indicates that the results are in agreement with the analytical data.

The primary fill and drain system development valve test was shut down after 3000 hours in 1000F lithium. Excessive seat leakage resulting from a mismatch of lapped plug and seat pairs prompted this early termination. At the shutdown, the valve had been cycled (open-close-open) 1000 times. Fig 13, 14, and 15 show posttest photographs of the plug, seat, and primary bellows seal, respectively. Visual examination of these parts showed no apparent defects. The Stellite surfaces of the plug and seat were measured for reflectance and then cut for metallographic examination. Preliminary examination has revealed no corrosive attack or surface deterioration. A helium mass spectrometer leak check and Zyglo examination of the bellows also showed no apparent defects. Metallographic examination of the bellows is currently in progress. This valve is being rebuilt with a new plug and seat incorporating a 60-degree contact angle and a new primary bellows seal.

FIG 12

SHIM MOTOR STACK TEST SPECIMEN, PRE-TEST

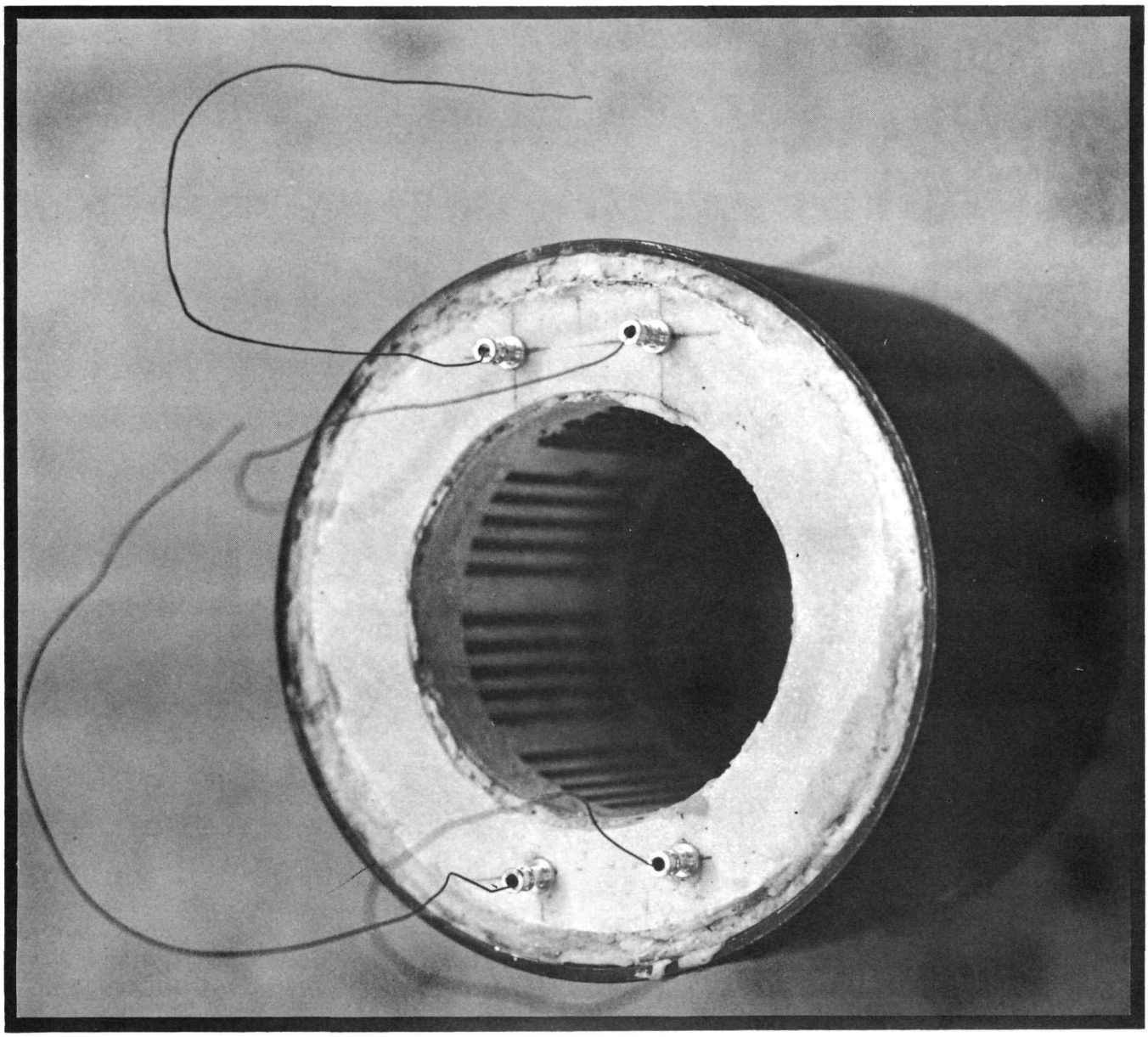

PLUG-ISOLATION VALVE TEST

(3000 HOURS, 1000F LITHIUM)

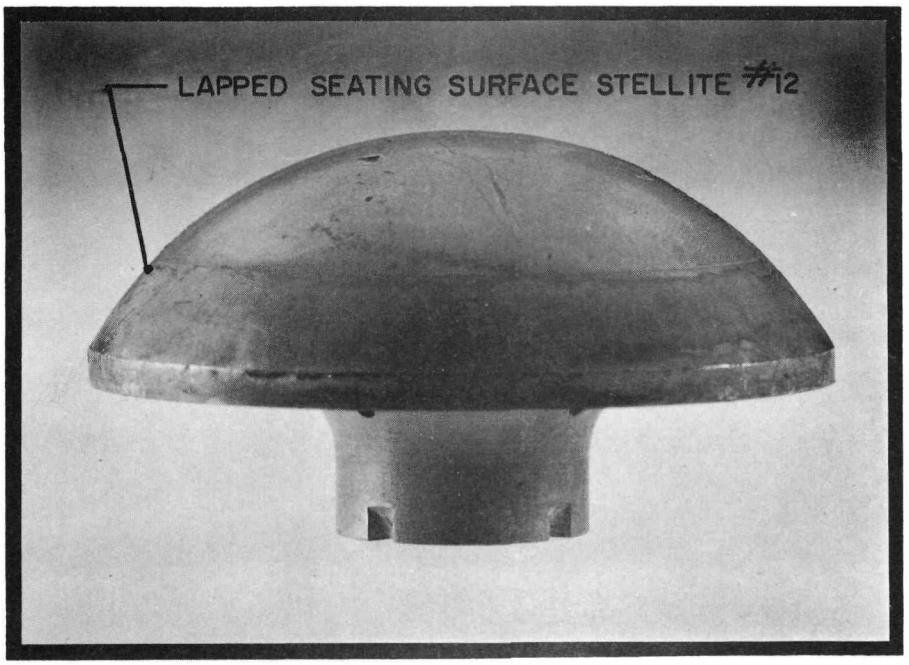

FIG 14

SEAT-ISOLATION VALVE TEST

(3000 HOURS, 1000F LITHIUM)

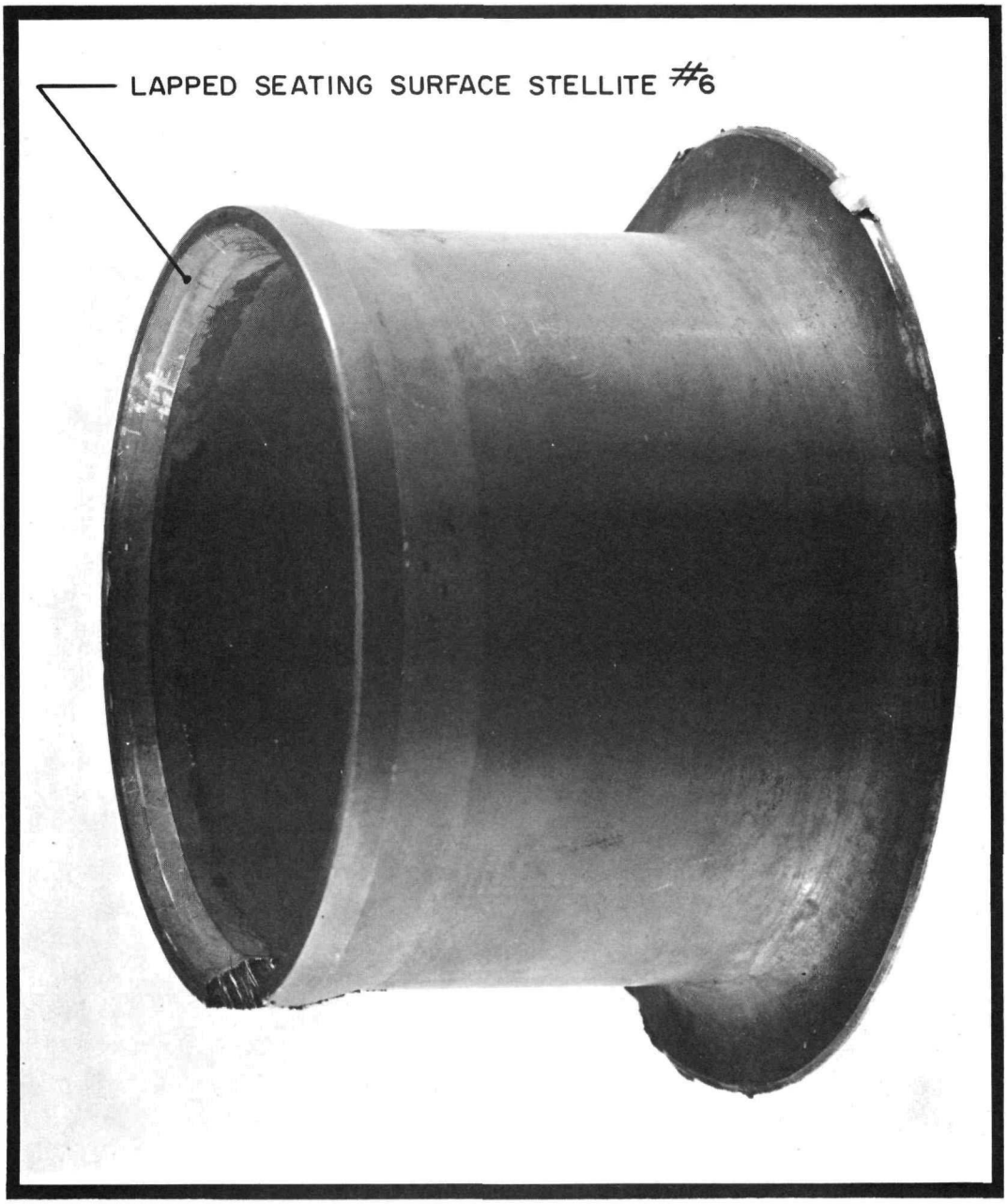

FIG 15

PRIMARY BELLOWS - ISOLATION VALVE TEST

(3000 HOURS, 1000F LITHIUM)

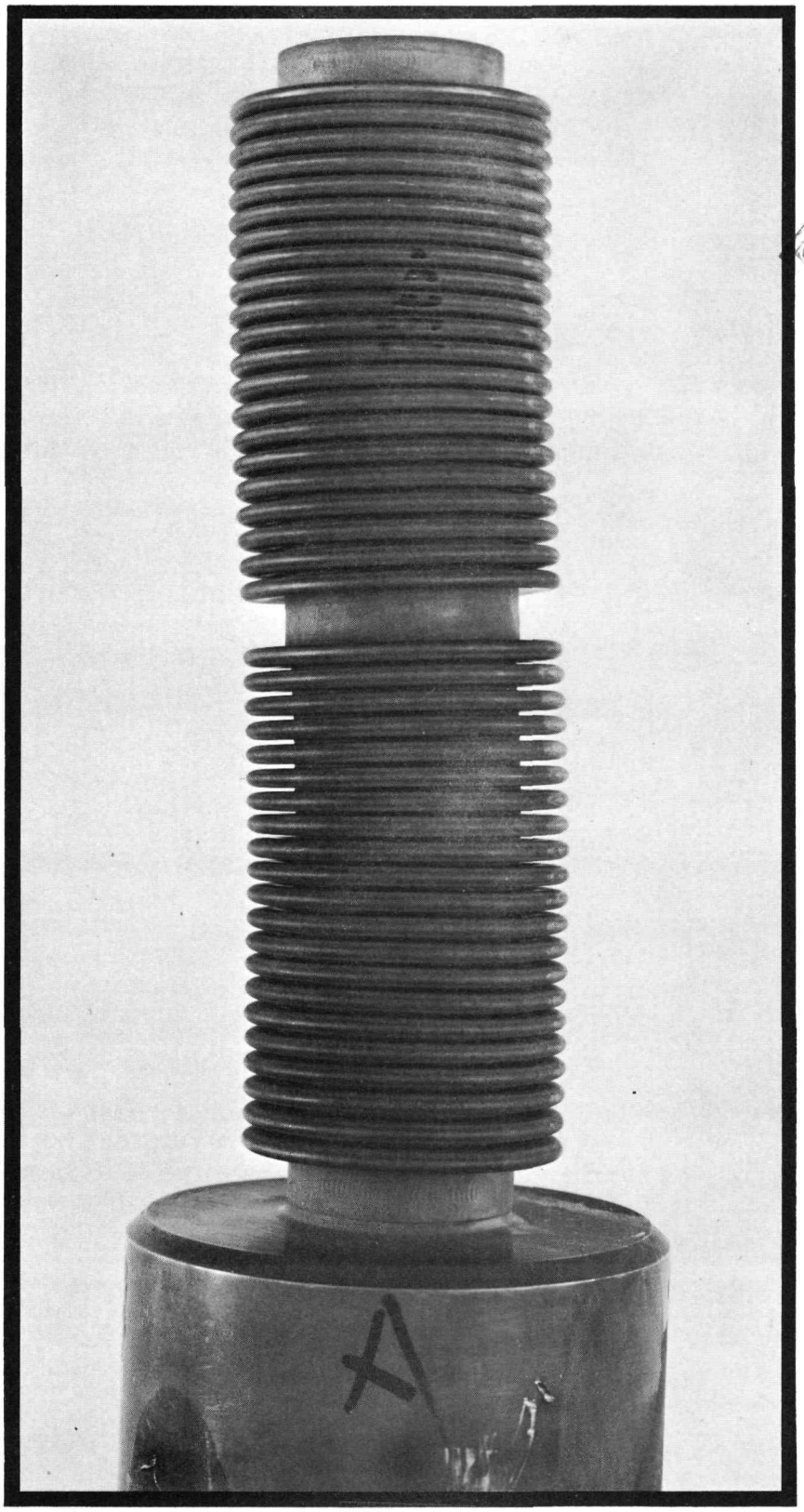

Installation of the second development punch valve in the test stand was completed and testing started. The diaphragm of this valve was cut after having contained 1000F lithium for the scheduled 1000 hours. The design pressure of 80 psi in the actuator was used to accomplish the cutting. Cycling and isolation testing are now being performed. Seat leakage was measured at less than 20 cc of lithium per day during isolation testing. To date, 1258 hours of testing at 1000F have been accumulated.

Corrosion testing of 0.025-inch thick, type 316 stainless steel sheet punch valve diaphragms continued. Satisfactory resistance to corrosion in 1000F lithium for periods to 7000 hours has been demonstrated.

The valve designs for the primary and reflector coolant system are shown in Fig 16.

Testing was completed on the series of development vapor trap cores discussed in two previous quarterly reports, PWAC-630 and PWAC-631. On the basis of these tests, Core Number IX, which has a constant one-quarter-inch fin pitch, was selected as the best for the LCRE application. The performance of this trap is compared to the performance of a unit having a one-half-inch fin pitch in Fig 17. Although Trap IX meets the criteria originally established for the LCRE, the small amount of lithium in the trap effluent may be great enough to ultimately plug the control valve in the primary pump sweep gas system downstream of the vapor trap. To eliminate this possibility, a second stage of trapping is being investigated which, at present, consists of a tank containing a rather large cross-section. The velocity of the gas, as it passes through this tank, is reduced so that the residence time is sufficiently increased to allow settling. Portable effluent analyzers and transparent sections are being used to evaluate the performance of the test units. In addition, vapor traps similar to the LCRE units are being tested in conjunction with the primary pump tests. Additional test stands are being fabricated to test the traps at the fill and drain tank conditions.

A scheduled shutdown of the second seal endurance rig (Fig 18) was effected after 10,364 hours of satisfactory operation. This unit was operated at a constant shaft speed of 5600 rpm and incorporated the prototype bearings and seals for the lithium pumps. This testing exposed the bearings and seals to a simulated LCRE pump operating environment, with the exception that they were not exposed to lithium. The average leakage rates observed for the oil shaft face seals were 1.5 cc/hour for the upper, and 1.1 cc/hour for the lower seal, respectively. The helium leakage past the dry gas shaft face seal varied during the test. While the leakage with a one psi differential was less than 0.01 scfh for about the first 6500 hours of test, the leakage increased to about 1.0 scfh for a 0.5 psi differential during the latter part of the test. The Kennametal K162B cermet face piece for this seal was brazed into the retainer with Coast Metals 52 alloy. Further efforts to evaluate brazed seals are in progress.

The disassembly and evaluation of the second seal endurance unit have been essentially completed. A photograph of the interior of the heated pot surrounding the shaft below the face seals is shown in Fig 19. The conditions inside the pot were similar to those for the first seal endurance test (15,045 hours) with only light film deposits of carbonaceous material in evidence. A view of the shaft region in the area of the dry gas shaft face seal is shown in Fig 20. No oily deposits were found, but light deposits of carbonaceous material were visible on the seal flange and on the shaft. Upon disassembly, the wear of all shaft

LCRE PRIMARY SYSTEM VALVE DESIGNS

PRIMARY SYSTEM FILL AND DRAIN

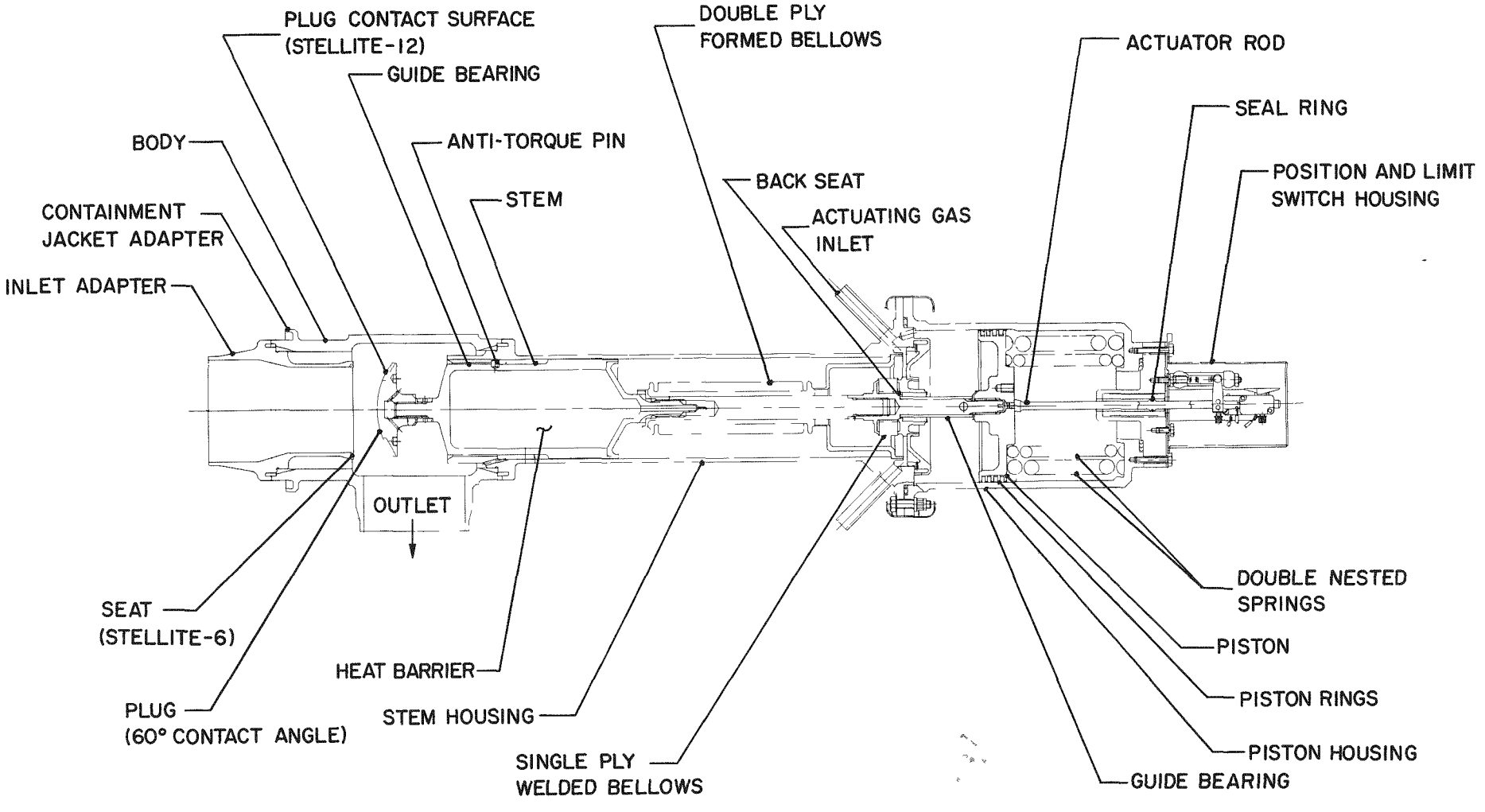

LCRE PRIMARY SYSTEM VALVE DESIGNS

REFLECTOR SYSTEM FILL AND DRAIN
(CONTINUED)

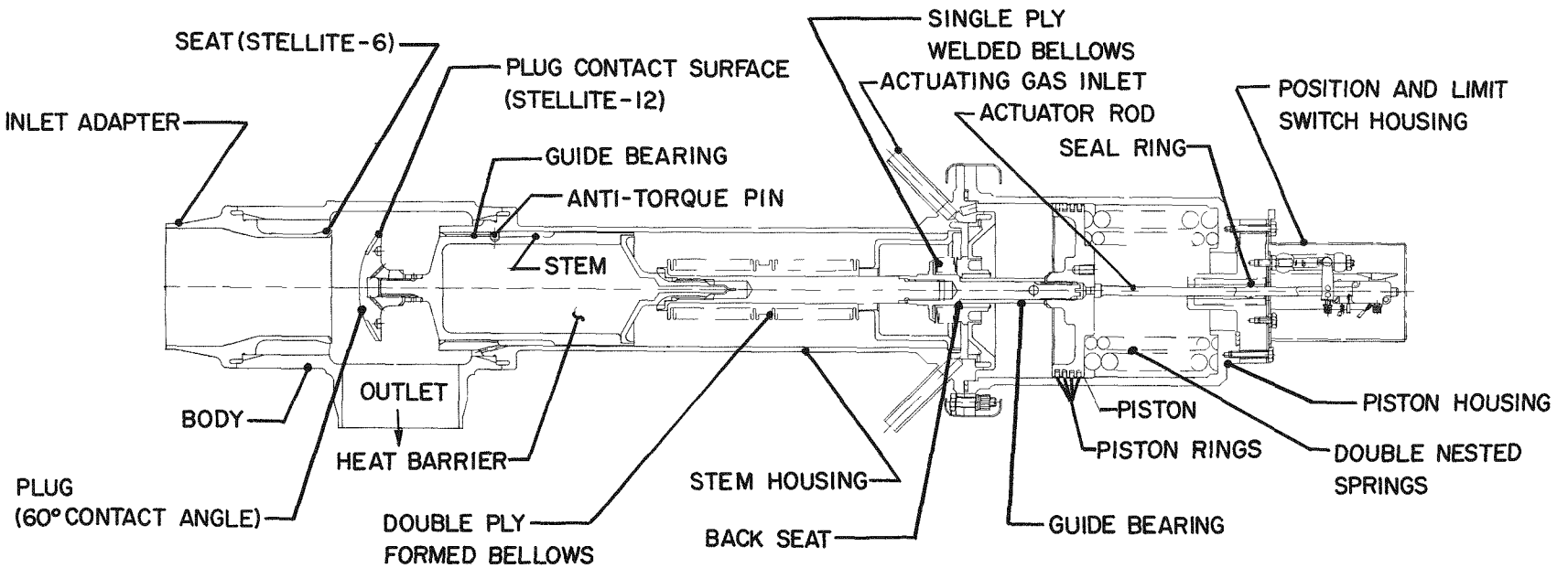

LCRE PRIMARY SYSTEM VALVE DESIGNS

LITHIUM-6 ADDITION SYSTEM THROTTLE
(CONTINUED)

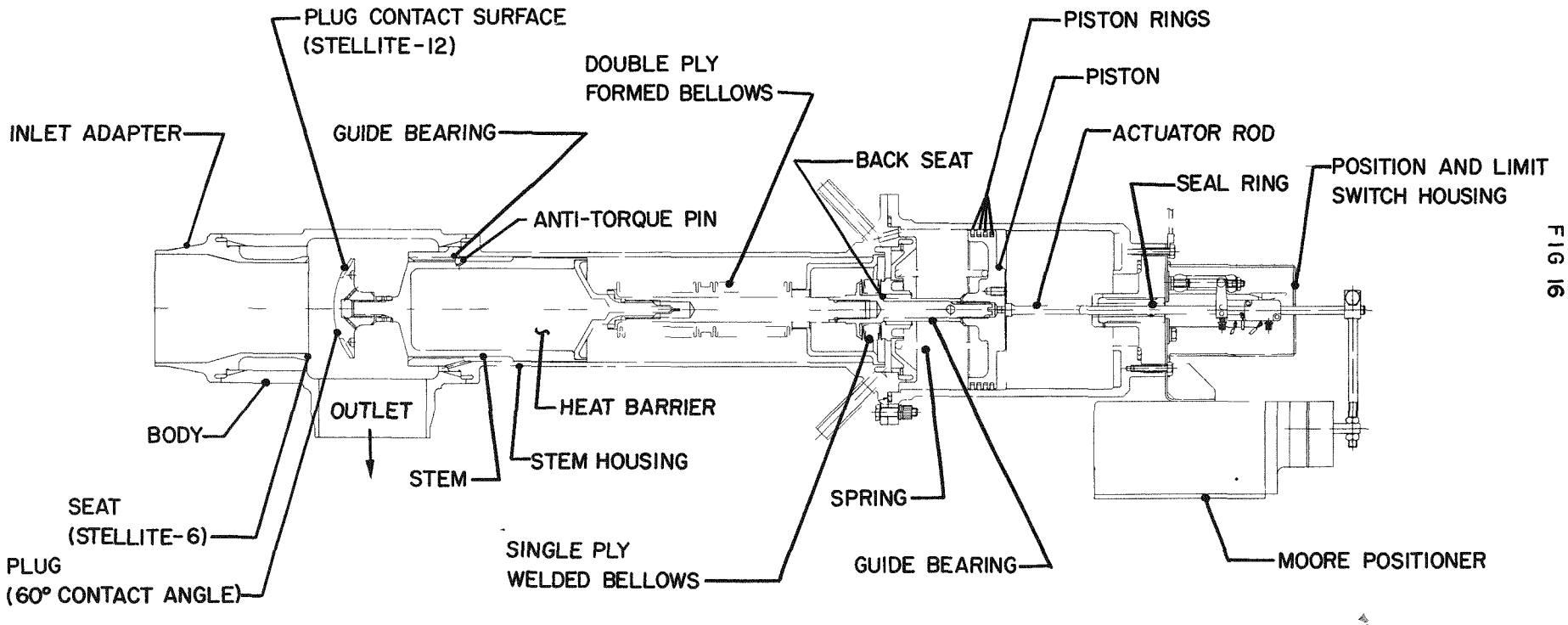

LCRE PRIMARY SYSTEM VALVE DESIGNS

LITHIUM-6 ADDITION SYSTEM PUNCH
(CONTINUED)

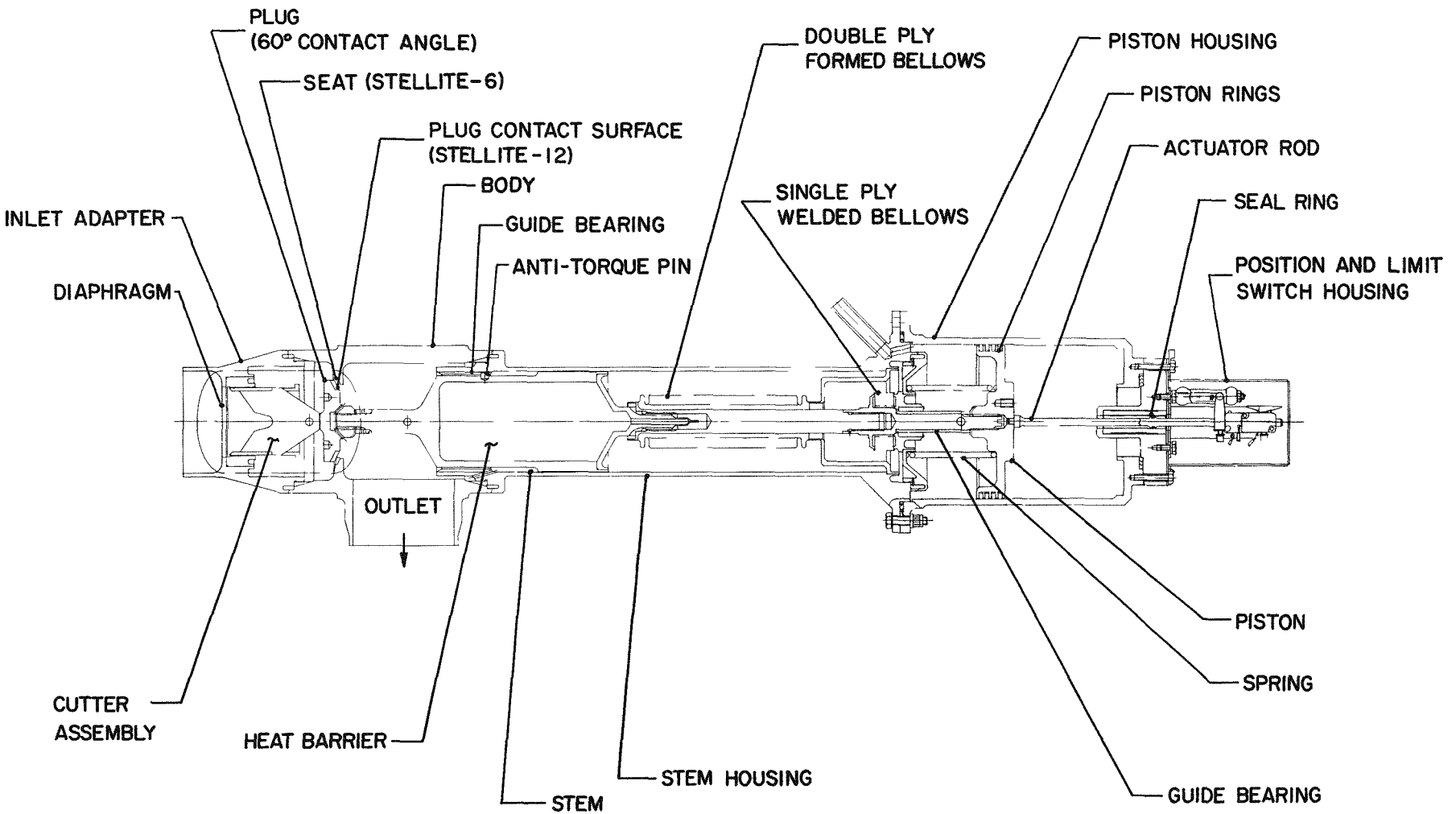

FIG 17

COMPARATIVE PERFORMANCE OF VAPOR TRAPS IX AND X WITH 1000F LITHIUM

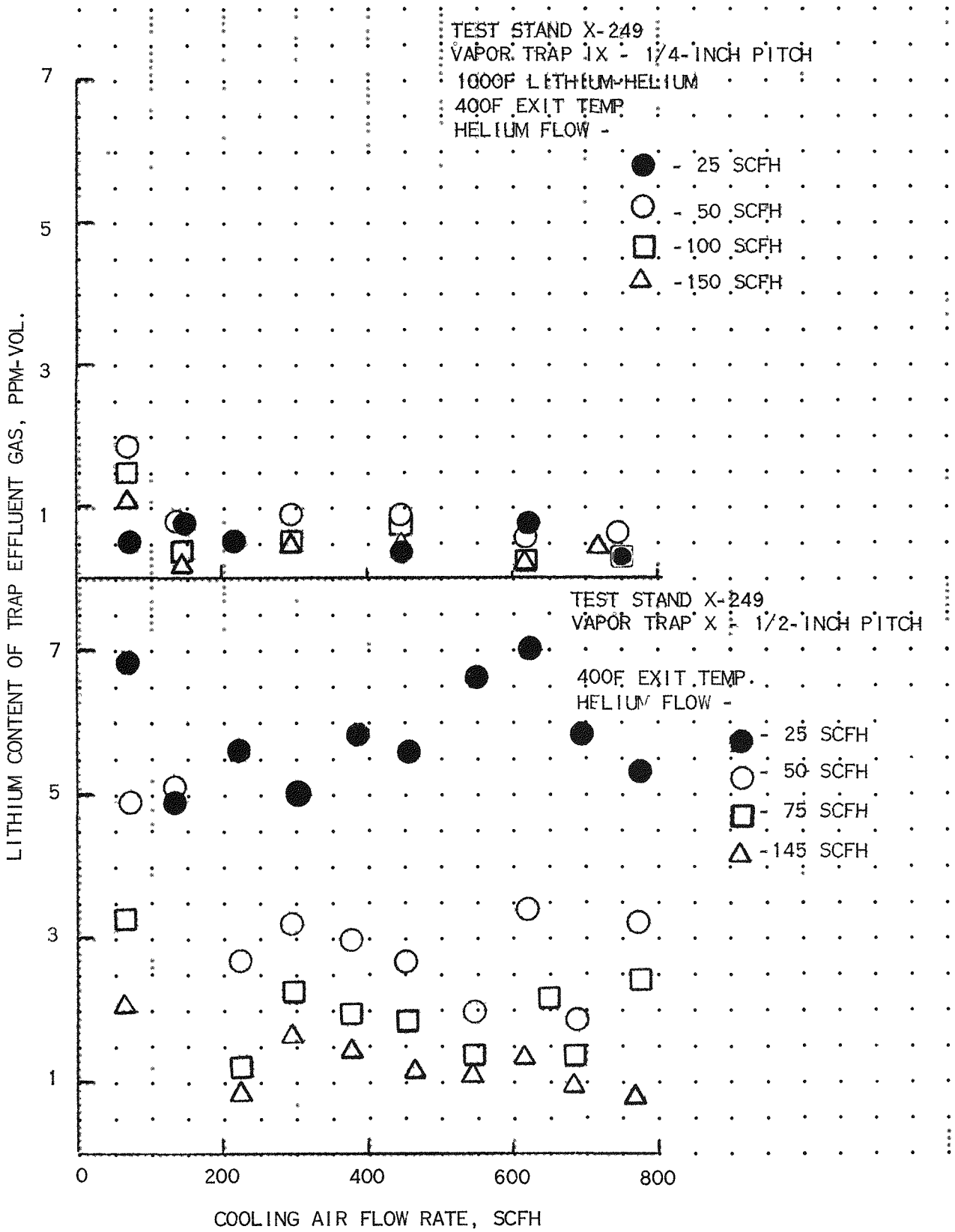

FIG 18

SECOND SEAL ENDURANCE RIG

AFTER 10,364 HOUR TEST

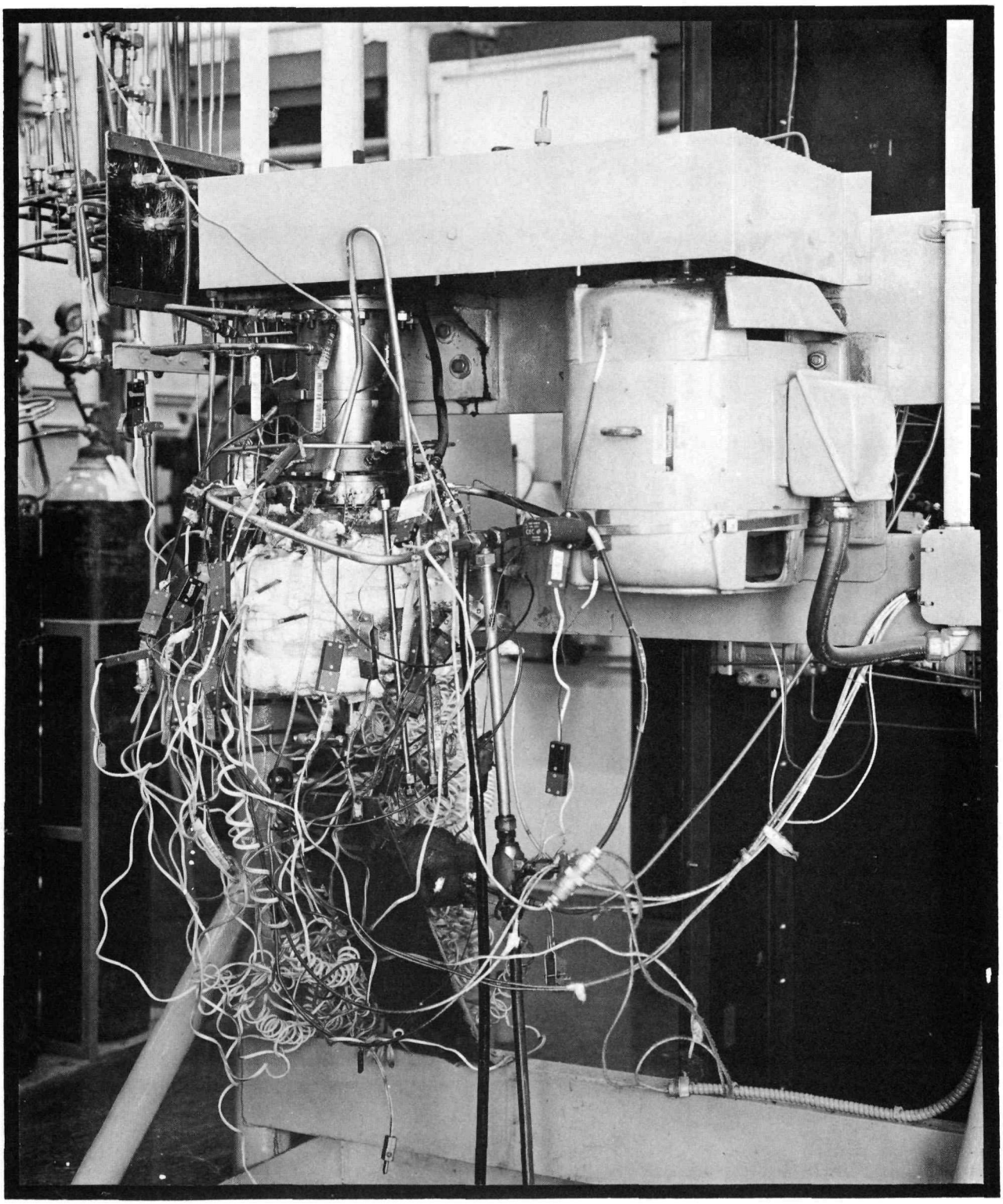

FIG 19

SECOND SEAL ENDURANCE RIG

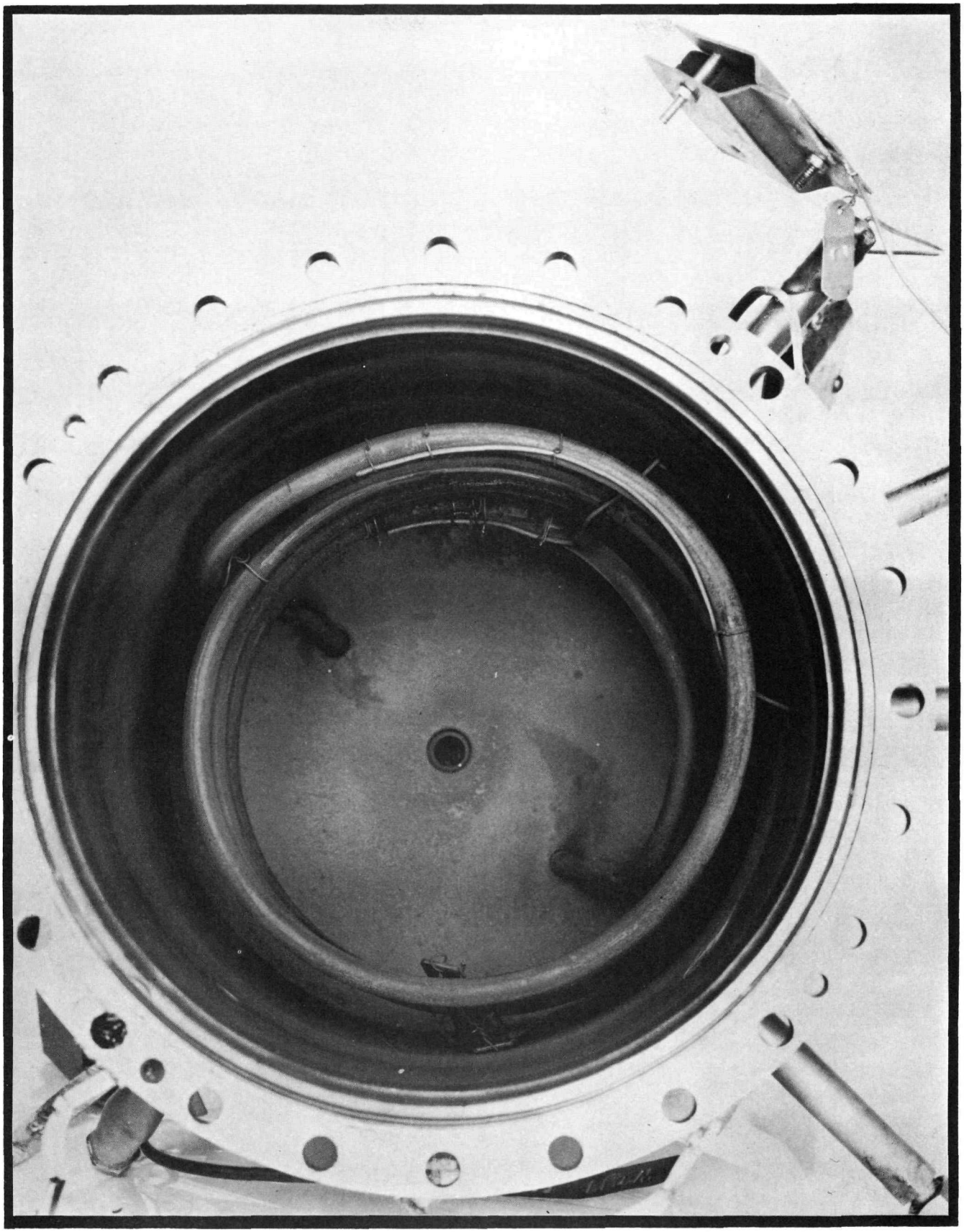

FIG 20

SECOND SEAL ENDURANCE RIG

PARTIAL DISASSEMBLY OF TEST UNIT

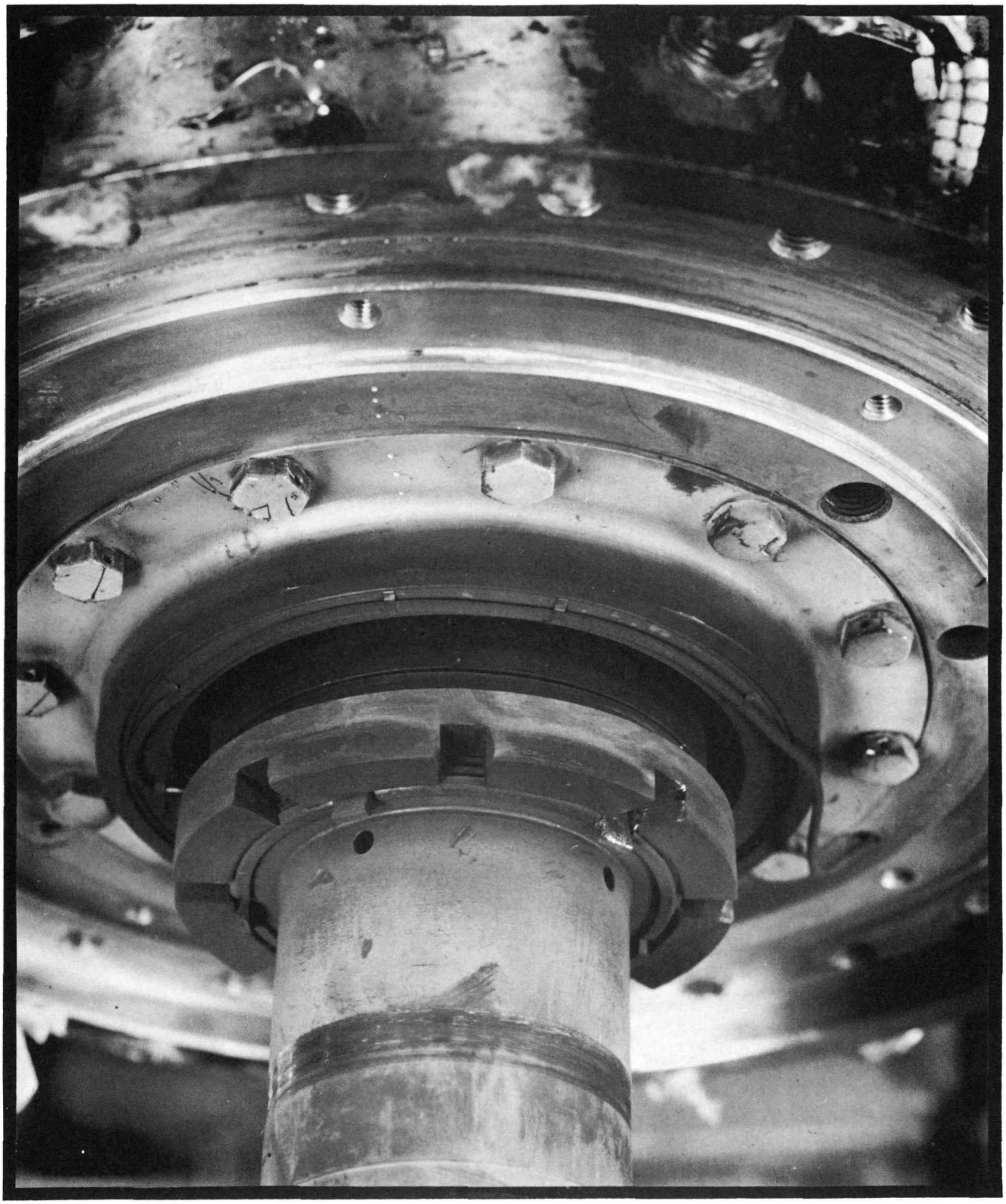

face seals was measured. The combined rotor and stator wear for both oil seals was found to be less than 0.0002 inch, which was comparable to that found on the first seal endurance test. For the dry gas shaft seal, the combined rotor and stator wear was found to be less than 0.010 inch. A film of oil was observed on the cermet faces of this seal, however, which was not present on the dry gas seal for the first endurance test unit. It is probable that this oil film on the seal faces formed only during the latter part of the test when the increased leakage across the seal occurred. The mechanical condition of all bearings and seals was found to be excellent. The excessive wear noted for the lower half of the duplex thrust bearing on the first seal endurance unit was not found for any of the bearings on this test.

The face seal component development has been stepped up for both dry gas seals and oil seals to ensure satisfactory operation of these seals in the long-term endurance tests of liquid metal pumps. Studies of the contour profiles of the cermet rubbing faces of these seals, as determined by optical flats, have shown that definite waviness patterns exist on seals after they have been run, although all were originally prepared to a flatness of about one helium light band. This observation has prompted an investigation of lapping techniques to produce selected waviness contours on cermet face seals prior to test. Preliminary tests of dry gas shaft seals lapped to a contoured surface are showing extremely low wear, low temperature rise, and low gas leakage.

One of the seals which prompted the investigation is shown in Fig 21. As shown, this seal had completed 1994 hours of operation at 6000 rpm with a leakage rate of only 7 scc/minute of argon for a pressure differential across the seal faces of 0.5 psi. This seal ran in one of the monobloc seal test units with a temperature of only 100F as measured by a thermocouple attached to the cermet face. Although the seal faces had been lapped to a 1.0 AA finish before test, the posttest examination revealed four apparent points of contact on the stator face with wavy depressions of about five light bands of helium between the points of contact. This same seal was previously tested for 3736 hours under similar conditions with an observed leakage rate of 28 scc/minute of argon. The total face load for both of these tests was 2.2 pounds. The seal wear for these tests was not measurable and the surfaces retained a mirror finish throughout the tests.

Testing of the second hot center section test unit was terminated in the PT-5B test stand after 6696 hours of operation. This caused a leakage of lithium through the stainless steel jacket surrounding the Cb-1 Zr alloy pot. A view of this leakage around the pot after the jacket was removed is shown in Fig 22. The test unit was completely disassembled and detailed visual, mechanical, and metallurgical examinations were conducted on the various components. Although it is strongly suspected that the liquid metal leakage occurred through the seal weld joining the pot to the center section housing, detailed metallurgical examination has so far been unable to determine a definite area of leakage. This test unit ran very well without any plugging problems inside the unit. A partially disassembled view of the lower shaft region and the dry gas shaft face seal is shown in Fig 23. A thin layer of oxides of lithium is noted on the shaft above the region of the gas sweep inlet and a film of lithium is also noticeable around the dry gas seal flange. This indicates that a small amount of lithium vapor did diffuse back up the shaft tunnel against the gas sweep flow, but no measurable plugging occurred. A photograph of the area around the lower oil seal is shown in Fig 24. This region, as well as the bearing cavity, was completely free of all traces of lithium. Mechanical inspection of the bearings and seals revealed that they were

CONFIDENTIAL

8C-10148
8C-10149

DRY GAS SHAFT SEAL AFTER 1994 HOUR TEST

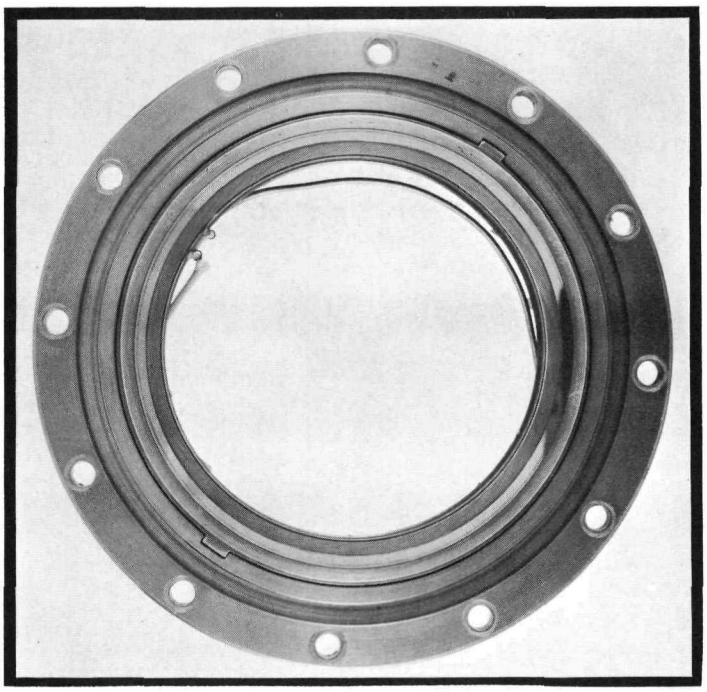

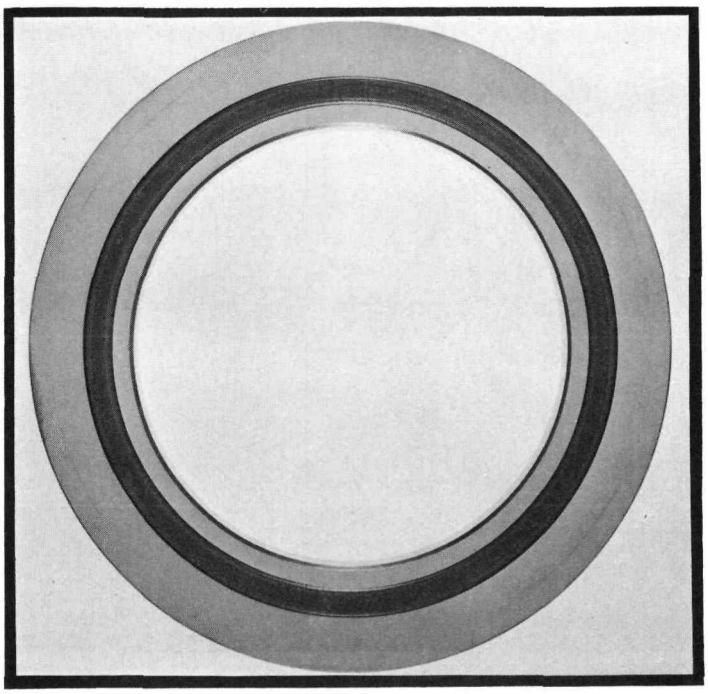

CONFIDENTIAL

FIG 22

SECOND LITHIUM CENTER SECTION

LEAKAGE AROUND POT

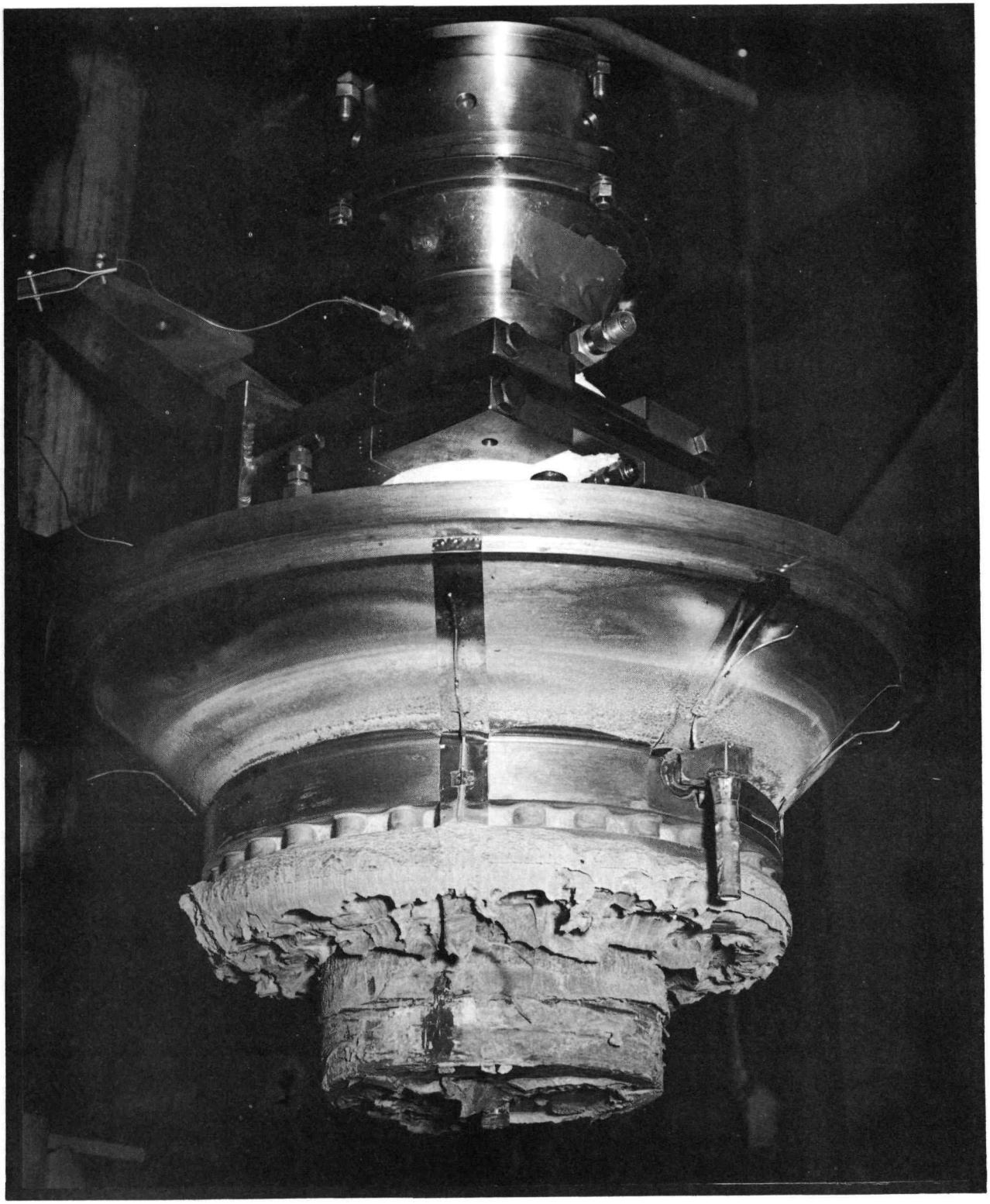

FIG 23

SECOND LITHIUM CENTER SECTION

DRY GAS SEAL REGION DURING DISASSEMBLY

FIG 24

SECOND LITHIUM CENTER SECTION

LOWER OIL SEAL REGION DURING DISASSEMBLY

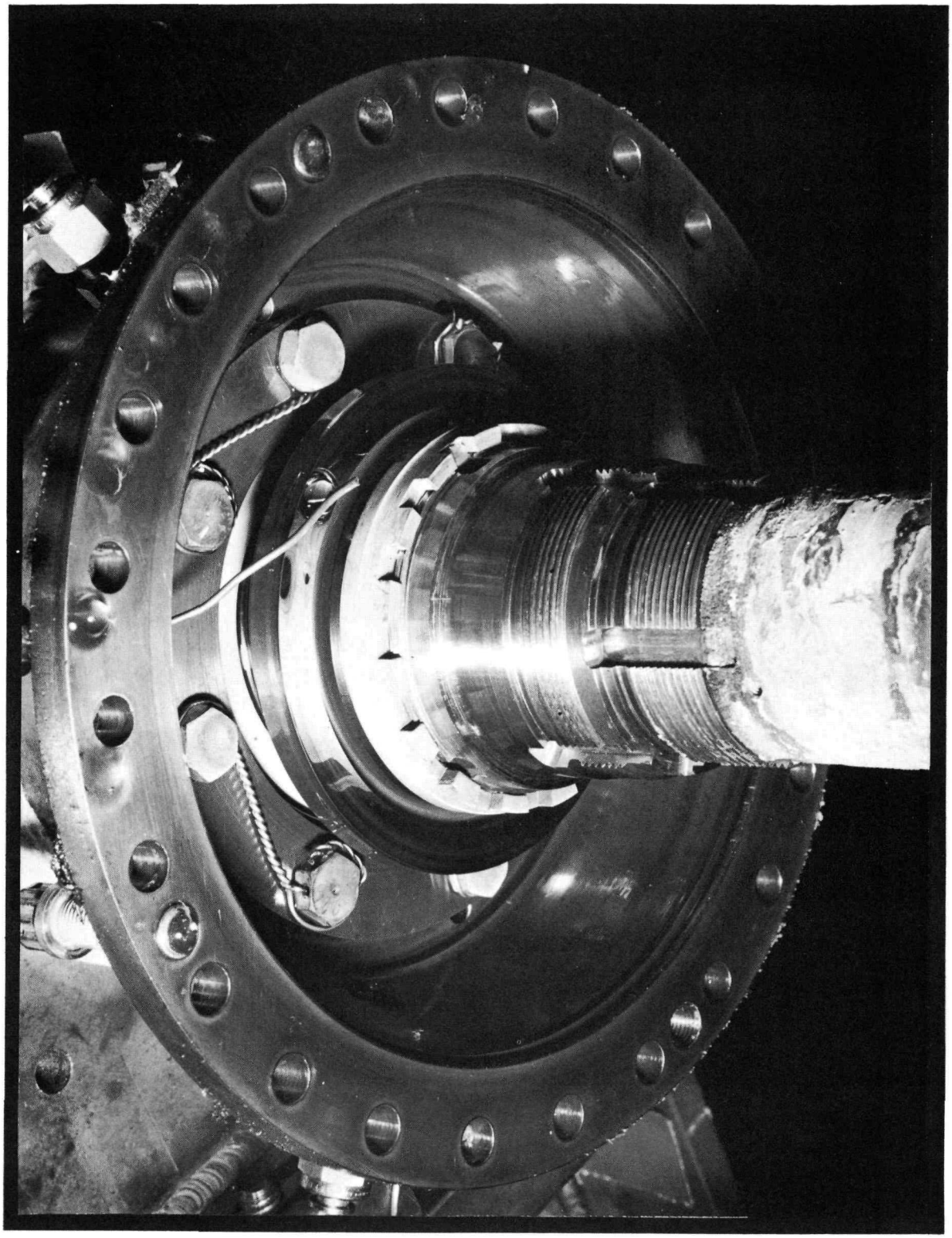

all in excellent condition. Heavy wear was noted on the faces of the dry gas shaft face seal and one convolution of the seal bellows was found to be fractured. This seal had malfunctioned at the beginning of the endurance test and ran with a balanced pressure across the seal for the remainder of the test. The wear on both the lower face seal rotor and stator was negligible and the average oil leakage past this seal during the test was 0.09 cc/hour. The wear on the rotor of the upper oil seal was also negligible, whereas the measured wear on the stator was 0.0009 inch. The average oil leakage past this seal was 5.3 cc/hour, although the leakage was not measurable for the first 3300 hours of the test. A design layout of modifications to be incorporated into the next assembly of this center section has been completed and detail fabrication drawings are in progress.

A scheduled shutdown of the first hot center section test unit in the PT-5A test stand was accomplished after 10,292 hours of test. Upon disassembly from the test stand, the tantalum foil wrapping around the Cb-1 Zr alloy pot was found to be intact and in excellent condition, as shown in Fig 25. This test unit experienced an inadvertent flooding of lithium up the shaft when a drive motor failure occurred after 4340 hours of test. The evidence of this flooding is shown in Fig 26 where deposits of lithium oxides are shown on the shaft and on the housing enclosing the slinger below the dry gas shaft seal. This oxide buildup in the gas sweep tunnel around the shaft resulted in periodic plugging problems during the test. A view of the shaft and dry gas shaft seal region is shown in Fig 27. Only small amounts of lithium are shown deposited on the dry gas seal flange, a deposition similar to that found for the second center section test unit.

No evidence of lithium was found in the region of the oil face seal or in the bearing cavity. Mechanical inspection of the bearings and seals revealed that the oil-lubricated bearings and face seals were in excellent condition. The dry gas shaft face seal was in very good operating condition, but the cermet rubbing faces were roughened and the combined rotor and stator wear was about 0.010 inch. This seal had operated satisfactorily with a pressure differential of 0.5 psi throughout the test. The wear on the upper oil seal stator was negligible and the stator was found to have a 1.0 AA finish after test. The measured wear of the rotor for this seal was 0.0001 inch and the finish was 2.0 AA after test. Average oil leakage for the upper seal was 0.46 cc/hour during the endurance test. A wear of 0.0006 inch was measured on the lower oil stator and the finish was 0.3 AA. Negligible wear occurred on the lower oil rotor and the finish after test was found to be 0.5 AA. There was no measurable leakage of oil past this seal throughout the test.

The design layout of necessary modifications to the hot center section test unit has been completed and detail fabrication drawings are being prepared. The modifications include a redesigned seal weld and a method of taking liquid metal samples during test operation. The latter feature is being incorporated in the next test of the first center section unit but not in the second section unit. Design of a third center section test unit is in progress. This will accelerate development of the primary pump.

Both of the lithium pump and sump hot flow test units have continued to function very satisfactorily. The first and second units have now accumulated totals of 8398 hours and 3247 hours, respectively. The second unit installed in the PT-5D test stand incorporated the auxiliary components scheduled for the LCRE installation.

A view of the assembled reflector coolant pump test unit is shown in Fig 28. A successful dry run of the unit to check out the operation of the shaft face seals has been completed. The pump unit is being prepared for assembly into the completed sump and loop assembly shown in Fig 29. The reflector pump and sump hot flow test unit is constructed predominantly of type 316 stainless steel and will be tested with NaK-78. Construction of the associated test stand is nearing completion and testing will be initiated during the next quarter. The design of two hot center section test units is in progress to accelerate the development tests of the reflector coolant pumps.

FIRST LITHIUM CENTER SECTION

AFTER 10,292 HOUR TEST

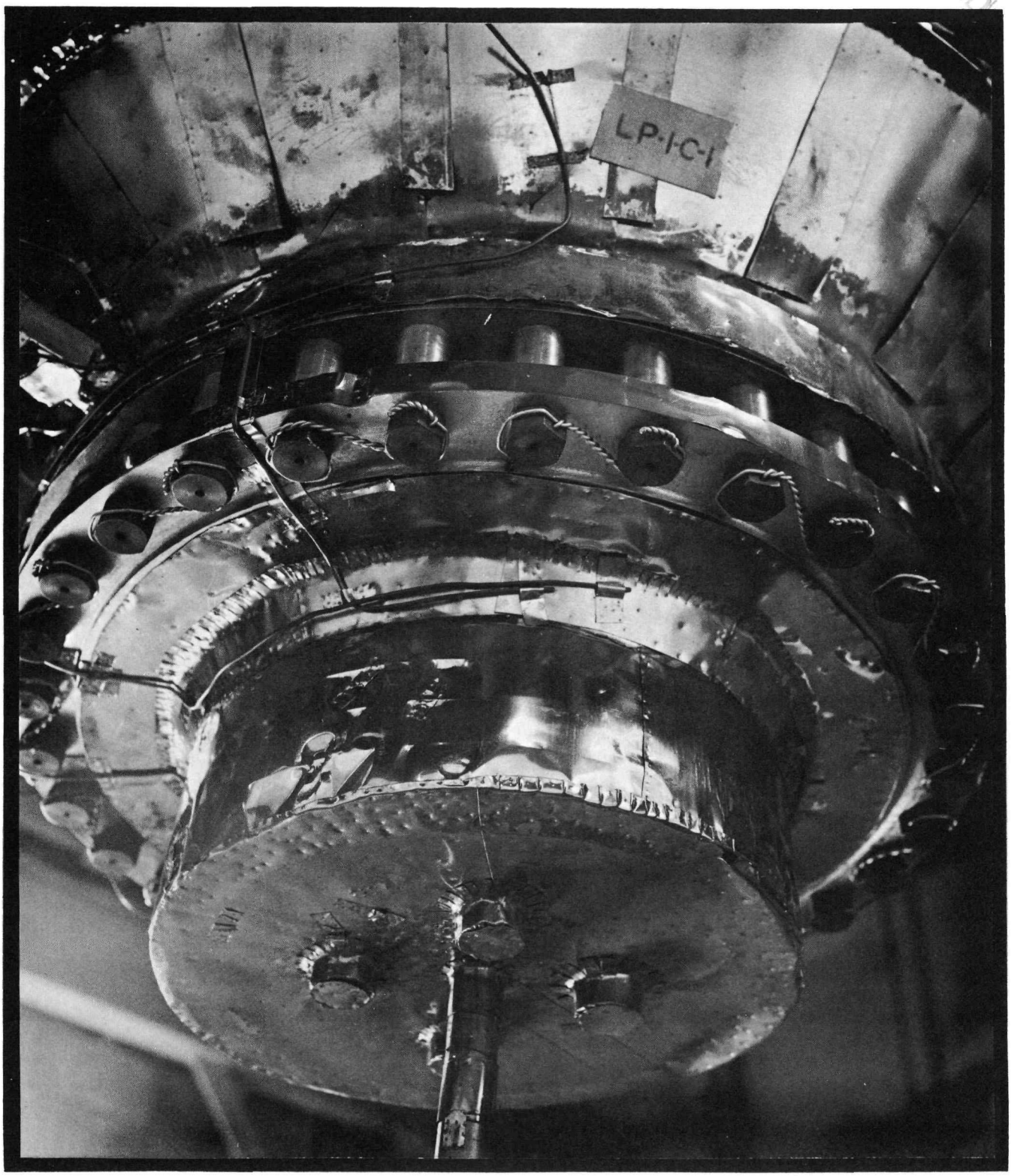

FIG 26

FIRST LITHIUM CENTER SECTION

LOWER SHAFT REGION DURING DISASSEMBLY

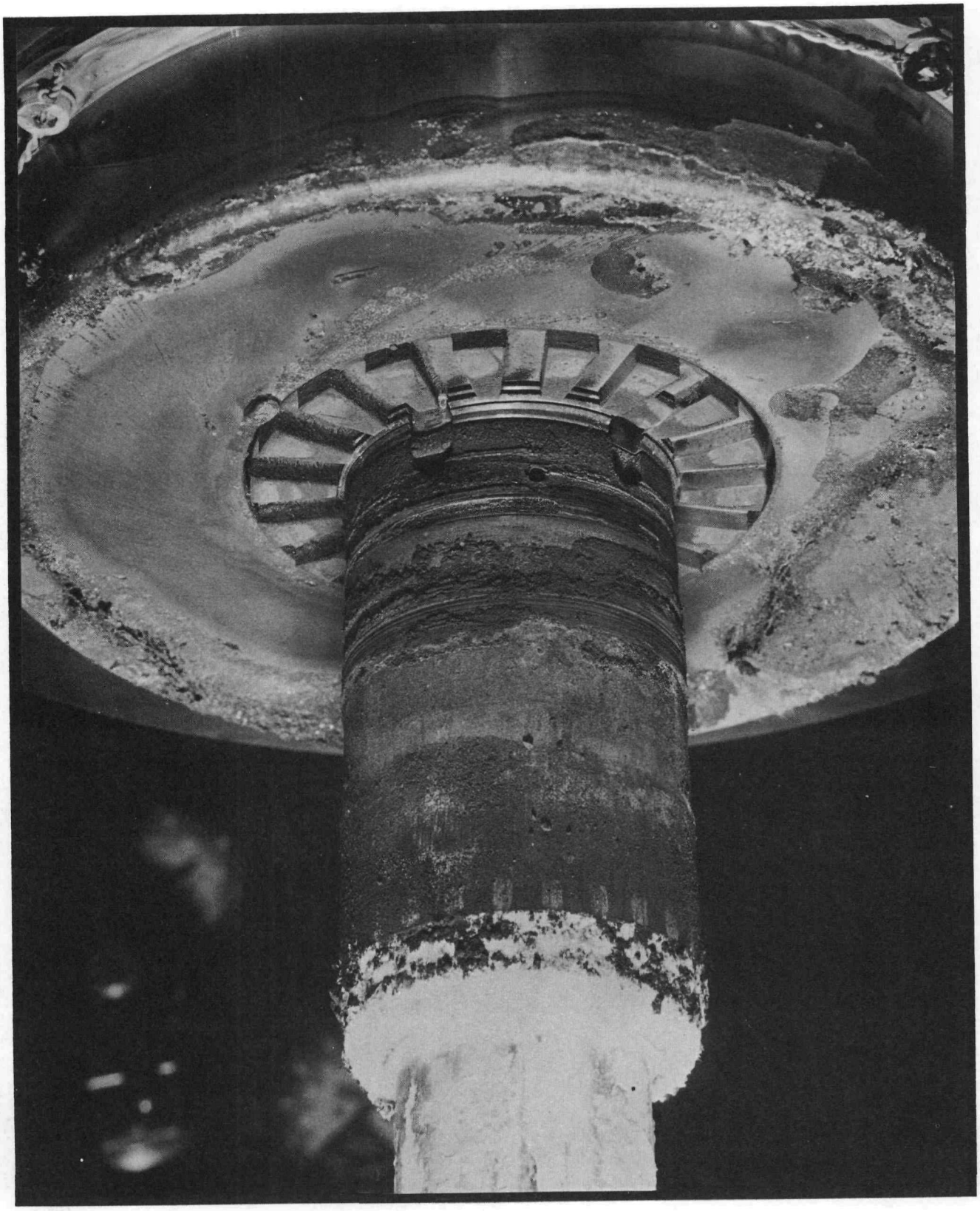

FIRST LITHIUM CENTER SECTION

DRY GAS SEAL REGION DURING DISASSEMBLY

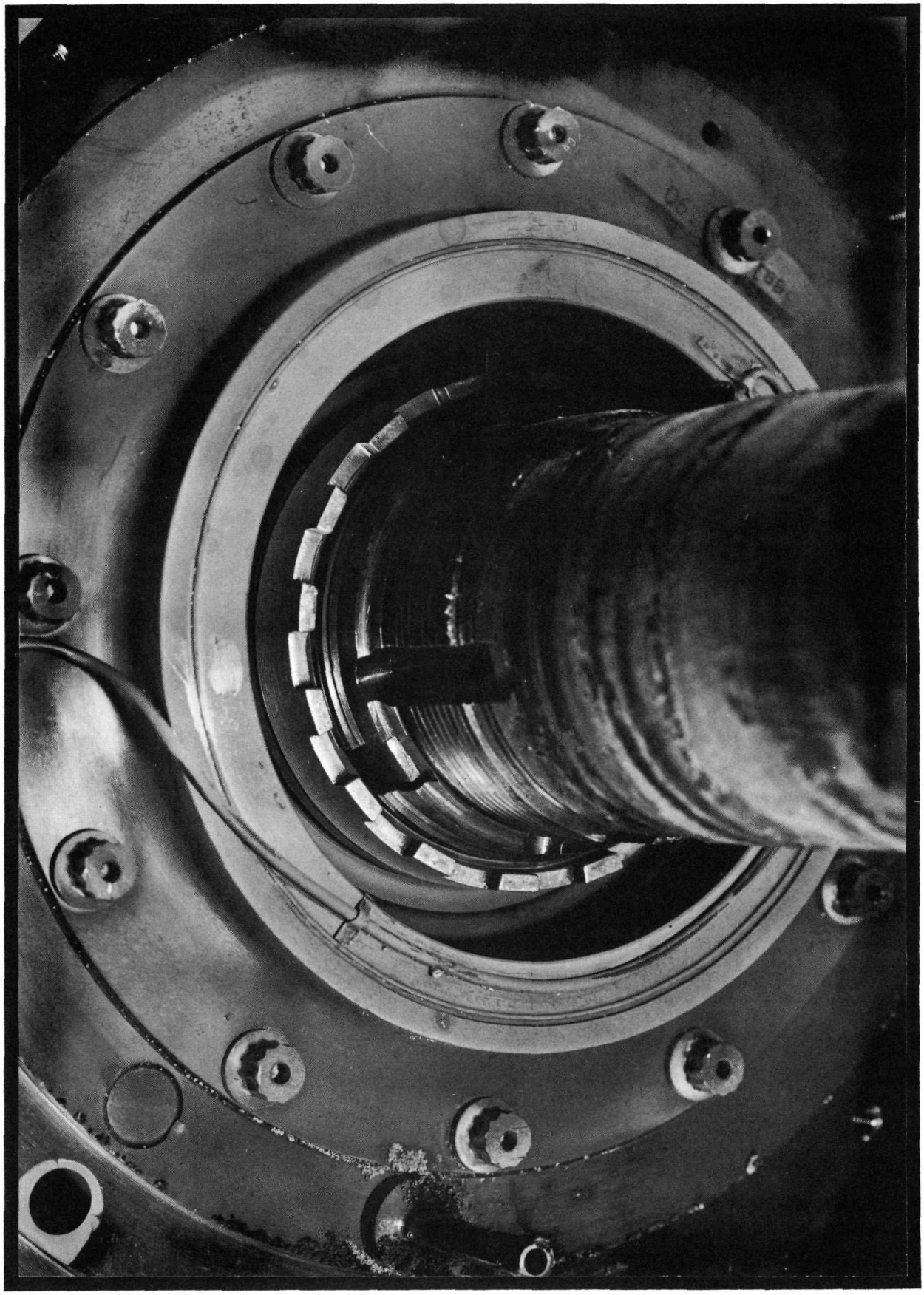

FIG 28

REFLECTOR PUMP TEST UNIT

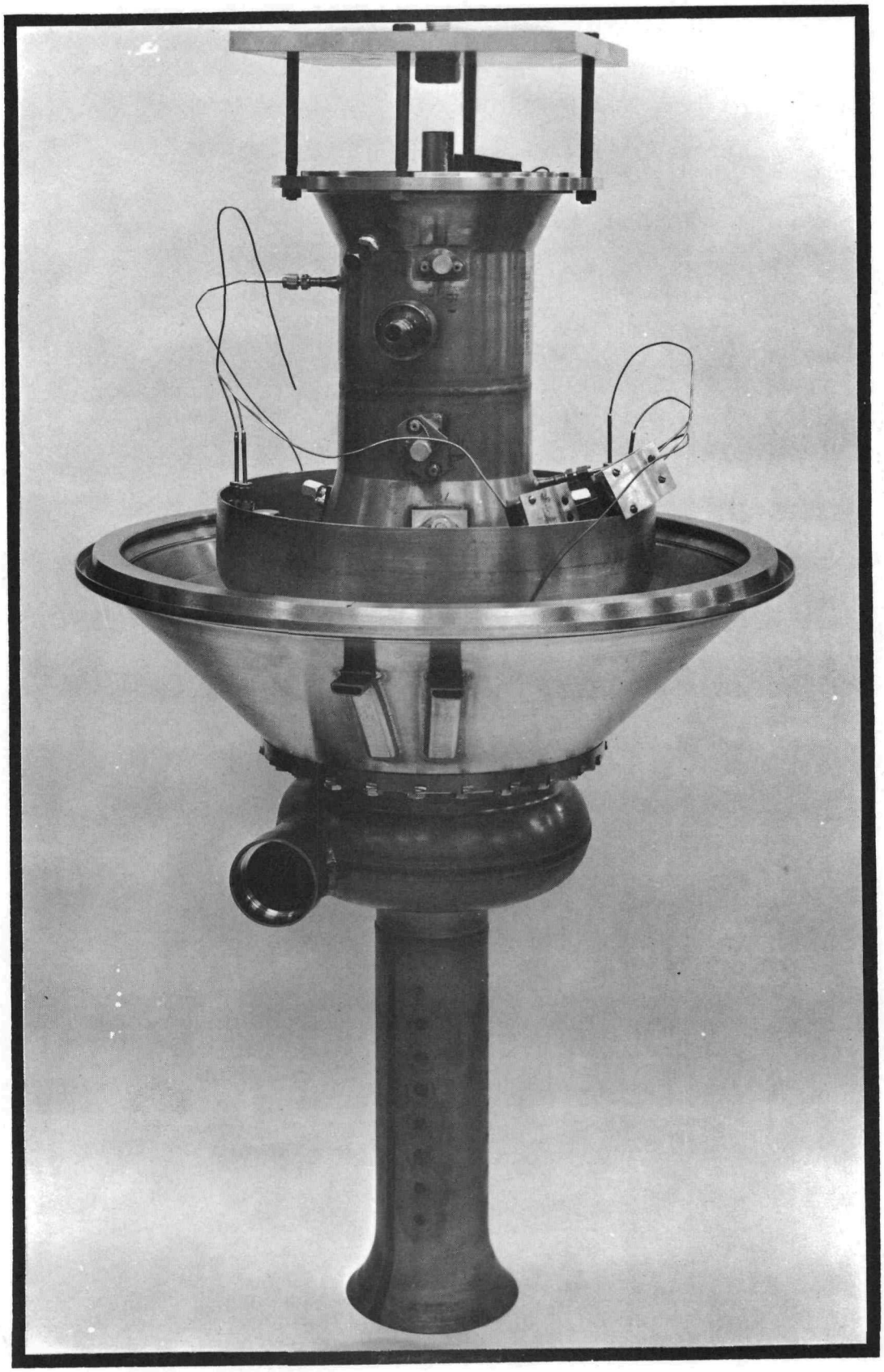

FIG 29

REFLECTOR PUMP TEST SUMP AND LOOP

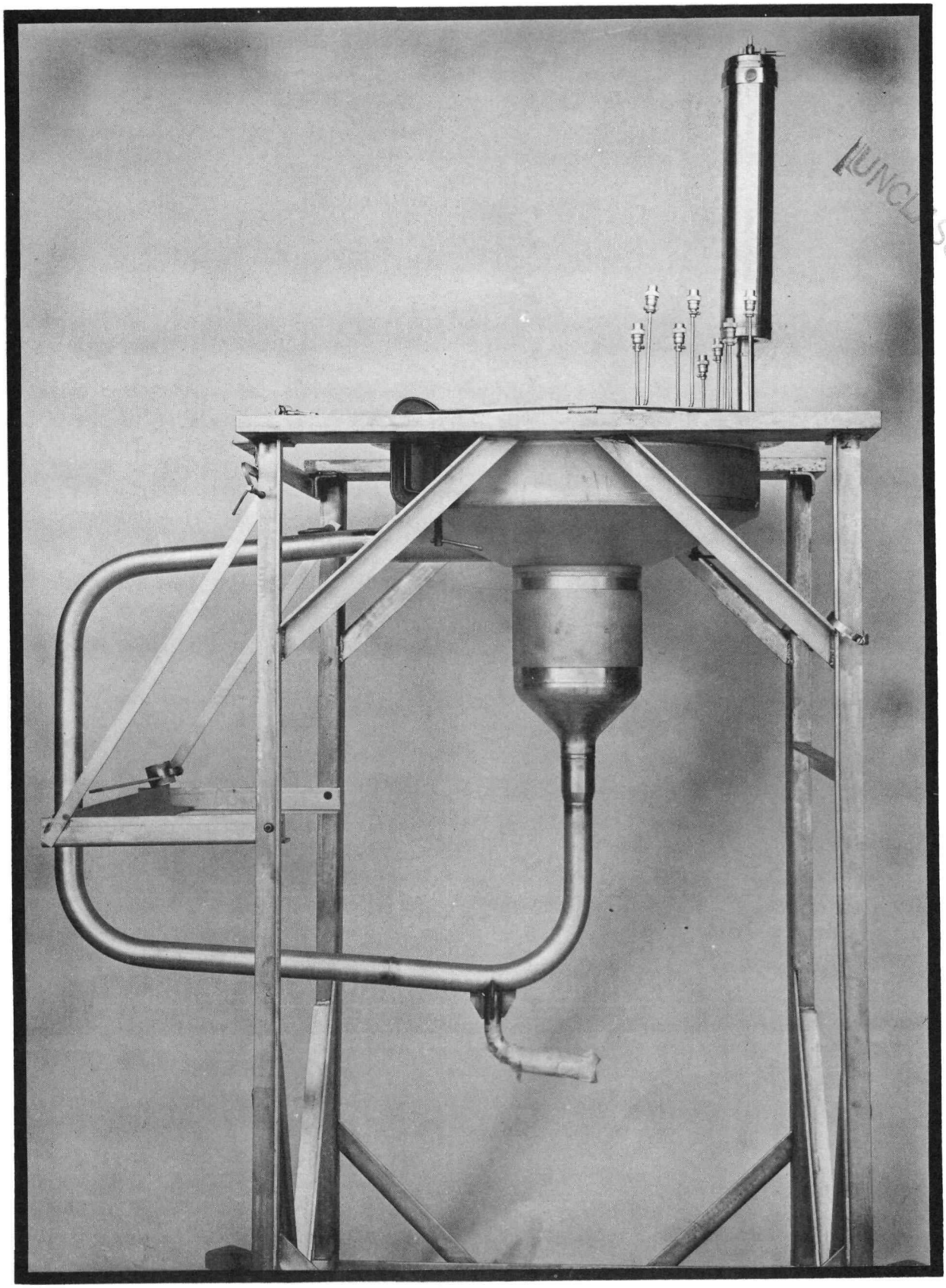

7. Secondary System Components

Water tests were conducted of the secondary coolant pump impellers (Fig 30) with a stainless steel partial shroud brazed to the vane tips. Data comparison (Figs 31 and 32) of the same impeller without a shroud indicated improved performance with a partial shroud. Results of other tests indicate that fully-shrouded impellers give markedly poorer performance than unshrouded impellers. An optimum performance level for the partially-shrouded impeller is being sought.

Testing of the modified hot center section unit (Fig 33) was begun and a total of 388 hours in NaK-78 at 700F have been accumulated. The modifications consisted of adding a radial vaned impeller at the end of the shaft to simulate the head rise generated by the secondary pump impeller, and adding a simplified sump around the center section to simulate the operating environment for the sump type pump. An improved vapor trap has also been incorporated into the test stand.

The hot flow test of the secondary pump and sump has continued to operate successfully for a total of 5516 hours in NaK-78 at about 695F. The current operating point is at a flow rate of 395 pgm and a head rise of 143 feet. This corresponds to a shaft speed of 4580 rpm. Minor plugging indications have persisted in the gas sweep circuit, but have not caused any operational difficulties.

Modifications to the secondary pump water test unit are being made in the area of the dynamic seals to satisfy the new head rise and flow rate requirements for the LCRE application. The PT-4 test stand of the Pump-Turbine Laboratory is also being modified to conduct the water calibration studies of the secondary pump and sump test unit.

The first of four development isolation valves completed the scheduled 10,000 hour test. This valve, which was operated in the 1200F to 1500F range, is being disassembled for examination and evaluation. Preliminary examination indicates the valve to be in excellent condition.

A rebuilt isolation valve, with the new 60 degree plug and seat contact angle, has accumulated 2450 hours in 1200F NaK and has been cycled approximately 775 times. Fig 34 shows this new plug design.

The valve designs selected for the secondary system as a result of the development valve testing are shown in Fig 35.

Vapor trap core, Type IX, the type selected for the lithium application, out-performs all other types tested in NaK-78. The development program on this unit closely parallels the lithium development discussed in the section of this report on the Primary and Reflector System Components.

The two, 3-1/4-inch diameter Cb-1 Zr alloy-to-type 316 stainless steel co-extruded joint tests, containing NaK at 1200F with an internal effective pressure of 64.5 psi, were completed during this period. Each of the tests successfully completed the scheduled 10,000 hours of endurance testing.

SECONDARY COOLANT PUMP IMPELLER

WITH PARTIAL SHROUD

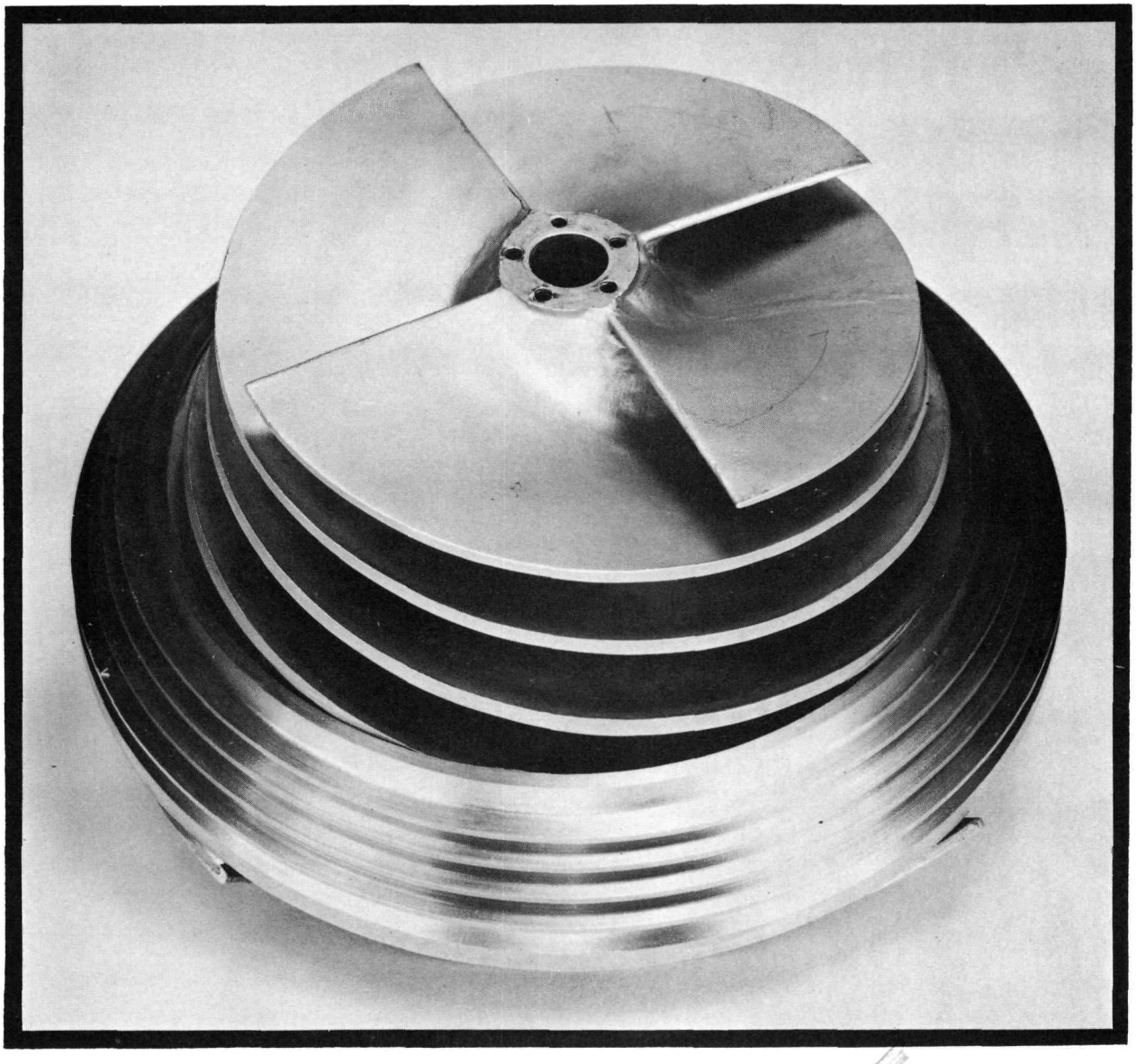

HEAD VERSUS FLOW COMPARISON

SECONDARY COOLANT PUMP IMPELLERS

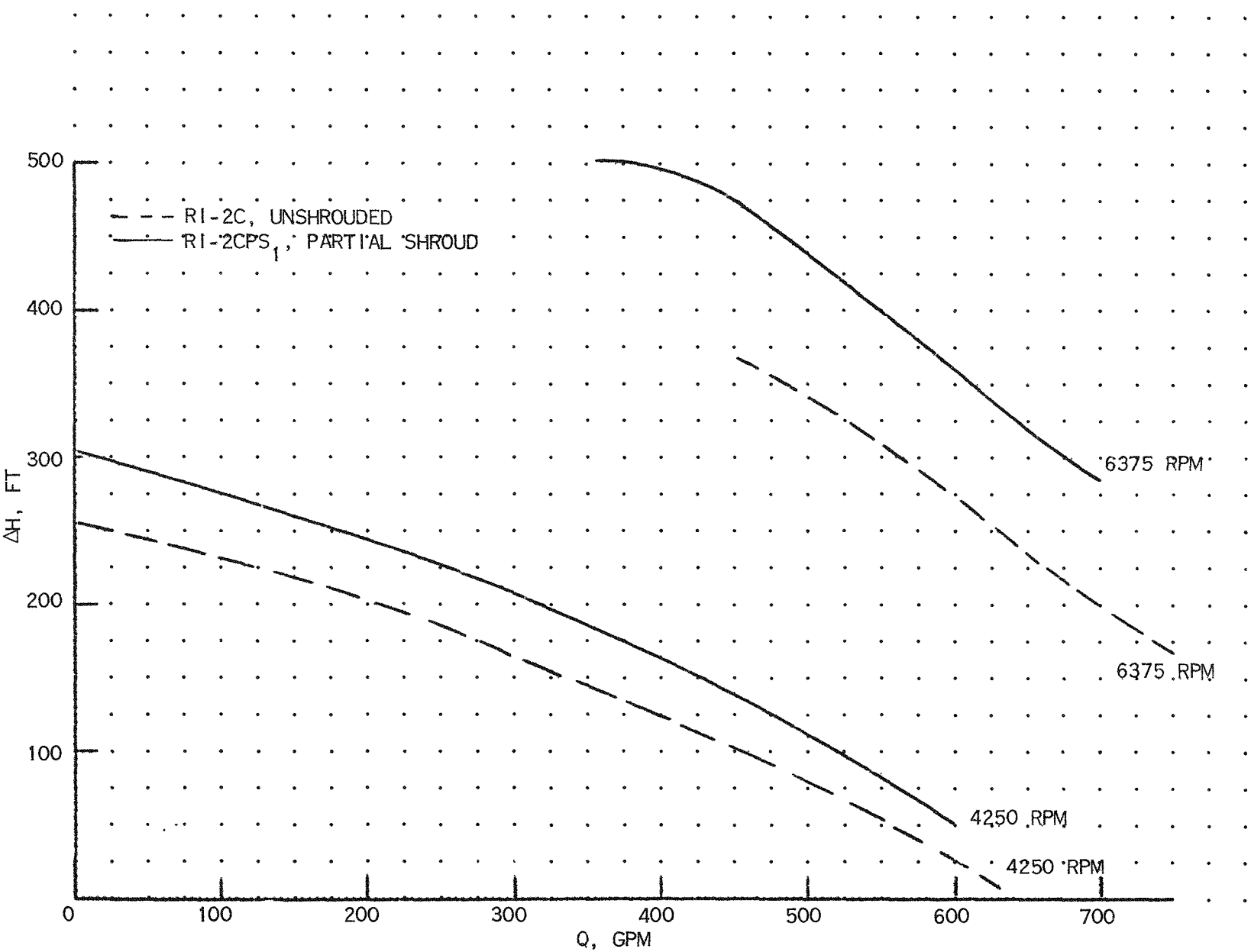

PWAC-632
FIG 31

EFFICIENCY VERSUS FLOW COMPARISON

SECONDARY COOLANT PUMP IMPELLERS

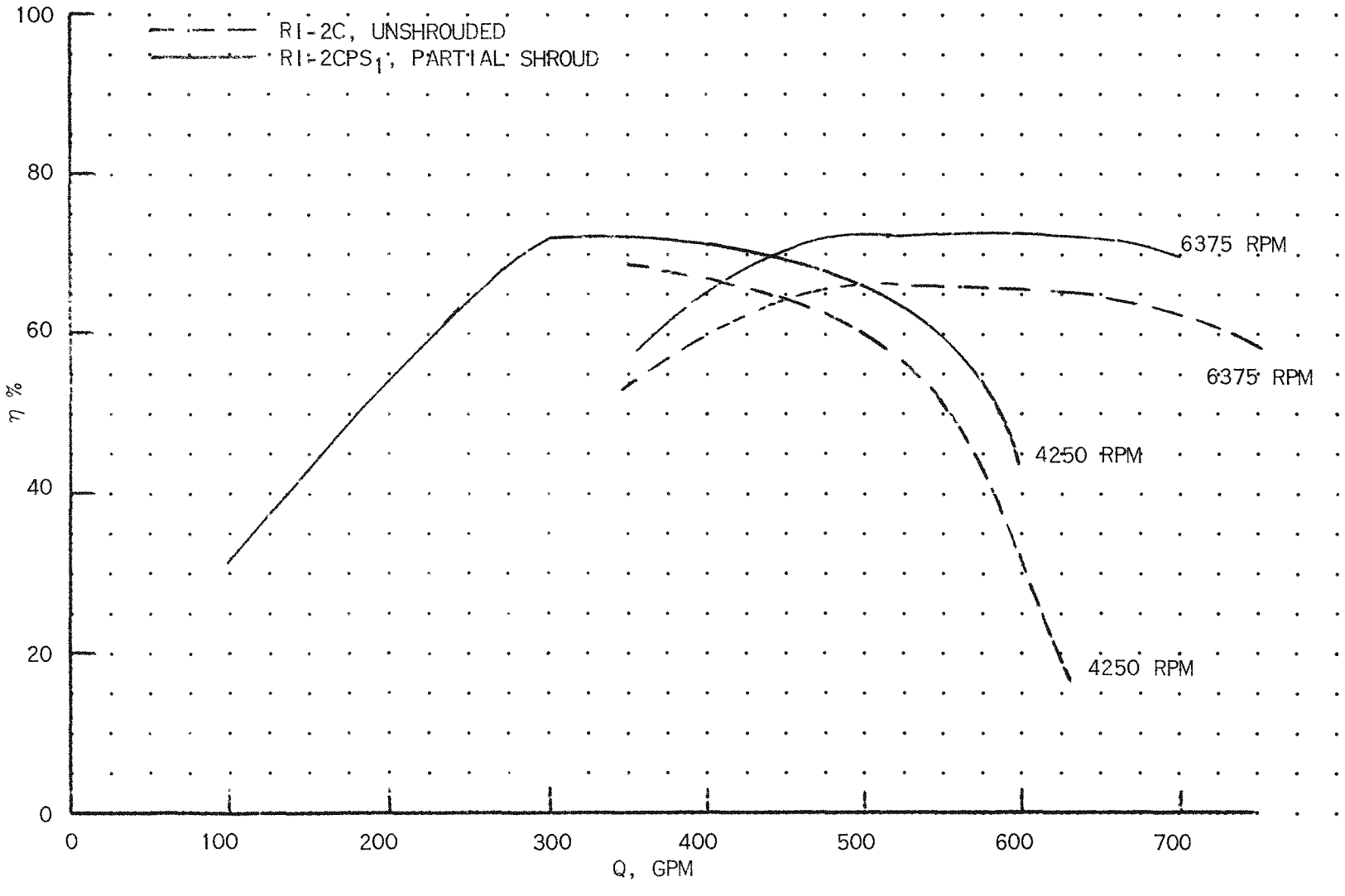

PWAC - 632
FIG 32

SECONDARY COOLANT PUMP CENTER SECTION

MODIFIED UNIT ON TEST

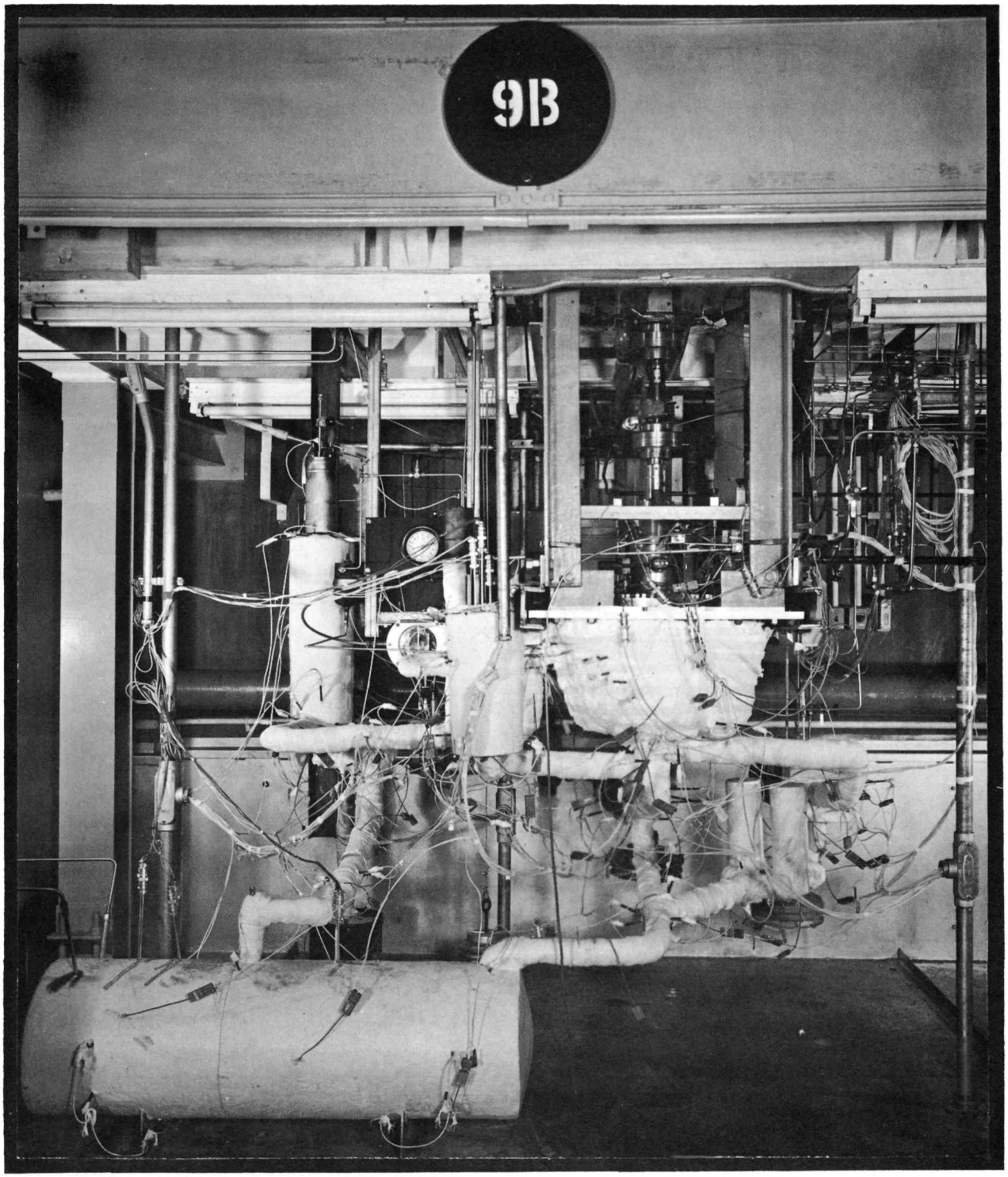

PROTOTYPE LCRE VALVE PLUGS

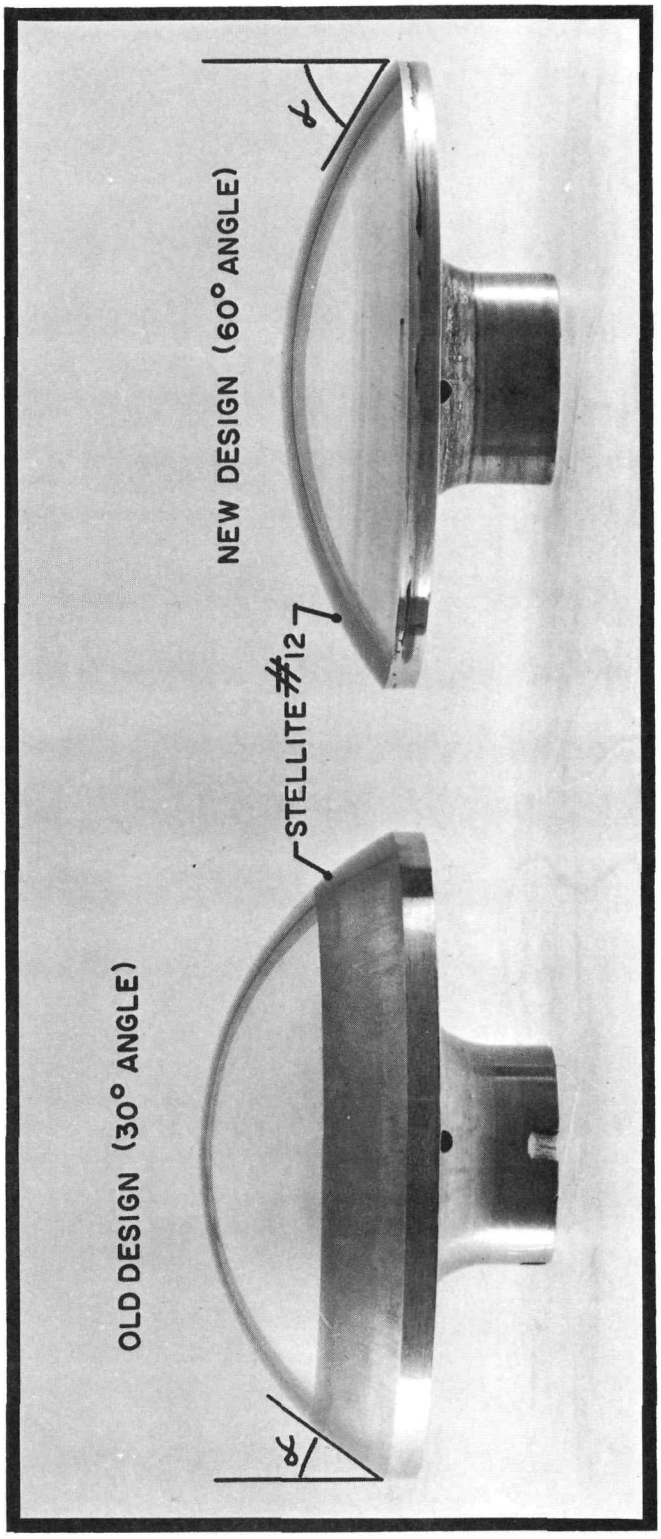

LCRE SECONDARY SYSTEM VALVE DESIGNS

SECONDARY SYSTEM FILL AND DRAIN

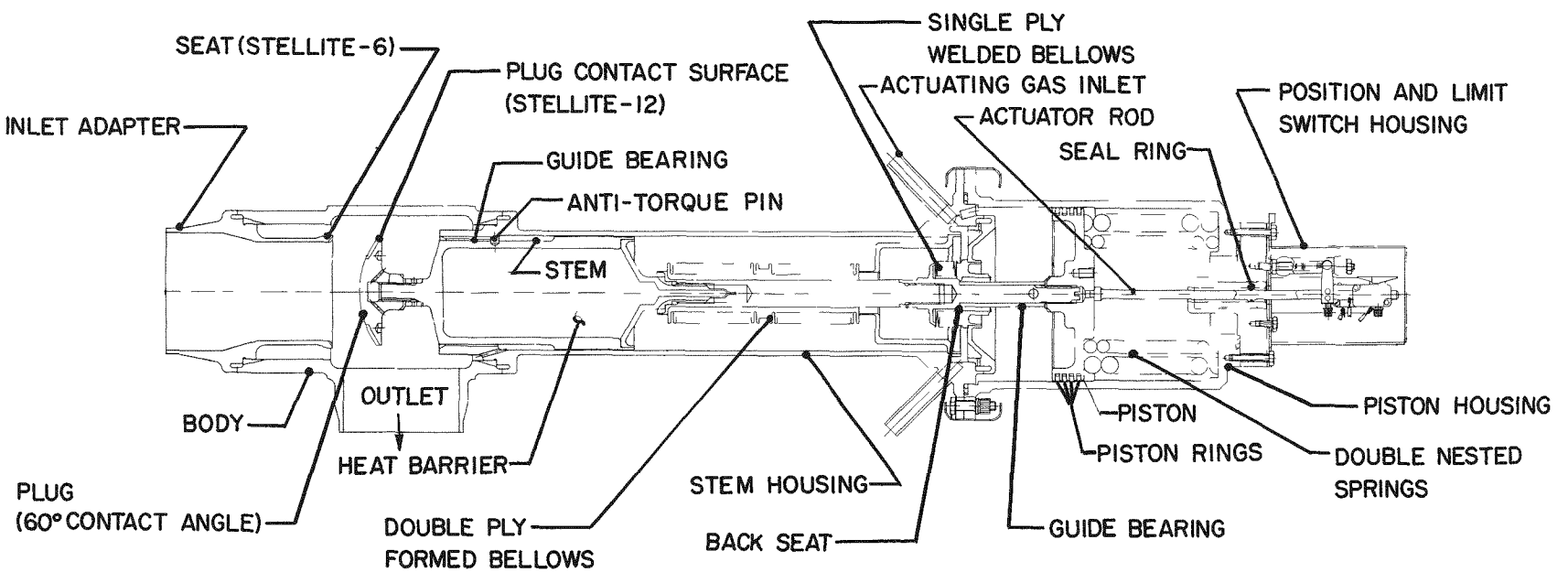

LCRE SECONDARY SYSTEM VALVE DESIGNS

SECONDARY SYSTEM ISOLATION
(CONTINUED)

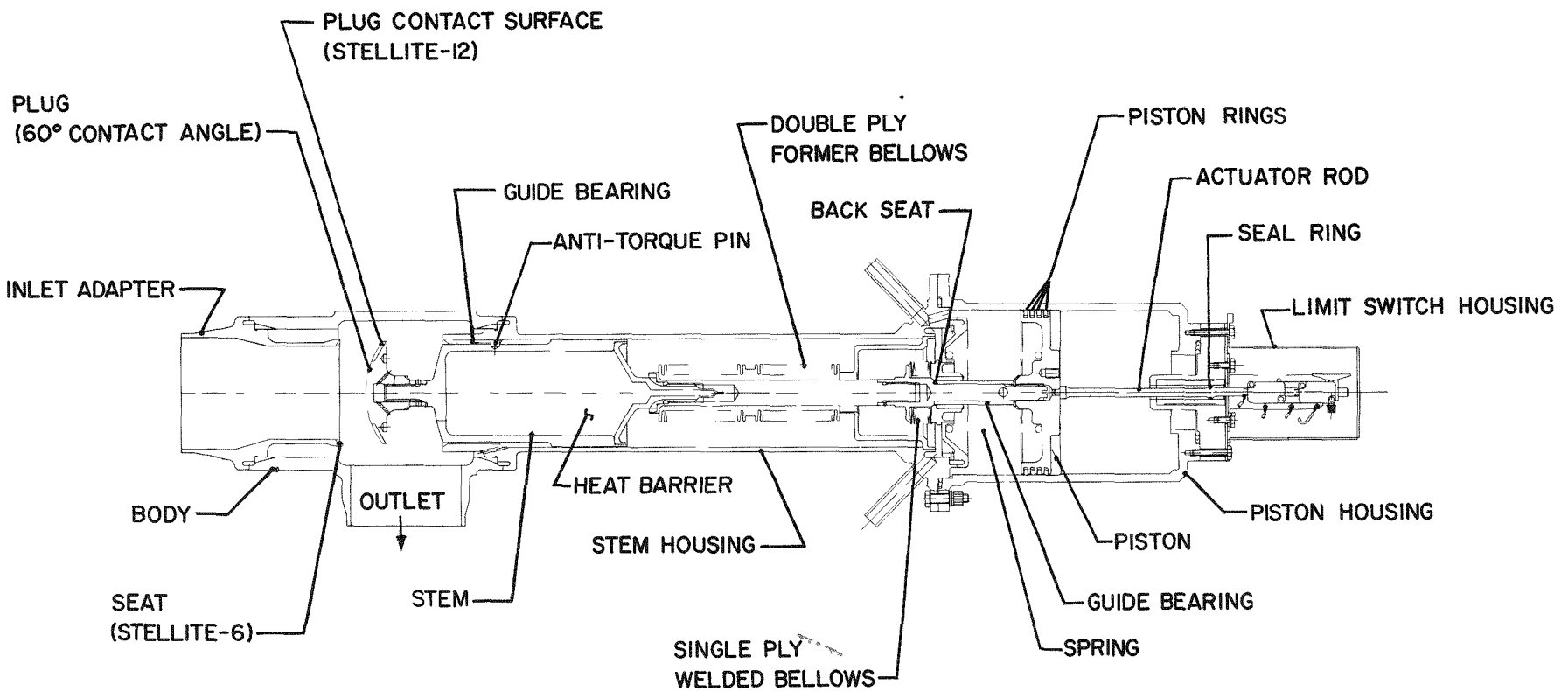

8. Non-Nuclear Systems Test

Rebuilding of the system, necessitated by an electrical short at the center terminal of the I^2R heater, was completed. All systems were started, a calibration program completed, and design point operation initiated on June 22. By the end of June, 206.5 hours of continuous operation at the design point (5 Mw and 2000F) had been completed without incident.

A drawing representing a sectional view through the center terminal seal, as it was rebuilt, is shown in Fig 36. The materials were selected for this arrangement on the basis of electrical insulating properties, structural characteristics, off-gassing and thermal stability characteristics, and availability. Viton-A seal rings, and NEMA G-7 and Super Mica 500 insulators make up the critical parts of the assembly. Prior to installation, bench tests were performed on this assembly in the non-nuclear systems test to determine sealing and permeability characteristics.

The start-up of the non-nuclear systems test was similar to the start-up reported in the last quarterly report, except that all phases of the start-up were accomplished in a much shorter time.

The results of the calibration program are shown in tabular form in Fig 37. This program was formulated to determine the heat transfer characteristics of the system as a function of liquid metal flow rate, temperature level and power transfer across the system. As shown on the chart, data was obtained at 11 different operating conditions, the eleventh point being the design point endurance condition. Performance predictions for the LCRE heat removal systems are confirmed by this data.

Plans call for operating the system at the design point for an extended period of time. The shroud gas system is being operated as a stagnant system, with make-up gas being added as necessary to replenish the gas removed for analysis. During the endurance run, a performance point will be calculated daily from the observed data to provide a basis for comparison of system performance as a function of operating time.

9. Instrumentation Development

Forty-seven, 10,000-hour endurance tests of 1/8-inch diameter Cb-1 Zr alloy-clad thermocouples are proceeding satisfactorily. Sixteen, W-5 Re/W-26 Re thermocouples have operated within tolerance limits of one percent for 3400 hours at 1950F in pure argon. The operating histories of these latter couples are shown in Fig 38. Maximum and minimum errors, as well as mean error in degrees F, are plotted for each of two groups of eight thermocouples. Two groups of ten chromel/alumel thermocouples, with junctions insulated from the cladding, show an average error of five degrees after 3200 hours under the same conditions (Fig 39). Seven Mo/W-26 Re thermocouples show no drift after 2600 hours under these conditions, but remain offset 60 degrees from the standard curve for this material (Fig 40). All of these thermocouples were fabricated and operated in a manner which excludes moisture and oxygen from the alumina insulation.

An order has been placed for calibrated tungsten/rhenium thermocouples, fabricated to the post-irradiation composition calculated for two representative neutron doses (refer to PWAC-631). These calibrations will confirm the maximum error expected in LCRE thermocouples due to transmutation.

Thermocouples have been fabricated of W-5 Re/W-26 Re, using a bimetallic sheath comprising AMS 5573 and Cb-1 Zr alloy tubes welded to a co-extruded joint before swaging. These thermocouples parted at about 1000F in the first heating portion of thermal cycling tests. Similar failure in AMS 5573 clad W-5 Re/W-26 Re couples indicates that the break-

NON-NUCLEAR SYSTEM TEST REPAIR

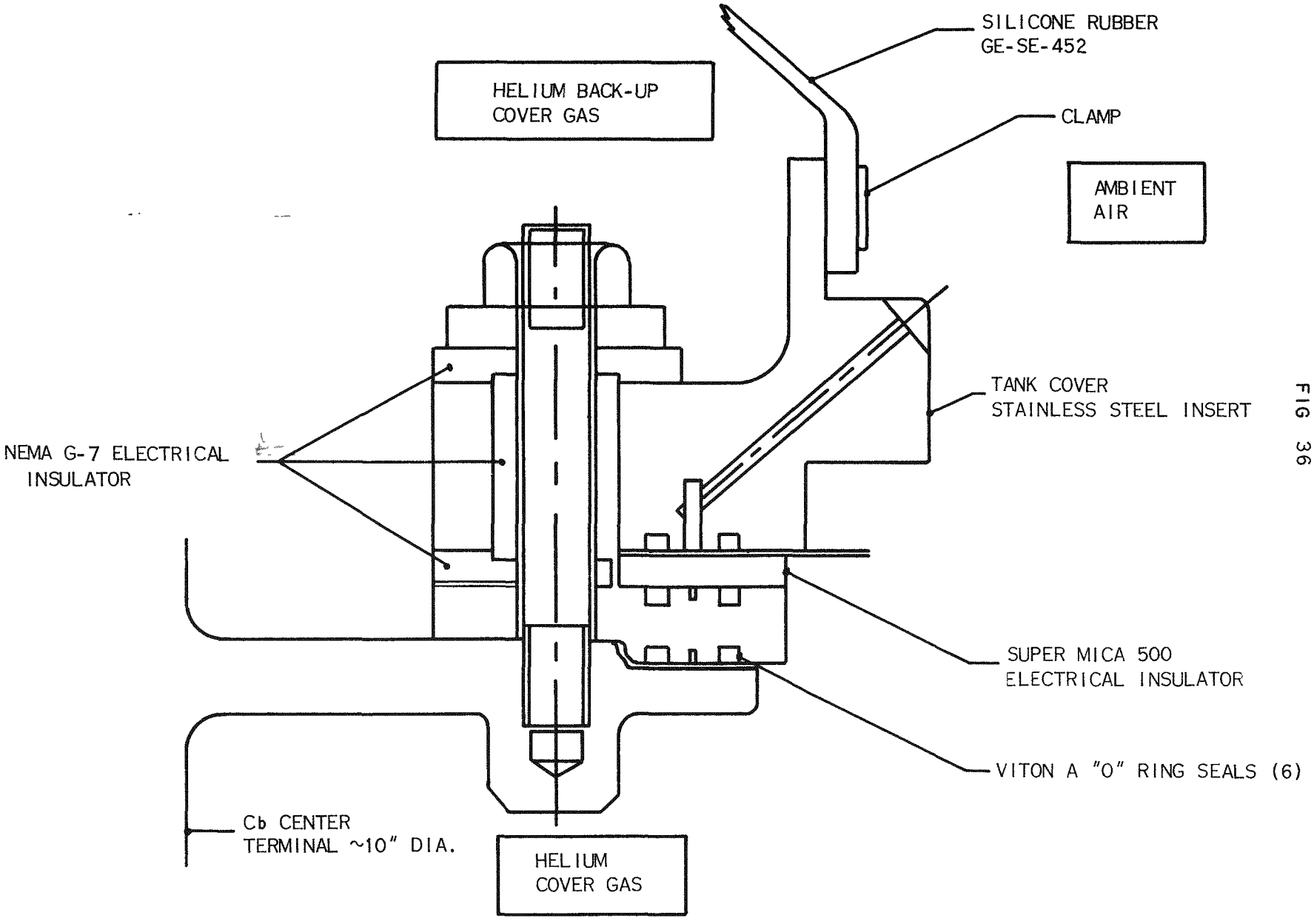

FIG 37

NON-NUCLEAR SYSTEM TEST OPERATING DATA

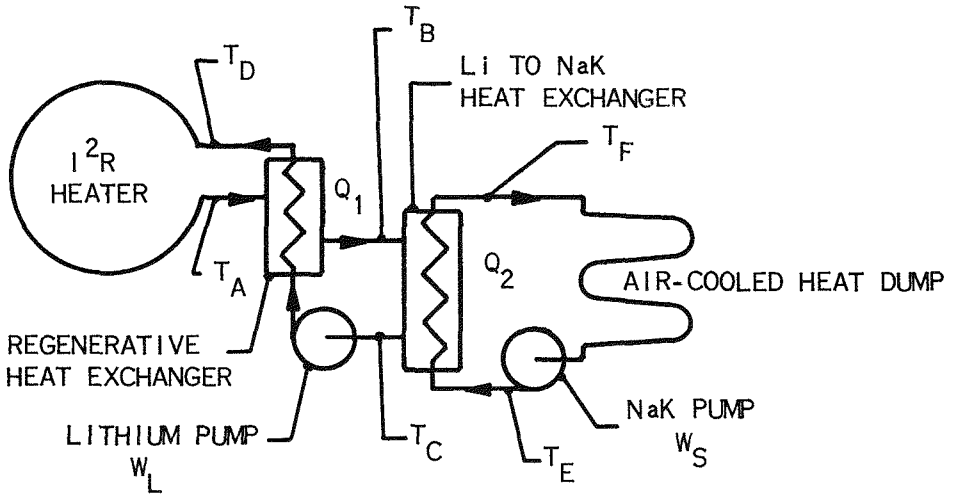

Performance Point	Q_2 (Mw)	Q_1 (Mw)	W_L (gpm)	W_S (gpm)	T_A (F)	T_B (F)	T_C (F)	T_D (F)	T_E (F)	T_F (F)
1	0.95	1.45	185	392	932	823	752	861	705	806
2	1.93	3.14	188	392	1192	953	813	1048	714	928
3	3.05	4.86	189	395	1459	1083	850	1223	713	1037
4	3.25	5.15	191	487	1462	1071	825	1213	709	992
5	2.79	4.75	168	472	1459	1046	804	1214	709	959
6	2.50	4.48	154	431	1463	1036	801	1222	712	952
7	2.15	4.15	138	386	1466	1031	799	1235	720	947
8	1.84	3.88	123	340	1455	999	780	1242	703	930
9	1.53	3.41	107	300	1434	978	762	1233	704	915
10	3.70	6.17	185	394	1703	1191	897	1399	714	1112
*11	5.02	8.43	190	395	1997	1319	921	1595	680	1211

*Endurance Conditions

OPERATING HISTORY OF EIGHT, 1/8 INCH DIA., Cb CLAD, W-5 Re/W-26 Re THERMOCOUPLES

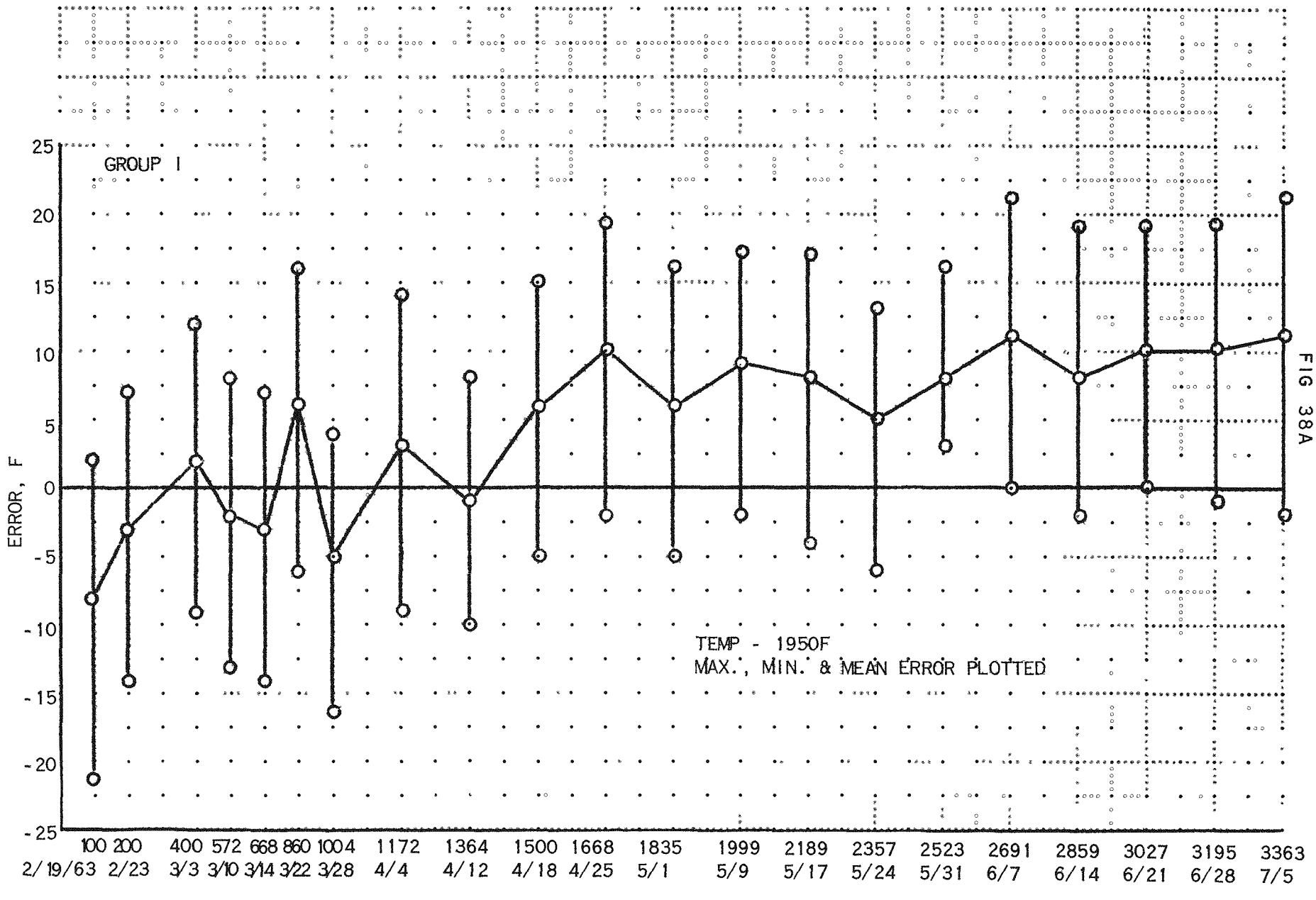

FIG 38A

OPERATING HISTORY OF EIGHT, 1/8 INCH DIA., Cb CLAD, W-5 Re/W-26 Re THERMOCOUPLES

(CONTINUED)

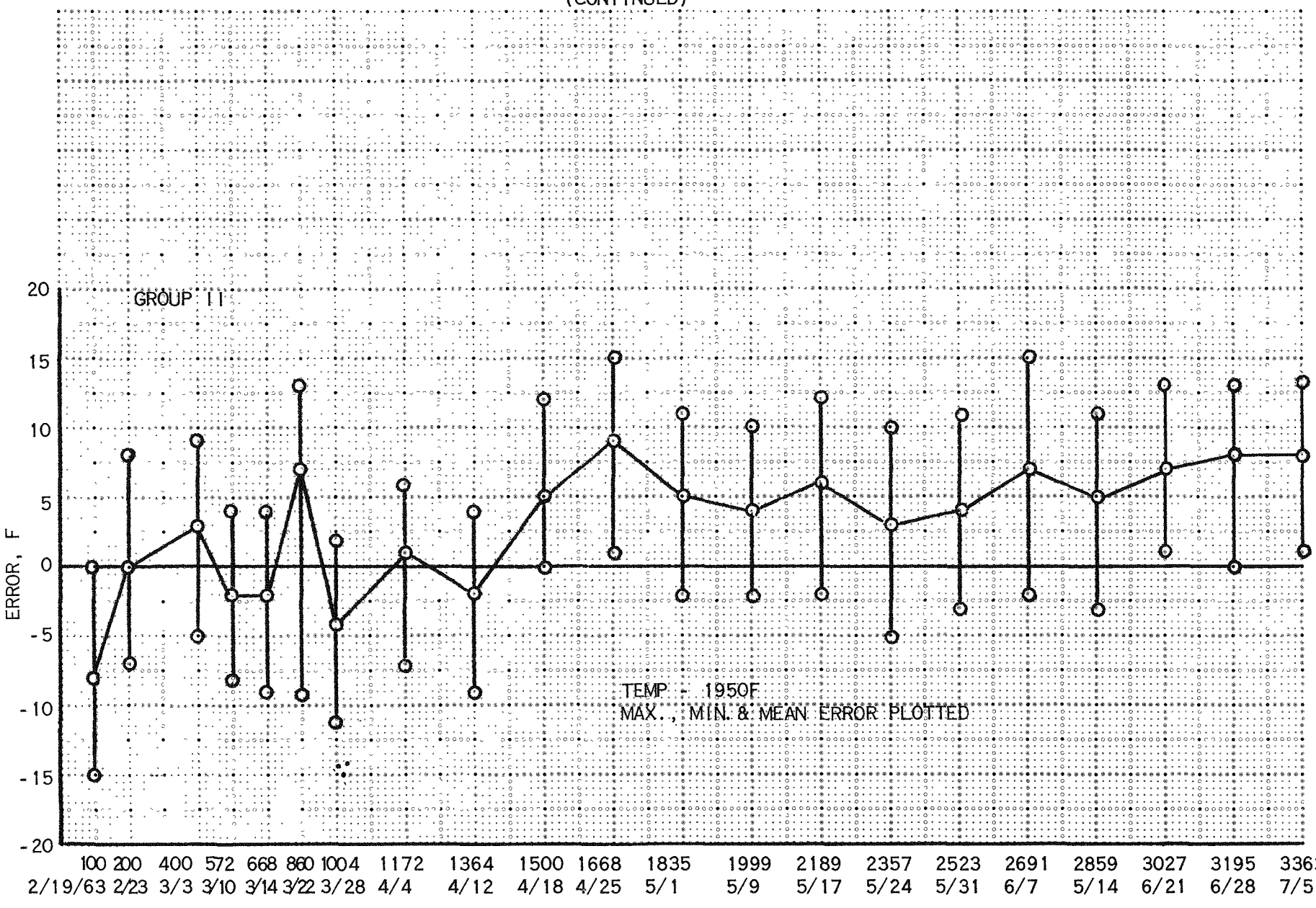

FIG 38B

OPERATING HISTORY OF TEN, 1/8 INCH DIA., Cb CLAD, CHROMEL/ALUMEL THERMOCOUPLES

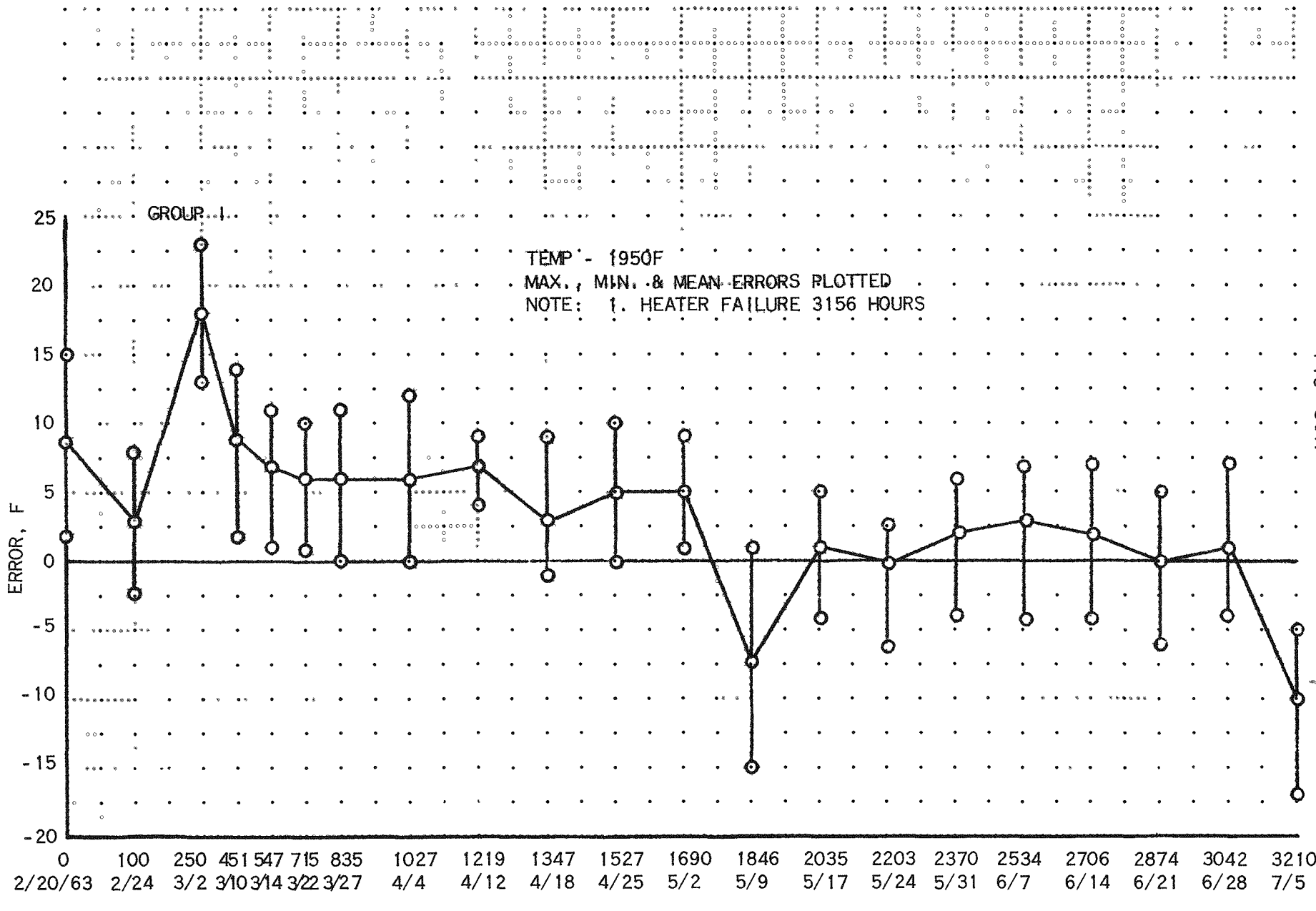

FIG 39A

OPERATING HISTORY OF TEN, 1/8 INCH DIA., Cb CLAD, CHROMEL/ALUMEL THERMOCOUPLES

(CONTINUED)

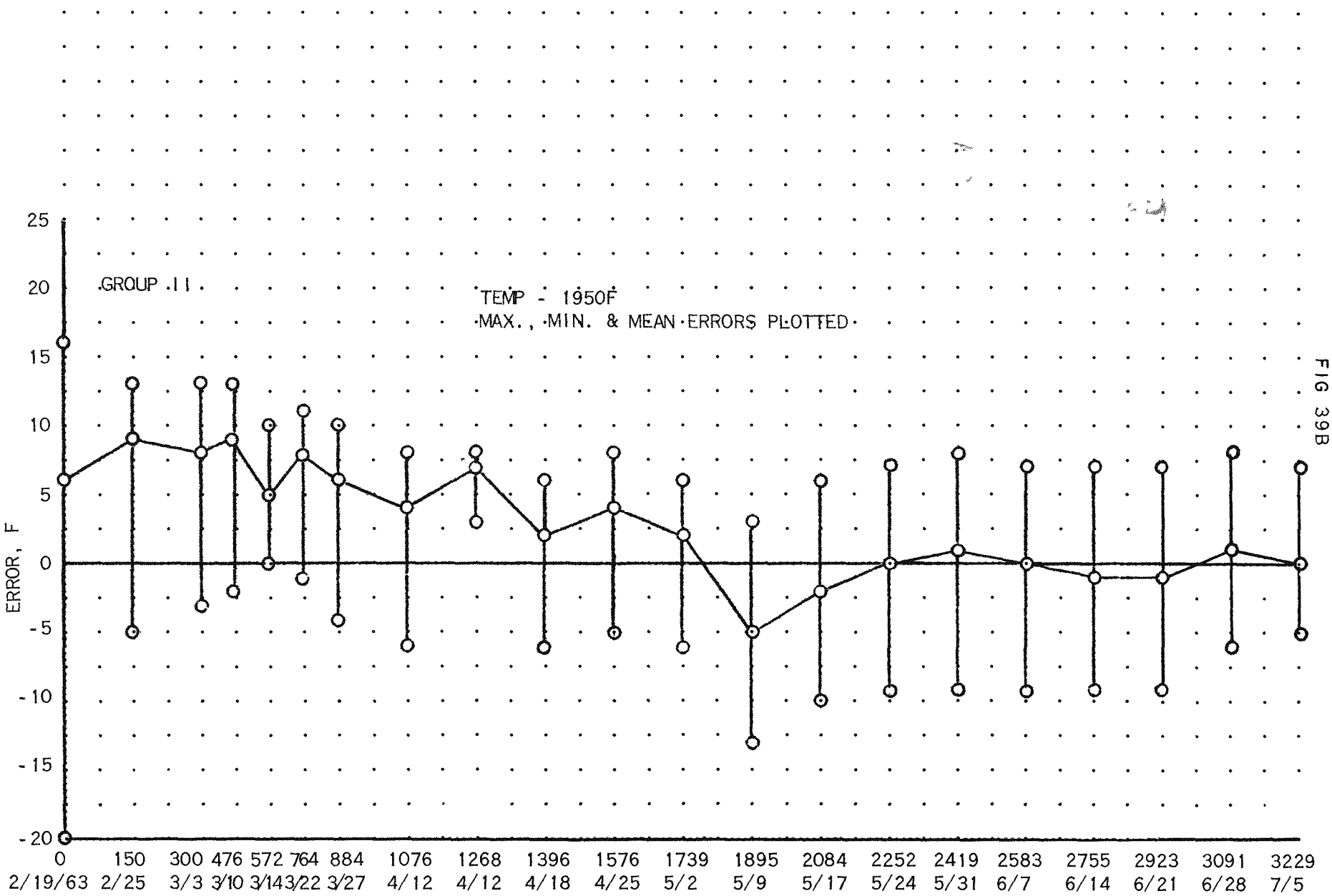

FIG 39B

OPERATING HISTORY OF SEVEN, 1/8 INCH DIA., Cb CLAD, Mo/W-26 Re THERMOCOUPLES

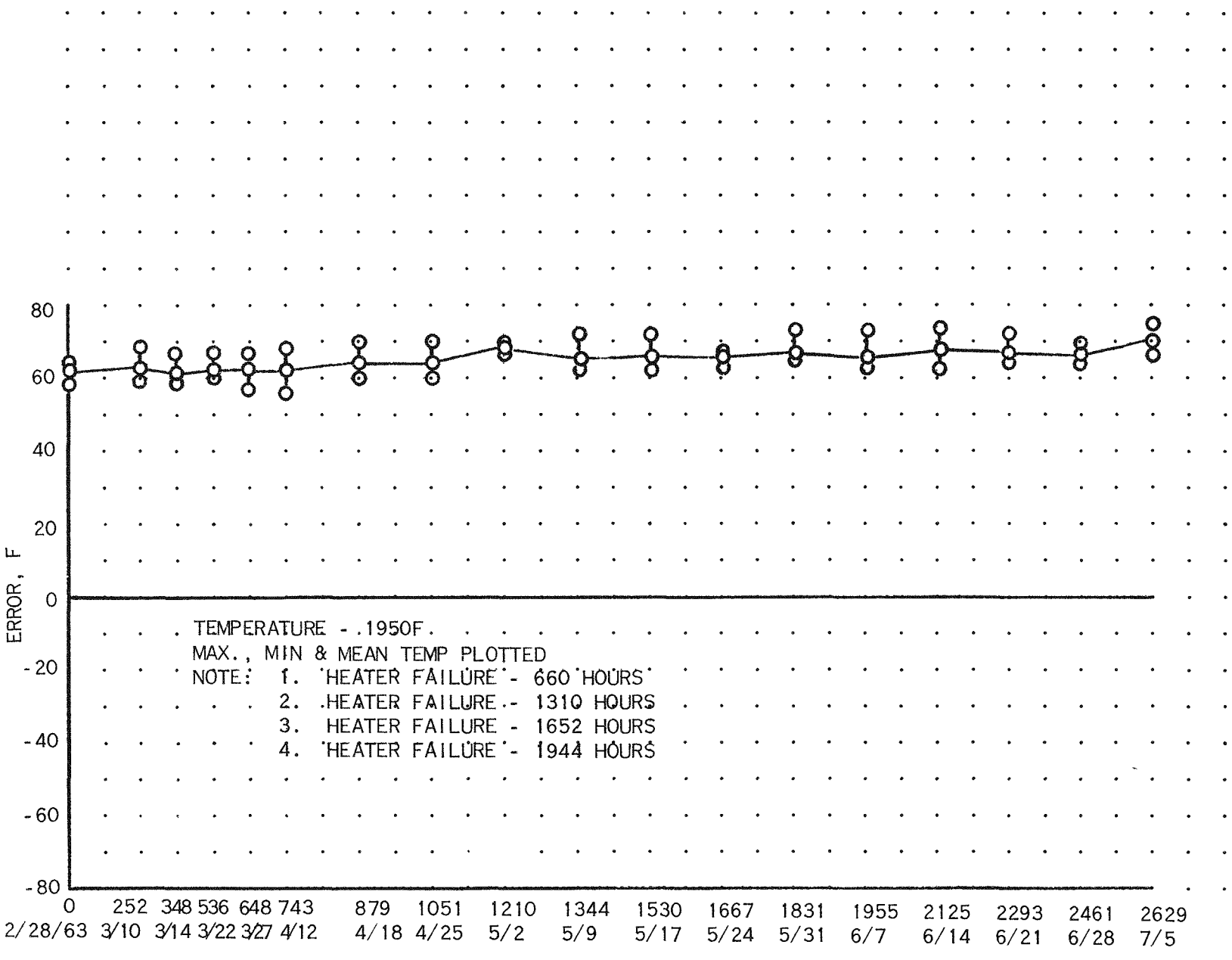

age is directly caused by differential thermal expansion. Since stainless steel-clad thermocouples previously fabricated from a different batch of W-5 Re/W-26 Re wire were successfully cycled many times over a 1000-hour period, the present difficulty seems to be due to either differences in wire or in the manufacturing process. Bimetallic-clad thermocouple samples, now being fabricated by vendors will be fabricated with less elongation in the wires in swaging, and will be thermal-cycled at CANEL. W-3 Re/W-25 Re wire is being evaluated as a substitute, since it apparently has greater ductility. The stability and transmutation characteristics of these new alloys should be comparable to those of the present alloys, but confirmation will be obtained by tests.

One of the ten Cb-1 Zr alloy continuous liquid metal probes on test in lithium at 1000F failed at 1300 hours. Posttest examination showed the failure to be a seal failure at the cold end, with resultant diffusion of air into the insulation. This was confirmed by leak-testing the seal. Since the probes are tested in pairs, the examination of this probe terminated the testing of a second probe, which was operating normally. The remaining eight probes are operating normally after 2800 hours, under the above conditions. Ten probes each of titanium and Cb-20 Ti alloy alternate materials are being fabricated for similar tests.

Inpile testing of four LCRE ion chambers and four fission counters in the Battelle Research Test Reactor was continued through this period. At 1500 hours, a test cable failed in one of the fission counter capsules, due to condensation of moisture evolved from a concrete shield plug. The capsule was removed and dried, the cable was replaced and the test resumed. One ion chamber was removed after 2156 hours of successful operation at 400F for posttest examination. The total dosage experienced by this chamber was 3.6×10^{11} ergs/gram (C) gamma, 8.6×10^{16} nvt thermal, and 7.5×10^{15} nvt fast neutrons. The exposed chamber is shown in Fig 41. The fiberglass electrical insulating tape cover was discolored to varying shades of brown, without detriment to its insulating function. Preliminary tests of the internal leakage resistances do not indicate significant decrease. One fission chamber was removed after 2180 hours of successful operation at 400F for posttest examination, which will be performed upon its receipt at CANEL. The remaining ion chambers and fission counters are operating satisfactorily after exposure times up to 2800 hours. Radiation sensor and preamplifier assemblies for additional proof testing are being fabricated.

10. Materials Development

a. Columbium-1 Zirconium Alloy

Evaluation of methods for developing improved strength in Cb-1 Zr alloy fuel pin cladding was continued. Methods included approaches for treating finished (CS-1831) tubing by carburizing, nitriding, and solution heat treatment. In addition, work was continued on modifications to melting and fabrication practices.

During the past quarter, 29 rupture tests in lithium were completed on specimens of fuel tubing. Three specimens remain on test. Results of these tests, summarized in Fig 42, confirmed that solution-treating finished tubing for one-half hour at 3100F resulted in a 10 to 15 percent increase in strength (PWAC-631). Raising the carbon content of finished tubing to the 500 ppm level was accomplished by coating the tubing with a graphite slurry and heating at 2000F to 2200F. Further treatment of this material at 2600F to 3100F enhanced the carbon distribution through the wall and produced significant increases in stress-rupture strength. Specimens of finished tubing with carbon restored in this manner were evaluated for stress-rupture strength after treatments of 6, 24, and 30 hours at 2600F, one hour at 2700F, one hour at 2900F, and one-half hour at 3100F. Compared to un-

REUTER-STOKES ION CHAMBER

MODEL RSN-83A SERIAL B-632 (90 INCHES OVER-ALL)
P&W CAPSULE NO. 392-1
AFTER 2156 HOURS OF IRRADIATION

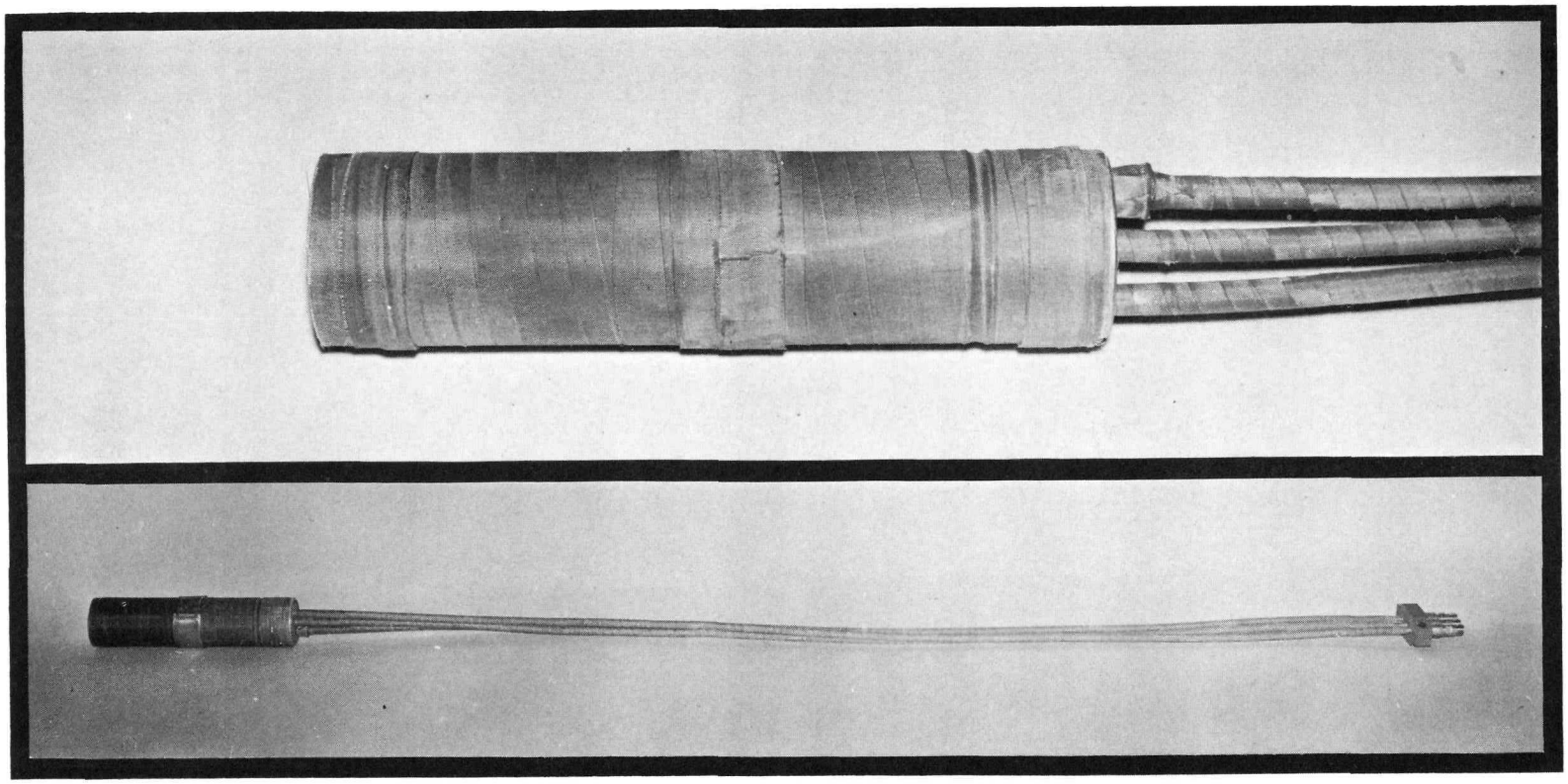

PWAC - 632
FIG 41

FIG 42

FUEL PIN CLADDING TUBE BURST TEST IN LITHIUM

(ALL TESTS HAVE RUPTURED UNLESS OTHERWISE NOTED)

Test Temp, F	Heat Code	Max. Test Stress KIPS	Test Time, hr.	Equivalent 2200F/10,000 hr. Rupture Stress, psi	Remarks
2400	PJHH	2.0	53	980	Nitride + 2200F/4 hr. anneal
		2.0	144	1250	Carbon + 2600F/6 hr. anneal
		2.0	221	1450	Nitrided + 3100F/1/2 hr. anneal
2200	PIHH	4.0	6	800	5 percent swage
2400		2.0	100	1100	Carbon + 2600F/30 hr. anneal
		2.0	112	1100	Carbon + 2600F/24 hr. anneal
		2.0	99	1100	Carbon + 2900F/1 hr. anneal
		2.0	200	1400	Carbon + 2900F/1 hr. anneal
2200	PIXY	4.0	12	840	5 precent swage
2200	PJVI	2.0	2757	1450	Carbon + 3100F/1/2 hr. anneal
2400		2.0	77	1080	Nitrided + 2200F/4 hr. anneal
		2.0	104	1150	Carbon + 2600F/6 hr. anneal
2200	PJVH	2.0	2970	1500	Carbon + 3100F/1/2 hr. anneal
2400		2.0	84	1080	Nitrided + 2200F/4 hr.anneal
		2.0	95	1100	Carbon + 2600F/6 hr. anneal
2200	PILY	4.0	140	1430	Carbon + 2700F/1 hr. anneal
		3.0	249	1150	Carbon + 2700F/1 hr. anneal
		3.0	223*	1100	Carbon+ 2900F/1 hr. anneal
		2.2	321	880	As rec'd + 3100F/1/2 hr. anneal
2400		2.0	181	1350	Nitrided + 3100F/1/2 hr. anneal
		2.0	48	960	Nitrided + 2200F/4 hr.anneal
		2.0	66	1000	Carbon + 2600F/6 hr. anneal
2200	GC-46 (Cb-1Zr-.05C)	4.0	89	1320	2700F/1 hr. anneal
		3.0	116**	960	2700F/1 hr. anneal
2400		2.0	24	820	As rec'd
		2.0	49	950	As rec'd
		2.0	351**	1600	2900F/1 hr. anneal
		2.0	660*	1800	2900F/1 hr. anneal
2200	GC-47 (Cb-1Zr-.14C)	4.5	28	1050	As rec'd
		2.6	145**	920	As rec'd
2400		2.0	62	1030	As rec'd
		2.0	641*	1780	2900F/1 hr. anneal

Note: All specimens were annealed at 2200F for two hours prior to test.

* Still on test

** Specimen had internal cracks which affected test results

treated, finished tubing, a strength increase of 40 to 50 percent was realized by the 2600F and 2700F heat treatments, and an increase in strength of 50 to 100 percent was realized by heat-treating for one hour at 2900F. Over 100 percent increase in strength was achieved by the 3100F, one-half hour anneal. However, this treatment produced an undesirably large grain size.

Similar experiments on gas-nitrided Cb-1 Zr alloy tube specimens, heat-treated at 2200F (four hours) or 3100F (one-half hour) showed 50 and 100 percent increase in strength, respectively. However, nitrogen restoration does not appear as promising as carbon restoration. Higher strengths are realized by carbon addition, and nitrogen tends to be depleted in a flowing lithium system. Evidence was obtained to indicate that whereas, carbon is comparatively stable in Cb-1 Zr alloy when exposed to lithium, nitrogen is removed by leaching. Carbon-restored tubing exposed for 500 hours in a 2000F maximum temperature in the LCCD-1 test system, 400F thermal gradient loop, showed no appreciable change in carbon content. Nitrogen-restored tubing similarly exposed showed a loss of 600 ppm from a pretest analysis of 1400 ppm. Two small melts of Cb-1 Zr alloy with 500 and 1200 ppm carbon were fabricated into tubing and evaluated for creep-rupture strength in the as-fabricated condition, and after 2700F and 2900F heat treatments. The as-fabricated tubing showed a 20 to 50 percent increase in strength compared to Cb-1 Zr alloy (CS-1831) tubing in the same condition. Heat treating at 2700F for one hour raised the strength level in one test by almost 100 percent. The 2900F, one-hour treatment appears very promising for this material. Specimens still on test are exhibiting about 150 percent increase in strength. Although two ruptures on specimens of this material revealed low strength, defects were discovered in subsequent examination.

Production of larger quantities of modified Cb-1 Zr alloy tubing (500 to 800 ppm C) is proceeding on material whose strength will be initially evaluated in the 2900F, one-hour, heat-treated condition.

Creep-rupture testing of Cb-1 Zr alloy specimens, machined from heavy plate, continued. Five creep tests in lithium completed 10,000 hours and were discontinued. Four other tests ruptured. Seven specimens were continued in test. Current status of uniaxial tests is as follows:

Uniaxial Creep-Rupture Tests in Lithium
(Heat Code PJDL Unless Noted)

Test Temp, F	Max. Test Stress, KIPS	Test Time, hr.	Total Extension, %	Remarks [1]
1600	6.0	10,000	0.565 [2]	Discontinued
	12.0	10,004	1.29 [2]	Discontinued
1800	3.5	10,000	0.96 [2]	Discontinued
	7.0	8,942	27.7 [2]	Ruptured
2000	1.75	9,591	0.73 [2]	In test
	2.0	10,000	1.3 [2]	Discontinued
	2.0	6,150	8.3	Code PHUM Extruded Pipe in Test

Test Temp, F	Max. Test Stress, KIPS	Test Time, hr.	Total Extension, %	Remarks[1]
	2.5	10,028	3.8	Discontinued
	3.0	6,461	19.2	In Test
	3.0	5,026	8.7	In Test, Weld
2200	1.2	8,677	3.6[2]	In Test
	1.75	2,688	49.2[2]	Rupture
	2.0	1,579	11.8[2]	In Test, Weld
	4.0	177	29.0[2]	Rupture
2400	0.75	9,197	34.4[2]	In Test
	1.5	415	44.6[2]	Rupture

[1] All specimens annealed at 2200F prior to test.

[2] Measured elongation after completion of test; all other extension measurements are from external dial gauge readings.

Two rupture tests were conducted in vacuum to provide short rupture data and primary creep data.

Creep Tests in Vacuum
(Specimens annealed at 2200F prior to test)

Temp, F	Heat Code	Max. Test Stress, KIPS	Test Time, hr	Total Extension, %	Remarks
2400	PJHJ	3.0	33.5	75.3	Rupture
2400	PJHJ	3.0	57.4	60.4	Rupture

Biaxial tube burst tests in lithium were continued for the purpose of evaluating long time creep-rupture behavior of typical reactor system weldments. The specimens were originally prepared from heavy wall, extruded pipe. Eight specimens were continued on test, one was discontinued because of rig malfunction, and one ruptured. Data is as follows:

Biaxial Tube Burst Tests in Lithium

Test Temp, F	Heat Code	Max. Test Stress, KIPS	Test Time, hr	Remarks[(3)]
1600	PGSG(2)	6.0	4,696	In Test
1600	PJYT(2)	9.0	210	In Test
1600	PHNF(2)	21.0	210	In Test
1800	PJYT(2)	3.5	3,857	In Test
1800	PHNF(2)	5.0	810	In Test
1800	PHNF(2)	7.0	210	In Test
2000	PGSI(2)	2.0	5,730	In Test
2000	PGSG(2)	3.0	5,552	Disc't; furnace failure
2000	PGSI(2)	4.0	2,682	Rup't; 48% growth
2000	PGSI(1)	5.0	15,271	In Test

Biaxial Tube Burst Tests in Lithium
(continued)

Note: (1) Tube-to-plate weld
(2) Girth weld
(3) All specimens annealed at 2200F prior to test

b. Reactor Materials Compatibility

Liquid metal compatibility testing of B_4C samples from vendor-supplied, LCRE reflector material, was completed at temperatures of 650F, 800F, and 1000F. No change occurred in specimens exposed to sodium at temperatures up to 1000F. Complete disintegration of the tested compacts occurred in potassium at 650F and above and in NaK at 800F and above. Disintegration occurred within five minutes of contact (Fig 43). The disintegrated material, even after 5000 hours exposure to 1000F eutectic NaK, was retained by a 160-micron, stainless steel filter. Tests at 1000F for 10,000 hours of B_4C and eutectic NaK in type 316 stainless steel capsules have shown that disintegration of the B_4C causes no detrimental carbon or boron transfer into the type 316 stainless steel.

Tests have been initiated with B_4C specimens, recently available from a second vendor. In contrast to the behavior of B_4C discussed above, these specimens have not been affected by exposure to NaK or potassium under identical test conditions. Specimens completed 1500 hours in 1000F eutectic NaK without evidence of attack. Analyses and testing are being continued to determine the reasons for this difference in behavior.

It has been determined that the dark region previously reported (PWAC-624, page 68) in beryllium coupled with type 316 stainless steel, was caused by galvanic corrosion which occurred when beryllium and stainless steel were polished together, using an alumina slurry. Addition of sodium nitrate to the polishing media eliminated the effect. As previously reported (PWAC-631, page 71) spectrographic analyses of material from zones immediately adjacent to the beryllium-stainless steel interface confirmed the absence of foreign material. Tests of the beryllium-eutectic NaK, type 316 stainless steel, erosion and corrosion loops NSBA-1 and NSBA-2 were shut down after completing scheduled tests of 5000 and 2000 hours, respectively. Posttest examination of these beryllium specimens will be performed. Evaluation of beryllium specimens exposed to 800F eutectic NaK alloy for 5000 hours in a pumped loop will be completed during the next quarter.

An investigation was started of the rate of lithium attack as a function of oxidation contamination on Cb-1 Zr alloy. Specimens of 0.032-inch wire having large equiaxed grains were prepared with oxygen in solid solution produced by a quench from 3700F and with the more stabilized structure produced by a one or two hour, 2200F heat treatment. Previous studies (PWAC-621 and PWAC-622) have shown that lithium attack can occur if the concentration of oxygen in solid solution exceeds 250 ppm or if the oxygen concentration of the stabilized alloy exceeds a nominal 3000 ppm. In this investigation, short time corrosion behavior was studied by inserting wire specimens for predetermined intervals into a beaker of 1500F lithium contained in purified inert gas. The evaluation of liquid metal attack was performed metallographically on a 0.5 inch section from the center of the region contacting the lithium. The results of testing are presented as follows:

FIG 43

INTERACTION OF BORON CARBIDE COMPACT SAMPLES WITH MOLTEN ALKALI METALS

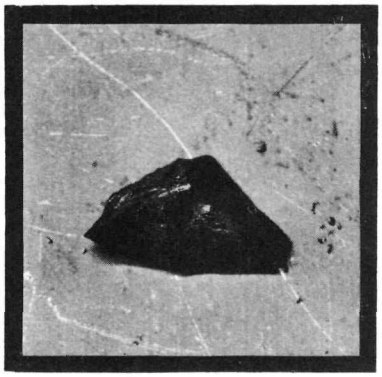

PRETEST

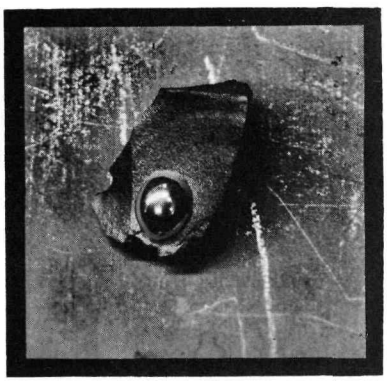

650F NaK

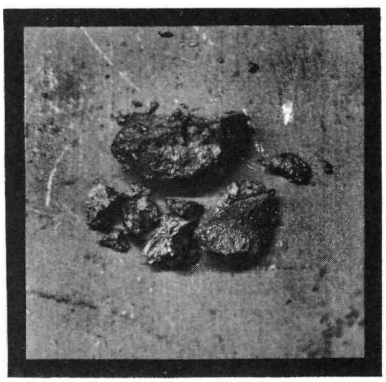

650F POTASSIUM

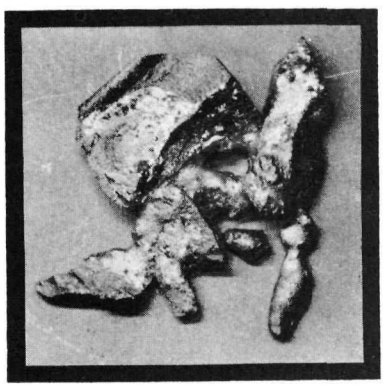

800F NaK

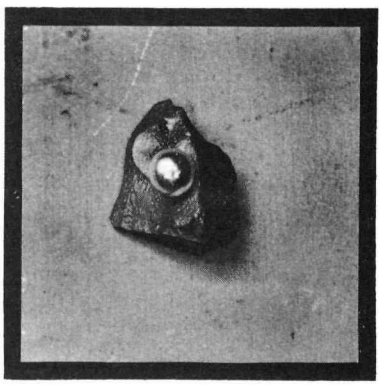

1000F SODIUM

MAGNIFIED: 1X

SHOWING THE DELETERIOUS EFFECT PRODUCED BY 5 MINUTES CONTACT WITH POTASSIUM AND POTASSIUM ALLOY (NaK; 78% K)

Cb-1 Zr Alloy Specimens Containing
Oxygen in Solid Solution as Quenched from 3700F

Oxygen, ppm	Exposure to 1500F Li, Minute	Results
195	1	No attack
195	5	No attack
180	10	No attack
180	20	No attack
300	1	No attack
300	10	No attack
500	1	No attack
500	5	10 percent of grain boundaries penetrated
560	10	20 percent of grain boundaries penetrated
560	20	50 percent of grain boundaries penetrated

Cb-1 Zr Alloy Specimens Containing Oxygen
Stabilized by One Hour-2200F Heat Treatment

Oxygen, ppm	Exposure to 1500F Li, Minute	Results
2000	1	Single grain boundary 0.003 inch penetration
2000	5	No attack
2600	10	No attack
2600	20	No attack
3000	1	No attack
3000	10	50 percent of grain boundaries penetrated
3700	1	50 percent of grain boundaries penetrated
3700	5	60 percent of grain boundaries penetrated
3500	10	100 percent of grain boundaries penetrated
3500	20	100 percent of grain boundaries penetrated

Examination of this data shows that with an oxygen concentration of 300 ppm in solid solution, no lithium attack was observed even after 10 minutes exposure. Previous experience has shown that similar Cb-1 Zr alloy specimens would be attacked by lithium in 50 hours. The columbium alloy specimens containing 3000 ppm oxygen, stabilized by a 2200F heat treatment, showed lithium attack after ten minutes exposure to lithium, but not after one minute. Specimens containing 3700 ppm oxygen were attacked within one minute. It was concluded that the rate of attack by lithium is extremely rapid and relatively insensitive to oxygen concentration within the range tested.

It is interesting to note that only intergranular penetration was observed in these short-time exposures, whereas, transgranular attack also has been observed in similar specimens after 50-hour exposures. These results suggest that the transgranular penetration is a much slower process. The specimen containing 2000 ppm oxygen, which exhibited a 0.003 inch penetration in one grain boundary, apparently contained a localized contamination and must be considered an anomaly. Additional testing will be directed toward determining the onset of transgranular penetration, the effect of a fine grain structure and the effect of higher and lower temperatures.

c. Materials Fabrication and Processing Development

A study is in progress to evaluate protective coating as a means for minimizing contamination of Cb-1 Zr alloy, lithium containment vessels during protracted exposure to inert gases at elevated temperatures. A four-inch diameter SnAl-1 coated, Cb-1 Zr alloy pressure vessel, operating in a purified helium atmosphere at 2000F, gave indications of failure after 7564 hours of test, but, because of a plugged lithium supply line, the leak was considered negligible. The test was continued to 7923 hours before termination, due to rupturing of the Inconel shroud by lithium attack. Penetration of air through the ruptured shroud resulted in pressure vessel oxidation which obscured the failure site. A similar test, in which contamination prevention is provided by tantalum foil wrapping, completed 8102 test hours at 2000F in a helium atmosphere containing 100 ppm air and flowing at the rate of 50 cc per minute.

Testing of the third in the series of tantalum foil-wrapped loops (LCCBK-9) was interrupted after 1359 hours, due to a helium blower motor failure. Repairs were completed and testing was continued to 1504 hours of a 5000-hour scheduled test. The SnAl-1 coated, Cb-1 Zr alloy corrosion loop LCCBK-6 completed 3303 hours of a scheduled 5000-hour test at a maximum lithium temperature of 2000F and a thermal gradient of 1000F. Contamination levels of the helium cover gas have been maintained below one ppm.

Work was continued on the development of seizure-resistant, columbium surface layers on Cb-1 Zr alloy parts. The carburizing process involves thermal treatment of a cold-sprayed graphite slurry coating in vacuum or inert atmosphere. Carbide layer thickness data was determined for various conditions of firing time and temperature and mathematical relationships were established. The carbide layer thickness data tabulated below is plotted in Fig 44. The effects of processing time and temperature for the range of conditions studied, fit the equation:

$$\text{Log}\ \frac{s^2}{t} = K\,T^{-1}$$

where: s = carbide layer thickness, mils

t = time, hours

K = proportionality constant, $(\text{mils})^2/\text{hr/deg., K}$

T = absolute temperature, degrees K

The calculated activation energy for the growth of the carbide layer by this process is -72.5 kcal/mole, which is in good agreement with -78.8 kcal/mole reported in Battelle Report No. BMI-1445. The calculated effective diffusivity of the elements in columbium carbide layer is 1.1×10^{-10} $cm^2/sec.$ at 2600F. Comparison between the results of this study and accepted literature values for the temperature dependence of the diffusivity of carbon in columbium metal, -27 to -33 kcal/mole, reveals that transport through the carbide layer represents the rate controlling step in this surface carburizing process.

FIG 44

TEMPERATURE DEPENDENCE OF COLUMBIUM CARBIDE FILM GROWTH RATE

3 MG/CM^2 GRAPHITE SLURRY ON Cb-1 Zr ALLOY

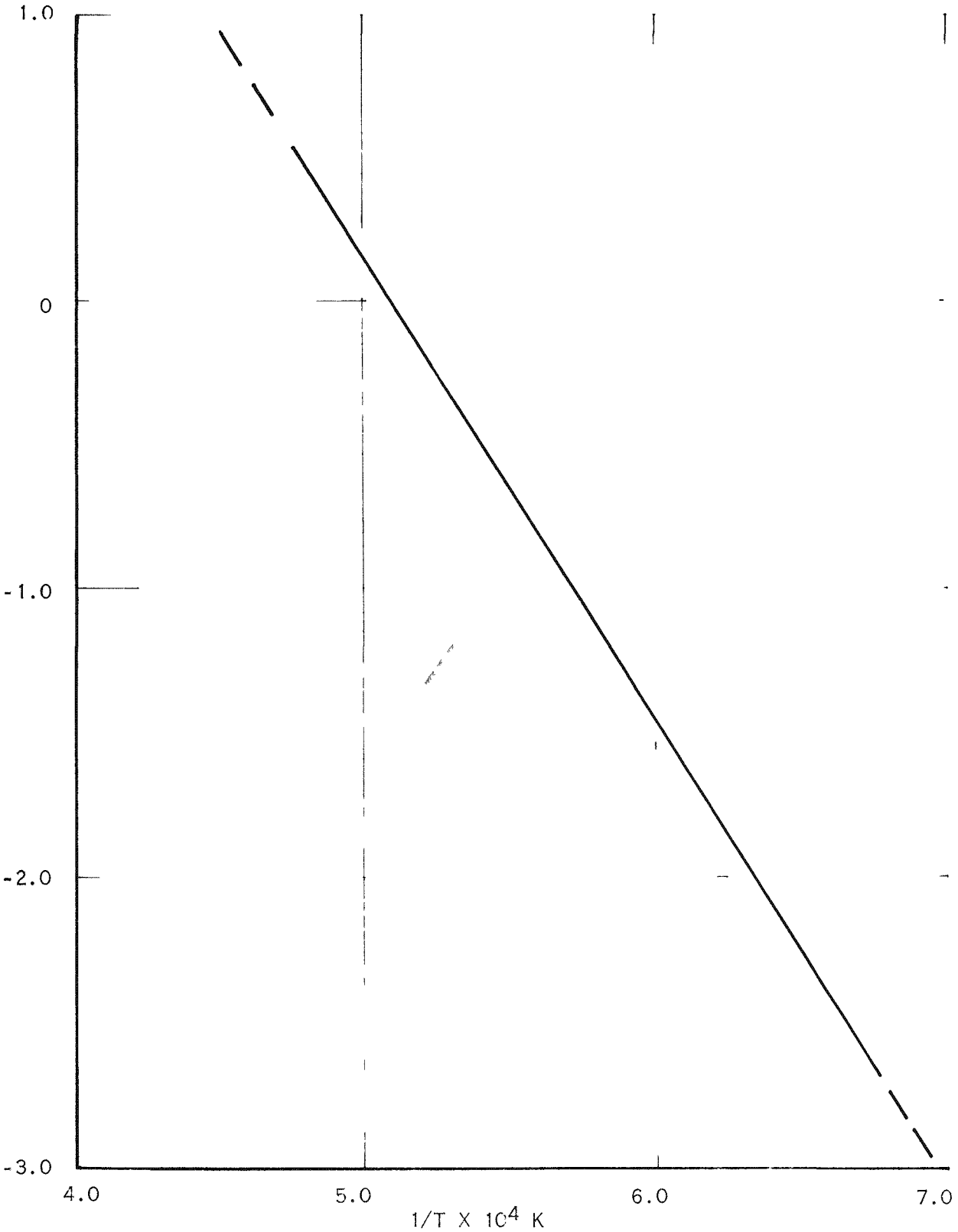

Processing Data for Slurry Carburization of Cb-1 Zr Alloy*

Specimen No.	Firing Temp, F	Time, hr	Carbide Layer Thickness, mils
1	2200	4.0	0.09
2	2400	1.0	0.1
3	2600	0.5	0.17
4	2600	4.0	0.45
5	2600	1.0	0.63
6	2800	1.0	0.51
7	3100	0.5	0.70
8	3300	0.5	1.25

*Initial slurry coating weight on each specimen was 2.8 to 3.0 mg/cm^2

Friction and wear test evaluation of slurry-deposited columbium carbide layers has not begun, but metallographic analysis is complete. Photomicrographs showing the effect of firing time and temperature upon carbide case thickness are presented in Figs 45 and 46.

An investigation of the use of methane-argon mixtures for high temperature carburization of Cb-1 Zr alloy parts is partially finished. This work was undertaken as an alternate carburizing method in case the problem of excess carbon removal from slurry-coated parts should become an obstacle to the processing of particular Cb-1 Zr alloy shapes. Carbide layers, 0.1 to 0.2 mils thick, have been obtained during a six-hour, 2200F treatment in an argon-five volume percent methane atmosphere flowing at the rate of 20 retort volume changes per hour. This work will be reported in detail upon completion of a program of chemical analyses.

The investigation of the interdiffusion of Cb-1 Zr alloy with type 316 stainless steel has been completed. Extrapolation from data reported in PWAC-623 indicated that a diffusion layer approximately 0.1 mil thick could be expected on specimens heated for 10,000 hours at 1350F. Electron microscopy examination of specimens heated at 1350F for 115, 400, and 900 hours showed diffusion had occurred to depths of 0.015, 0.02 and 0.03 mil, respectively. A log-log plot (Fig 47) of these diffusion zone widths against time indicated a diffusion zone of approximately 0.07 mil would be formed in 10,000 hours. The validity of these extrapolations has been demonstrated in Figs 48 and 49 by results of optical and electron metallographic examination. These revealed a 0.06 mil diffusion zone on a diffusion couple heated at 1350F for 9300 hours.

It should also be noted that a large volume of a second phase, identified as sigma by X-ray diffraction, has developed in the stainless steel. Particles of this phase appear to have bonded to a continuous layer formed at the bond interface. This layer was identified by electron diffraction as CbC.

Electron microprobe analysis of the diffusion couple showed an increase in the chromium concentration at the interface and an increase in sigma phase concentration. The iron was found to be lower in concentration in the sigma phase than in the matrix, with the nickel concentration following the iron concentration changes. From this data, it was assumed that the $CR_{23}C_6$ was the source of chromium for the sigma and, also, the source of carbon for the formation of CbC. It was postulated on this basis that the CbC

COLUMBIUM CARBIDE SURFACE LAYERS ON Cb-1 Zr ALLOY

EFFECT OF TIME AND TEMPERATURE ON CARBIDE LAYER THICKNESS

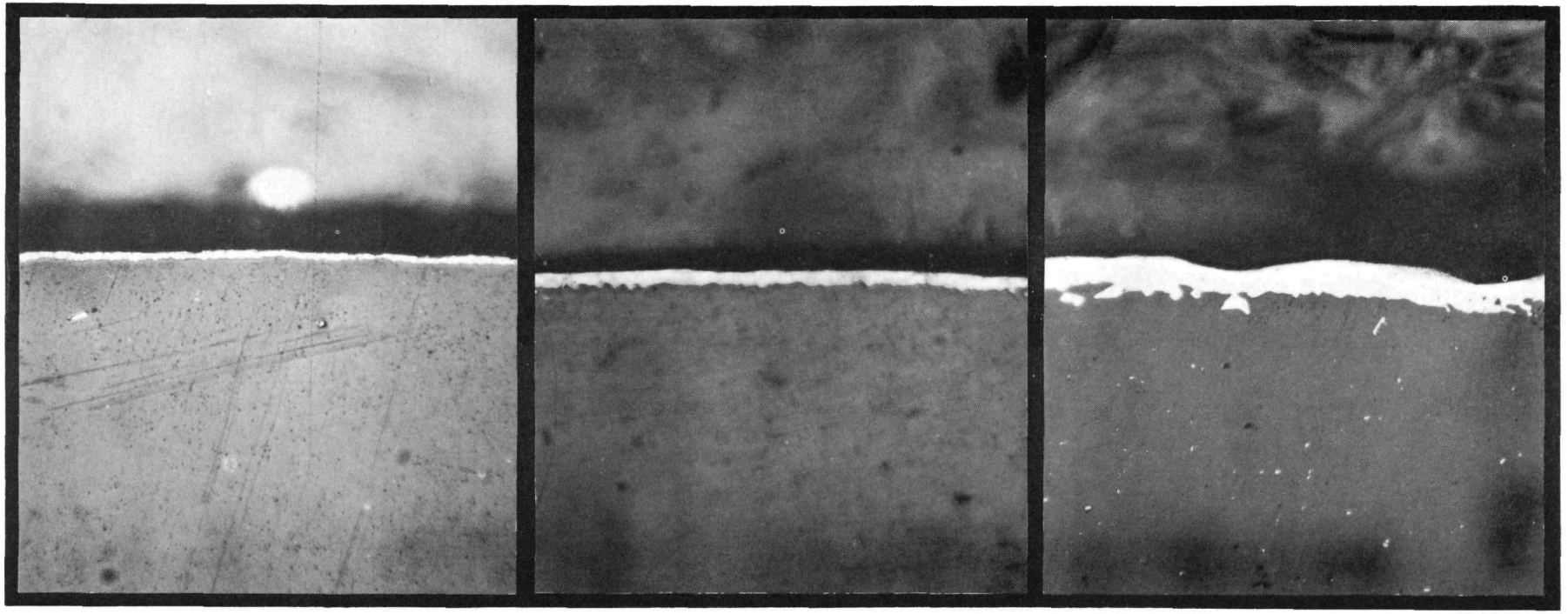

	MAGNIFIED: 500X	MAGNIFIED: 1000X	MAGNIFIED: 500X
SLURRY COATING WEIGHT (MG/CM^2)	3.0	3.0	3.0
FIRING TIME, HRS	4	1	6
FIRING TEMPERATURE, F	2200	2400	2600
CASE THICKNESS, MILS	0.09	0.1	0.63

2679-2
2597-70
2597-80

COLUMBIUM CARBIDE SURFACE LAYERS ON Cb-1 Zr ALLOY

EFFECT OF TIME AND TEMPERATURE ON CARBIDE LAYER THICKNESS

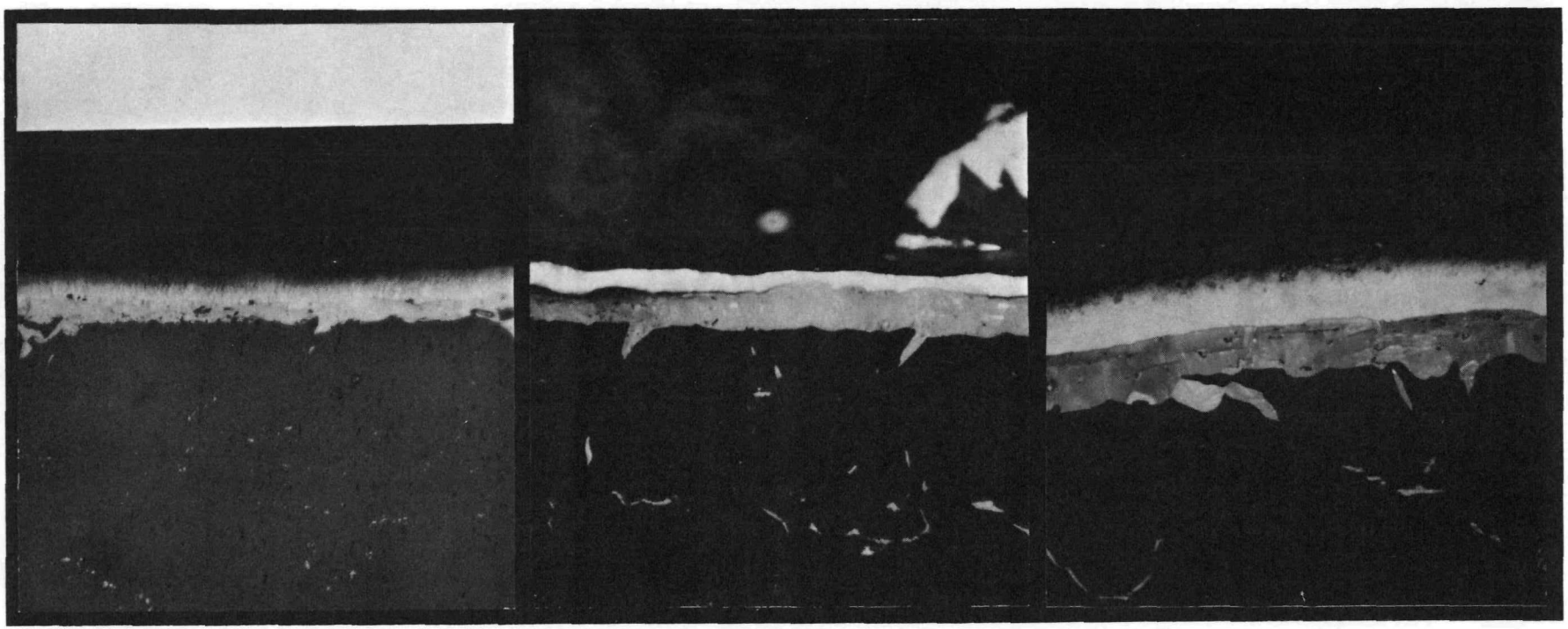

	MAGNIFIED: 500X	MAGNIFIED: 500X	MAGNIFIED: 500X
SLURRY COATING WEIGHT (MG/CM^2)	3.0	3.0	3.0
FIRING TIME, HRS	1	0.5	0.5
FIRING TEMPERATURE, F	2800	3100	3300
CASE THICKNESS, MILS	0.51	0.70	1.25
	2597-92	2597-108	2597-102

FIG 47

COMPARISON OF Cb-1 Zr ALLOY-TYPE 316 STAINLESS STEEL DIFFUSION ZONE WIDTHS

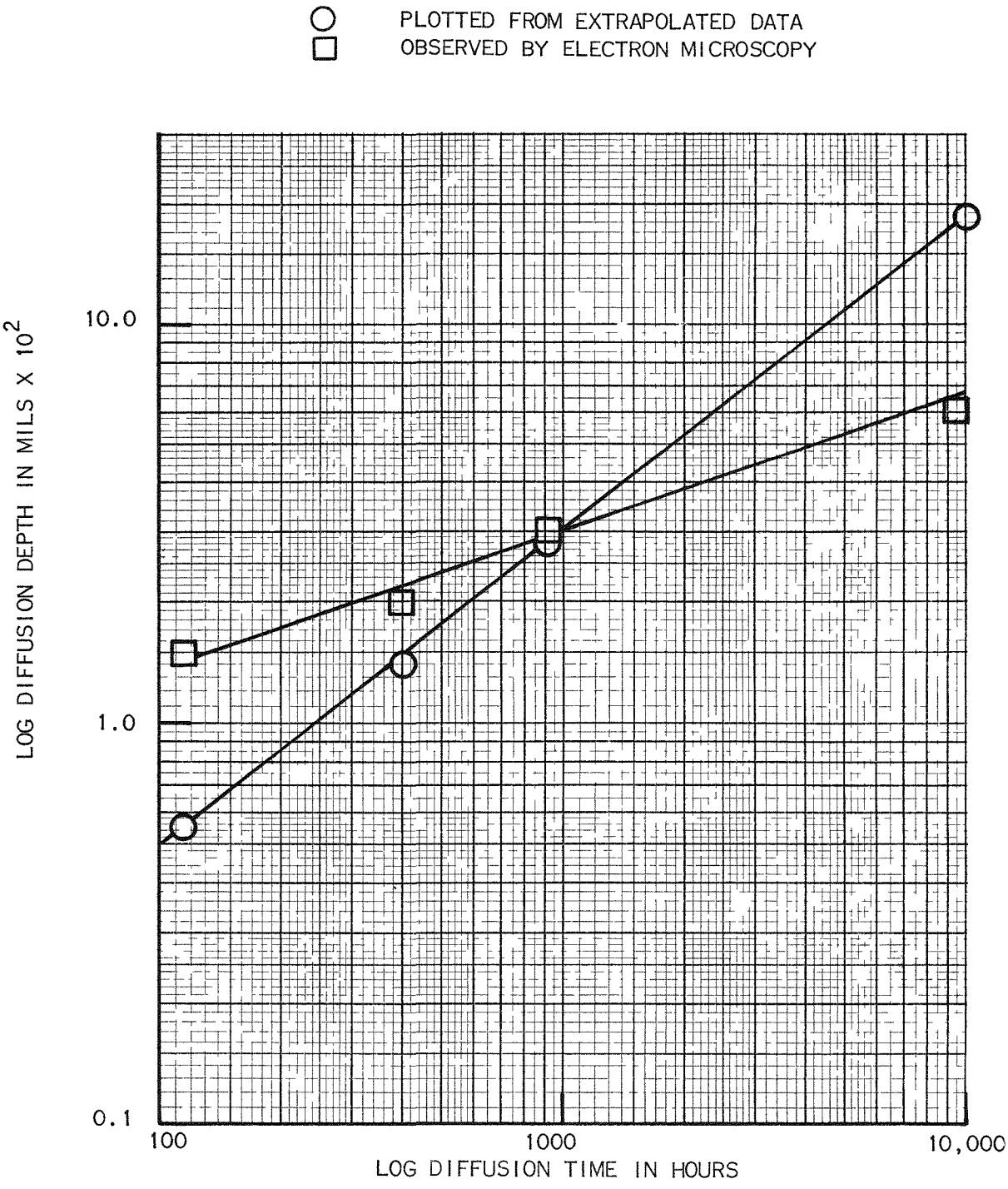

OPTICAL AND ELECTRON PHOTOMICROGRAPH SHOWING INTERDIFFUSION OF Cb-1 Zr ALLOY WITH TYPE 316 STAINLESS STEEL

DIFFUSION ANNEALED AT 1350F FOR 9300 HOURS

Cb-1 Zr ALLOY

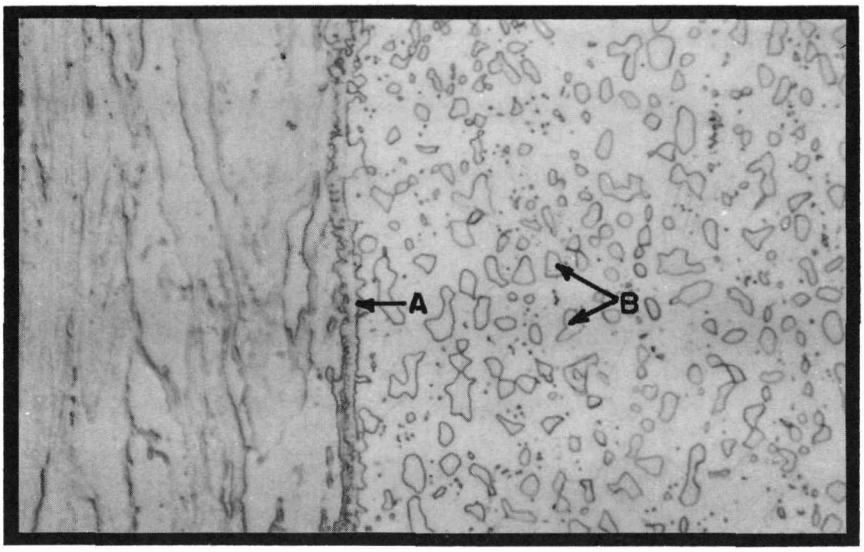

TYPE 316
STAINLESS STEEL

ETCHANT: 10 H_2O, HNO_3, 3 HF MAGNIFIED: 1000X

A DIFFUSION ZONE
B SIGMA PHASE

ELECTRON PHOTOMICROGRAPH SHOWING INTERDIFFUSION OF Cb-1 Zr ALLOY WITH TYPE 316 STAINLESS STEEL

DIFFUSION ANNEALED AT 1350F FOR 9300 HOURS

Cb-1 Zr ALLOY

TYPE 316 STAINLESS STEEL

1μ

CATHODIC ETCH
CARBON REPLICA - Pt SHADOWED

MAGNIFIED: 1000X

A DIFFUSION ZONE

zone acted as a barrier to the diffusion of the metals at temperatures of 1000 and 1350F. At temperatures in the order of 1600F, this barrier was apparently disrupted to allow metal diffusion and the subsequent formation of the intermetallic compounds based on the iron-columbium system.

From this study of a Cb-1 Zr alloy-type 316 stainless steel couple, it was concluded that intermetallic diffusion in a bimetallic joint of these materials would occur to only a limited extent when subjected to temperatures of 1400F for periods of approximately 10,000 hours.

A semi-quantitative method was developed for the spectrographic determination of metallic impurities in the 10 to 1000 ppm levels in alkali metals. Ten milligrams of the alkali metal carbonate were mixed with five milligrams of graphite containing cobalt as an internal standard and excited in a 20 ampere dc arc. Intensity ratios, obtained by ratioing the intensity of the element line to the intensity of the 3048.8 Angstrom cobalt line, were compared to intensity ratios of standard curves to determine the concentration of the elements in a sample. Standard curves have been established for the determination of titanium, cadmium, sodium, boron, silicon, zirconium, calcium, columbium, molybdenum, iron, chromium, nickel, magnesium, sodium, potassium or lithium. Using this method of analysis, an accuracy of about 30 percent of the reported value is obtained.

Work has been concluded on the chlorine extraction method and determination of the rare earths, gadolinium and samarium, from Cb-1 Zr alloy reported in PWAC-631. Experiments have shown recoveries in the order of 70 percent of the amount added at the 2.5 and 10 microgram levels with coefficients of variation of $\pm$ 6 percent of the amount reported.

11. Reliability

The Reliability Data Center became fully operational during this quarter. Data from Trouble and Failure Reports are being stored on the Bendix G-15 computer and programs prepared for rapid searching of this data. Another program permits searching and printout of a monthly tally to establish frequency rates of failure modes.

The critical parts list for LCRE is under final review and the mechanics for a system which provides quick access to complete fabrication history of these parts have been worked out with the Operations Department.

D. LCRE FABRICATION

1. Reactor

All work has stopped on the fabrication of the core pressure vessel, core support, and core spacers, pending redesign of the fuel element assemblies. Changes in tooling and procedures are being made to accommodate the longer fuel pins called for in design modifications.

Fabrication of the Reflector and Control Assembly is continuing. The upper reflector support with manifold has been welded, stress-relieved, and is awaiting the inner reflector case before further fabrication can continue. Flow-turning of four stainless steel inner reflector cases did not produce an acceptable LCRE part. Salvage of a fifth flow-turned case is being attempted. No further flow-turning of inner reflector cases can be performed until additional forgings are received. Because of the difficulties experienced in flow-turning, a parallel effort was started to produce both inner and outer reflector cases by welding and machining. Fabrication of two inner and two outer-welded reflector cases is now in progress. Machining of the outer reflector case forgings has been completed. Flow-turning of the cases has begun.

Delivery of beryllium reflector shapes will be delayed, caused by a strike at the fabricator's plant.

The control drum drive gear box, reactor start-up source drive, harmonic bearings, drum thrust and radial bearings were placed on order this period. Major items awaiting vendor quotations are the pile oscillator transmission, and two chamber check source drives. Fabrication continued on the six nuclear instrument drives, harmonic region gas containment cans, and all hardware associated with the power range neutron sensors. All scram motors and limit switches placed on order the previous quarter have been received and are now being inspected.

2. Primary and Reflector Coolant Systems

Work on the fabrication of Cb-1 Zr alloy primary system piping by the vendor was temporarely delayed because of retort cracking on one length of pipe. Ten 14-foot lengths of the 2-1/4 inch outside diameter and five 16-foot lengths of the 3-1/4 inch outside diameter pipe have been received, inspected, and are being fabricated into detail parts for use in the primary system.

A review of the as-bent pipe details for the LCRE mockup has been completed. This review has shown that parts can be bent to acceptable tolerances for the LCRE piping system. Contamination of the pipe during bending operations can be eliminated by careful control of the handling procedures and cleanliness of the equipment.

Primary sump inlet duct forgings were received with numerous surface cracks and laps and were returned to the vendor for cleanup.

Thermocouples for the LCRE are on order to be fabricated in accordance with the requirement for exclusion of moisture and oxygen from the alumina insulation.

Ten-inch by ten-inch billets of CS-1100 raw material were received and inspected. These billets were made from double-vacuum arc melted ingot, chemically equivalent to type 316 stainless steel. The billets were then drawn to various sizes and upset-forged to obtain completely worked material. During the draw-down and upset-forging operations, hairline cracks appeared on the surfaces and some of the forgings were cracking at the center on the ends. Work continued on the forging operations by locally grinding surface cracks as they appeared. In the meantime, metallurgical and chemical analyses of this material are being performed. It will be used for machining liquid metal containing parts whose shape will not permit the use of grain-oriented material.

Fabrication of two of the four Cb-1 Zr alloy heat exchangers required for the LCRE was completed (Figs 50 and 51). The other units are scheduled for completion during the next quarter.

Following welding of the primary sump inlet adapters to the body of the original sump, an inspection revealed cracks in the heat-affected zone of the inlet adapter. Attempts to locally grind, polish, and acid-etch these defects were unsatisfactory and the sump was placed in storage for back-up purposes. A weld evaluation program was started in order to evaluate and improve the high stress welding procedures required for this particular configuration. Prior to welding the inlet adapters on the second sump, several trial samples of the adapter-to-sump body welds were fabricated and evaluated. These welds indicated that acid-etching after welding and before annealing may be detrimental. Sample welds which were acid-etched at that stage produced crack-like defects in the weld and parent metal after annealing. A weld sample annealed immediately after welding (with no acid etching) showed no defects. Based on weld sample investigations, the acid etch treatment immediately after welding was eliminated. However, in order to assist in making any weld repairs, the acid-etch treatment was permitted after the part had been annealed. The welding of the inlet adapters to the second sump body is scheduled for completion early next quarter.

The reflector system double pump sump fabrication continued satisfactorily during this period. The sump assembly was prepared for machining prior to welding the sump cover in place. Some weld distortion apparent prior to machining was corrected and fabrication continued. Fig 52 is a photograph of the reflector system double sump, partly assembled.

3. Secondary and Air Systems

The contract to fabricate and assemble three NaK-to-air radiators was awarded and design work was initiated by the vendor. The contract for the fabrication of the air system butterfly valves was awarded. Design drawings, received from the vendor for approval, were returned with comments and corrective suggestions. The air system blower and drive package contract was awarded. Design work was initiated by the vendor and is approximately 30 percent completed.

Release of the fabrication drawings for the secondary pump is scheduled for July. Evaluation of potential vendors is in progress for sump fabrication.

Seamless stainless steel tubing materials (AMS-5573C) for the secondary system piping were received from the vendors and were inspected at CANEL. The two-inch outside diameter by 0.095-inch wall tubing was reviewed and accepted with minor repair work necessary. The 3.500-inch outside diameter by 0.120-inch wall tubing was returned to the vendor as unacceptable for use in a liquid metal system. Inspection review has not been completed for the 1.000-inch outside diameter by 0.095-inch wall tubing.

FIG 50

A-11384
A-11385

LCRE Li- TO-NaK HEAT EXCHANGER

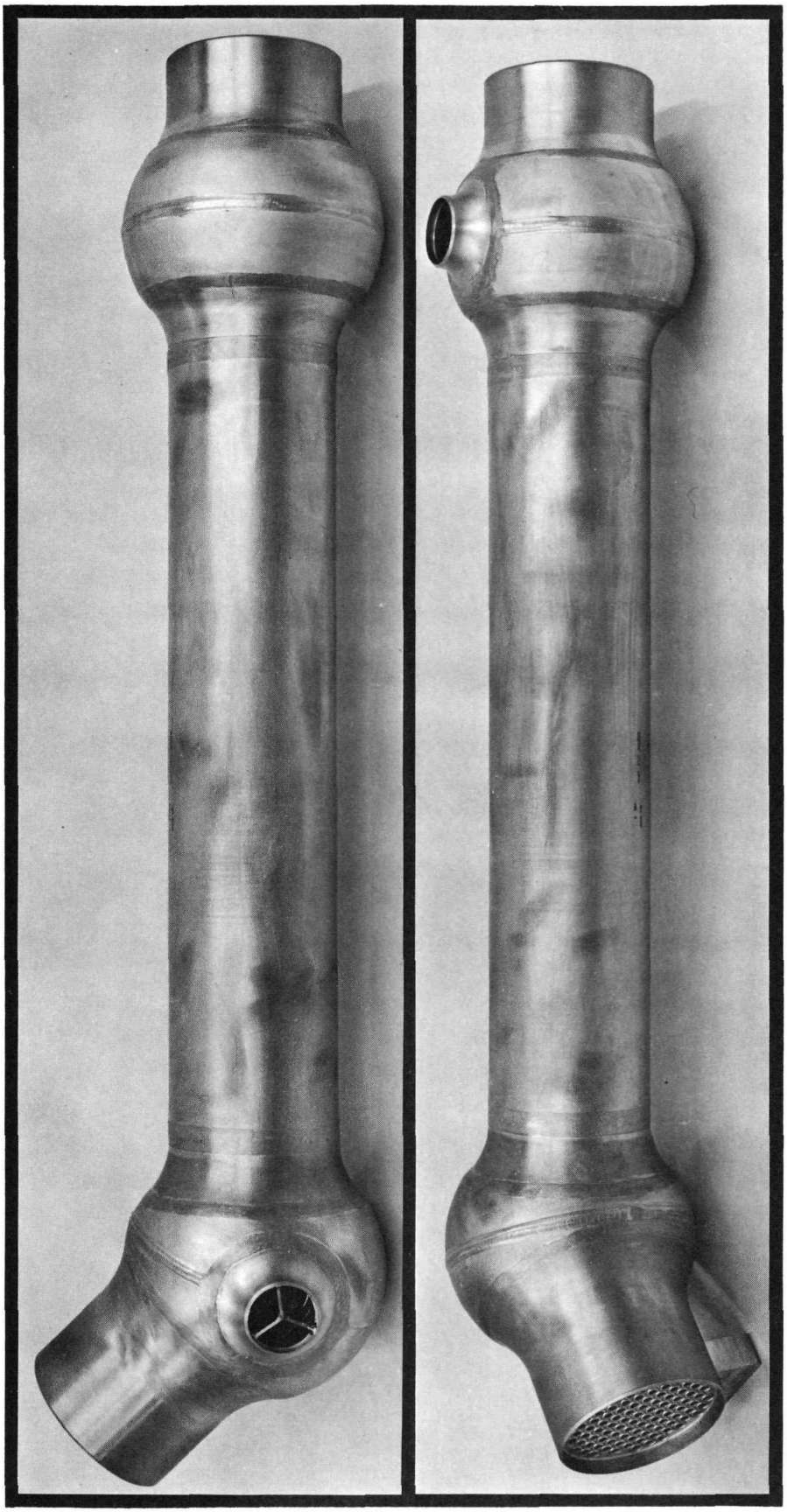

A-11386
A-11387

LCRE Li-TO-Li REGENERATIVE HEAT EXCHANGER

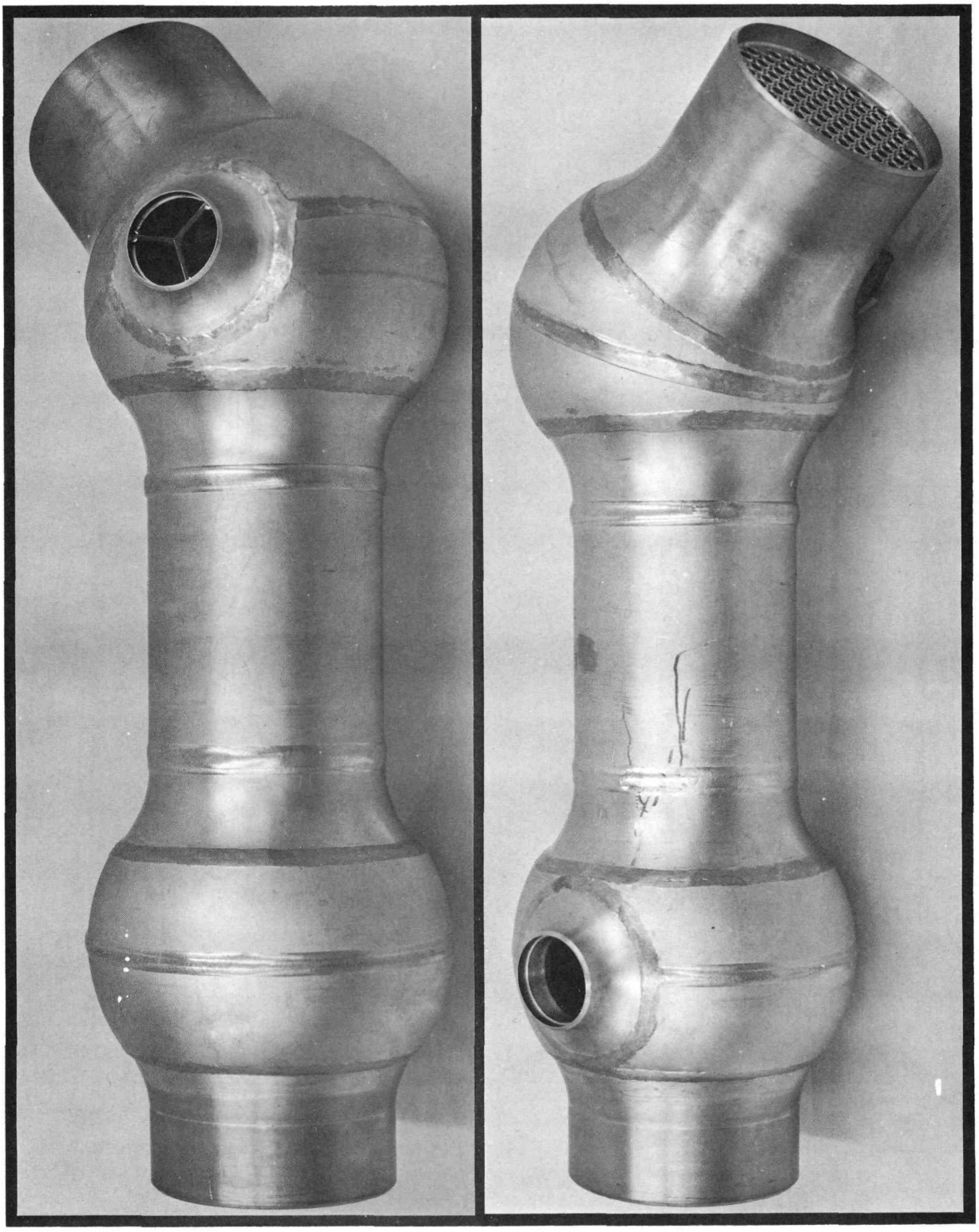

LCRE REFLECTOR SYSTEM DOUBLE PUMP SUMP

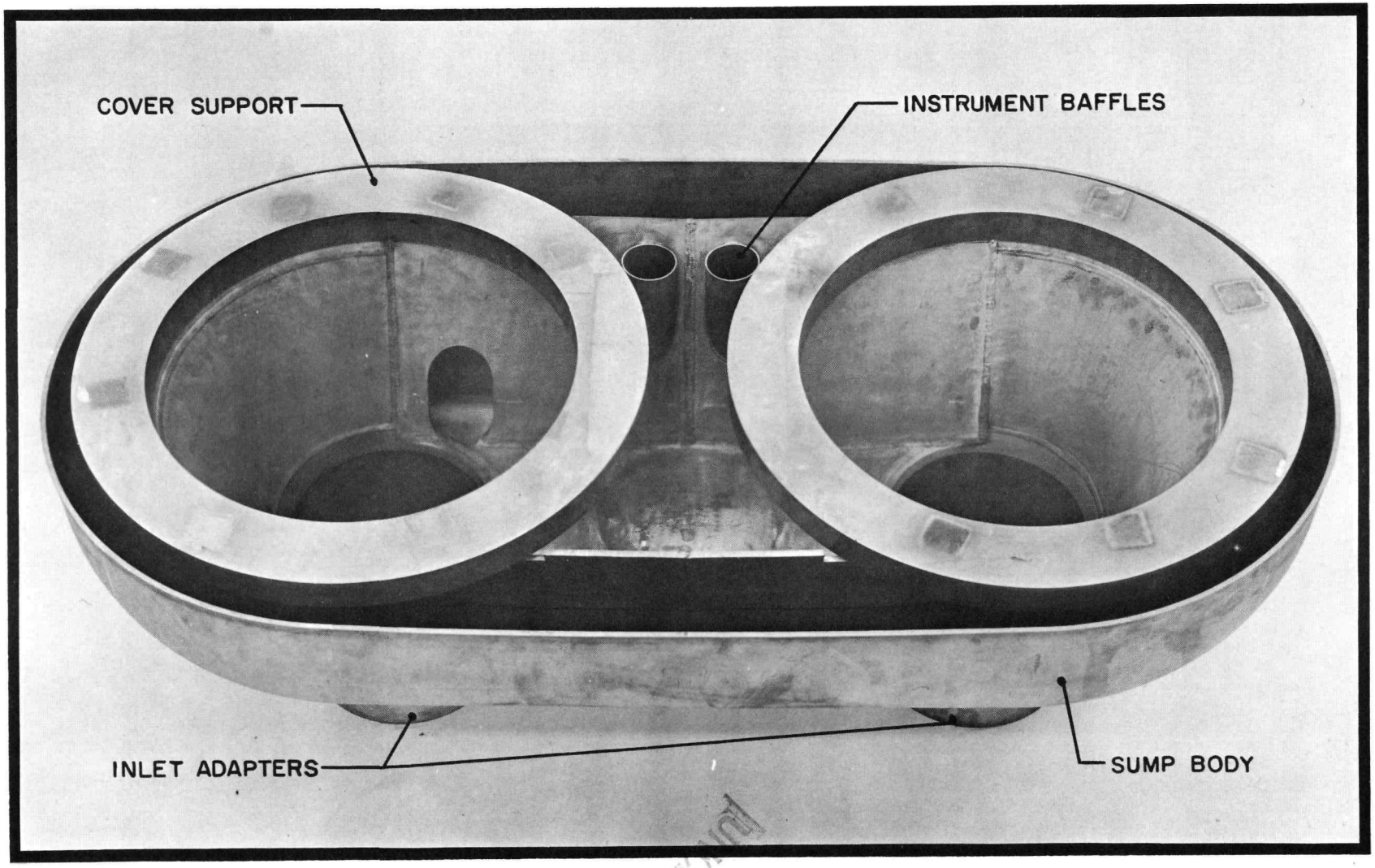

4. Auxiliary Systems

Proposals to complete the installation and checkout of the LCRE Auxiliary Systems at NRTS were reviewed and rejected. The bids were not comparable and, after careful review of the work to be completed on these systems prior to start of installation in Idaho, it was concluded that the work should be bid on a CPFF basis and the selection of a single contractor could be delayed until the first quarter of FY 64 without compromising the LCRE schedule. The new specification (FPS-E-418, Revision 1) was completed on June 30, and covers installation design and procurement, fabrication, and installation of 39 Auxiliary Systems. This work to be performed by the Auxiliary System Contractor (ASC) requires company specialization in the engineering and/or installation of control and process systems in the nuclear power field. Except for one system, Cryogenic Trap-Nuclear Instrumentation (a radiation monitoring system), requiring special design knowledge, the design of these systems will be completed by CANEL. This does not include such work as is directly concerned with installation (wiring diagrams between areas, installation design of mechanical and electrical equipment, etc.). The work was divided into the following five major categories to help define and control the work:

I. Reactor Instrumentation and Control Systems

II. Liquid Metal Systems Instrumentation

III. Primary, Secondary, and Gas Line Heating Systems

IV. Gas Systems

V. Mechanical and Electrical Systems and Equipment

Six bidders have been requested to return proposals by August 9, 1963, and after evaluation of the proposals, it is planned to award the Auxiliary Systems contract during September, 1963.

A source has been selected for cleaning instrumentation and control components for use in the clean gas systems. This vendor demonstrated ability to clean components of complex geometry (pressure transmitters) to the requirements of CANEL Cleanliness Specification 309B (CS-309B). Examination of the parts was performed in the CANEL clean room. At least two more component cleaning vendors will be located and qualified during the next quarter. All instrumentation and control components for use in the clean gas systems, which cannot be purchased clean, will be upgraded by using these cleaning services.

Work on 21 construction tasks has been activated with the construction contractor for the LCRE control and safety circuit chassis. These tasks cover 109 of approximately 120 chassis required for the LCRE installation.

The control console structural bays, wedges, doors, side panels, and hardware have been received and are in assembly.

The procurement of "P" Area (PWAC-631, Fig 2) racks and associated hardware was initiated during the month.

Two vendor proposals were received covering the scram battery power supply systems. Neither proposal was found adequate and, following engineering conferences with their representatives, both vendors were requested to resubmit proposals.

Proposals are being evaluated for 60 cps to 400 cps frequency convertors for use with the drum position readout instrumentation.

The present overall status of direct procurement by CANEL of Auxiliary and Control Systems instrumentation, components, and equipment is shown in Fig 53. Specifications have been completed for 53 percent and vendors have been selected for 38 percent of the procurement packages. The remainder of these systems will be procured by the Auxiliary System Contractor when this contract is awarded.

FIG 53

STATUS OF PROCUREMENT BY CANEL OF AUXILIARY AND CONTROL SYSTEMS

Category[1]		Description of Procurement Package	Specs. and/or Drawings Sent Out for Bids	Bids Evaluated and Vendor Selected	Vendor Drawings Approved	Inspection and/or Acceptance Test Complete	Material Delivered
I.	Reactor and Instrumentation and Control Systems						
Battery Power Supply	1.	Complete battery power supplies	Yes	In process	--	--	--
Pile Oscillator	2.	Variable frequency power supply	Yes	Louis Allis	In process	--	--
Control Panels	3.	Control console and instrumentation	Yes	Yes	Assembly by CANEL begun	--	--
	4.	"P" area rack					
		Rack structures	In process	In process	To be assembled by CANEL	--	--
		Rack assembly (1-31, 38-41, 46, 51, 52) including instrumentation					
	5.	"S" area rack assemblies (47-52) including instrumentation	Yes	Burns & Roe, A. D. Little	In process	--	--
	6.	"D" area control panels	Yes	In process	--	--	--
	7.	Instruments for					
		Pump drive system	Yes	G.E./M.H.[2]	--	--	--
		Heat sink blowers and valves	Yes	Assembly Prod.	--	--	--
TV Monitoring Systems	8.	Cameras, monitors, camera mounts and positioning mechanisms	In process	--	--	--	--
II.	Liquid Metal Systems Instrumentation						
Coolant Circuit Instrumentation	9.	Primary, reflector, and secondary circuit instrument and components	Yes	M.H./G.E./ Electro Mech/et al	In process	In process	In process
LM Fill and Drain Systems	10.	Primary, reflector, and secondary fill and drain instruments and components	Specs for Source Evaluation	Electro Mech, Research Control Foxboro	--	--	--
	11.	Coolant addition instruments and components	Specs for Source Evaluation	Electro Mech, Research Control Foxboro	--	--	--
III.	Gas Systems						
Helium Supply and Purification	12.	Inconel pipe	Yes	Huntington Alloy, Int. Nickel	--	--	--
	13.	Inconel pipe caps	Yes	In process	--	--	--
	14.	Inconel tubing	In process	--	--	--	--
	15.	Instruments and components	In process	--	--	--	--
Pump Seal and Sweep Gas, Primary Coolant Jacket Gas, Gear Box Gas	16.	Primary, secondary, and reflector seal and sweep gas instruments and components	Yes	Manning, Max. & Moore, Foxboro Research	In process	--	--
	17.	Jacket gas instruments and components	Specs for Source Evaluation	Foxboro Research Electro Mech.	--	--	--
	18.	Gear box gas instruments and components	Specs for Source Evaluation	Foxboro	--	--	--
	19.	Test cell isolation valve actuators	Specs for Source Evaluation in process	--	--	--	--
Cryogenic Trap System and Exhaust Headers	20.	Cryogenic non-nuclear process system	Yes	A. D. Little	In process	--	--
IV.	Mechanical and Electrical Systems Equipment						
LM Coolant Pump Drives	21.	Pump drives and transfer switchgear	Yes	In process	--	--	--
	22.	Pump drive instruments and components	Yes	M.H., G.E., Electro Mech., Anadex	In process	In process	In process
Coolant Pump Lube Oil Systems	23.	Lube oil units	In process	--	--	--	--
	24.	Instruments and components	Yes	Electro Mech., Anadex	--	--	--
Heat Sink Systems	25.	Blowers and drives	Yes	Bayley Blowers	In process	--	--
	26.	Butterfly valves and operators	Yes	Golden Anderson	In process	--	--
	27.	Instruments and components	In process	Assembly Prod. Foxboro, M.H.	In process	In process	In process
LM Handling Systems	28.	NaK shipping container	In process	--	--	--	--
	29.	Li shipping and gettering tanks	In process	--	--	--	--
	30.	Ti sponge	In process	--	--	--	--
	31.	LM transfer lines	In process	--	--	--	--
	32.	NaK	In process	--	--	--	--
	33.	Li^7	In process	--	--	--	--
	34.	Li^6	In process	--	--	--	--
	35.	Instruments and components	Specs for Source Evaluation	In process	--	--	--
Test Cell Pass-Thrus	36.	Triaxial fitting pass-thrus (13)	Specs for Source Evaluation	In process	--	--	--
	37.	Power pass-thrus (162)	Specs for Source Evaluation	In process	--	--	--
	38.	Control and T/C pass-thrus (47)	Specs for Source Evaluation	In process	--	--	--
	39.	Gas line pass-thrus (37)	Specs for Source Evaluation	In process	--	--	--
Fuel Loading Experiment	40.	Temporary support structure and working platform	In process	In process	--	--	--
	41.	Fuel handling equipment	In process	--	--	--	--
	42.	Instruments	In process	--	--	--	--
Pretest Gas Analysis	43.	Gas analysis dollies	In process	--	--	--	--
	44.	Evacuation dollies	In process	--	--	--	--
Core Installation	45.	Core installation dolly	In process	--	--	--	--

(1)Ref. FPS-E-418, Revision 1
(2)G.E. - General Electric
M.H. - Minneapolis Honeywell

E. LCRE TEST FACILITY

1. Test Facility

Title II drawings and specifications were essentially completed during the quarter. The Title II design work remaining consists of minor detailing of piping locations and supports and the preparation of component and system test specifications. Plans and specifications were issued to the construction contractor for use in procurement and for the preparation of final schedules and cost estimates.

The following construction work was completed during the quarter: demolition, pile driving and the installation of drilled piers in the Test and Diesel Generator Buildings, excavation, installation of reinforcing steel and concrete placement for the Cryogenic Trap Pits, Shield Cooling System Room, Test Cell Foundation Mat, and Diesel Generator Building grade beams.

Fig 54 shows construction work in progress in the Test Cell and Shield Cooling System Room area during June, 1963.

2. Support Facility

Title I design was completed in April. Title II design is in progress and is scheduled for completion in August. Specifications for long lead time equipment and material were completed and have been issued to the construction contractor.

CONSTRUCTION OF LCRE TEST FACILITY SHOWING TEST CELL AND SHIELD COOLING SYSTEM AREAS - JUNE 20, 1963

F. LCRE OPERATIONS

All abstracts and other information necessary for writing the operating procedures for the fuel loading and final core assembly phase of LCRE assembly were received and about 70 percent of the procedures have been drafted.

An outline of the Operations Manual covering the operations from liquid metal fill through after-heat removal was prepared and the pertinent information and data requested. The technical abstracts for this portion of the procedures are essentially complete.

Planning and preparations were begun for testing and training personnel at CANEL in using the tools and equipment being designed for the fuel loading phase of LCRE assembly.

All approved Auxiliary Systems flow diagrams were reviewed for operational consistency. A review of facility system drawings and flow diagrams was started.

A review of over-all manpower and schedule requirements resulted in postponing the start of the operator training course until the middle of July. A revised outline of the training program was issued defining the extent of the course and the responsibilities for each area of instruction. Preparation of individual lesson outlines and lesson plans was started.

Preparation of the Operator Training Manual was started. This manual will include the organization of the training program, a syllabus of the course, the requirements for qualification of each type of operator, and the methods for maintaining records of operating personnel.

Studies of possible problems encountered in the reactor disassembly are continuing, and alternate procedures are being developed to overcome these problems should they occur. Liason is continuing with the Physics Group in regard to criticality aspects of disassembly and the results of the calculations are being utilized in the design of the poison shroud, NaK tank for core disassembly, and various tools to be used in conjunction with the latter.

Disassembly tooling requirements have been compiled. Design specifications are approximately 50 percent complete.

An estimate has been made of the amounts and levels of radioactive waste which will have to be disposed of during the disassembly and examination of LCRE. At present, a waste handling procedure is being written which will eventually be incorporated into the Disassembly Manual.

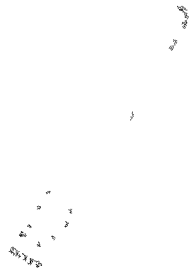

III. SNAP-50/SPUR

A. POWERPLANT

1. System Analysis and Design

The SNAP-50/SPUR Powerplant Development Plan describing the engineering program required to develop the powerplant through flight test was prepared and issued.

Powerplant engineering studies of the first flight powerplant were continued, resulting in changes to the powerplant design requirements discussed in PWAC-631. The major revision concerns reduction in the powerplant pump power requirements and, consequently, in the alternator gross electrical output. The pump power requirements are influenced by losses in dynamic seals, hydrostatic bearings and ceramic-lined electric motors. The previous estimates of these losses were found to be too high and new estimates have been made. The dynamic seal losses which are proportional to the fifth power of the seal radius have been reduced by the use of a two-stage seal. The estimate of motor efficiency was increased from 70 percent to 80 percent as a result of discussions with motor manufacturers. As a consequence of these changes, the electric power load of the motor pumps has been reduced approximately 50 percent.

An additional change in alternator power requirements is the elimination of 15 kilowatts as a parasitic load for alternator frequency regulation. Analog simulation studies of the powerplant have shown that the pump discharge throttle valve is adequate for control during steady state operation and the electric parasitic load may be needed only during transients. The SNAP-50/SPUR First Flight Preliminary Design Specifications, with these revisions incorporated, was prepared and issued.

The selection of the temperatures and pressures of the powerplant are being reviewed with respect to reducing powerplant weight and radiator size. As a part of this review, a digital computer program was prepared for calculating performance and weights for use in an optimization study. The preliminary results of these studies indicate that a number of changes in design conditions may be desirable. The most significant change would be an increase in the turbine exhaust temperature, resulting in reduced radiator area. In addition, small changes in temperature drops and pressure drops for heat exchanger components may be anticipated.

A change in the power conversion circuit is being studied. This would utilize interstage bleed vapor from the turbine to preheat the potassium prior to entering the boiler. The vapor would condense in the preheater and drain to the suction side of the centrifugal pump. This modification would decrease the magnitude of temperature differences at the boiler inlet which is 870F without turbine bleed and 370F with turbine bleed. The larger temperature difference is considered a potentially difficult mechanical design problem.

A digital computer program is being prepared to estimate off-design performance characteristics. This program is necessary for evaluating part-load characteristics and component requirements, and for analyzing control modes. Sufficient component characteristics are not presently available for a detailed off-design performance program but by using simplified representations of components, the general characteristics for part-load and stability can be estimated and the component requirements described.

A powerplant arrangement layout based on the preliminary design specification was completed. Review and evaluation of this layout with respect to structural support, minimization of piping, preheating, meteoroid protection and system compactness is in progress to define modifications and revisions for a second arrangement layout.

Preliminary evaluation of the powerplant piping sizes, and weights and system coolant inventories was accomplished to provide improved weight data for system evaluations and initial system accumulator volume requirements.

The study was based on the preliminary system design requirements and the initial powerplant arrangement layout. The study indicated that a revision of the main heat rejection system piping and radiator arrangement should be accomplished to reduce the system piping weight. The auxiliary heat rejection system specific weight as a function of temperature for the 300 Kwe powerplant was determined for use in electrical equipment parametric studies.

Preliminary analytical studies have been completed to determine the feasibility of using thermal insulating shrouds for the primary and main heat rejection systems, in order to minimize the loss of stored heat in the powerplant prior to startup in orbit. These studies were based on the assumption that the time interval between launch and powerplant startup in orbit will not exceed ten hours. A two-dimensional IBM-7090 heat transfer program was used to determine the temperature-time history of the primary system, assuming an initial preheat temperature of 1000F and continuous circulation of lithium. The temperature-time history curve is shown in Fig 55A. The analytical model for the primary system assumed a BeO meteoroid barrier and a concentric stainless steel thermal shield around the components and piping. As shown in Fig 55A, the lithium temperature would decrease to 450F in a period of ten hours. Although this temperature is above the lithium freezing point of 375F, an increased safety margin could be obtained by either utilizing additional insulation or by supplying supplemental heat in orbit. The results of an analysis to determine the primary system lithium equilibrium temperature in orbit as a function of heat input are shown in Fig 55B. This heat could be supplied through the dissipation of pump work, since it is proposed to circulate the lithium at reduced flow during orbit to minimize local cold spots.

The feasibility of preheating and maintaining the main heat rejection radiator at a temperature sufficient to preclude freezing in orbit prior to startup was investigated. It was assumed that the radiator , encased in an insulating shroud, would be ground-preheated to a temperature of 600F. The temperature-time history shown in Fig 56A was determined by means of a one-dimensional heat transfer code, treating the stainless steel-copper radiator as a slab having a weighted density and specific heat. Linde Super-insulation, which is composed of alternate layers of glass fiber mat and aluminum foil having a conductivity of about 0.0001 Btu/hr-ft-F, was selected as the shroud material. As an alternate to preheating, the powerplant radiator was assumed encased in an aluminum shroud having a high solar absortivity but low emissivity and orientated perpendicular to the sun in orbit. Preliminary results, shown in Fig 56B, indicate that this method is also capable of maintaining the NaK (78 percent potassium) above freezing for the required time period. In both schemes, the radiator shrouds are jettisoned in orbit during powerplant startup.

Analytical studies continued to investigate the first flight radiator configuration and to provide parametric performance data. A parametric analysis of planar radiators, fabricated of type 316 stainless steel tubes, copper fins, and utilizing eutectic NaK as the coolant, was completed. The parameters included in this study were radiator weight and area as a functio of fluid inlet temperature, pressure drop, temperature difference and heat rejection rate. Analytical studies to investigate radiators of cylindrical configuration continued, following modification of the IBM radiator code.

A study to evaluate electro-magnetic pumps for some, or all, of the SNAP-50/SPUR pumping requirements was initiated.

A mathematical model of the 300 Kwe SNAP-50 powerplant system has been developed and checked out on the CANEL electronic analog computer. The model is non-linear and requires about 225 operational amplifiers, over 100 function multiplications and seven arbitrary function generators. Temperature control of the reactor has been shown to be feasible and stable. Two system control modes were also shown to operate satisfactorily with the system data which is now available. In one, a parasitic load is used to control generator speed with off-center positioning of the parasitic load control driving the potassium flow valve and reactor temperature in the proper directions. In the other, the generator

FIG 55

SNAP-50/SPUR PRIMARY SYSTEM TEMPERATURES

LAUNCH TO ORBITAL STARTUP

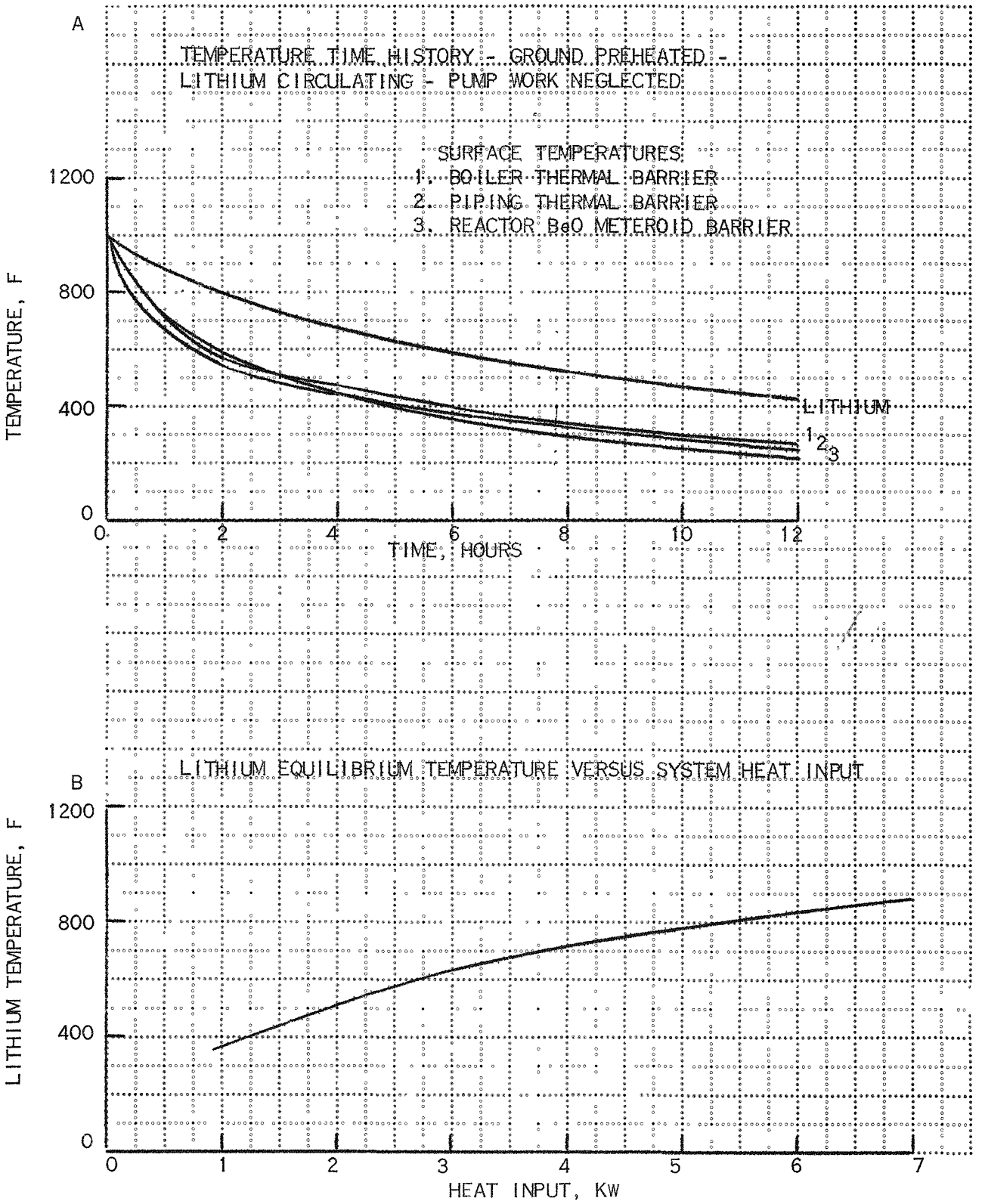

FIG 56

SNAP-50/SPUR RADIATOR TEMPERATURE-TIME HISTORY

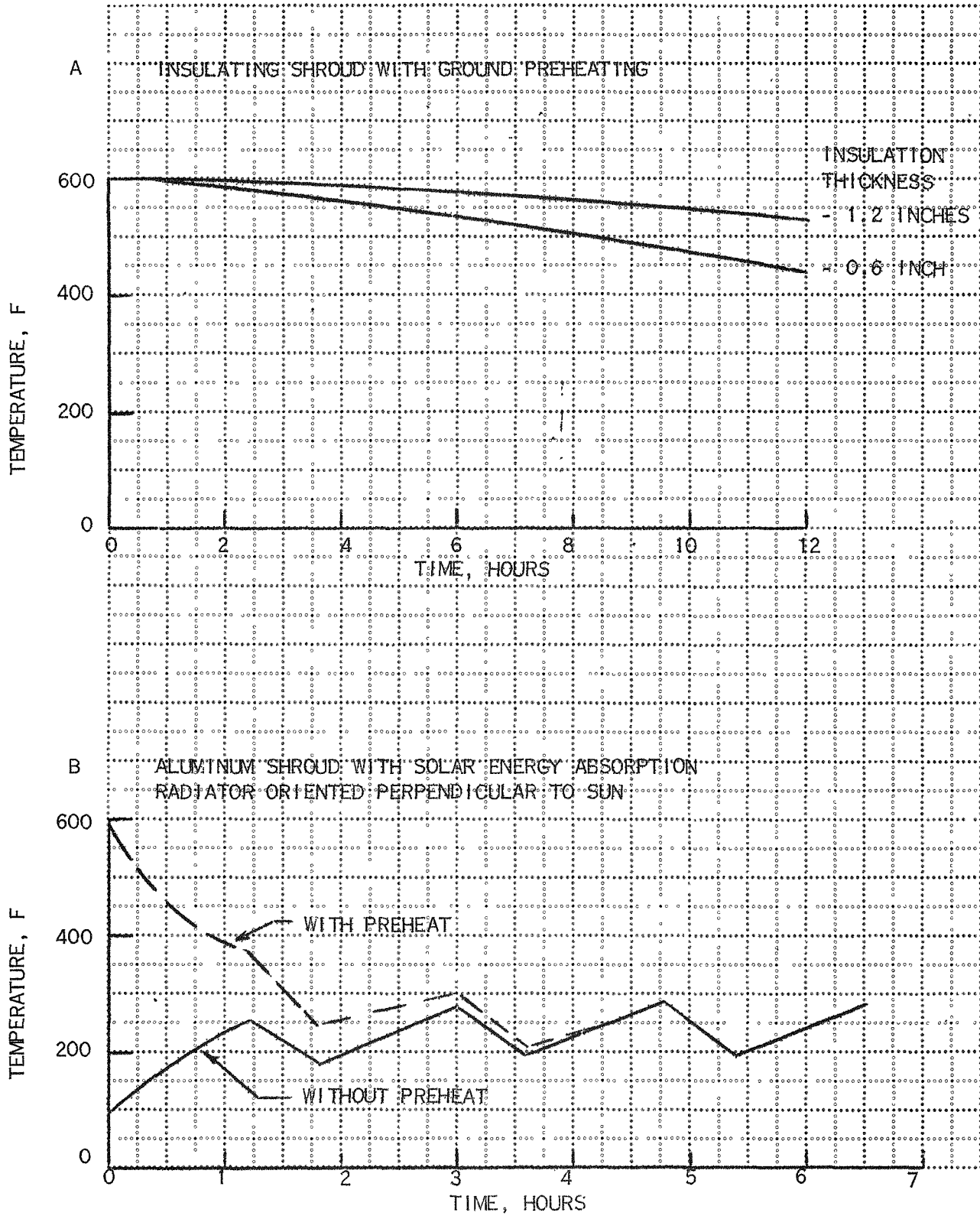

speed error drove the valve directly with reactor temperature programmed from valve position. The second mode was somewhat slower in correcting speed errors and was slightly less stable than the first. System off-design temperature and pressure trends were investigated. The study showed that boiler outlet vapor quality must be kept high to avoid potassium flow instabilities. The reactor was able to recover from step reactivity disturbances as large as 20 cents as shown in Fig 57. With either speed control it was possible to drop and pick up about 20 kilowatts of generator load without undue disturbance. Fig 58 shows this feature without the dissipative load.

2. Systems Test

An engineering study of the Nuclear Powerplant Test Facility was conducted by the architect/engineer to define more concisely the layout of the powerplant test cell, the shielding requirements, vacuum tanks and associated pumping equipment. Analysis and review of system requirements were continued in preparing the preliminary facility design criteria.

A conceptual arrangement of the Non-Nuclear Powerplant Test Facility in the CANEL Radiator Laboratory was prepared.

3. Hazards

a. Discussions were held with personnel at AeroJet-General Nucleonics, Atomics International, and Sandia Corporation to review the scope and organization of the SNAP-50/SPUR aerospace nuclear safety program. These programs have been surveyed to investigate the possibility of including a SNAP-50/SPUR experimental effort and to assist in establishing a basic aerospace nuclear safety program.

b. Some preliminary calculations were completed to determine the criticality hazards which might be encountered in handling a typical uranium carbide core under various conditions of moderation and reflection. Calculations indicated supercriticality with infinite reflectors of water, iron, or NaK.

c. Preliminary planning for the preliminary hazards summary report has scheduled completion of the final draft by mid-February, 1964 with final approval by August, 1964.

FIG 57

RESPONSE TO A 20 CENT REACTIVITY DISTURBANCE

DISSIPATIVE LOAD SPEED CONTROL

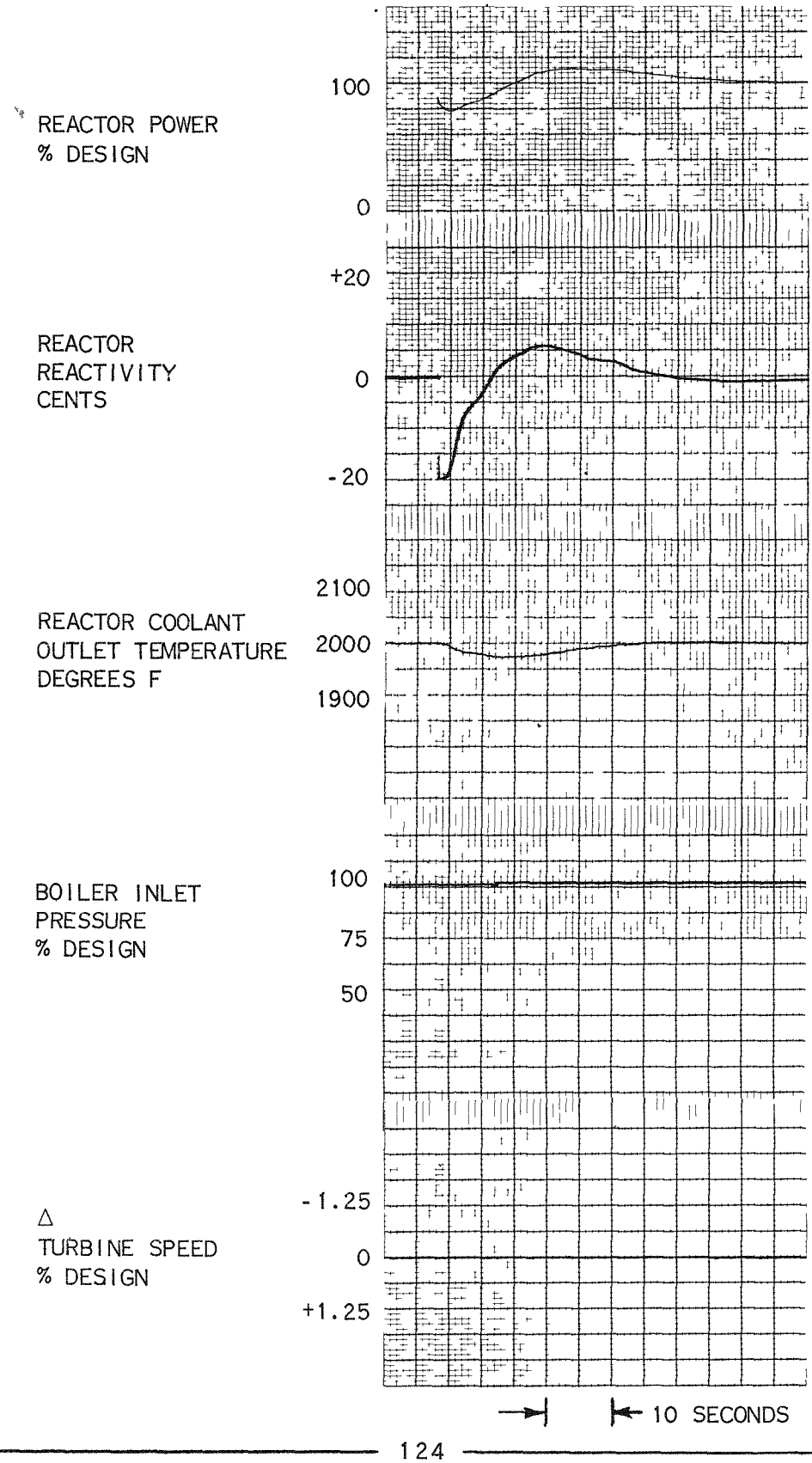

RESPONSE TO A 6.5 PERCENT STEP CHANGE OF LOAD

THROTTLE VALVE SPEED CONTROL

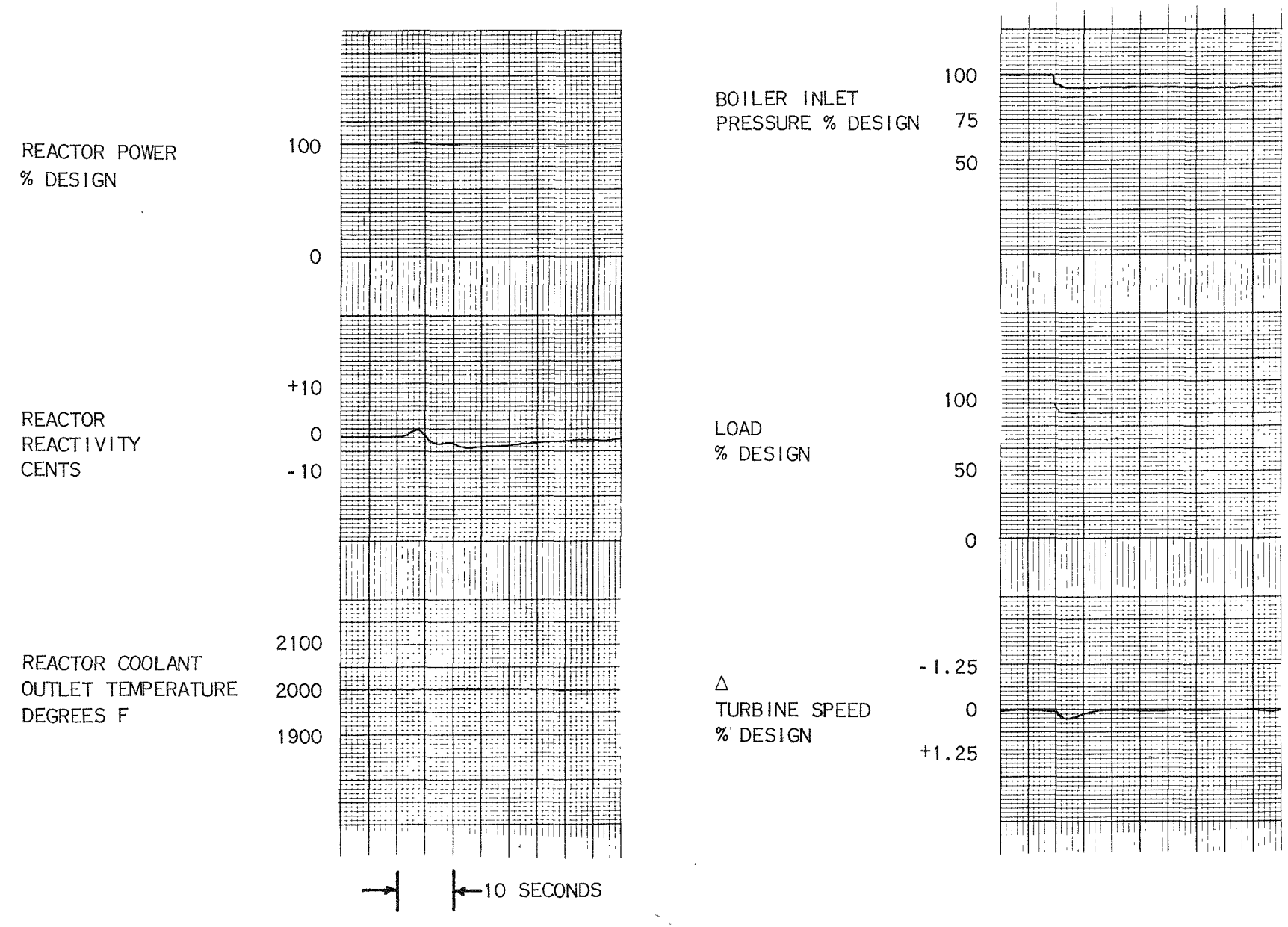

PWAC - 632
FIG 58

B. SNAP-50/SPUR RESEARCH AND DEVELOPMENT

1. Fuel

Work continued on installation of the SNAP-50/SPUR fuel fabrication equipment. The automatic powder compacting press was installed and leak-checked. Operation of the underfill feature was corrected. The devices for lubrication of die cavity walls and punch faces are not adequate and corrections are in progress. Installation of the cold wall, vacuum sintering furnace is nearly complete. Vacuum boxes for the furnace, powder conditioning equipment and for loading and unloading the powder synthesis rigs were received. Installation of their associated vacuum systems is in progress. Fabrication of components for the powder synthesis rigs was initiated.

In the hope of improving the rate-limiting step in the synthesis of uranium carbide powder, (i.e., hydrogen removal from the methane-hydrogen gas mixture over the reacting hot uranium metal), a hydrogen diffusion cell consisting of a number of parallel, thin-walled, Pd-5 Ag alloy tubes was installed on the pilot uranium carbide synthesis rig. Preliminary results indicate that hydrogen was removed selectively from the mixed gases and that this method may be an improvement over the present use of uranium at room temperature as a hydrogen getter.

Difficulties in achieving consistently high density uranium carbide and uranium nitride pellets were traced to the structure of the uranium used as starting material in powder synthesis. Lower density pellets resulted from use of powder synthesized from cast uranium whereas high density pellets resulted when heavily worked uranium metal was used for powder synthesis. A specification was written for the use of worked material.

A potential problem associated with scale-up from the laboratory to production-scale processing is pressing-die lubrication. If a suitable lubricant or binder could be mixed with the fuel powder, the problem would be minimized. Preliminary experiments with internal lubricants indicated that a solution of two percent mechanical vacuum pump oil in toluene resulted in pellets with the least detrimental effects upon sintered density or chemical composition. Other lubricants investigated with poorer results included paraffin, zinc stearate Carbowax 400, camphor and cetyl alcohol in normal hexane.

A series of 3000-hour, 2200F uranium carbide fuel-to-cladding compatibility tests were completed and examined. These are summarized in Fig 59. Specimens consisted of hyperstoichiometric uranium carbide pellets in both unlined and tantalum-lined, Cb-1 Zr alloy cladding. The cladding of half of the specimens was intentionally defected and all specimens were immersed in lithium. Sound, tantalum-lined specimens provided further confirmation of the effectiveness of tantalum as a barrier between this fuel and its cladding. Defected specimens with and without tantalum barrier liners exhibited general bulging of the cladding in the region corresponding to the fuel pellets, and local reactions and bulging at the ends of the fuel pellets stack, Fig 60. These local reaction spots contained uranium, as indicated by radiographic inspection of specimens. Contrary to the previous report, these effects were observed only in these 3000-hour tests and not in 1000-hour tests.

Metallographic examination of sound, unlined specimens showed agglomeration of U_2C_3 phase and migration of carbon to the pellet periphery, Fig 61. An electron beam microprobe analysis of the peripheral region showed approximately five percent columbium. It is believed that the presence of this third component may alter the activity of carbon in the fuel, thereby contributing to migration. In the case of the sound, tantalum-lined

RESULTS OF COMPATIBILITY TESTS C-202 AND C-203

($UC_{1.08}$ VERSUS Cb-1 Zr ALLOY IN 2200F LITHIUM FOR 1019 AND 3015 HOURS)

Cladding	Cb-1 Zr		Cb-1 Zr		Cb-1 Zr		Cb-1 Zr	
Barrier	None		None		2-mil Ta		2-mil Ta	
Defective	Yes		No		Yes		No	
Time, hours	1019	3015	1019	3015	1019	3015	1019	3015
Fuel Composition, w/o C								
Pretest	5.08	5.08	5.08	5.08	5.21	5.21	5.21	5.21
Posttest	4.61	4.4	5.04	4.9	4.56	4.6	5.18	5.17
Cladding Reaction, mils								
Carburization	Fw*	Fw	0.5	Fw	Nil	Fw	Nil	Nil
U-Cb Alloying	Fw	Fw	Nil	Nil	Nil	Fw	Nil	Nil
Barrier Reaction, mils								
Carburization	--	--	--	--	2	Fw	1.0	2
U-Ta Alloying	--	--	--	--	0.5	Fw	Nil	Nil

*Fw - Full cladding or barrier wall thickness

FIG 60

URANIUM CARBIDE VERSUS Cb-1 Zr ALLOY COMPATIBILITY SPECIMENS

(AFTER 3015-HOUR TEST IN 2200F LITHIUM)

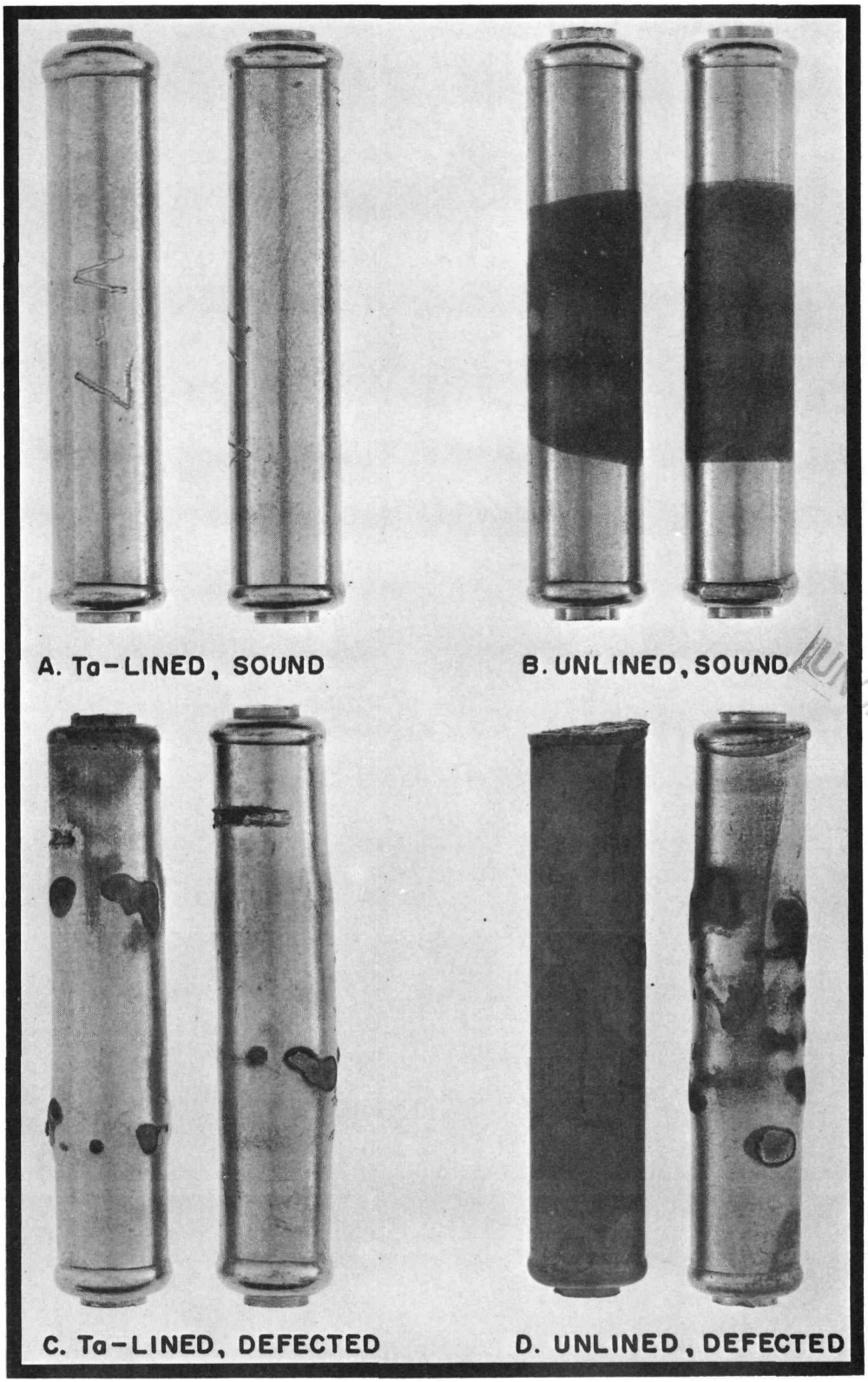

2666-32
2666-42

FIG 61

HYPERSTOICHIOMETRIC URANIUM CARBIDE FROM SOUND COMPATIBILITY SPECIMENS

(AFTER 3015 TEST VERSUS Cb-1 Zr CLADDING IN 2200F LITHIUM)

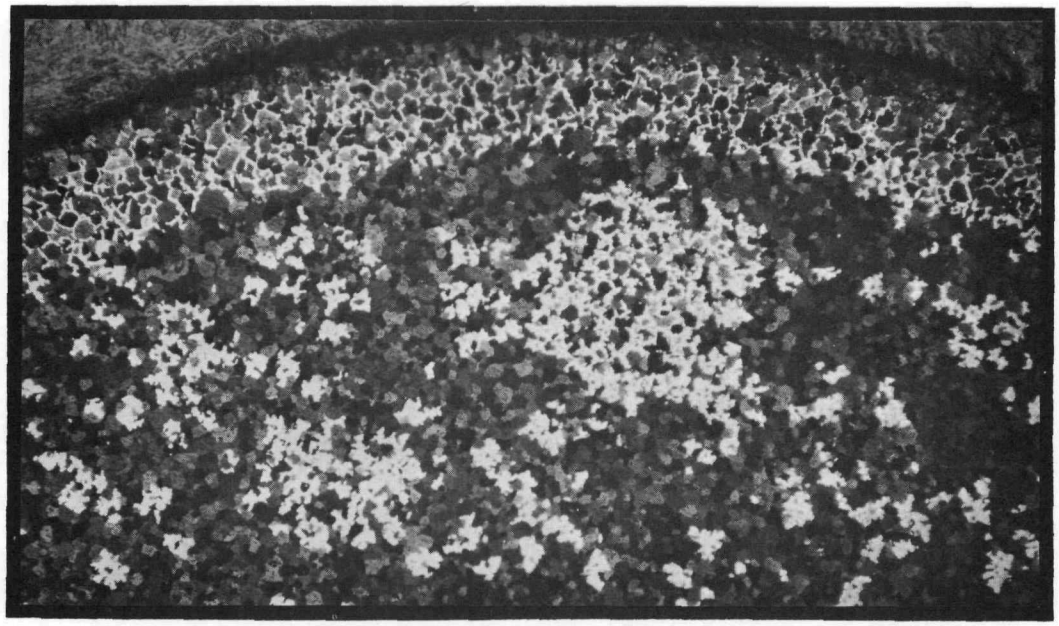

ETCHANT: 1 HNO_3, 1 CH_3COOH, 1 H_2O MAGNIFIED: 50X

A UNLINED SPECIMEN SHOWING AGGLOMERATION OF U_2C_3 (LIGHT PHASE) AND MIGRATION OF CARBON TO PERIPHERY

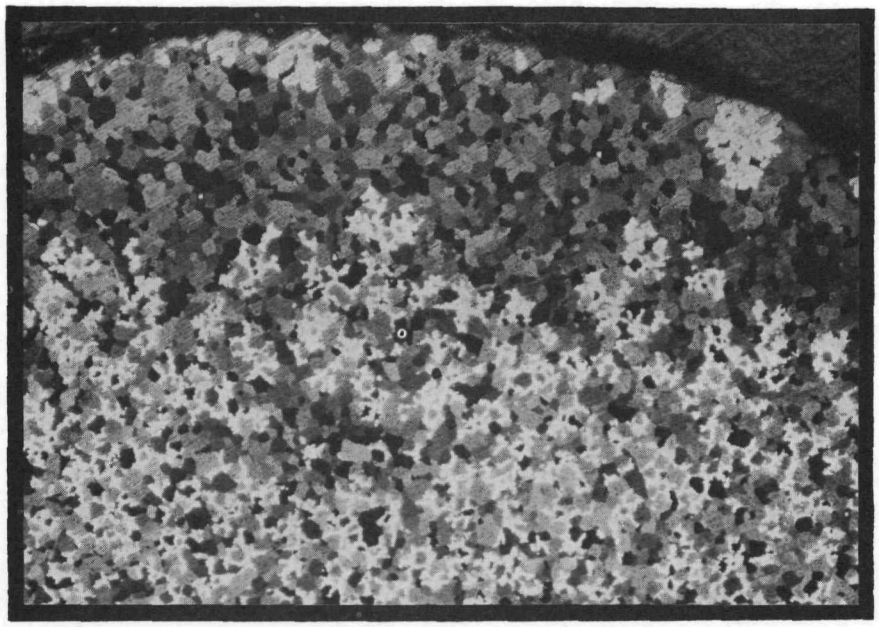

ETCHANT: 1 HNO_3, 1 CH_3COOH, 1 H_2O MAGNIFIED: 50X

B TANTALUM-LINED SPECIMEN SHOWING AGGLOMERATION OF U_2C_3 AND DEPLETION OF CARBON FROM PERIPHERY

specimens, agglomeration of U_2C_3 and depletion of carbon from the peripheral region occurred, (Fig 61), and no tantalum was detected by electron beam microprobe analysis. Carburization of the tantalum occurred but no carbide phase was observed in the Cb-1 Zr alloy cladding. In contrast to the 1000-hour test, tantalum did not prevent uranium diffusion into the cladding in defected specimens. This result indicated that tantalum is effective in delaying the reaction in defected specimens for times up to 1000 hours.

Excellent compatibility of stoichiometric uranium carbide against tungsten-lined Cb-1 Zr alloy continued to be demonstrated by diffusion couple tests under vacuum at 2200F for tests of 4000 and 5000 hours. Tests at temperatures of 2400F, 2600F, 2800F and 3000F showed no reaction after 100 hours. Similar results were observed for tests of massive tungsten or W-26 Re alloy against stoichiometric uranium carbide after 5000 hours at 2200F and 100 hours at 3000F. Additional tests for 100 hours at 3300F have shown extensive reaction of the diffusion couple. A series of 1000-hour, 1900F tests of stoichiometric uranium carbide versus tungsten-lined Cb-1 Zr alloy cladding were completed. Examination of both sound and defected specimens, tested in lithium, showed embrittlement of the tungsten, but no carbide particles or uranium in the Cb-1 Zr alloy. The embrittlement of the tungsten foil is attributed to either impurities in the foil or a slight excess of carbon over the stoichiometric composition in the pellets.

Evaluation of tungsten, vapor-deposited on the inside diameter of Cb-1 Zr alloy tubing, was started. This composite cladding material is being investigated on the basis of the promising out-of-pile compatibility results of tungsten foil liners reported above. The unsuccessful performance of tungsten foil liners in irradiation tests, reported below, appears to be related in part to mechanical and chemical deficiencies of the foil and may not represent the best performance of tungsten. Evaluation of the composite material showed excellent bonding of tungsten to Cb-1 Zr alloy, Fig 62. Hydrogen contamination of the Cb-1 Zr alloy was reduced from 80 ppm to 5 ppm by a vacuum heat treatment following vapor deposition. Pickling of the tubing outside diameter and/or purification of the helium used during the coating process may be necessary to reduce oxygen pickup. Coating thickness in preliminary specimens was non-uniform and tended to taper from gas entrance end to gas exit end. Most specimens showed a two-mil coating thickness variation over the 1.5-inch length. Heat treatments for six hours at high temperatures resulted in the following diffusion zone between the coating and the substrate:

Temp, F	Diffusion zone thickness, mils
2500	0.18
2800	0.28
3100	0.47
3400	0.50
3600	0.60

Good welds resulted between tubes and Cb-1 Zr alloy end caps when coating was removed from the end face of the Cb-1 Zr alloy and where the weld did not overpenetrate into the coating. Tubes cold-swaged 5 mils showed only minor cracking. Efforts will be made to warm-work the composite to avoid cracking the tungsten, and compatibility specimens will be prepared and evaluated.

Tantalum was ineffective as a barrier between uranium nitride and Cb-1 Zr alloy, as predicted. A diffusion couple compatibility test utilizing 5-mil thick tantalum foil was tested for 100 hours at 2200F. Examination showed uranium diffusion through the tantalum and into the Cb-1 Zr alloy, Fig 63.

TUNGSTEN VAPOR DEPOSIT ON ID OF Cb-1 Zr ALLOY TUBING

(SHOWING BOND AFTER 2 HOUR VACUUM ANNEAL AT 2200F)

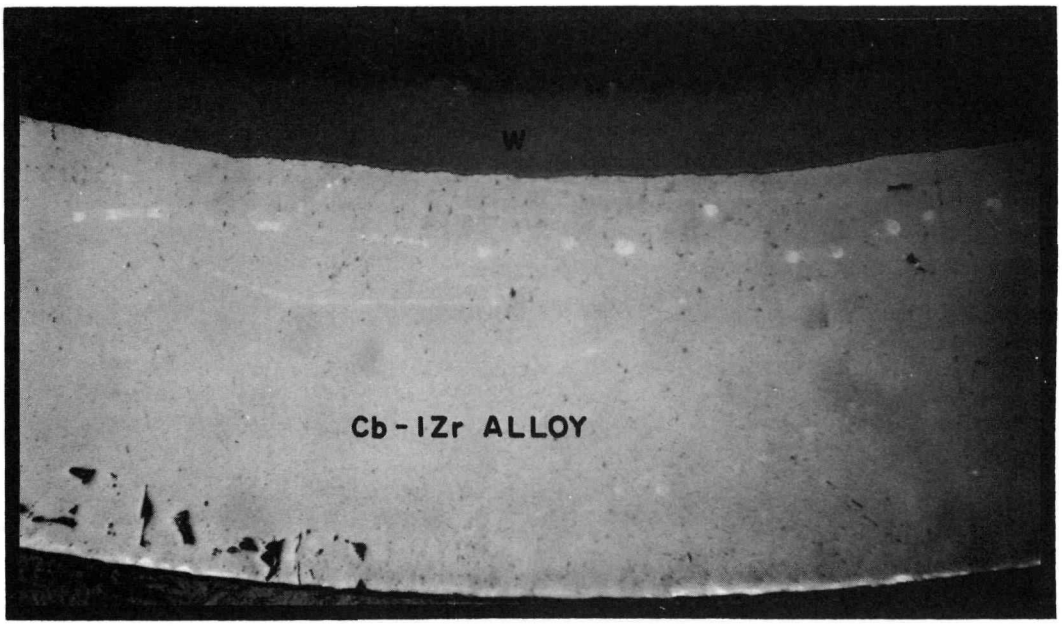

UNETCHED MAGNIFIED: 100X

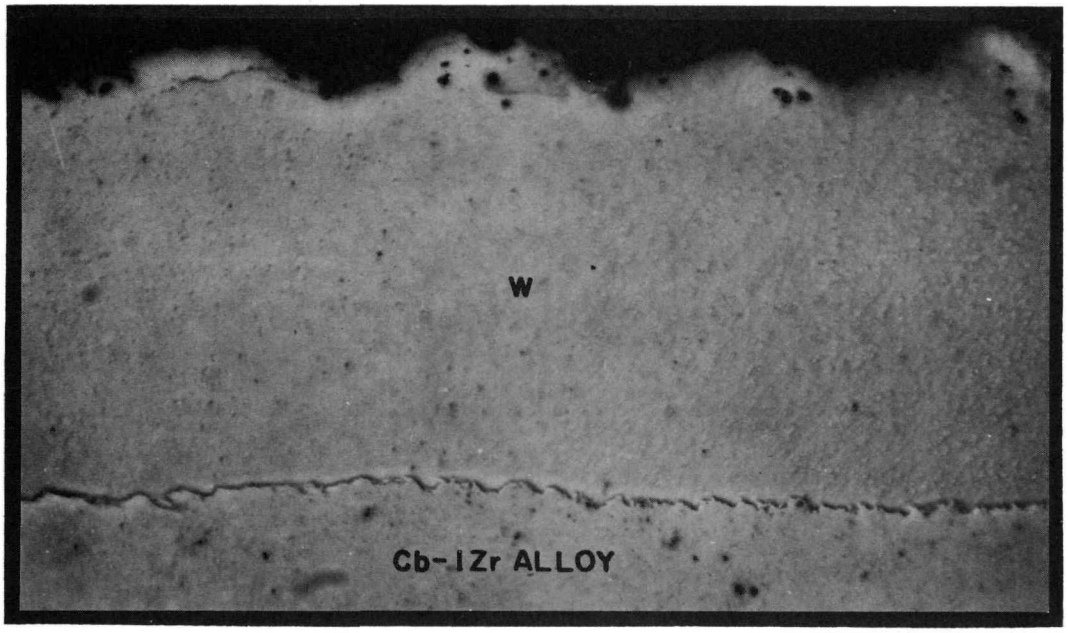

UNETCHED MAGNIFIED: 500X

FIG 63

TANTALUM-LINED Cb-1 Zr ALLOY

(AFTER 100 HOUR TEST VERSUS URANIUM NITRIDE IN VACUUM)

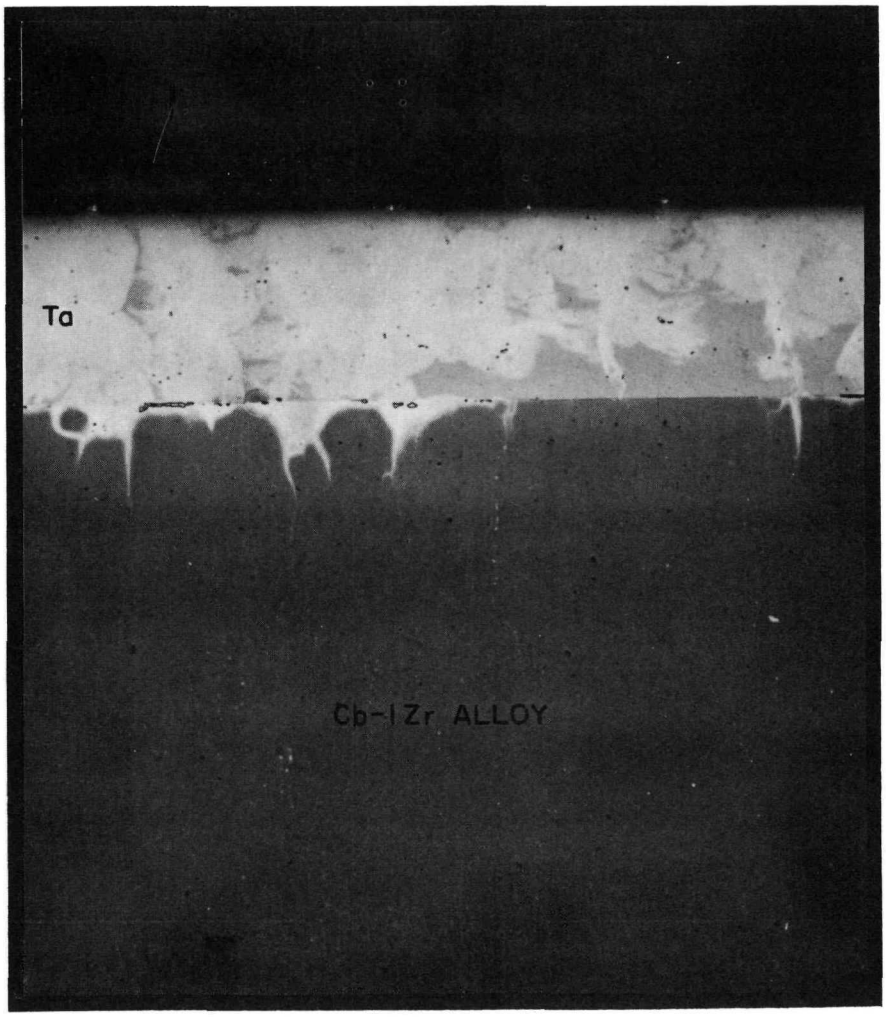

ETCHANT: ANODIZED MAGNIFIED: 200X

SHOWING PENETRATION OF URANIUM THROUGH TANTALUM AND INTO Cb-1 Zr ALLOY

Compatibility tests of uranium nitride versus tungsten-lined Cb-1 Zr alloy were extended to 5000 hours at 2200F. No evidence of reaction was noted except in one spot where diffusion zones of columbium-tungsten-uranium, columbium-uranium and columbium-nitrogen formed. However, no uranium was detected in the tungsten by electron beam microprobe analysis and it is therefore postulated that a chip of uranium nitride had gotten behind the tungsten foil and reacted with the unprotected Cb-1 Zr alloy. A 6000-hour test currently nearing completion should help to evaluate this postulation.

Status of irradiation tests of the high temperature (2200F maximum cladding surface), low enrichment (10 percent U^{235}) series is tabulated in Fig 64.

Fig 65 summarizes data from all capsules of this series examined to date.

Examination of inpile capsule PW26-191, containing stoichiometric uranium carbide in tungsten-lined Cb-1 Zr alloy cladding, was completed. Results were generally similar to those for the shorter time test, PW26-190. Reaction occurred between fuel and cladding where the tungsten barrier was cracked and also in areas where tungsten appeared unbroken. Adjacent to the top of the pellet stack, the tungsten barrier was reacted and contained dispersed phase particles and continuous layers on both sides, (Fig 66). A reaction zone believed to be columbium-uranium alloy was observed to approximately five mils into the Cb-1 Zr alloy, adjacent to the center of the pellet stack. Beyond this zone, a 0.5-mil thick band of carbide and some intergranular and dispersed particles were also present in the cladding. The extensive reaction observed may be due to cracking of the tungsten barrier, excess carbon or impurities in the fuel, contamination of tungsten, or reaction of fuel with Cb-1 Zr alloy spacers at the top of pellet stacks. As in capsule PW26-190, fission gas release was high and external specimen diameter increased less than one percent. However, no significant longitudinal bulging of fuel pellets was observed as in PW26-190.

Examination of inpile capsules PW26-150 and PW26-153, containing hyperstoichiometric uranium carbide in tantalum-lined Cb-1 Zr alloy cladding, was begun. Results continue to demonstrate that tantalum is an effective barrier against cladding-fuel reactions. Specimens from both capsules showed generally uniform carbide layers in the tantalum foil barrier with some intergranular carbide phase extending through the two-mil thick foil. No carbide was observed in the Cb-1 Zr alloy cladding. Results were generally similar to those for specimens from capsule PW26-150C and PW26-151.

Inpile capsule PW26-170, containing hyperstoichiometric uranium carbide versus bare Cb-1 Zr alloy cladding, showed extensive reaction of fuel with cladding and with the specimen container. Preliminary metallographic examination showed complete reaction of fuel with and rupture of cladding and large voided areas in the center of the specimens. Reaction was observed out to the thermocouple flutes in the specimen container. This test demonstrated the need at these temperatures for a barrier between uranium carbide and Cb-1 Zr alloy and the failure of the hyperstoichiometric composition alone to circumvent the compatibility problem.

Examination of inpile capsule PW26-220, containing nitride versus bare Cb-1 Zr alloy cladding, was started. Significant reaction occurred between fuel and cladding with a 2 to 13-mil-thick reaction zone observed in the Cb-1 Zr alloy cladding (Fig 67). Slight amounts of metallic phase particles were observed in the fuel. Inpile specimens lost significant amounts of weight and exhibited diameter increases of less than one percent. Density of irradiated fuel pellets decreased 1.9 to 6.0 percent. The specimens showed a zone of second phase, 2-mil thick, at the outside diameter of specimen cladding. This test has further demonstrated the need for a barrier between uranium nitride and Cb-1 Zr alloy.

SUMMARY OF CAPSULE IRRADIATION PROGRAM

Capsule Number	Duration of Irradiation, hr	*** Average Operating Temp of Specimen Surface, F	Test Facility Thermal Flux, nv	*** Cesium^{137} U^{235} Burnup, %	Fission Density Fissions/cc	Power Density Kw/cc	% Xe Release	Cladding OD Change, mils	Cladding Reaction	Irradiation Dates
A. Pin-type specimens, Cb-1 Zr alloy cladding (with Ta barrier) and end caps, 0.296 OD x 0.025 wall cladding, UC matrix 10% enriched, 0.244 inch D x 0.65 inch long pellet height, 1.5 Kw/cc in Li at 2200F										
PW26-150	2,562	2122+	6.2×10^{13}	13.0	--	--	--	--	--	11/62-5/63
PW26-151	1,027	2175	7.0×10^{13}	6.6	2×10^{20}	1.6	7.5	+5.0	Nil	12/62-2/63
PW26-152	10,000*	2198	7.0×10^{13}	40.0*	--	--	--	--	--	3/63-8/64*
PW26-153	679	2208	6.0×10^{13}	40.0*	--	--	--	--	--	4/63-5/63
PW26-154	10,000*	2200*	6.2×10^{13}*	40.0*	--	--	--	--	--	7/63*-12/64*
B. Pin-type specimens, Cb-1 Zr alloy cladding (with Ta barrier) and end caps, 0.296 OD x 0.025 wall cladding, UC matrix of alloy metal 10% enriched, 0.244 inch D x 0.65 inch long pellet height, 1.5 Kw/cc in Li at 2200F design										
PW26-160	3,000*	2204	5.4×10^{13}	--	--	--	--	--	--	4/63-10/63*
C. Pin-type specimens, Cb-1 Zr alloy cladding and end caps, 0.296 OD x 0.025 wall cladding, UC matrix 10% enriched, 0.244 inch D x 0.65 inch long pellet height, 1.5 Kw/cc in Li at 2200F design										
PW26-170	2,210	2172	6.5×10^{13}	14.7*	--	--	--	--	--	1/63-5/63
PW26-171	892	2135	7.0×10^{13}	5.5	1.7×10^{20}	1.7	0.2	+2.5	Nil	1/63-3/63
PW26-173	10,000*	2222	6.3×10^{13}	40.0*	--	--	--	--	--	3/63-9/64*
PW26-174	10,000*	2221	6.2×10^{13}	40.0*	-	--	--	--	--	4/63-10/64*
D. Pin-type specimens, Cb-1 Zr alloy cladding (with W barrier) and end caps, 0.296 OD x 0.025 wall cladding, UC matrix of alloy metal 10% enriched, 0.242 inch D x 0.65 inch long pellet height, 1.5 Kw/cc in Li at 2200F design										
PW26-181	3,000*	2212	6.5×10^{13}	14.7*	--	--	--	--	--	5/63-11/63*
E. Pin-type specimens, Cb-1 Zr alloy cladding (with W barrier) and end caps, 0.296 OD x 0.025 wall cladding, UC matrix 10% enriched, 0.242 inch D x 0.65 inch long pellet height, 1.5 Kw/cc in Li at 2200F design										
PW26-190	1,069	2055	6.2×10^{13}	6.8	2.1×10^{20}	1.7	76.0	+1.0	Intermittent	
PW26-191	1,830	2103	6.5×10^{13}	8.5***	2.6×10^{20}	1.2	44.3	1.9	--	11/62-3/63
PW26-192	10,000*	2188	6.5×10^{13}	40.0*	--	--	--	--	--	3/63-9/64*
PW26-195	10,000*	2200*	6.2×10^{13}*	40.0*	--	--	--	--	--	7/63*-12/64*
PW26-196	10,000*	2200*	6.2×10^{13}*	40.0*	--	--	--	--	-	7/63*-12/64*
F. Pin-type specimens, Cb-1 Zr alloy cladding and end caps, 0.309 OD x 0.035 wall cladding, UN matrix 31.5% enriched, 0.237 inch D x 0.65 inch long pellet height, 1.5 Kw/cc in Li at 2200F design										
PW26-210	1,092	2119	3.0×10^{13}	1.3	1.4×10^{20}	1.1	3.3	Nil	Spotty	10/62-12/62
G. Pin-type specimens, Cb-1 Zr alloy cladding and end caps, 0.309 OD x 0.035 wall cladding, UN matrix 10% enriched, 0.237 inch D x 0.65 inch long pellet height, 1.5 Kw/cc in Li at 2200F design										
PW26-220	1,690	2149	6.3×10^{13}	9.7	3.1×10^{30}	1.5	11.7	2.3	2-13 mils	1/63-4/63
H. Pin-type specimens, Cb-1 Zr alloy cladding (with W barrier) and end caps, 0.312 OD x 0.035 wall cladding, UN matrix 10% enriched, 0.237 inch D x 0.65 inch long pellet height, 1.5 Kw/cc in Li at 2200F design										
PW26-230	853	2215	6.2×10^{13}	6.3	2.0×10^{20}	1.9	0.8	Nil	Spotty	1/63-3/63
PW26-231	3,000*	2220	7.1×10^{13}	14.0*	--	--	--	--	--	2/63-8/64*
I. Pin-type specimens, Cb-1 Zr alloy cladding (with W barrier) and end caps, 0.296 OD x 0.025 wall cladding, UN matrix 10% enriched, 0.241 inch D x 0.65 inch long pellet height, 1.5 Kw/cc in Li at 2200F design										
PW26-240	3,000*	2201	6.5×10^{13}	11.5*	--	--	--	--	--	4/63*-10/64*
PW26-241	1,000*	2215	6.7×10^{13}	3.8*	--	--	--	--	--	4/63*-6/63
PW26-242	3,000*	2200*	5.7×10^{13}*	11.5*	-	--	--	--	--	--
PW26-243	10,000*	2200*	5.7×10^{13}*	38.2*	--	--	--	--	--	--
PW26-244	10,000*	2200*	5.7×10^{13}*	38.2*	--	--	--	--	--	--

* Design value
** Average to date
*** Mass spec. B.U.
\+ Average before heater failure

RESULTS OF SNAP-50/SPUR FUEL IRRADIATION

Data	PW26-190	PW26-191	PW26-150	PW26-151	PW26-153	PW26-170	PW26-171	PW26-210	PW26-220	PW26-230
Fuel Composition	$UC_{1.0}$	$UC_{1.0}$	$UC_{1.08}$	$UC_{1.08}$	$UC_{1.08}$	$UC_{1.08}$	$UC_{1.08}$	UN	UN	UN
Barrier	W	W	TA	Ta	Ta	None	None	None	None	W
Cladding	Cb-1 Zr	Cb-1 Zr	Cb-1 Zr	Cb-1 Zr	Cb-1 Zr	Cb-1 Zr	Cb-1 Zr	Cb-1 Zr	Cb-1 Zr	Cb-1 Zr
Test Duration, hour	1069	1830	2562	1027	679	2210	892	1092	1690	853
Cladding Temperature, F**	2055	2154***	2094*	2175	2208	2172	2135	2119	2149	2215
Specimen Weight Loss, grams	Nil	ND	0.34	Nil	0.21	ND	0.014	0.016	0.13	0.075
Cover Gas Pressure, psia	38.2	48.3	9.6	11.5	7.9	ND	9.5	9.2	21.0	9.8
Fuel Density, % Theoretical	ND	ND	-5.2	ND	-4.1	ND	-2.2	-1.0	-6.0	-2.6
Pretest	92.4	92.3	94.2	95.2	94.7	96.8	97.2	95.9	94.3	96.0
Posttest	ND	ND	89.0	ND	90.6	ND	95.0	94.9	88.3	93.4
Specimen Diameter Δ, mils	+1	+2	+4	+5	+2	ND	+2.5	Nil	+2	Nil
Fission Burnup, % U^{235}	6.8	8.5	13.0	6.6	ND	ND	5.5	1.3	9.7	6.3
Fission Density, 10^{20} x f/cc	2.1	2.6	4.0	2.0	ND	ND	1.7	1.4	3.1	2.0
Power Density, Kw/cc	1.7	1.2	1.3	1.6	ND	ND	1.7	1.1	1.5	1.9
Fission Gas Release, % Xe	76.0	44.3	ND	7.5	ND	ND	0.2	3.3	ND	0.8
Reaction into Clad, mils	~1-2	~5	Nil	Nil	Nil	>25	2-13	~8	2-13	Nil

Data are for center specimen unless otherwise indicated

* First 1952 hours only. Heater failed. Full time average temperature = 1963F
** Time weighted average cladding temperature
*** First 1630 hours only. Heater failed. Full time average temperature = 2103F
ND Not determined

MIDDLE SPECIMEN, CAPSULE PW26-191

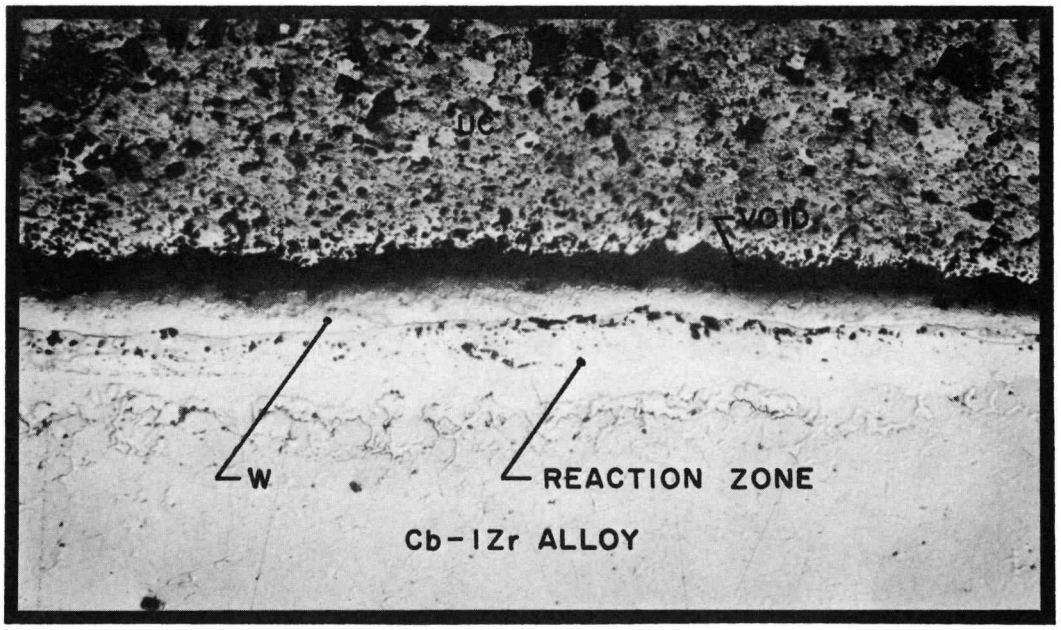

UNETCHED MAGNIFIED: 100X

A LONGITUDINAL SECTION THROUGH MIDDLE PELLET SHOWING REACTION IN Cb-1 Zr ALLOY BEHIND TUNGSTEN FOIL

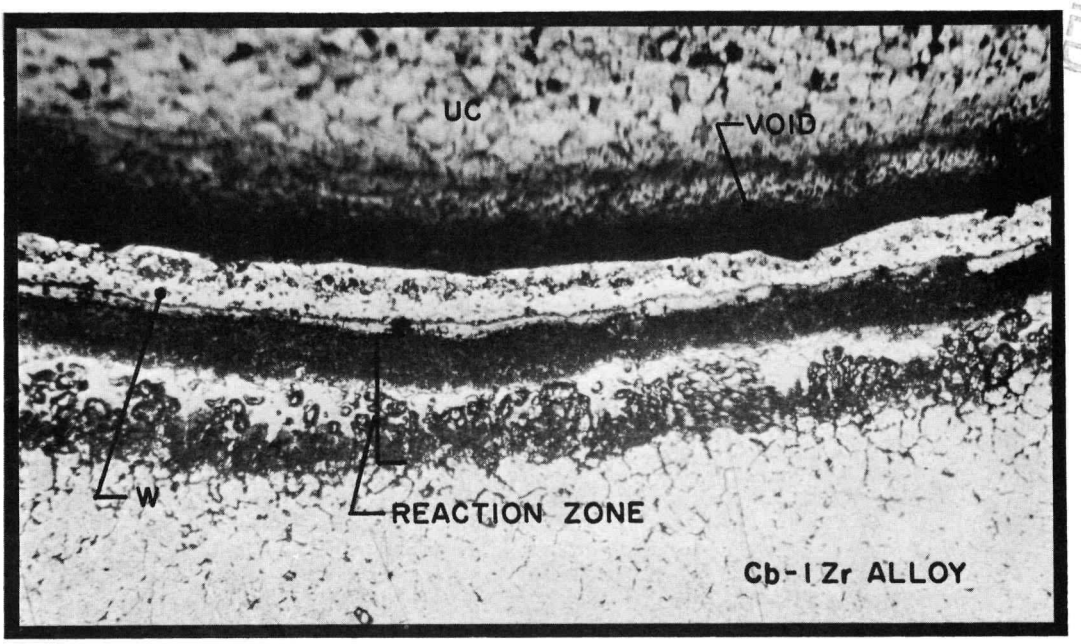

ETCHANT: 10 H_2O, 5 HNO_3, 2 HF (CLADDING) MAGNIFIED: 100X

B TRANSVERSE SECTION THROUGH TOP PELLET SHOWING REACTION OF TUNGSTEN AND Cb-1 Zr ALLOY

HM26220120

Cb-1 Zr ALLOY CLADDING FROM MIDDLE SPECIMEN CAPSULE PW26-220

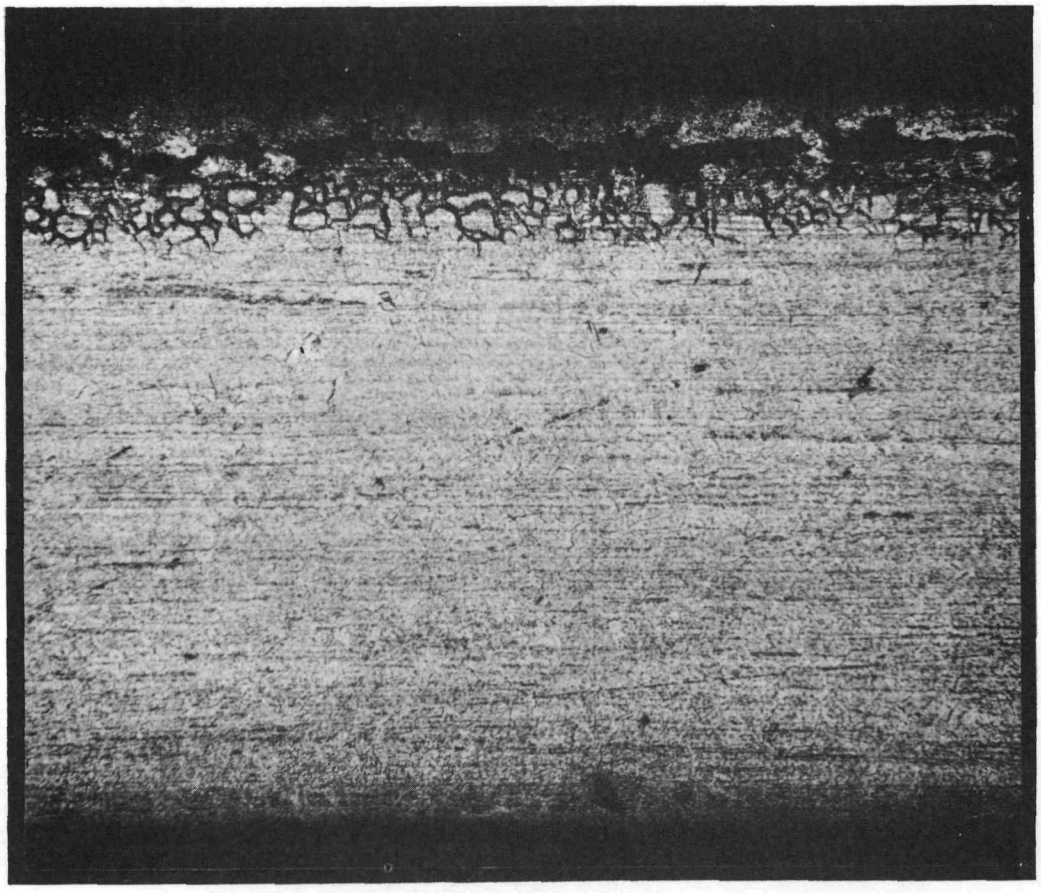

ETCHANT: 10 H_2O, 5 HNO_3, 2 HF MAGNIFIED: 100X

LONGITUDINAL SECTION SHOWING REACTION ZONE IN CLADDING AFTER CONTACT WITH URANIUM NITRIDE

Examination of inpile capsule PW26-230, containing nitride in tungsten-lined Cb-1 Zr alloy cladding, was completed. No significant change in diameter of specimens was observed, but specimens lost weight and fuel pellet densities decreased. Specimens were easily disassembled. Some cracking of the tungsten was observed, along with some associated evidence of incompatibility between fuel and cladding (Fig 68). Micro-examination of the fuel pellets showed slight amounts of a metallic phase. Fission gas retention was excellent.

The results from the fuel capsule irradiations examined to date (Fig 65) may be summarized as follows:

a. Effective barriers are required between either uranium carbide or uranium nitride and the Cb-1 Zr alloy cladding. The presence of second-phase carbides in hyperstoichiometric uranium carbide matrix did not prevent uranium-columbium alloy formation in the cladding.

b. Tantalum continued to demonstrate effectiveness as a barrier between hyperstoichiometric uranium carbide and Cb-1 Zr alloy. Carburization of the tantalum occurred as predicted, but no carbide phase or uranium was observed in the Cb-1 Zr alloy.

c. The usefulness of tungsten as a barrier between stoichiometric uranium carbide and Cb-1 Zr alloy demonstrated by out-of-pile tests has not been realized in inpile tests. The tungsten foil cracked during irradiation and allowed reaction with the Cb-1 Zr alloy. Reactions also occurred in areas where no cracks were apparent, although the possibility of cracks in adjacent planes is not discounted. Other variables such as purity of tungsten, contamination of pellets and contact with Cb-1 Zr alloy spacers at ends of fuel pellet stack may influence the extent of reaction.

d. Good fission gas retention appears to be associated with high pre-irradiation density for both carbide and nitride fuels. Gas retention may also be influenced by extent of reaction with cladding and with fuel composition.

e. Swelling of the fuel may be associated with higher fission gas retention.

A series of compatibility tests showed that uranium dioxide was extensively attacked in short times when exposed to 2200F lithium in defected Cb-1 Zr alloy clad specimens and that alloying between resultant uranium and the cladding was extensive. Compatibility specimens consisting of uranium dioxide pellets in sound and defected Cb-1 Zr alloy claddings were immersed in 2200F lithium for 50, 100, 200, 500 and 1000 hours. The 1000-hour test included 20 thermal cycles down to 1600F, performed during the last 300 hours of the test. The other tests were operated at isothermal conditions. The uranium dioxide pellets from defected specimens showed extensive reaction with the lithium, whereas those from sound specimens were unchanged (Figs 69 and 70). Metallic uranium was found at grain boundaries and on outer surfaces of the pellets exposed to lithium. Significant increases in grain size were also observed in the pellets of defected specimens. Alloying of uranium with the 13-mil thick Cb-1 Zr alloy cladding occurred to depths up to 12 mils. Magnitude of effects was dependent upon test duration but attack was observed in even the 50-hour specimens.

Only slight incompatibility in the form of finely-dispersed precipitates was observed in Cb-1 Zr alloy sections of uranium dioxide versus Cb-1 Zr alloy diffusion couple tests after 2327 hours at 2200F. A 1000-hour test at the same temperature exhibited no incompatibility.

HM26230014
HM26230010

TOP SPECIMEN, CAPSULE PW26-230

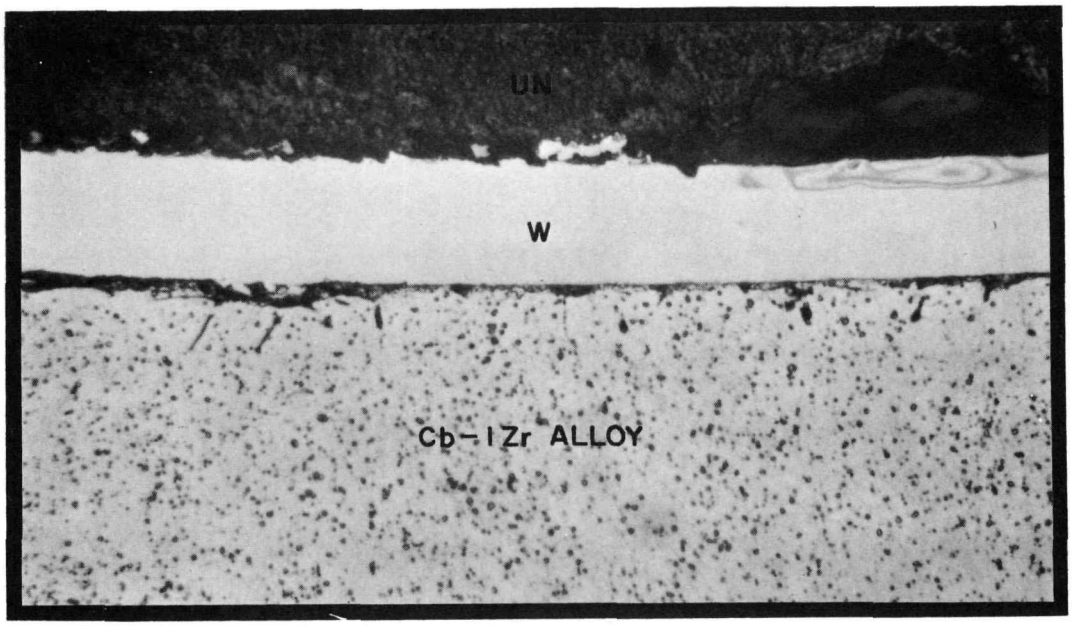

ETCHANT: 30 $CH_3CHOHCOOH$, 10 HNO_3, 3 HF, 30 H_2O MAGNIFIED: 500X

A TRANSVERSE SECTION THROUGH MIDDLE PELLET AND CLADDING SHOWING PROTECTION OF CLADDING BY TUNGSTEN FOIL

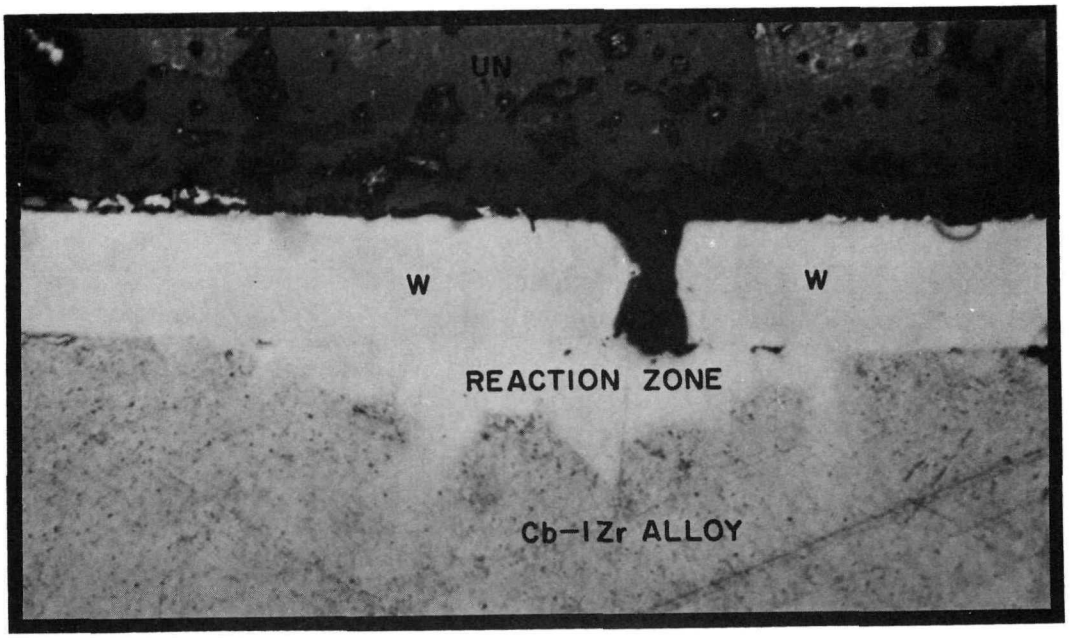

ETCHANT: 30 $CH_3CHOHCOOH$, 10 HNO_3, 3 HF, 30 H_2O MAGNIFIED: 500X

B TRANSVERSE SECTION THROUGH MIDDLE PELLET AND CLADDING SHOWING REACTION AT BREAK IN TUNGSTEN

URANIUM DIOXIDE VERSUS Cb-1 Zr ALLOY COMPATIBILITY SPECIMENS

(AFTER 500-HOUR TEST IN 2200F LITHIUM)

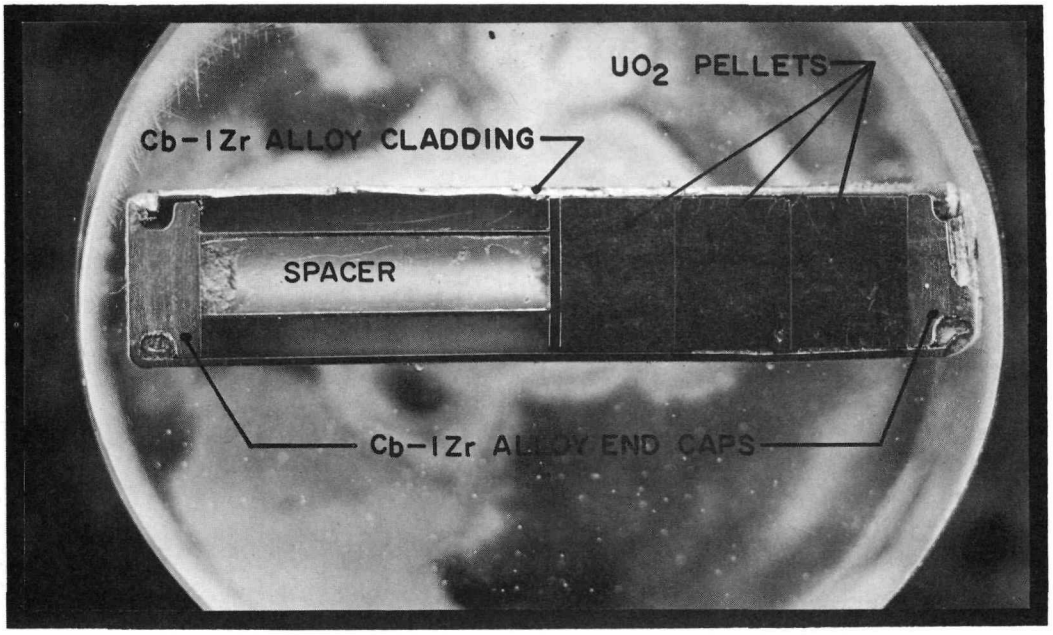

UNETCHED MAGNIFIED: 4X

A. LONGITUDINAL SECTION THROUGH DEFECTED SPECIMEN SHOWING CORROSIVE ATTACK OF UO_2

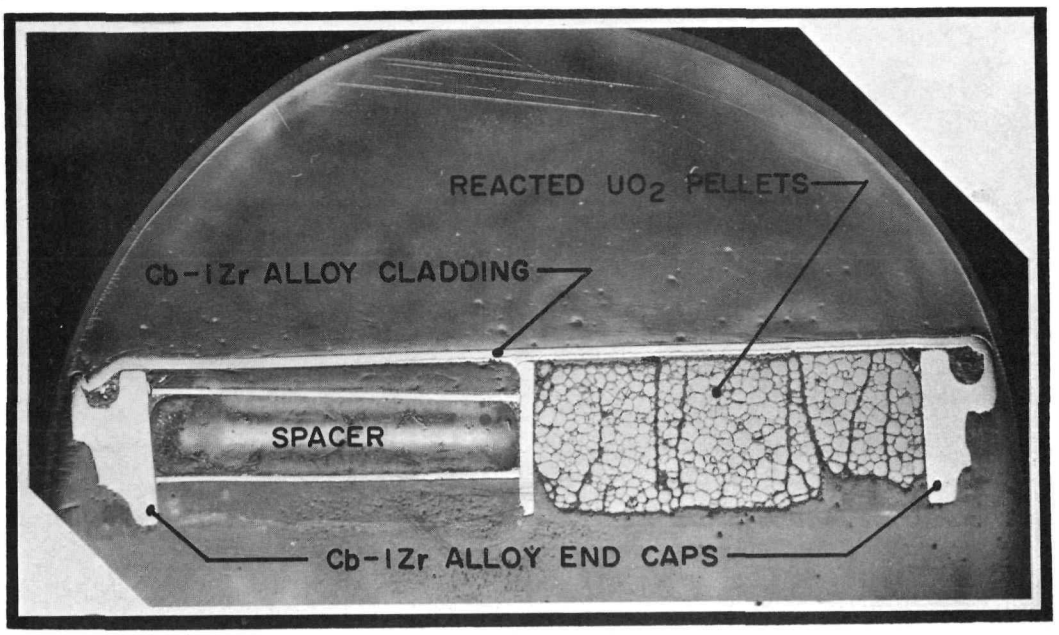

UNETCHED MAGNIFIED: 4X

B. LONGITUDINAL SECTION THROUGH SOUND SPECIMEN SHOWING NO ATTACK OF UO_2

FIG 70

2726-57
2726-61

URANIUM DIOXIDE FROM COMPATIBILITY SPECIMENS

(AFTER 500-HOUR TEST IN 2200F LITHIUM)

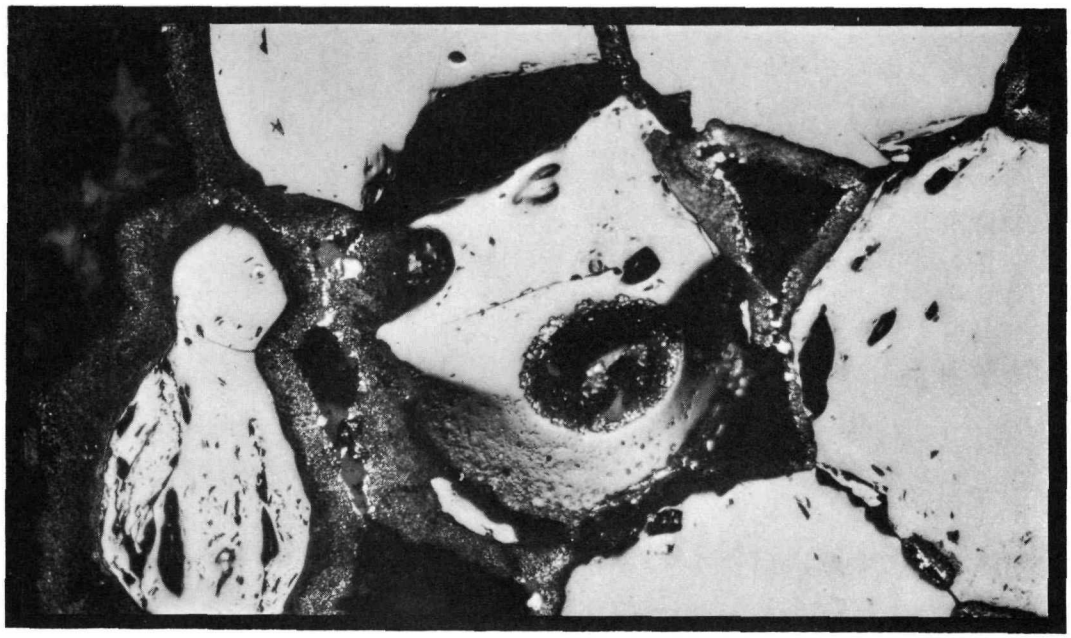

UNETCHED MAGNIFIED: 150X

A DEFECTED SPECIMEN SHOWING LARGE GRAIN SIZE AND EXTENSIVE ATTACK OF UO_2 GRAINS CAUSED BY LITHIUM

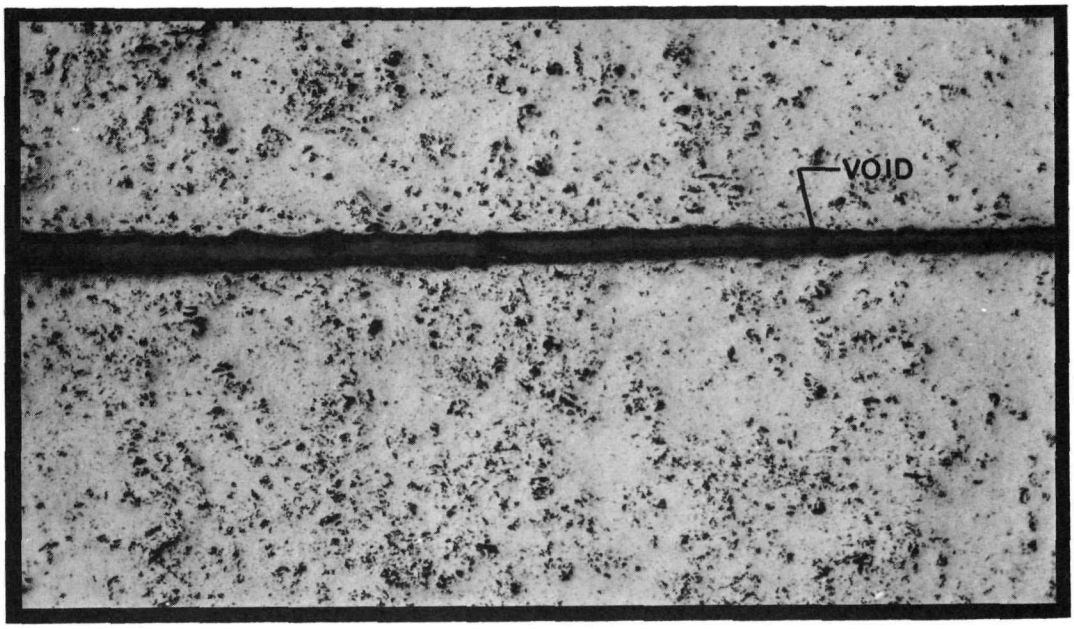

UNETCHED MAGNIFIED: 100X

B SOUND SPECIMEN SHOWING INTERFACE BETWEEN PELLETS

2. Reactor and Shielding

Initial experiment studies were performed on the CCA-7 critical assembly with a 12-inch diameter, 14-inch long core. The dimensions and material compositions of the base configuration are presented below:

Dimensions and Material Compositions by Region of CCA-7 (12x14) Base Configuration

Region	Dimensions (inches) Inner Radius	Outer Radius	Length	Composition ($gm/in.^3$) Al	BeO	C	Cb	SS
Core	-	6.10	14.18	3.14	-	3.08	67.0	1.24
Shell	6.10	7.07	20.00	4.70	33.2	-	-	3.11
Side Reflector	7.07	9.04	20.00	2.61	43.3	-	-	-
End Reflectors	-	6.10	3.00	2.86	34.9	-	9.64	1.24

The homogeneous critical mass of the base configuration was 103/kg of U^{235}. This was obtained after applying corrections for both the 1.45 dollar reactivity increase from incidental reflection by the critical assembly supporting structure, and for the 1.21 dollar increase from fuel lumping effects of the 1/8-inch-thick, 93 percent enriched, uranium blocks. The radial and axial fission rate distributions were investigated, and core-averaged reactivity coefficients were measured for selected materials as listed below:

Core-Averaged Material Reactivity Coefficients for CCA-7 (12x14) Base Configuration

Material	Reactivity Coefficient (cents/kg)
U^{235}	76.2
Al	25.8
Al_2O_3	32.0
BeO	67.2
C	58.4
Cb	5.72
Ta	-15.3
W	- 1.90

A series of investigations of the variations in the critical mass of the CCA-7 (12x14) with changes in reflector configuration were started. First, the beryllium oxide in the shell region of the base configuration was removed, leaving an annular region of low density aluminum and stainless steel between the core and side reflector. The critical mass for this configuration was found to be 119 kg of U^{235}. For the second alteration, columbium

was added to the shell region at a density of 102.2 gm/in^3, essentially filling the void left after removal of the beryllium oxide. The critical mass for this configuration was found to be 111 kg. Third, the approximate two-inch thickness of beryllium oxide outside the gap of the first side reflector alteration was increased to approximately three inches. The critical mass was found to be 109 kg. The dimensions and material compositions of the regions altered in this study are summarized below:

Dimensions and Material Compositions of Altered Regions of CCA-7 (12x14) in Side Reflector Studies

Alteration	Region	Dimensions (inches) Radius	Radius	Length	Composition (gm/in^3) Al	BeO	Cb	SS
1	Shell	6.10	7.07	20.00	4.70	-	-	3.11
2	Shell	6.10	7.07	20.00	4.70	-	120.0	3.11
3	Shell	6.10	7.07	20.00	4.70	-	-	3.11
	Side Reflector	7.07	10.09	20.00	2.61	43.3	-	-

Two physics parameter studies were completed on SNAP-50/SPUR type reactors, using UO_2-BeO fuel and UC fuel. The critical volume fraction of fuel was calculated as a function of the following five variable parameters over the indicated range of variation:

Variable Parameter	Range of Variation UC Study	UO_2BeO Study
Core Diameter, inches	9 - 12	12 - 17
Ratio of Core Height to Diameter	0.8 - 1.2	0.8 - 1.2
End Reflector Thickness, inches	0 - 5	0 - 5
Coolant Volume Fraction	0.1 - 0.3	0.10 - 0.25
Base Reactivity (Side Reflector Removed)	0.85 - 0.97	0.85 - 0.97

For any given set of five variable parameters, the fuel volume fraction was calculated with the side reflector removed using the TDC code. A second calculation was obtained using an estimated side reflector thickness and the effective multiplication with the side reflector on.

Engineering calculations have continued on several aspects of the preliminary reference design UC reactor. An elastic analysis of the transition region between the hexagonal core skirt and the conical flow divider was performed. The maximum effective stress, located at the upper end of the conical section, was estimated to be 1500 psi. An elastic analysis is in progress on the revised version of the lower dome of the pressure vessel. Excessive inlet and outlet coolant velocities led to redesign of this section. A Bendix G-15 computer program has been written for determining the location and magnitude of the maximum effective stress in a long cylindrical shell which contains a uniform internal pressure, edge moments and shearing forces. This program will be used to analyze an annular flow divider for an alternate core configuration.

It was determined that the afterheat generated after a 10,000-hour operation of an 8-Mwt SNAP-50/SPUR reactor can be removed by helium flow through the preheat jacket, starting 30 days after shutdown at a core temperature level of 1000F. The required helium flow was estimated to be 360 lb/hr with a pressure loss of approximately 0.5 psi, for an assumed 0.2-inch preheat gas gap. The maximum temperature level reached was 1380F.

A method for the calculation of SNAP-50/SPUR core hot channel factors was completed and incorporated into an IBM-7090 code for computation of the reactor temperature distribution.

Maximum temperature levels in the SNAP-50/SPUR reflector and cladding have been computed as a function of reflector thickness and emissivity for both 2 Mwt and 8 Mwt reactor operation.

Machine computer methods for performing parametric calculations of weight optimized reactors were completed. A series of parametric studies was started to incorporate recent data on Cb-1 Zr alloy creep strength, data on reduced fuel center line temperatures to reduce fuel fission gas release and/or swelling, and data on the improved physics analysis results. Corresponding revision of representative preliminary reactor specifications was initiated.

The feasibility of using depleted uranium and lithium hydride for the shield for 2 Mwt reactor operation was evaluated in a preliminary survey. An estimate was made of the secondary gamma dose rate from a shield of depleted uranium exposed directly to the reactor leakage flux. The result indicates that a depleted-uranium shield of about two-inch thickness or less can precede a lithium hydride neutron shield, and the secondary contribution will be less than about ten percent of the attenuated primary gamma dose rate.

A study was made of lithium hydride properties and their effects on the temperature in a radiatively cooled shield of this material. Inclusive knowledge of these properties prevents accurate shield temperature predictions. However, the acceptance of the most detrimental value in each property spectrum reported in the literature would not prohibit the use of lithium hydride for the neutron shield.

Nuclear heating rates in a uranium-lithium hydride shield were computed by approximate methods and a thermal analysis was performed to obtain an estimate of the shield temperatures. Maximum temperatures of 1000F to 1100F were obtained in the uranium and in the canned lithium hydride shield for 2 Mwt reactor operation. Heat loss was by direct radiation to space from shield surfaces which were assumed to have an emissivity of 0.8.

The feasibility of insulating a 2000F reactor coolant pipe through a lithium hydride shield was studied. Practical numbers of radiation baffles would not prevent lithium hydride melting. Computations suggest that insulation resistances of about 3.5 hr-ft^2-F/Btu are necessary for acceptable lithium hydride temperatures. One company has reported having developed an insulation for use in high vacuum and capable of providing such a resistance with a thickness of about one inch.

3. Primary Pump

Analyses of the SNAP-50/SPUR primary pump components are in progress. These studies include parametric data on over-all performance characteristics, as well as detailed de-

sign analyses of hydraulic, bearing, and motor components. The motor parametric studies and preliminary design work are being performed under separate contracts. Hydraulic designs include the main pump impeller and scroll, the bearing lubricant pump impeller, dynamic seals, and the liquid film thrust and journal bearings. A shaft speed of about 15,000 rpm has been tentatively selected, based upon a motor current frequency of 1000 cps. The pump parametric studies have indicated that significant gains in over-all pump efficiency are possible with increased values of shaft speed and reduced pump inlet pressures corresponding to higher values of suction specific speed.

Fabrication of parts for the high temperature rotating disk test unit is approximately 95 percent complete. The shaft assembly was scrapped as a result of damage incurred in attempting to shrink-fit the Cb-1 Zr alloy and stainless steel sections of the shaft. The procuremer of a second shaft was initiated. Fabrication of the liquid metal rotating disk test apparatus has been essentially completed. The feasibility of conducting tests of anti-friction bearings in 600F to 800F lithium with this apparatus is being studied.

The mechanical properties of several of the refractory metal alloys to be used in the cavitation damage program have been evaluated at room temperature, at 1700F, 1800F, 1900F, 2000F, and 2100F. These tests have included the tensile strength of Cb-1 Zr alloy for standard heat treatment and large grain structure, the hot hardness of Cb-1 Zr alloy for standar heat treatment and large and small grain structure, tensile strength and hot hardness tests for molybdenum-50 percent titanium as described above for Cb-1 Zr alloy, the tensile and hot hardness for Ta-10 W in the as-received condition, and the hot hardness for Ta-8 W-2 Hf in the as-received condition.

Additional tests with the rotating disk apparatus in water were also conducted with Cb-1 Zr alloy specimens. A photograph of a standard annealed Cb-1 Zr alloy specimen after four hours of test at 6000 rpm is shown in Fig 71. Cavitation damage data obtained under comparable test conditions on the rotating disk apparatus in water for aluminum, Cb-1 Zr alloy and type 316 stainless steel is shown in Fig 72. It is noted that the curve for the Cb-1 Zr alloy falls between the other two materials tested.

Screening tests of standard annealed Cb-1 Zr alloy specimens, together with annealed specimens of Ta-10 W and Ta-8 W-2 Hf, were conducted in a cavitating venturi apparatus in roor temperature water and mercury. The tests of both tantalum base alloys conducted in mercury indicated superior cavitation damage resistance over the Cb-1 Zr alloy and other materials previously tested, including stainless steel. Both tantalum base alloys also exhibited higher resistance than Cb-1 Zr alloy in water, but were not quite as resistant as stainless steel.

A view of the full-scale stainless steel primary pump impeller during fabrication on the tape controlled milling machine is shown in Fig 73. This impeller and its associated housings have been completed and are being made ready for water test in the PT-2 test stand of the Pump Turbine Laboratory. The initial test of a jet pump in conjunction with an unshrouded impeller is in progress in this test stand. An over-all view of the jet pump test apparatus is shown in Fig 74.

Fabrication of the detail parts of the first water rotor-dynamics test unit has been nearly completed and assembly will begin shortly. This unit was designed with the simulated motor rotor mass overhung from the journal bearings.

The second water rotor-dynamics test unit with the simulated motor rotor mass straddled by the journal bearings is shown in Fig 75. Test stand designs for both water rotor dynamics rigs have been initiated.

CAVITATION DAMAGE TO Cb-1 Zr SPECIMEN AFTER 4 HOUR TEST IN WATER

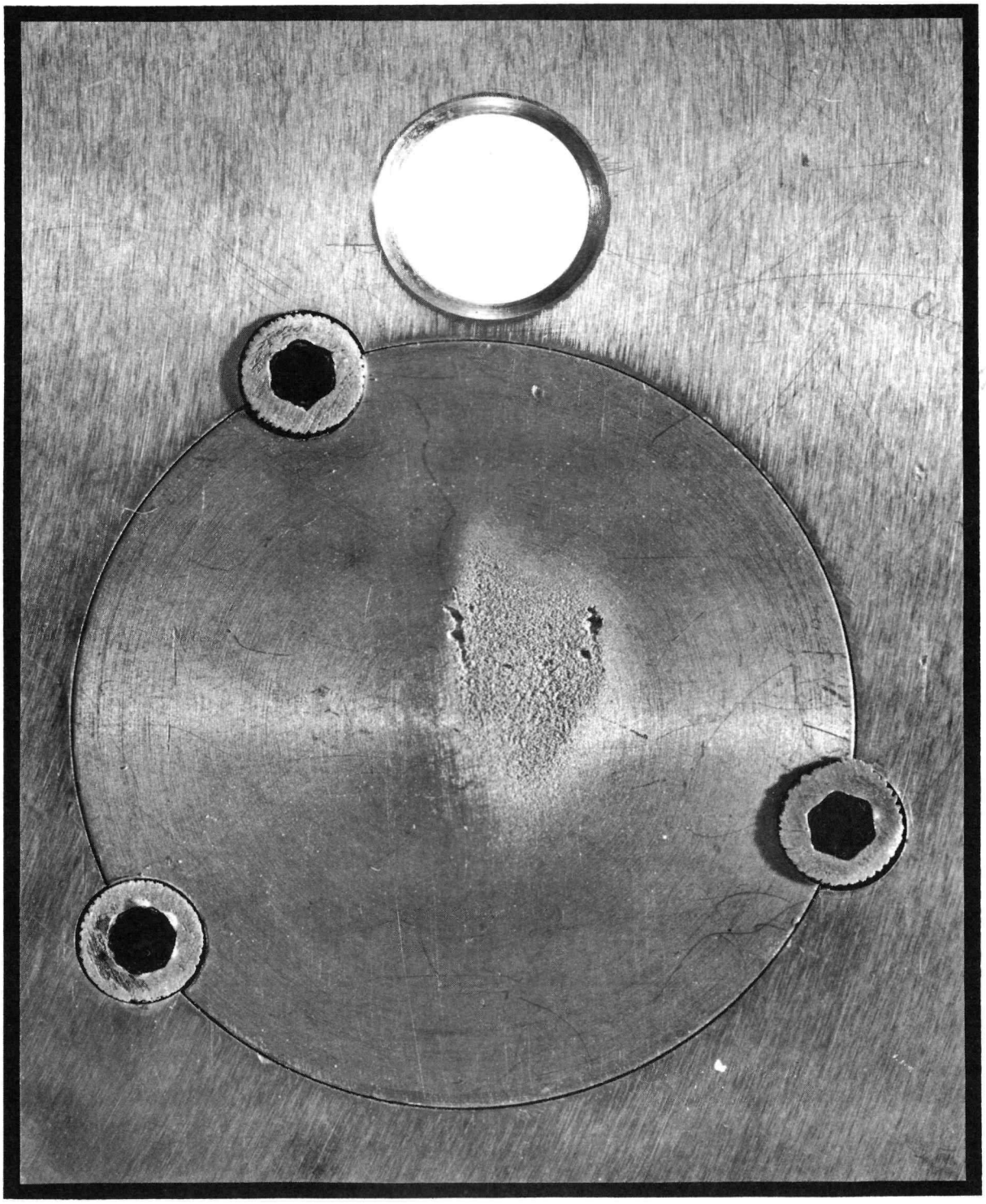

CAVITATION VOLUME DAMAGE RATE

SHAFT SPEED – 6000 RPM
POT PRESSURE – 10PSIG
VELOCITY – 162 FT/SEC

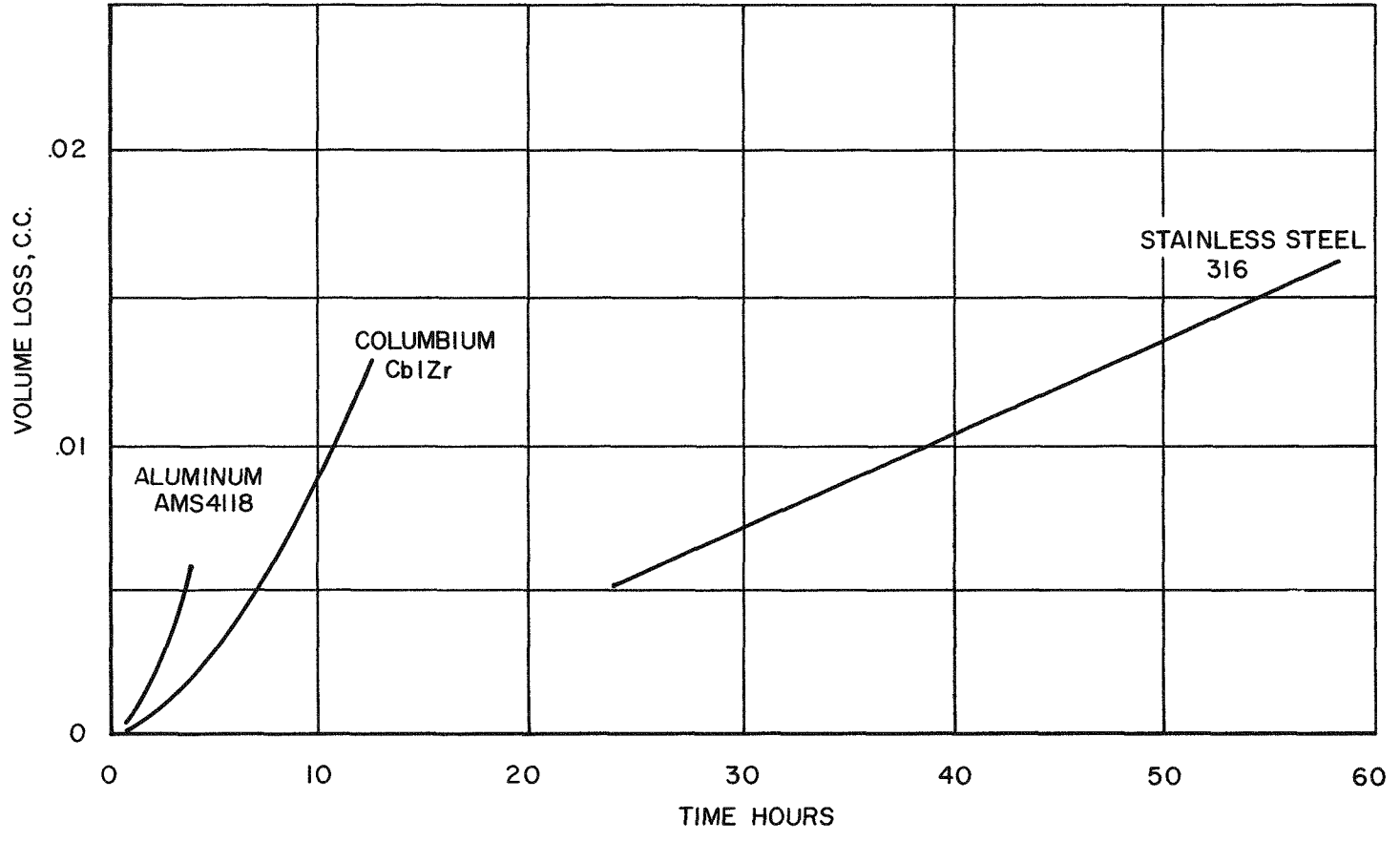

PRIMARY COOLANT PUMP IMPELLER

MACHINING OF STAINLESS STEEL MODEL FOR WATER TESTS

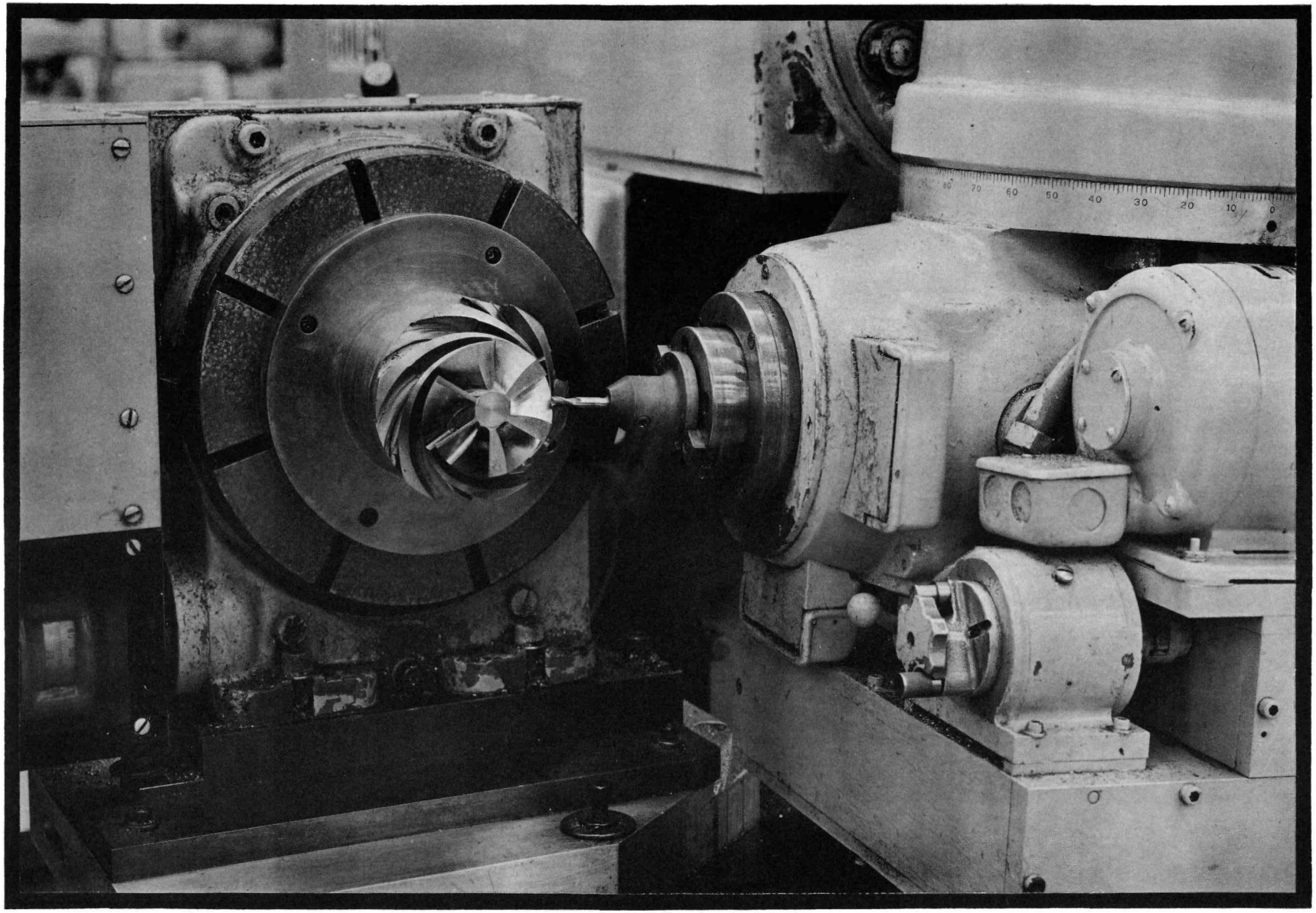

FIG 74

JET PUMP TEST IN WATER

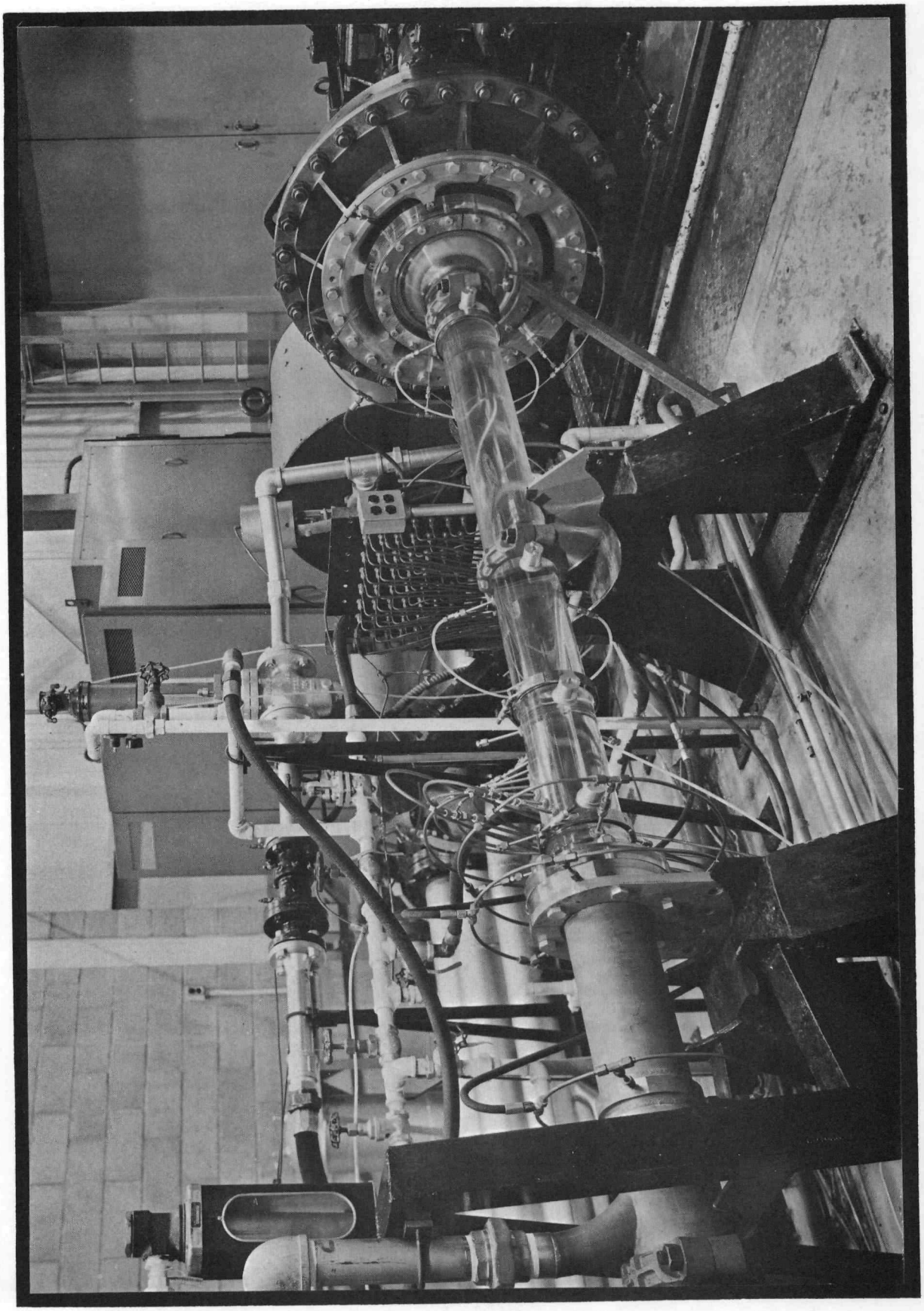

ROTOR DYNAMIC TEST UNIT FOR HYDROSTATIC BEARINGS WITH STRADDLED LOAD

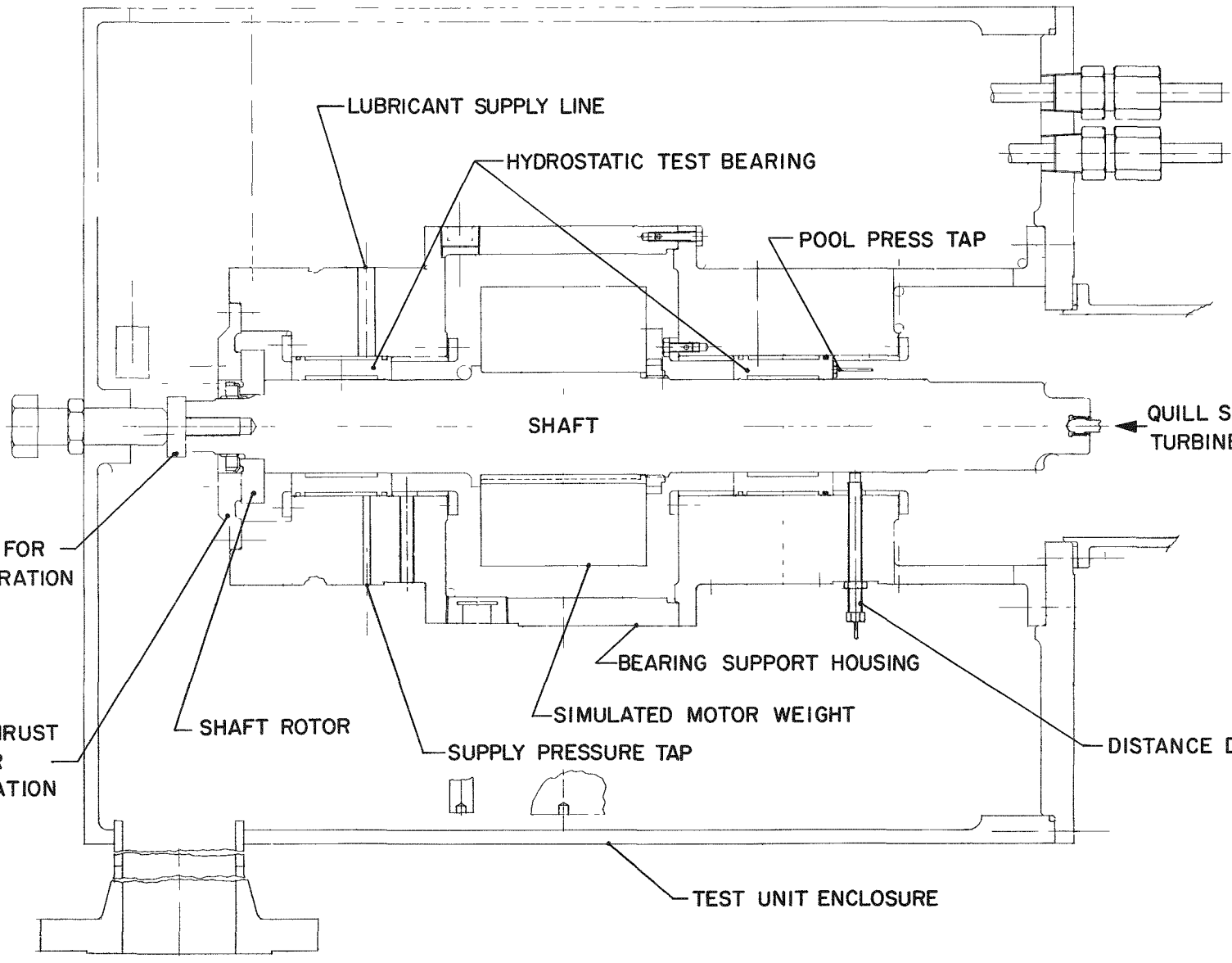

A photograph of the installed water, hydrostatic journal bearing test rig is shown in Fig 76. This rig was designed from modified turbopump parts and is driven by a partial-admission, single-stage turbine operating on compressed air. A view of a four-pool, orifice-compensated journal bearing for test in this rig is shown in Fig 77. Static flow calibration data of the first bearing is presented in Fig 78. It is noted that the data does not correspond closely with the data of Ramondi and Boyd. The principal discrepancy appears to be in the values of the orifice coefficients. This test rig is being prepared to conduct the first series of rotating tests with the same hydrostatic test bearing.

The lithium radial bearing test unit was shut down as planned after 2103 hours of test at 5000 rpm. The titanium carbide journal was 3.875 inches in diameter. The bearing was tungsten carbide. The test ran quite smoothly with applied radial loads ranging from 30 to 200 pounds in lithium at temperatures from 600F to 800F. From the records of the input power to the drive motor, it was observed that the bearing rig ran with very few power fluctuations at the higher radial loads. The test bearing and its journal are shown in Figs 79 and 80. The journal appeared in excellent operating condition with only very light rub marks

Portions of its surface were coated with a very thin black deposit of unknown composition. Areas of light rubbing were noted in one section of the bearing. It was also observed that a crack had developed in the bearing (Fig 79), but the cause of the cracking is not known.

The lithium-to-vacuum seal test unit is being assembled for test in the dry box and an endurance test in 800F lithium is scheduled for the next quarter.

4. Boiler

Fabrication and installation of the Haynes-25 alloy, 1800F boiling potassium, heat transfer loop were completed (Fig 81). Cover gas purification, liquid metal filling, and liquid metal purification were completed late in the quarter. Several days of two-phase operation have been completed, in addition to system flow and heat loss calibration runs. Extensive two-phase testing is now being accomplished with this rig.

Operation of the first stainless steel, boiling potassium loop which incorporated a twisted ribbon insert was terminated after about 200 hours of two-phase operation. Over-all heat transfer and pressure drop data from 0 to 100 percent quality was obtained on this loop, with up to 15 pounds per hour potassium flow rate. The test was terminated due to the limited range of stable operation attainable with the high vapor phase pressure drops in the boiler tube and in the tube between the boiler and condenser. The orifice used at the tube in let was too large to improve stability.

The second stainless steel loop (NKSS-B), an improved version of the first loop, with a helical slotted insert in the boiler tube, was installed in the test stand and filled with liquid metal. A photograph of this installation is shown in Fig 82. Several days of two-phase oper ation were completed by the end of the quarter, including a) 48 two-phase heat transfer data points, b) generation of vapor to 100 percent quality and with superheat, c) heat fluxes to 50,000 Btu/ft^2 hr, d) potassium flow rates to 32 pounds per hour and e) boiling temperatures to 1580F. A typical performance condition attained in these tests was vaporization of 21 lb/hrs of potassium to 100 percent quality in the five-foot long boiler tube with an average temperature difference of 75F between the sodium and potassium. The wider range of stable operation attainable on this loop is attributed to the more favorable ratio of liquid and vapor pressure drops realized by lowering the pressure drop of the boiler and increasing the pressure drop of the boiler inlet orifice.

The two-phase water screening tests were continued to include two sizes of tubing with integ ral helical fins and two sizes of dual-diameter tubes. Fig 83 shows the geometries being tested and Figs 84 and 85 show the heat transfer and pressure drop characteristics, respectively.

FIG 76

HYDROSTATIC JOURNAL BEARING WATER TEST RIG

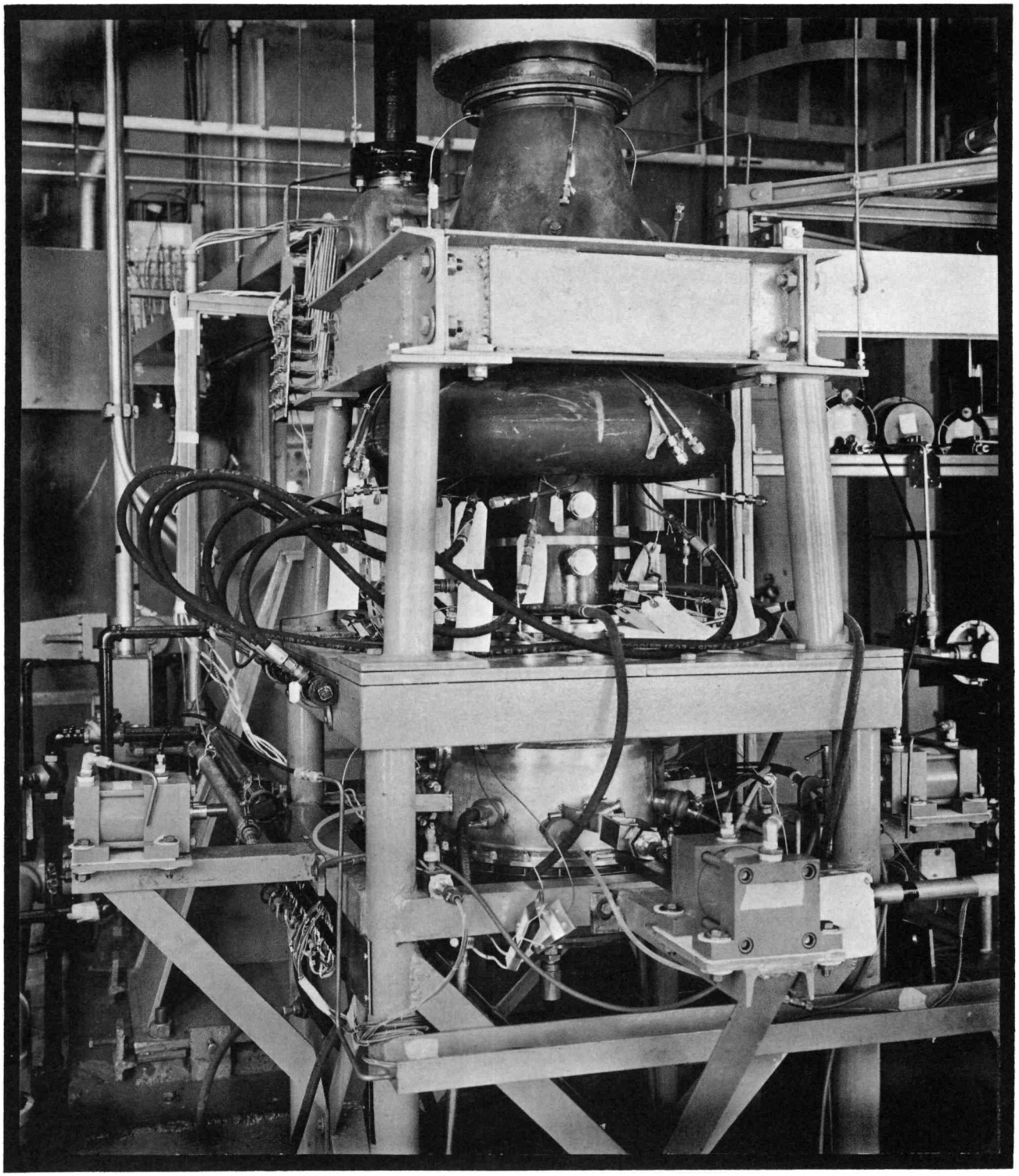

STAINLESS STEEL HYDROSTATIC TEST BEARING

UNCLASSIFIED

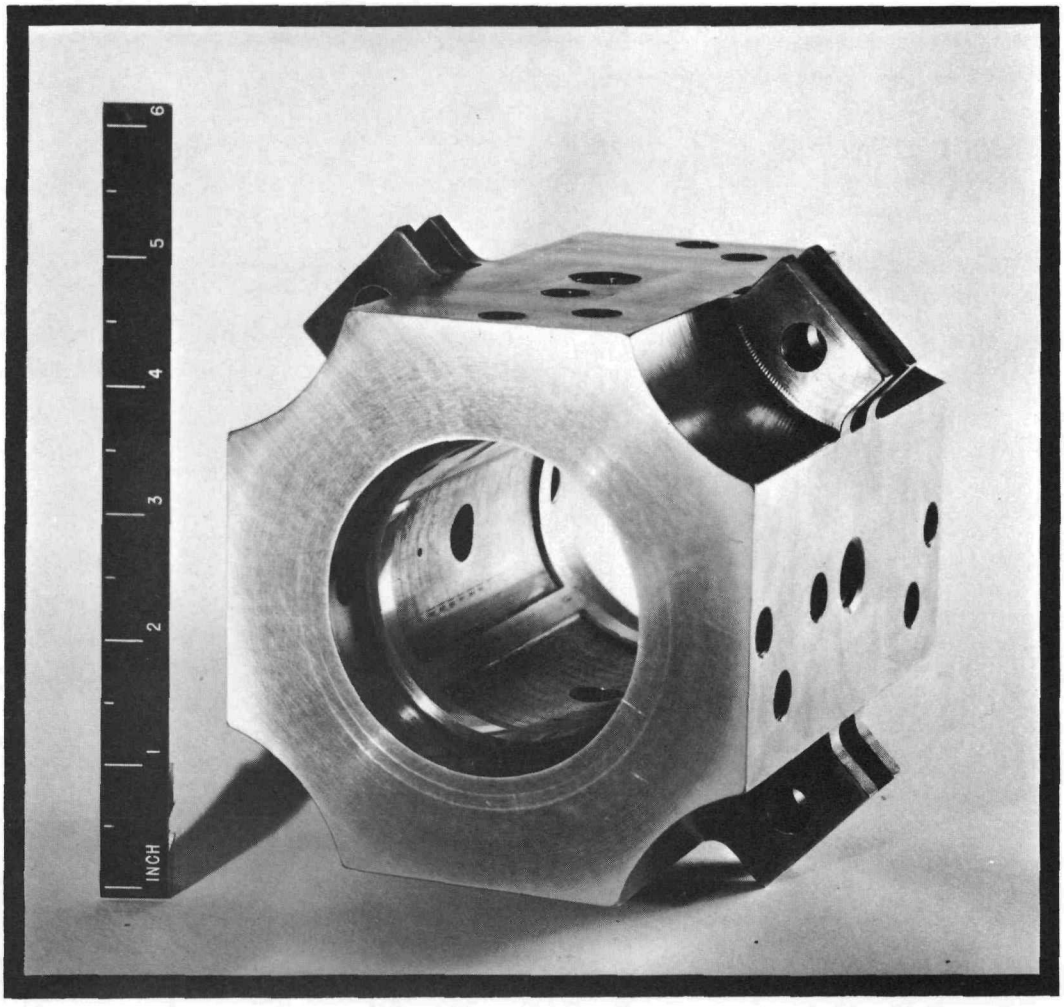

FIG 78

STATIC FLOW TEST OF ORIFICE COMPENSATED HYDROSTATIC JOURNAL BEARING

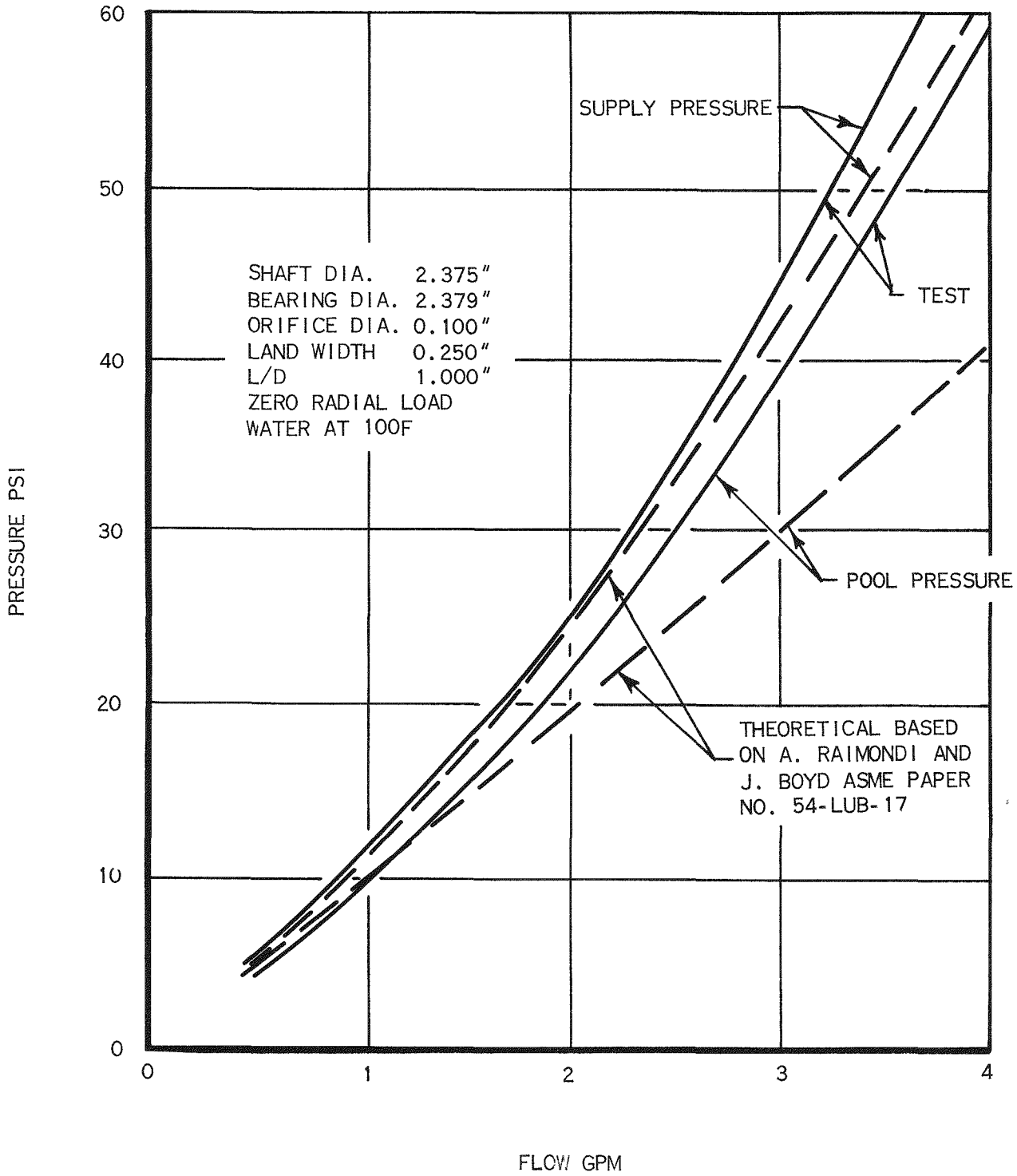

HYDRODYNAMIC BEARING AFTER 2103 HOUR TEST IN LITHIUM

FIG 80

HYDRODYNAMIC BEARING JOURNAL AFTER 2103 HOUR TEST IN LITHIUM

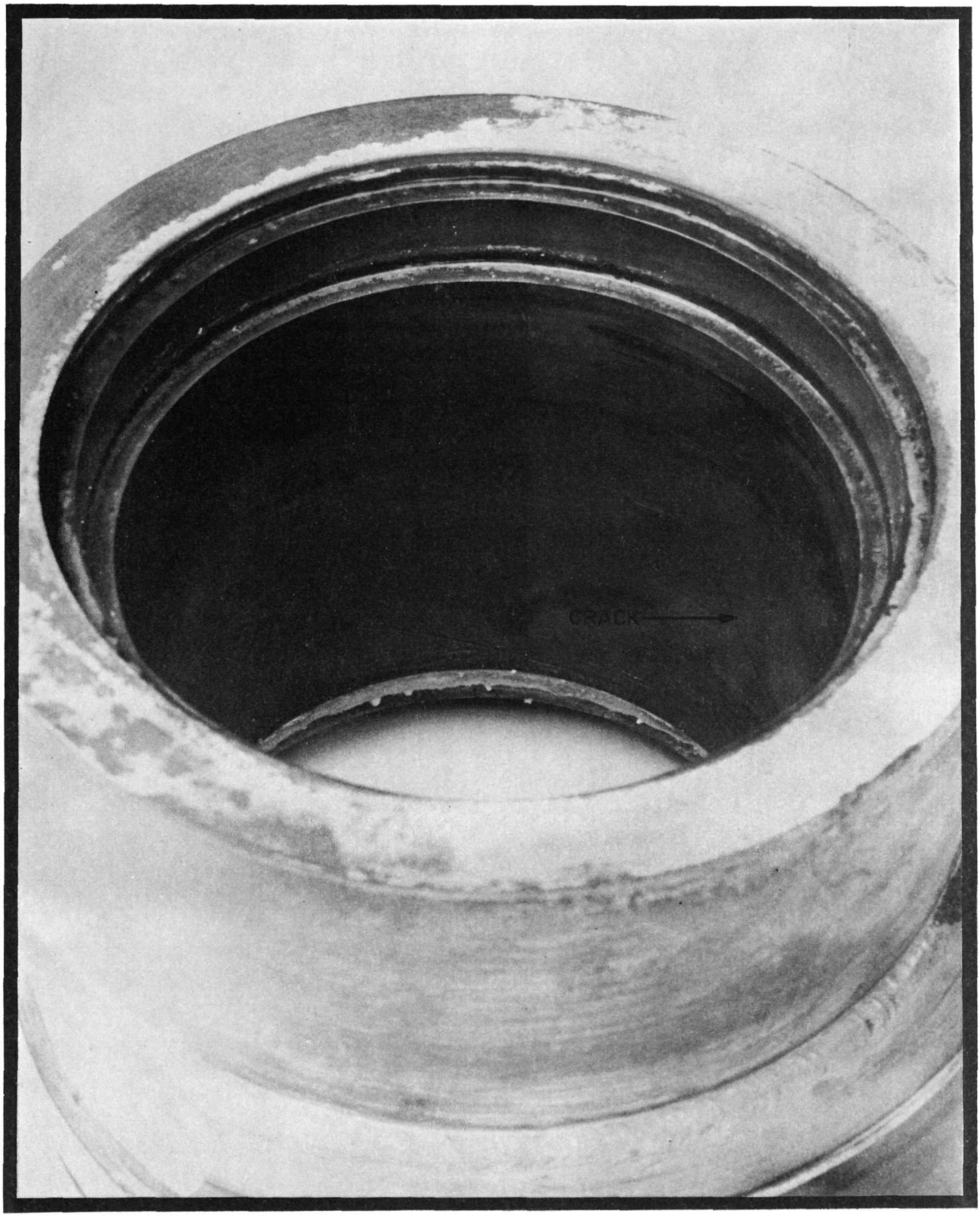

FIG 81

HAYNES 25 ALLOY BOILING POTASSIUM HEAT TRANSFER LOOP

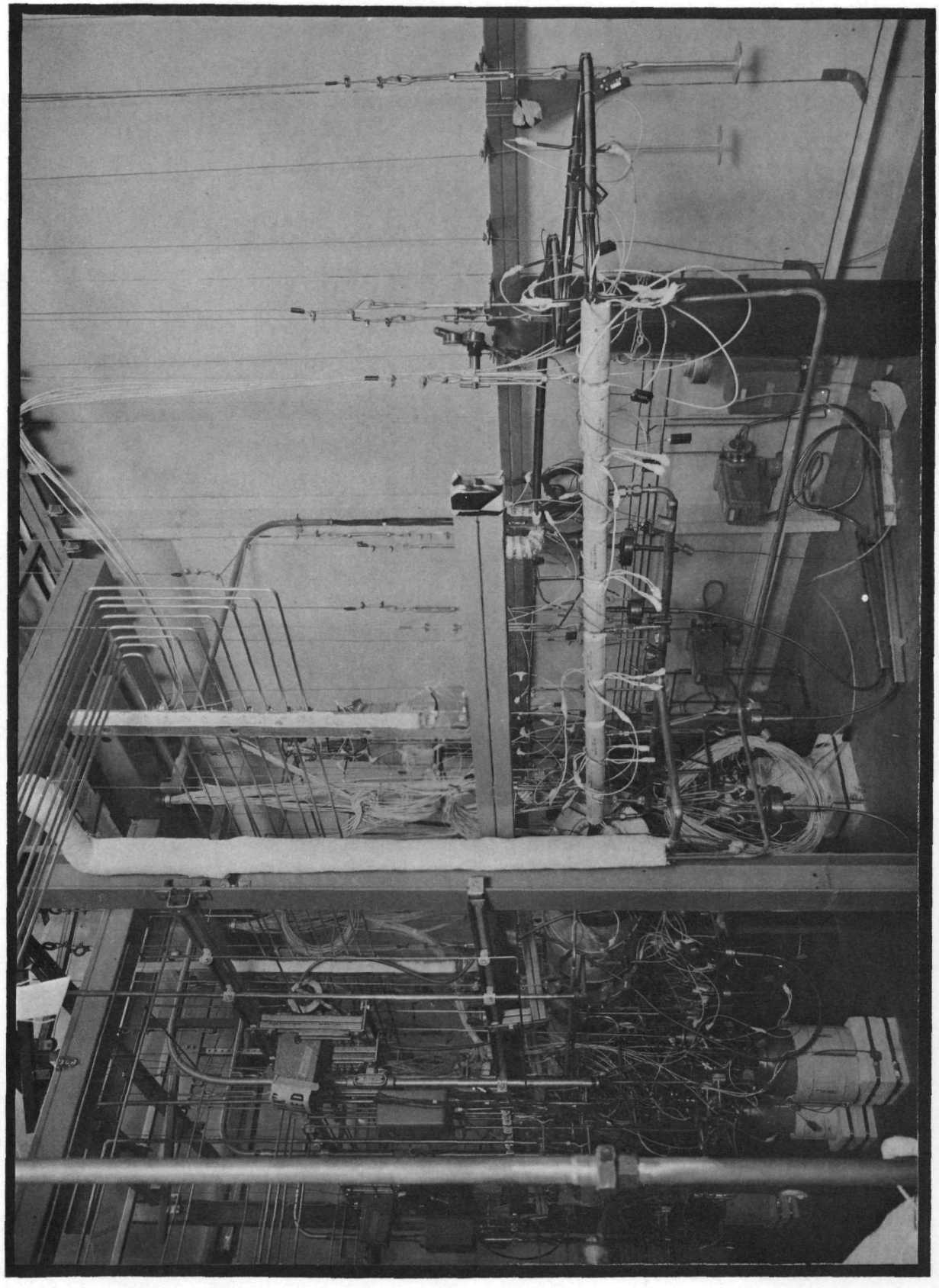

STAINLESS STEEL BOILING POTASSIUM HEAT TRANSFER LOOP NKSS-B

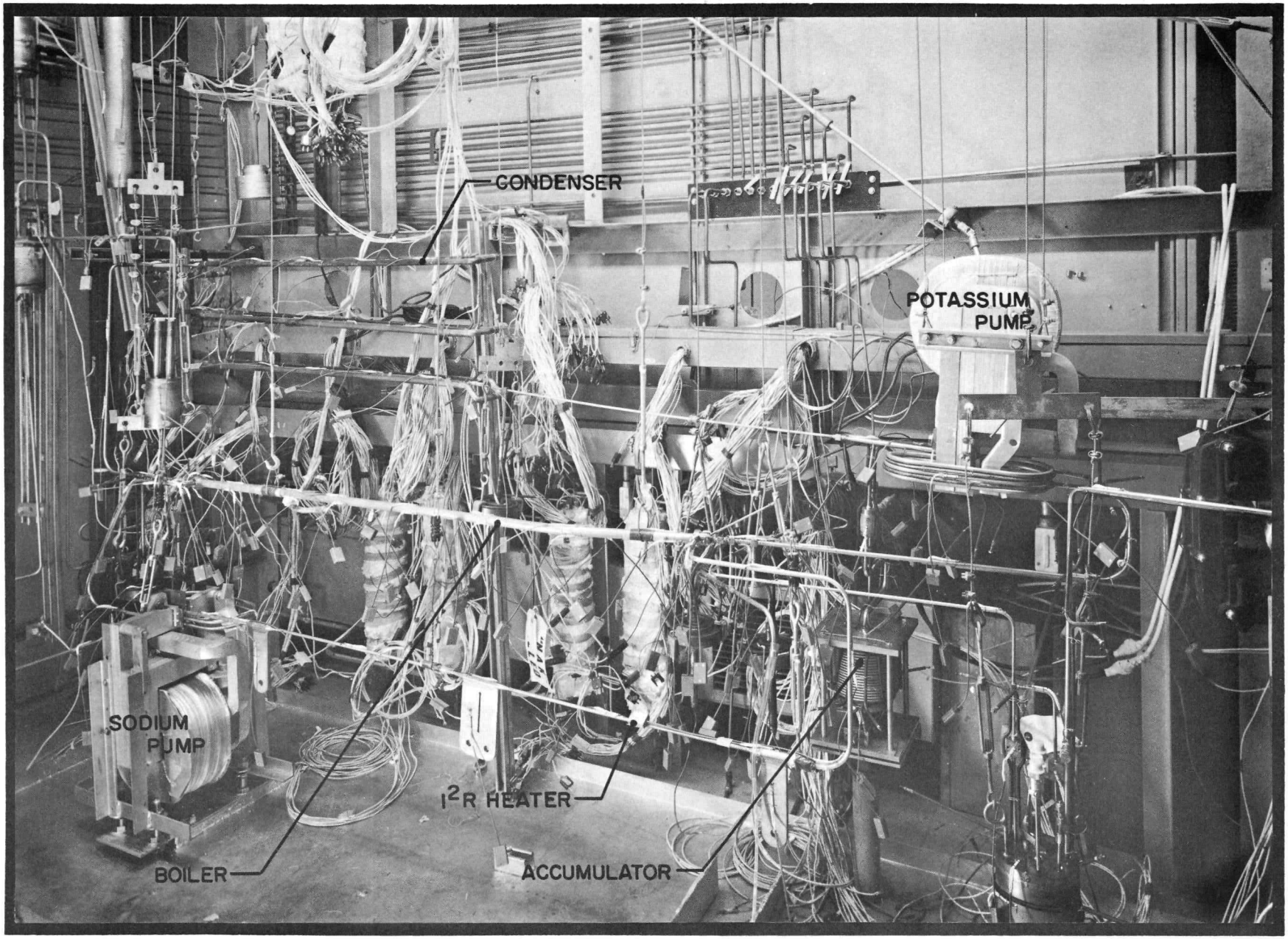

FIG 83

BOILER TUBE SAMPLES

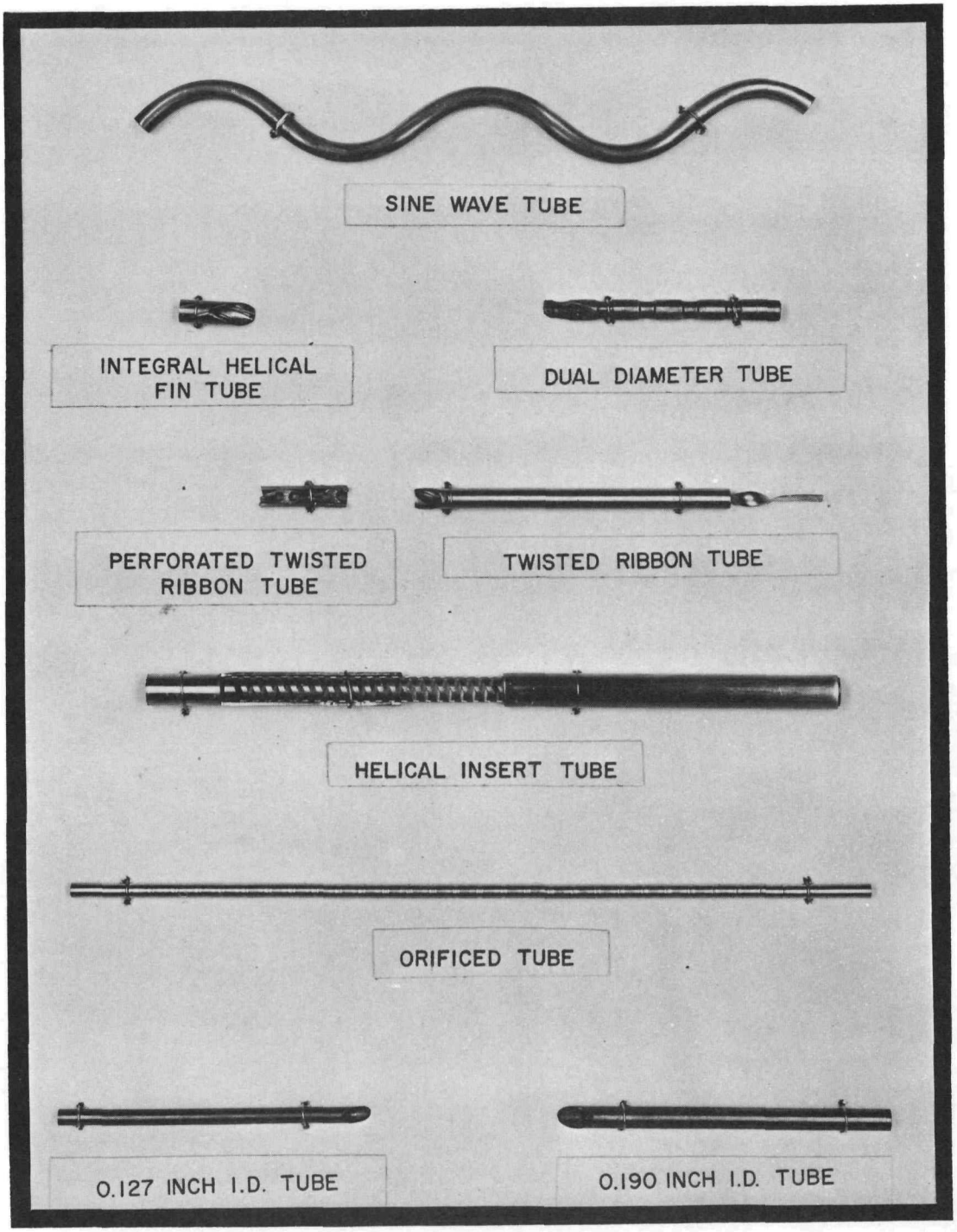

LOCAL HEAT TRANSFER COEFFICIENT VERSUS LOCAL QUALITY

TWO-PHASE WATER TESTS

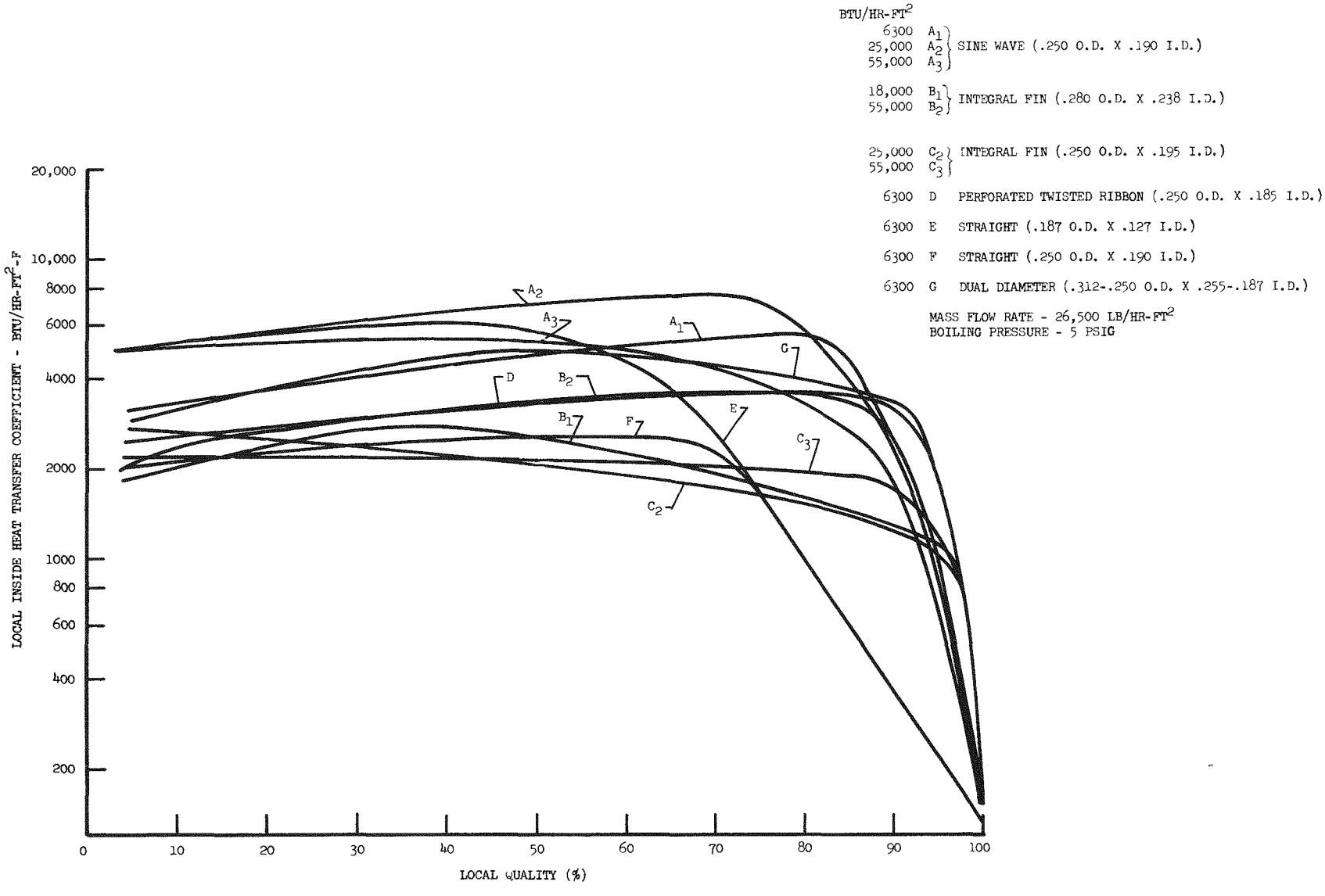

PWAC - 632
FIG 84

LOCAL PRESSURE DROP VERSUS LOCAL QUALITY

TWO-PHASE WATER TESTS

A. SINE WAVE (.250 O.D. X .190 I.D.)
B. INTEGRAL FIN (.280 O.D. X .238 I.D.)
C. INTEGRAL FIN (.250 O.D. X .195 I.D.)
D. TWISTED RIBBON (.250 O.D. X .185 I.D.)
E. STRAIGHT (.187 O.D. X .127 I.D.)
F. STRAIGHT (.250 O.D. X .190 I.D.)
G. DUAL DIAMETER (.312-.250 O.D. X .255-.187 I.D.)

MASS FLOW RATE - 26,500 LB/HR-FT^2
ΔP MEASURED LENGTH - 16 "
BOILING PRESSURE - 5 PSIG

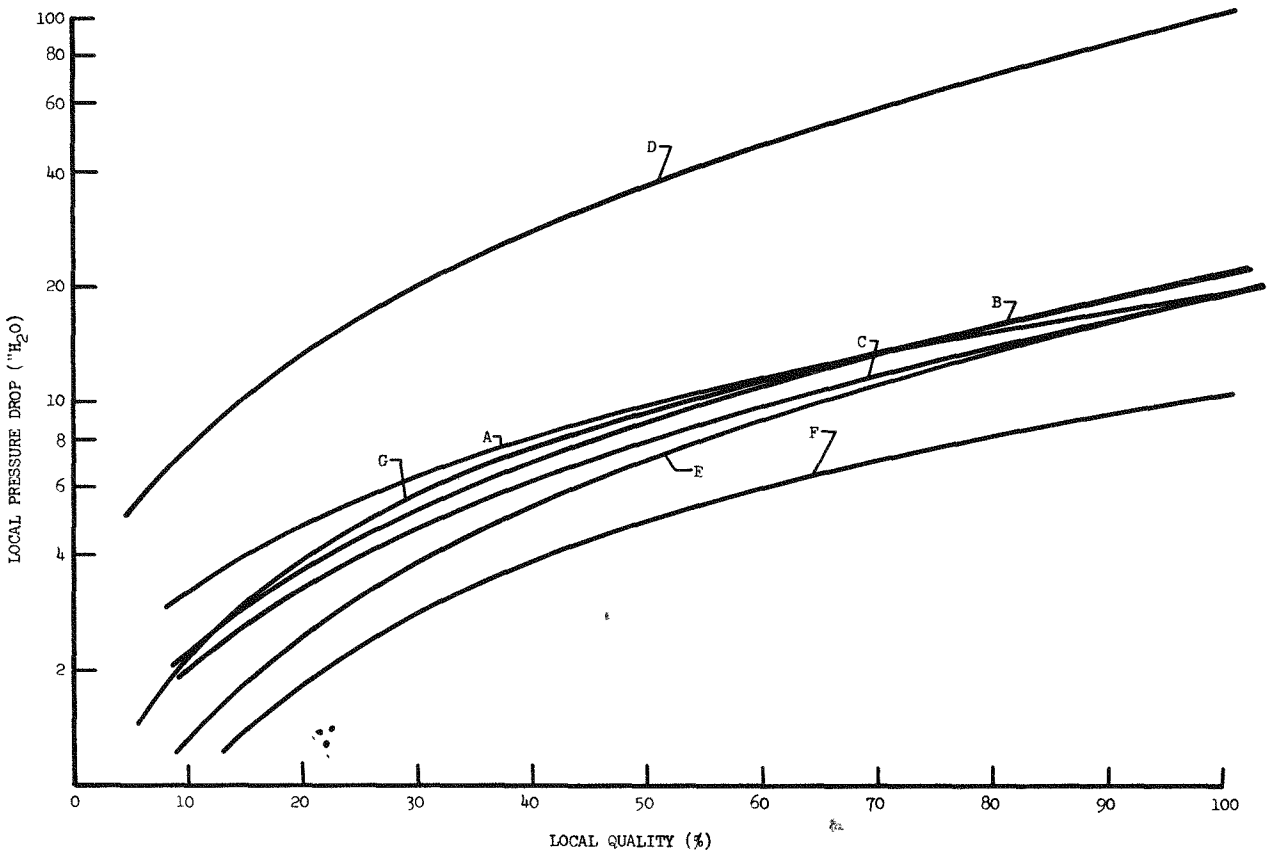

The efforts to produce columbium alloy samples with internal helical fins have not been too successful. Attempts are still being made by two vendors to produce tubing with integral, internal fins in a manner that would be acceptable for pilot lot production.

Planning and design efforts were continued during the quarter on Cb-1 Zr alloy on 19 tubes, test boilers and the Cb-1 Zr alloy test system. Layouts of two boiler designs have been completed, one using helical slotted inserts in the boiler tubes (PWAC-631, Fig 59) and the other using dual-diameter tubes (Fig 86). Figs 87 and 88 show these boiler layouts. Tubing material is on order from which either tube geometry can be fabricated. It is planned to operate these tests in an existing inert atmosphere chamber. Component arrangement studies have been conducted leading to the layout shown in Fig 89. A schematic of the proposed test system is shown in Fig 90.

Initial studies were conducted to arrive at flow systems satisfactory for testing full-scale boilers. A review of corrosion and mass transfer data available for NaK in Cb-1 Zr alloy-Haynes-25 bimetallic systems indicated that mass transfer might be a serious problem in a bimetallic boiling potassium system. On this basis, it was decided that both the lithium and potassium circuits should be fabricated from Cb-1 Zr alloy, thereby requiring that these systems be entirely enclosed in a controlled atmosphere container. Approximately 30 flow schematics were analyzed in these studies.

The capabilities considered desirable for the SNAP-50/SPUR boiler and condenser test facility included: 1) boiler test only, 2) simultaneous test of a SNAP-50/SPUR boiler and one or more SNAP-50/SPUR condensers, 3) boiler test using a modified SNAP-50/SPUR condenser and 4) condenser test only. Studies concentrating on the first facility capability included condensing the potassium vapor by removing heat with NaK, lithium, helium, water (with a helium barrier), and radiation to the containment walls. Of these possibilities, condensing with NaK appeared to have the greatest promise. Simultaneous testing of SNAP-50/SPUR boilers and SNAP-50/SPUR condensers requires inclusion of a turbine simulator section in the vapor line. Fig 91 shows one possible arrangement. Studies on the third facility capability revealed that a condenser which is prototype for the first flight powerplant (except for heavier shell and thicker tube sheets) would serve as a satisfactory workhorse condenser in a prototype boiler test. This possibility is diagrammed in Fig 92. In addition, the prototype boiler could be used to generate vapor at conditions suitable for a prototype condenser test as shown in Fig 93. This facility can also be designed to permit the addition of a SNAP-50/SPUR turbogenerator and other components when testing of the power conversion system (Fig 94) becomes desirable. Preliminary arrangement studies have shown the Heat Exchanger Laboratory at CANEL (refer to Section II, C, "Non-Nuclear Systems Test" of this report), with its existing high amperage dc power supplies and high temperature NaK coolers, to be quite adequate for two such boiling potassium test facilities.

5. Materials

Design of the primary coolant pump motor for SNAP-50/SPUR requires that a joint be made between Cb-1 Zr alloy and BeO. These materials will be used in canning the stator to protect electrical wiring from liquid metal attack.

The following braze alloys have shown promising results on producing a BeO to Cb-1 Zr joint:

Alloy	Heat No.	Melting Temp
Zr-8 Mo-8 Ni	CA-785	2370F
Zr-8 Mo-6 Fe	CA-787	2540F
Zr-8 W-8 Ni	CA-782	2370F

DUAL DIAMETER BOILER TUBE

Cb-1 Zr ALLOY BOILER TEST SYSTEM

(EXTERNAL VIEW)

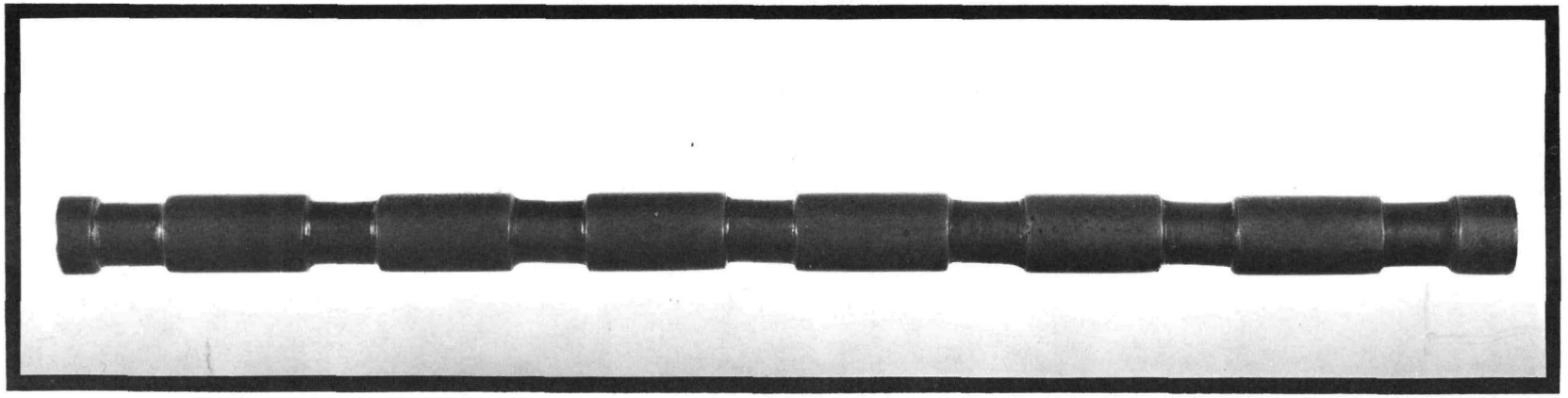

(SECTIONAL VIEW)

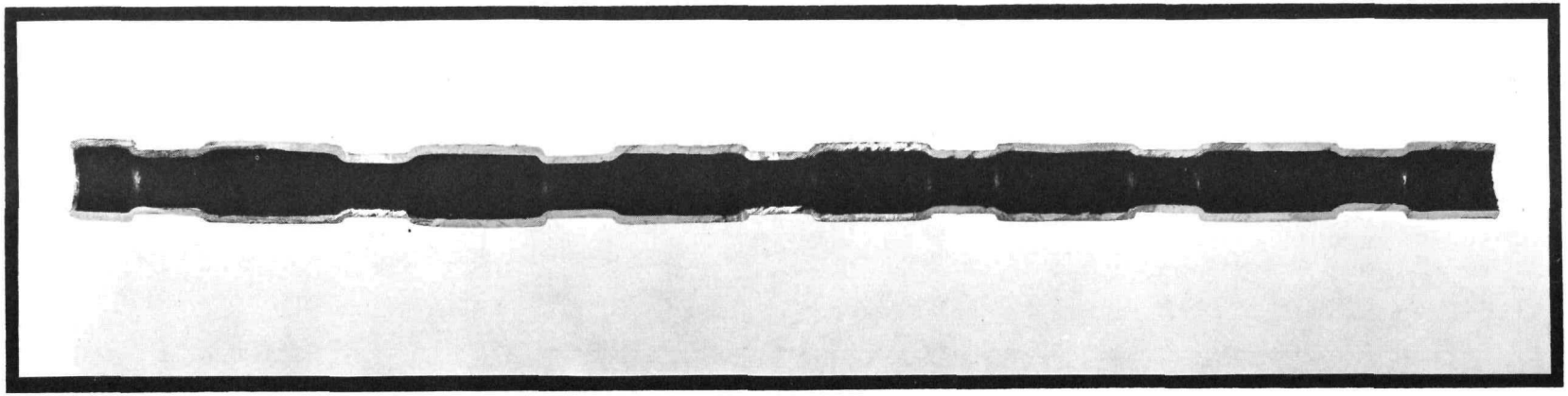

Cb-1 Zr ALLOY, 19 TUBE, TEST BOILER

HELICAL SLOTTED INSERTS IN TUBES

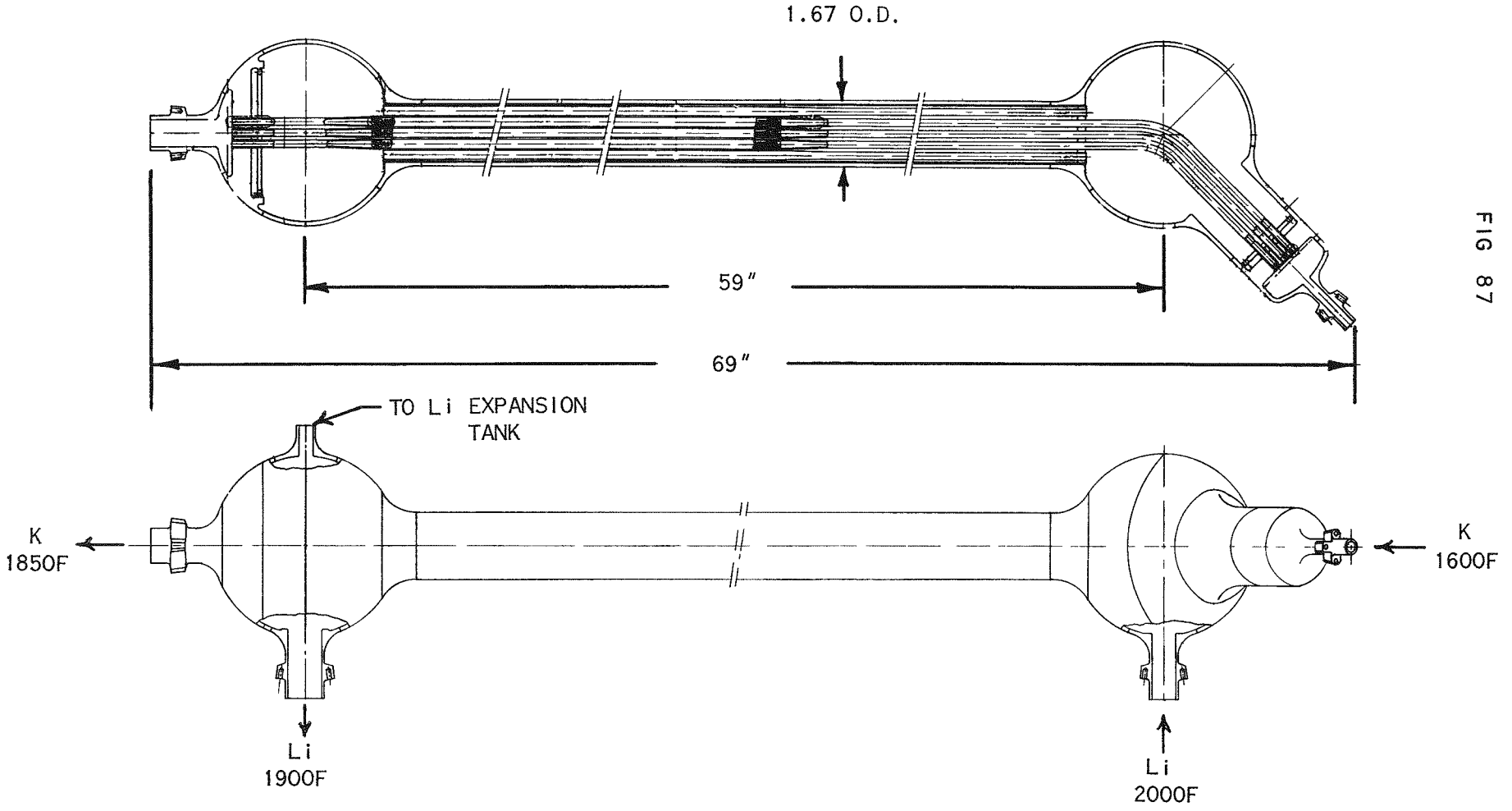

Cb-1Zr ALLOY, 19 TUBE, TEST BOILER

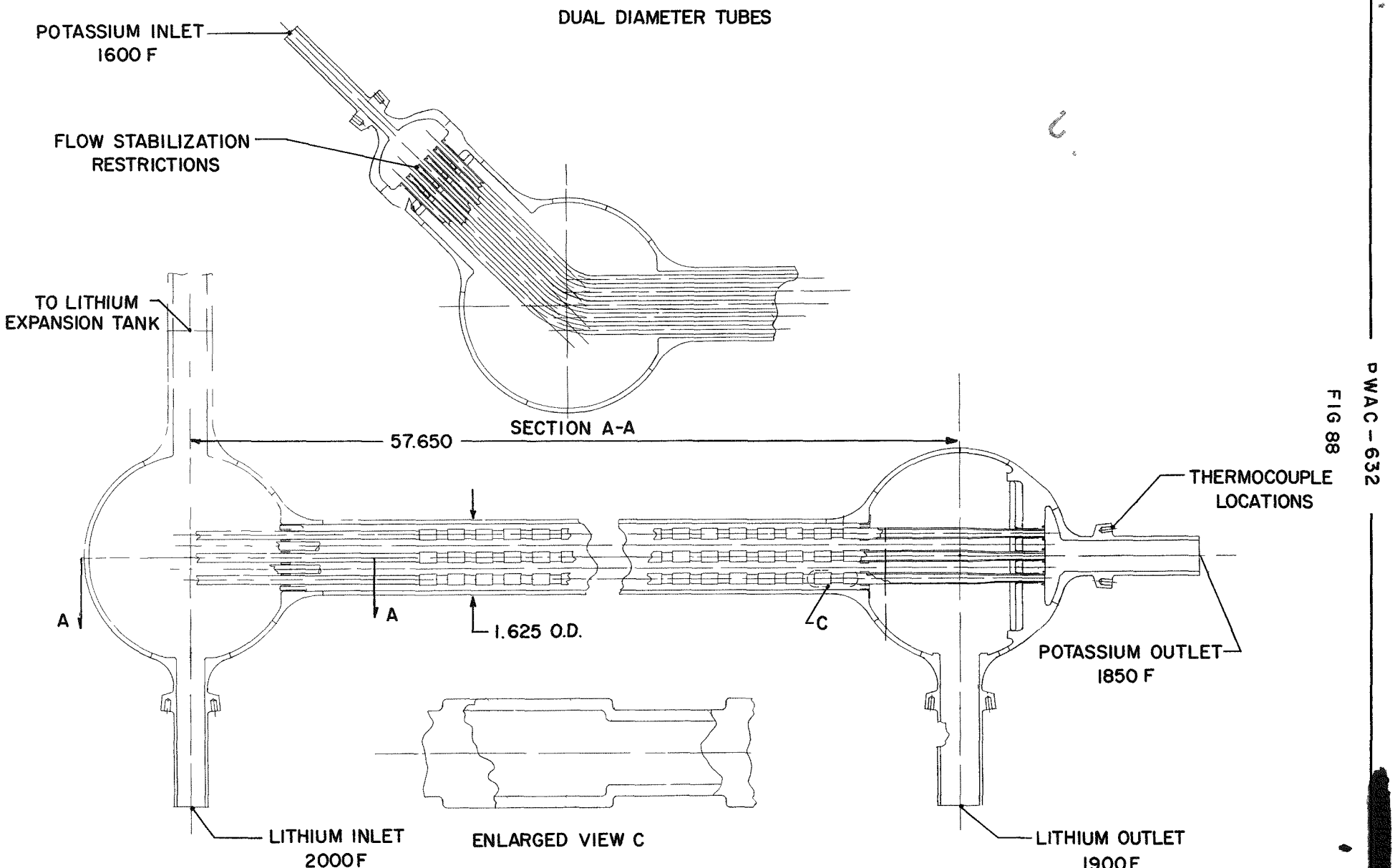

Cb-1Zr ALLOY BOILER TEST SYSTEM IN EXISTING INERT GAS CHAMBER

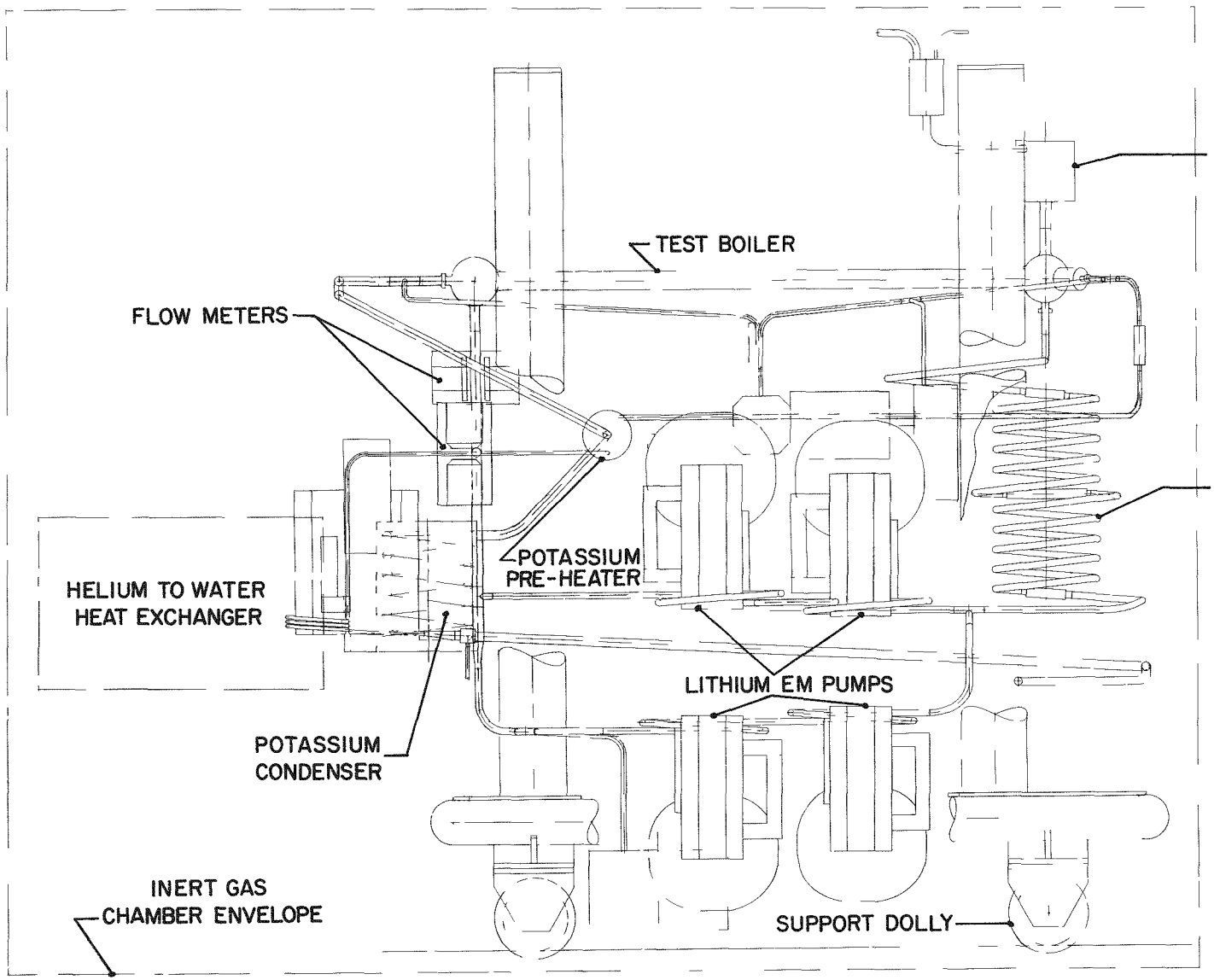

Cb-1Zr ALLOY BOILER TEST SYSTEM SCHEMATIC

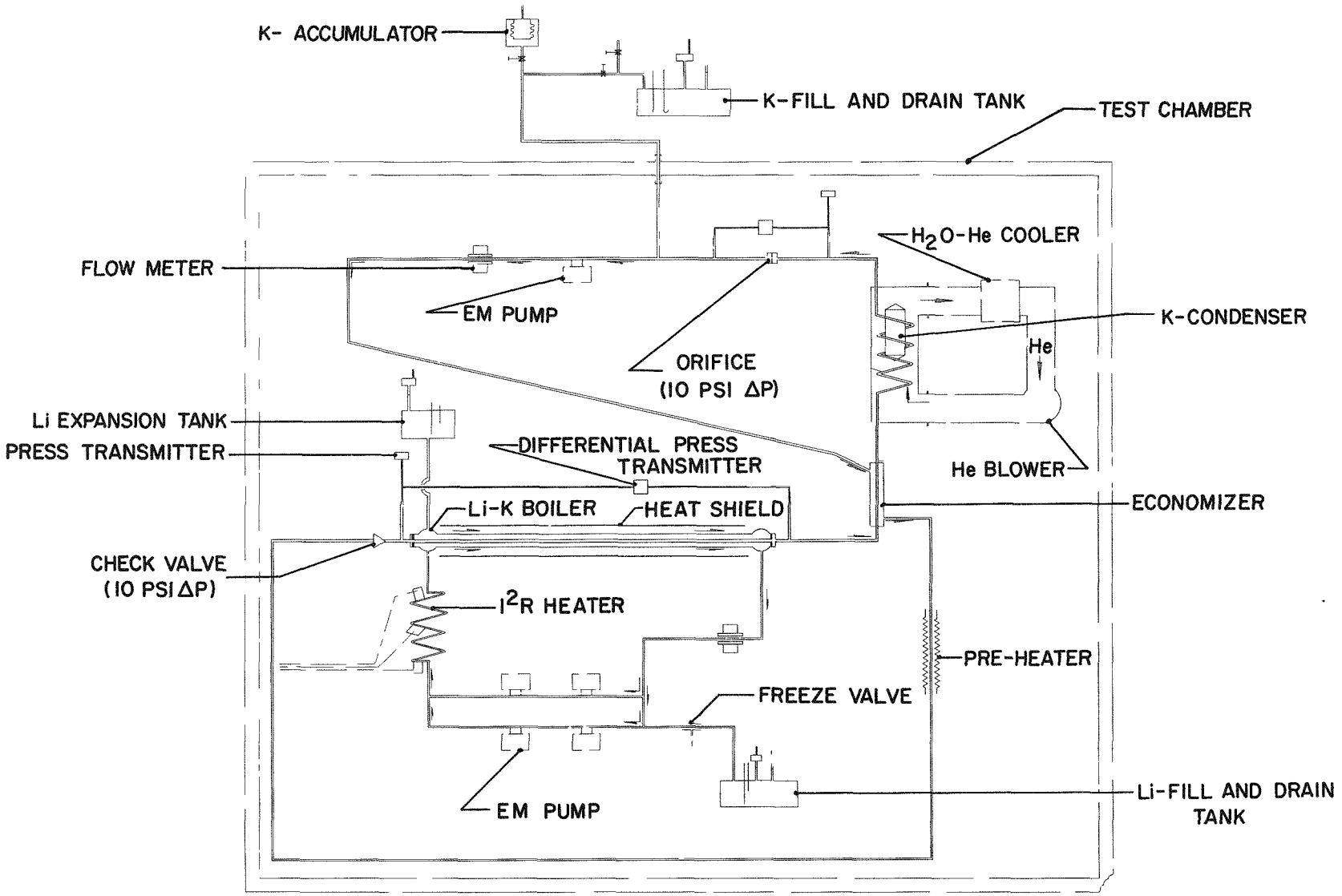

FIG 91

FULL SCALE BOILER AND CONDENSER TEST

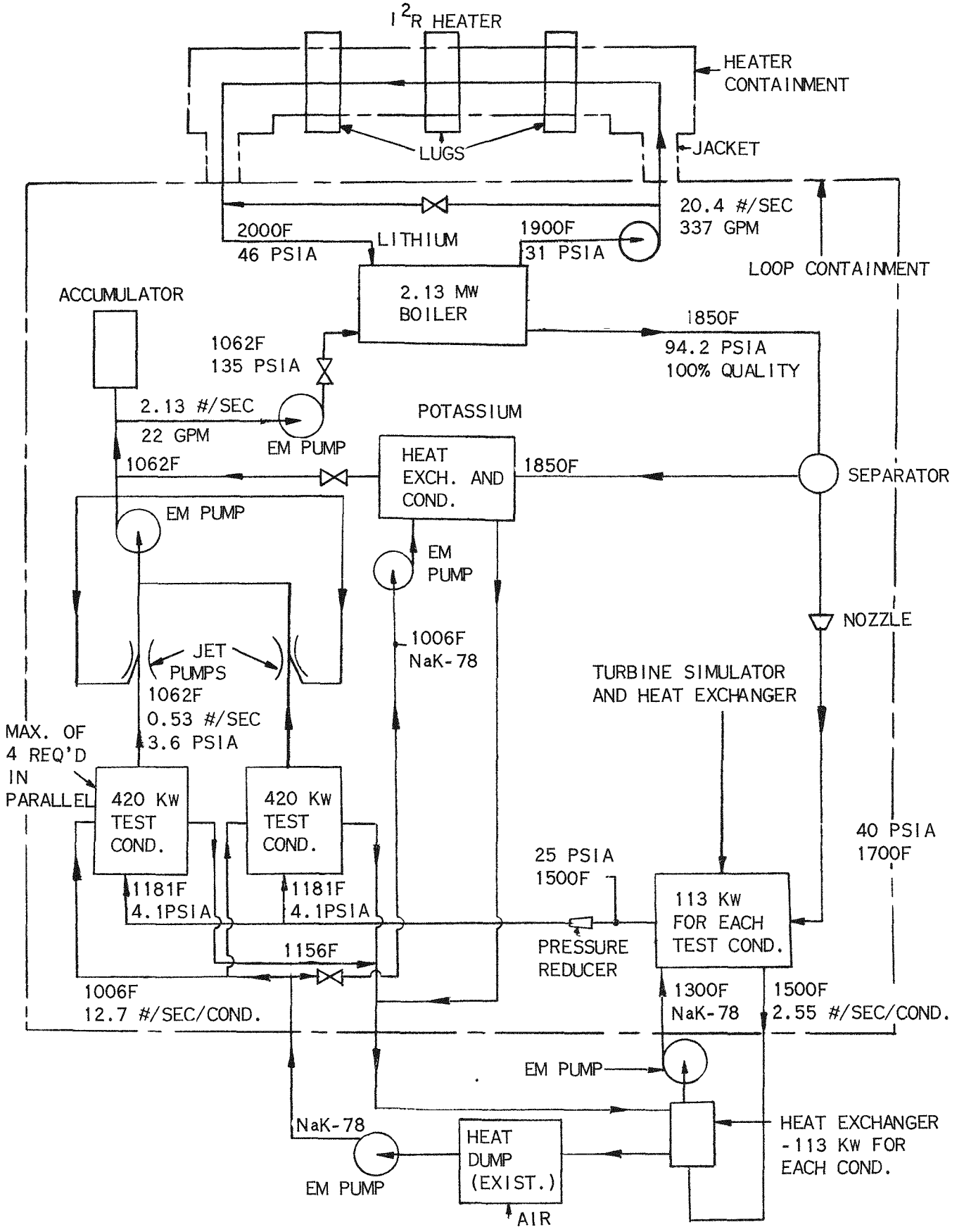

FIG 92

FULL SCALE BOILER TEST

PRELIMINARY SCHEMATIC

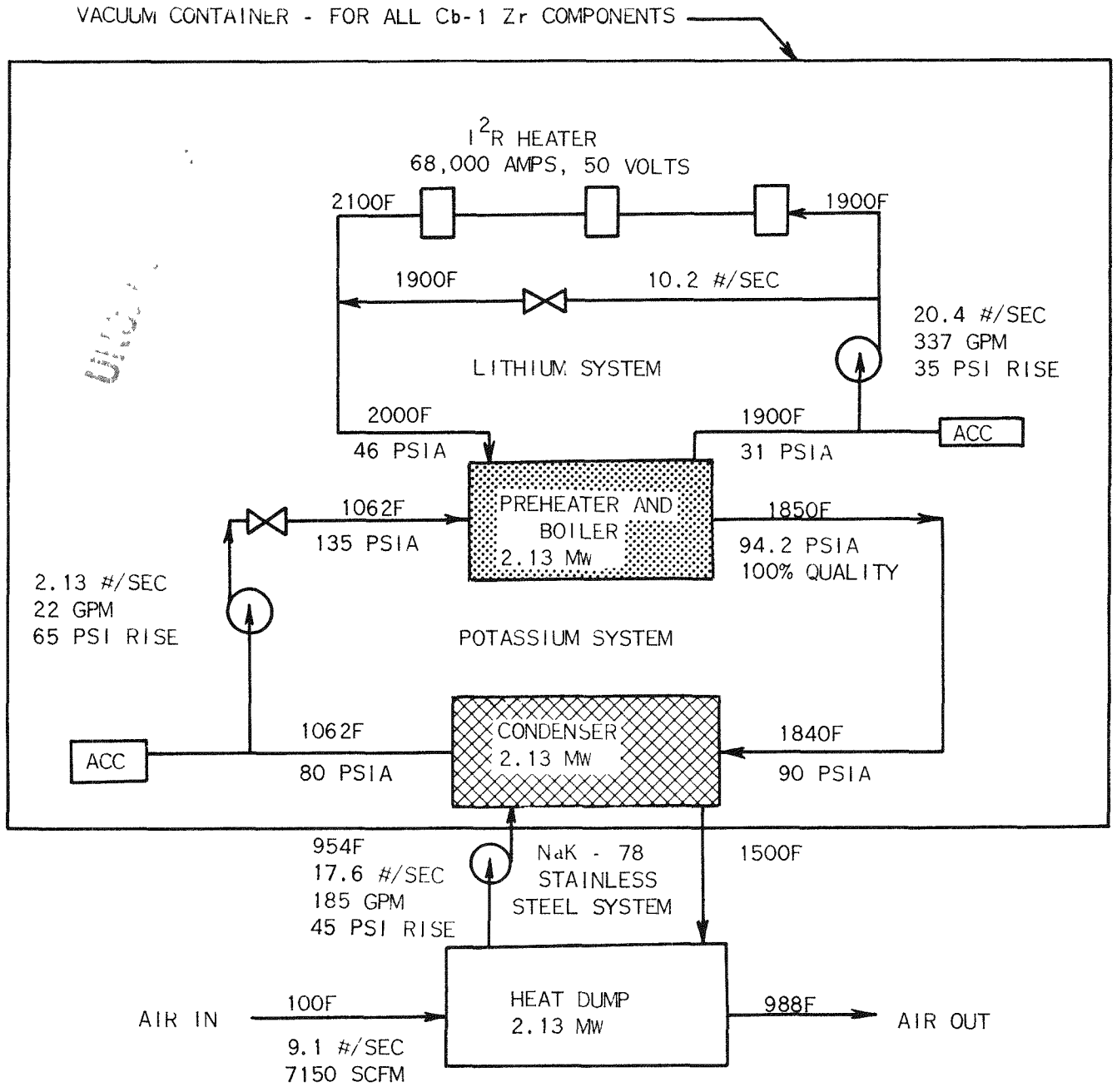

CONDITIONS STATED ARE APPROXIMATE - FOR PLANNING ONLY

PROTOTYPE COMPONENT OPERATING AT PROTOTYPE CONDITIONS

SEMI-PROTOTYPE COMPONENT OPERATING AT OFF DESIGN CONDITION

FIG 93

FULL SCALE CONDENSER TEST

PRELIMINARY SCHEMATIC

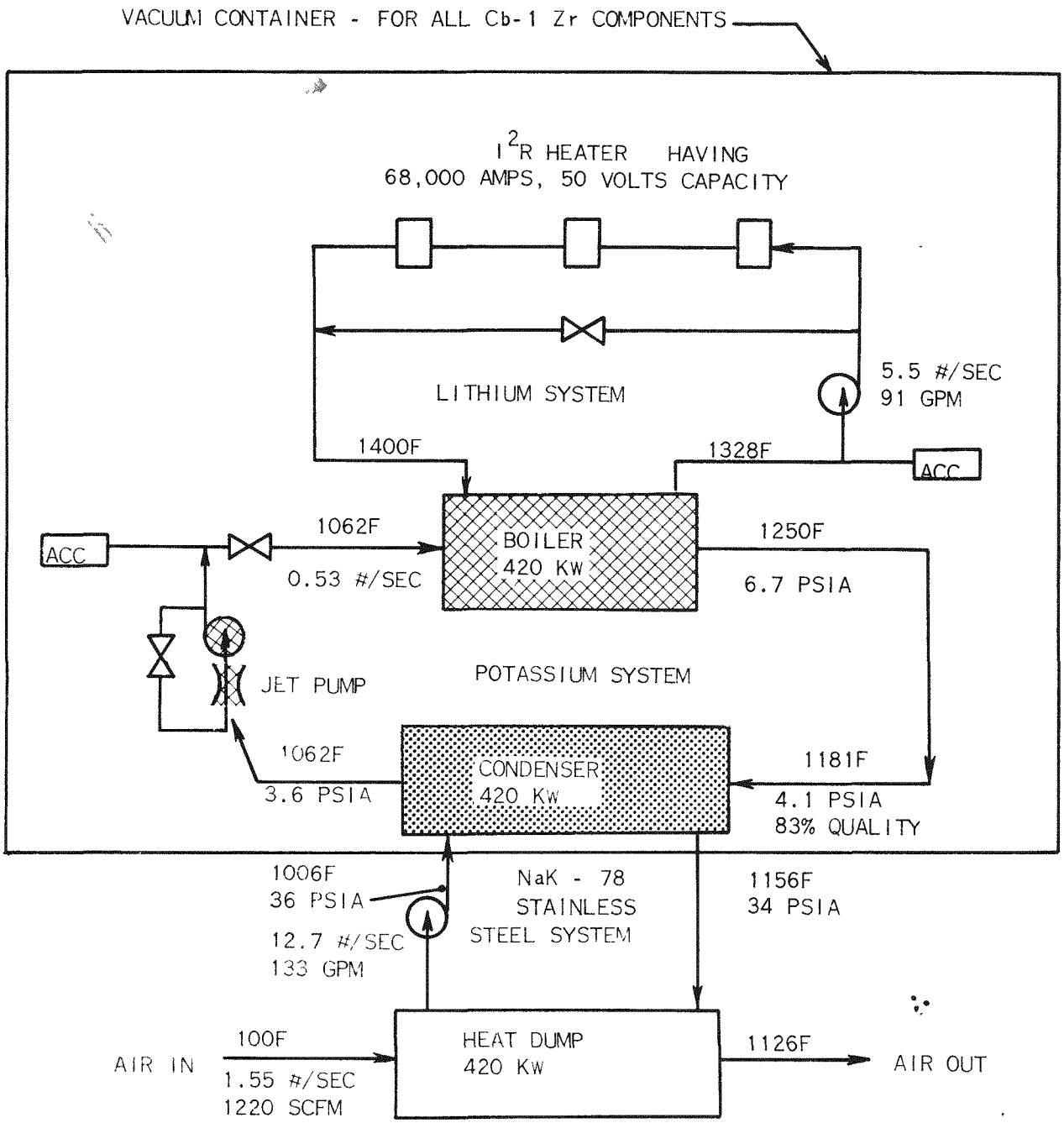

CONDITIONS STATED ARE APPROXIMATE - FOR PLANNING ONLY

PROTOTYPE COMPONENT OPERATING AT PROTOTYPE CONDITIONS

PROTOTYPE COMPONENT OPERATING AT OFF-DESIGN CONDITION

FIG 94

FULL SCALE POWER CONVERSION SYSTEM TEST

PRELIMINARY SCHEMATIC

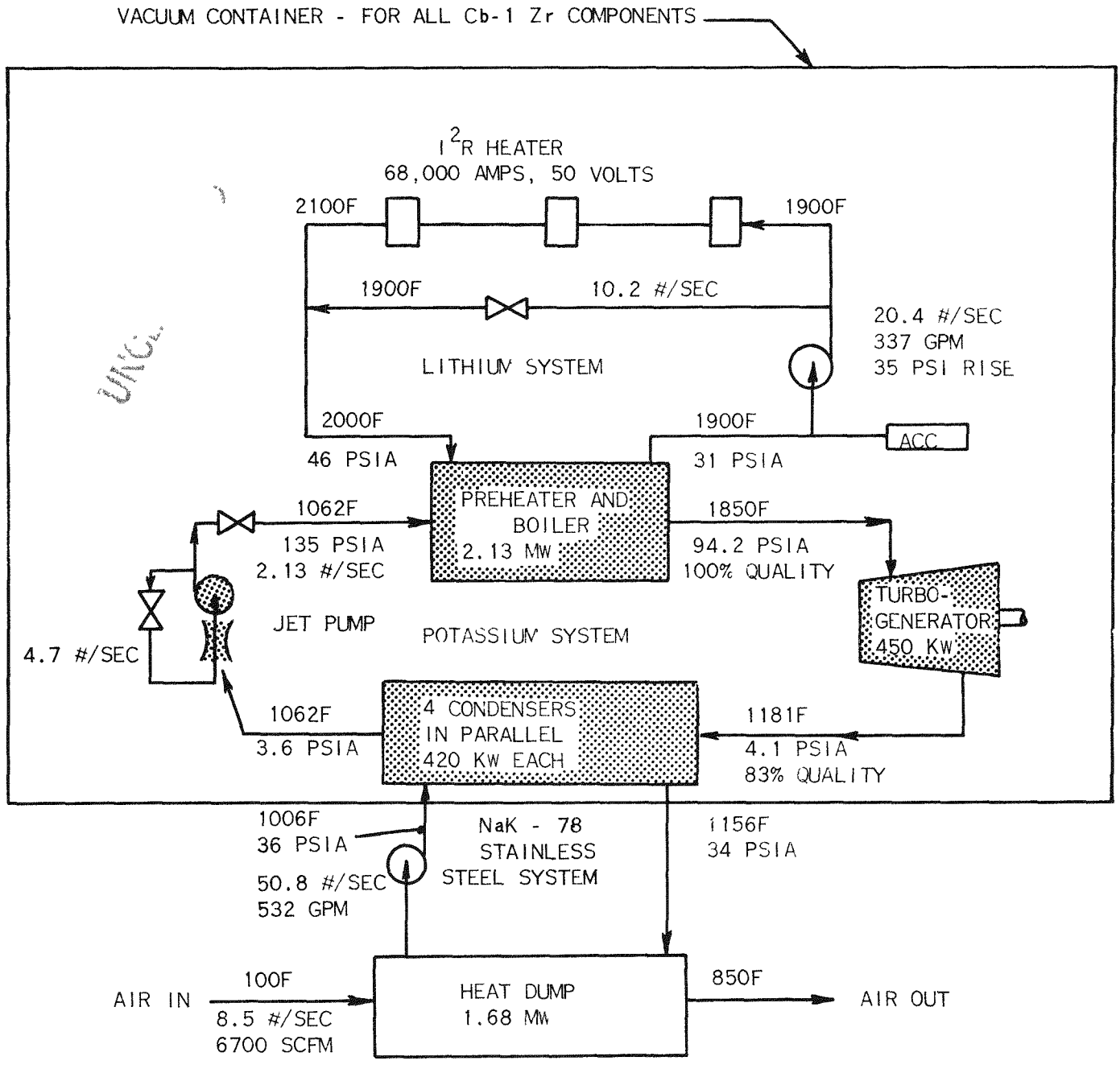

CONDITIONS STATED ARE APPROXIMATE - FOR PLANNING ONLY

PROTOTYPE COMPONENTS OPERATING AT PROTOTYPE CONDITIONS

Alloy	Heat No.	Melting Temp.
Zr-8 W-6 Fe	CA-784	2565F
Zr-28 V-16 Ti	CA-779	2280F
Ti-7 Fe	CA-761	2650F

Two methods of brazing to BeO have been investigated, 1) brazing directly on bare BeO, and 2) metallizing the BeO with titanium before brazing.

Alloys CA-782, 784, 785, and 787 have been brazed to bare BeO. The test specimen consists of a Cb-1 Zr alloy tube into which is inserted a BeO pellet. The braze joint is then made between the pellet outside diameter and the tube inside diameter. The specimens were induction brazed in an argon atmosphere with a two to three mil gap.

After brazing, the joints were leak-checked using a helium mass spectrometer. All four alloys produced leak-tight joints. The joints were then thermally-cycled from 600F to 1200F for five cycles, at a heating and cooling rate of 50F/hr. After thermal cycling, the joints were again leak-checked. All alloys produced leak-tight joints, except the Zr-8 W-6 Fe. The specimens were then sectioned for metallographic examination. An excellent bond was produced between the braze alloy and the BeO with the Zr-8 Mo-8 Ni (Fig95) and Zr-8 W-8 Ni alloys. The Zr-8 Mo-6 Fe and Zr-8 W-6 Fe showed some void areas and lack of bonding between the BeO and braze alloy. All alloys produced excellent joints between the Cb-1 Zr alloy and braze alloy. Liquid metal soak tests at 1200F in lithium for 500 and 1000 hours are scheduled.

All six alloys have successfully produced leak-tight joints between Cb-1 Zr alloy and titanium-metallized BeO. The joints were produced in the same manner as the above specimens, with the exception that a coating of titanium was deposited on the BeO. Thermal cycle tests are scheduled to be performed on these specimens. Those alloys producing leak-tight joints after thermal cycling will be subjected to liquid metal soak tests.

Evaluation of prospective bearing materials for compatibility in 1100F lithium and wear in 700F lithium has continued. Data from tests concluded during the past quarter is summarized in Fig 96. The CANEL-developed cermet, WC-Mo-CbC, showed negligible weight loss after a 500 hour compatibility test and excellent wear quality after a low-load 96-hour test in 700F lithium. This material appears to be the most satisfactory material tested to date. Specimens of Kennametal K-96 have been evaluated after completing 500 and 2000-hour tests. Metallographic examination showed no attack on lithium-exposed specimens. A network of fine cracks on one surface of the 2000-hour test specimen was attributed to physical damage in preparation or handling. Wear specimens of Kennametal K-96 operated under low load for 20 hours in 700F lithium and exhibited excellent wear quality. On the other hand, Kennametal K-162B specimens proved to be incompatible with 1100F lithium in 500 and 2000 hour tests because of lithium attack of the nickel rich binder. Wear specimens of Kennametal TiC-10 Mo, Carboloy-78, and plasma-sprayed CANEL cermet 113565 had fair wear quality under low load. Poor wear quality was exhibited by Clevite 300 at low load and cermet 113565 at high load.

Prospective materials for seal-welding of motor rotors have been under test. One specimen each of unannealed welds of Cb-1 Zr alloy to unalloyed titanium and Ti-6 Al-4 V alloy have completed 500 hours in 1100F lithium. Posttest examination showed no weight loss and no metallurgical difference from pretest material.

BeO TO Cb-1 Zr BRAZE JOINT

(Zr-8 Mo-8 Ni BRAZE ALLOY)

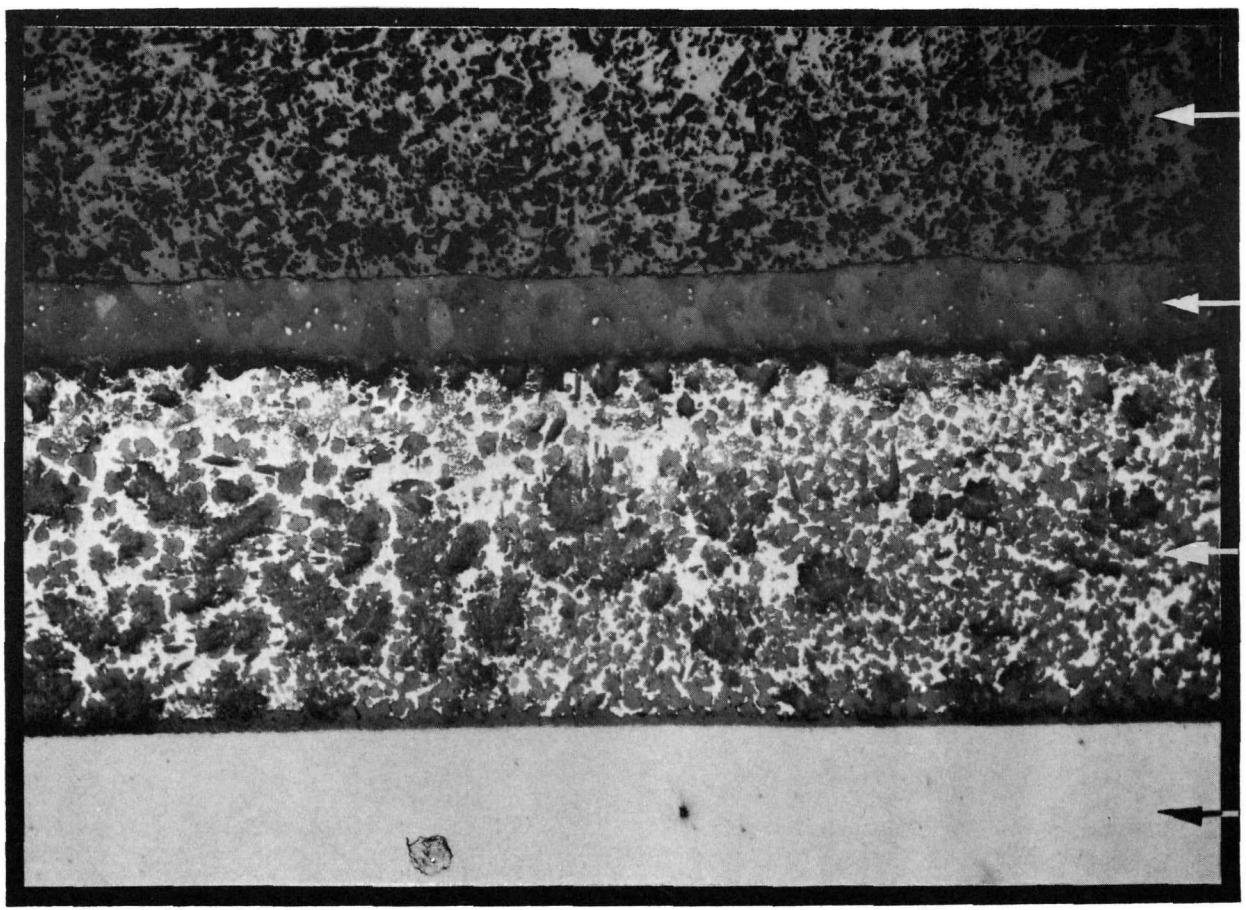

MAGNIFIED: 200X

PWAC - 632

FIG 95

2764-3

COMPATABILITY AND WEAR BEHAVIOR OF CERMETS IN LITHIUM

Material*	Source	Surface Treatment	Compatibility in 1100F Lithium: Duration, hr.	Compatibility in 1100F Lithium: Weight Loss mg/cm² 100 hrs.	Remarks	Wear and Friction ** in 700F Lithium: Duration, hr.	Wear and Friction ** in 700F Lithium: Remarks
K-96	Kennametal	-	500 2,000	0.06 0.07	Appears Compatible	20	Low load; excellent wear quality
K-162B	Kennametal	-	500 2,000	1.2 1.6	Incompatible		
WC-Mo-CbC	CANEL	-	500	Neglible		96	Low load; excellent wear quality
Cb-1Zr Alloy	CANEL	Plasma Spray 113565					Low load; fair wear quality High load; very poor wear quality
TiC-10 Mo	Kennametal	-				22.25	Low load; fair wear quality
Carboloy	G. E.	-				22.33	Low load; fair wear quality
Clevite 300	Cleveland Graphite Bronze					1.16	Low load; very poor wear quality

* Cermet compositions are as follows:

	WC	Co	(Ta, Cb)C	TiC	Mo	Ni
K-96	92	6	2			
K-162B			6	64	5	25
Carboloy	76	8	4	12		
Clevite 300						

** Wear and friction tests are performed in a modified Holman A-6 test rig described in PWAC-624. Low load - 22 pounds applied, high load - 85 pounds applied.

IV. ADVANCED APPLICATION STUDIES

IV. ADVANCED APPLICATION STUDIES

A preliminary analytical study for adapting the SNAP-50/SPUR space powerplant to provide electrical power for a manned lunar base was completed and published as PWAC-406. Two types of powerplants were considered in this study: a system with a net electrical power output of 100 to 300 Kwe, referred to as a first generation powerplant, and a system with a nominal net power output of 1 Mwe, referred to as a later generation powerplant.

The first generation powerplant proposes using the basic 300Kwe SNAP-50/SPUR powerplant designed for space operation with a single power conversion unit, but including those modifications required for operation on the lunar surface. This system, shown in Fig 4, PWAC-406, has a fixed radiator configuration as determined by the Saturn C-1B envelope and is assumed to utilize a naturally-occurring lunar crater for shielding. This system is expected to require a minimum of site preparation with installation and start-up accomplished by a few men.

The later generation powerplant incorporates components identical to the first except for the configuration of the radiators. The reactor, together with four power conversion units, are buried beneath the lunar surface with lunar soil functioning as shielding material, as shown in Fig 7, PWAC-406. The radiator panels are arranged vertically above the lunar surface. It is assumed that sufficient manpower and equipment would be available on the moon to provide for considerable site preparation and excavation, in addition to connecting and erecting radiator panels above the lunar surface.

The study considered those problems which are unique to operation of the SNAP-50/SPUR type powerplant on the lunar surface, such as radiator orientation, shielding, reactor side reflector cooling, decay heat removal and powerplant start-up. Based upon this study, the SNAP-50/SPUR type powerplant is a feasible electrical power-generating system for a lunar base. Furthermore, a powerplant specific weight of 10 to 15 lb/Kwe is well within the delivery capability to the lunar surface of the Saturn C-5 launch vehicle which is being developed for use in the Apollo Program.

A brief study was completed which examined SNAP-50/SPUR type powerplants scaled-up in net power output to 40 Mwe. The powerplant specific weight was found to increase from a value of about 10 lb/Kwe at 1 Mwe to about 17 lb/Kwe at 40 Mwe. This increase was due primarily to the added meteoroid shielding of the radiators, required for the larger systems. The reactor was the only component which would require complete re-design and could not be based upon scaled-up designs of current SNAP-50/SPUR components. Radiation cooling of the side reflector would no longer be feasible. Fuel loading would have to be increased significantly to accommodate fuel burnup and reactivity control associated with both high reactor power and long reactor life.

A study of the LCRE reactor for use in a portable electrical power-generating system was initiated. The system is designed to provide a net electrical power output of 1 Mwe and is capable of being transported by either ship or aircraft to any remote site. The basic power cycle consists of the lithium-cooled reactor which provides heat to air through an intermediate NaK circuit. The air enters Pratt & Whitney Aircraft's 500-hp, PT-6 aircraft engines where it is compressed, heated in liquid metal-to-air radiators located external to the engines, and expanded through the turbines, each of which is directly coupled to electrical generators.

RESTRICTED DATA

This document contains restricted data as defined in the Atomic Energy Act of 1954. Its transmittal or the disclosure of its contents in any manner to an unauthorized person is prohibited.